COORDINATION OF SOME MONODENTATE AND HYBRID MULTIDENTATE PHOSPHINE LIGANDS TO PLATINUM GROUP METALS

A thesis presented for the degree of

Doctor of Philosophy

in the

Department of Chemistry

of the

Faculty of Science

at the

University of Leicester

by

Roger Abdo Nassar

August 2000

ProQuest LLC
789 East Eisenhower Parkway
P.O. Box 1346
Ann Arbor, MI 48106-1346

I would like to dedicate this work to my father *ABDO*, my mother *COLETTE* and to my brother *TONI* for their love and support in all my endeavours.

This work is also dedicated to the memory of my late cousin *Rita J. Nassar* whom, I believe, is an angel in God's kingdom.

STATEMENT

The experimental work described in this thesis has been carried out by the author in the Department of Chemistry at the University of Leicester between July 1997 and August 2000.

The work has not been submitted, and is not presently being submitted, for any other degree at this or any other university.

Signed: R. NASSAR **Date:** 26 October 2000

Department of Chemistry
University of Leicester
University Road
Leicester
U.K.
LE1 7RH

Coordination of Some Monodentate and Hybrid Multidentate Phosphine Ligands to Platinum Group Metals

Roger Abdo Nassar

Abstract

A range of low-valent late transition-metal triarylphosphine complexes have been prepared and characterised by a combination of ^{1}H, ^{31}P and ^{19}F (as appropriate) NMR and IR spectroscopies and mass spectrometry. Some of these complexes have been isolated as single crystals and characterised by X-ray diffraction.

The triarylphosphine ligands used in this study were $P(4\text{-}CH_3OC_6H_4)_3$, $P(4\text{-}HOC_6H_4)_3$, $P(2\text{-}CH_3OC_6H_4)_3$, $PPh_2(2\text{-}CH_3OC_6H_4)$, $P(2\text{-}HOC_6H_4)_3$ and $PPh_2(2\text{-}C_2H_3C_6H_4)$ whilst the transition-metals were platinum(II), palladium(II), rhodium(I), rhodium(III), osmium(II) and ruthenium(II). This work has shown that the former four phosphine ligands act as monodentate ligands whilst the last two ligands act as hybrid multidentate ligands. The metal complexes of the *ortho*-hydroxy substituted ligand exhibit fluxional behaviour in solution, where the phosphine is interchanging between mono- and bi-dentate modes of coordination. In contrast, fluxionality has not been observed in the case of the *ortho*-vinyl substituted ligand.

A set of platinum(II)-, osmium(II)- and ruthenium(II)-fluoride triarylphosphine complexes have been prepared and characterised. The electron-donating substituents in the phosphine strengthen the metal-phosphine and metal fluoride bonds as compared to those for the non-substituted triarylphosphine ligand, PPh_3. Furthermore, these substituents affect the geometry at the metal centre in these complexes. In the reactions of $P(2\text{-}HOC_6H_4)_3$ with $[Pt(\mu\text{-}F)\{P(4\text{-}CH_3OC_6H_4)_3\}_2]_2$ or $[M(\mu\text{-}F)F(CO)_3]_4$ (M = Os, Ru), metal chelates are formed by the displacement of fluoride by phenoxide and liberation of HF, whereas, in the related reactions, the *ortho*-vinyl substituted ligand acted in a monodentate mode.

CONTENTS

Chapter Three

Coordination Chemistry of Monodentate ortho-Substituted Aryl Phosphine Ligands

Chapter Four

Coordination Chemistry of the tris-(ortho-Hydroxyphenyl)-phosphine Ligand

Chapter Five

Coordination Chemistry of the ortho-Vinylphenyl-diphenylphosphine Ligand

Chapter Six

Synthesis and Characterisation of Low-Valent Platinum Group Metal Fluoride Phosphine Complexes

Chapter Seven

Reactions of Low-Valent Platinum Group Metal Fluoride Complexes With Hybrid Multidentate Phosphine Ligands

Chapter Eight

Experimental

Acknowledgements

My deep thanks are due to Prof. John H. Holloway and Prof. Eric G. Hope for supervising my research and for their help and support throughout the last three years at Leicester University.

I would like to acknowledge Dr's John Fawcett, Gerry Griffith and Graham Eaton for their help in solving crystal structures, recording NMR and mass spectra respectively.

I wish to express my gratitude to the members of the fluorine group both past and present. In particular, I am grateful to Dr's Howard Clark, Alison Stuart and David Birdsall. Thanks goes to the project student, Antony Wood, for carrying out the experimental work related to $PPh_2(2\text{-}CH_3OC_6H_4)$. I would also like to thank all the members of the chemistry staff. A big thankyou goes to Anne Crane.

I am most grateful to everybody who made my time in England excellent. Here, a special thankyou goes to Jenny Holloway.

Finally, I would like to thank the Lebanese University (UL) for granting me a full scholarship and I would like to mention Dr Rafic El-Bacha for offering all the help that I needed from the UL.

Abbreviations

aHF:	Anhydrous hydrofluoric acid
Cy:	Cyclohexane
DCM:	Dichloromethane
DMSO:	Dimethylsulfoxide
ES:	Electrospray
e.s.d.:	Estimated Standard Deviation
FAB:	Fast Atom Bombardment
FEP:	Fluorinated ethylene-propylene co-polymer
HOMO:	Highest occupied molecular orbital
Kel-F:	Poly(chlorotrifluoroethylene)
LUMO:	Lowest unoccupied molecular orbital
NMR:	Nuclear magnetic resonance
SP:	*Ortho*-styryldiphenylphosphine
Cp*:	Pentamethylcyclopentadienyl
PTFE:	Polytetrafluoroethylene
RT:	Room temperature
r.b.f.:	Round bottom flask
THF:	Tetrahydrofurane

CHAPTER ONE

INTRODUCTION TO METAL PHOSPHINE COMPLEXES

CHAPTER ONE

INTRODUCTION TO METAL PHOSPHINE COMPLEXES

1.1 General Introduction:

Metal-phosphorus coordination compounds provide inorganic chemistry with many elegant illustrations of the various stereochemical requirements of metal elements. For many years, coordination chemists have used trivalent phosphorus ligands to stabilise a large variety of oxidation states of transition-metals.[1] The coordination can be viewed as an acid/base reaction in the wider Lewis classification.[2] The complexing ability of tertiary phosphines arises from the donation of the lone-pair of electrons on the phosphorus atom, and such phosphine belong to the "soft" base group of Pearson's hard/soft acid/base (HSAB) theory.[3-5] This theory predicts that phosphorus bases should bind more strongly to "soft" Lewis acids, such as transition-metal atoms in low oxidation states and, therefore, it is not surprising that low-valent late transition-metal phosphine complexes are well established and highly stable.

Phosphorus(III) ligands have a potential ability to act not only as σ-donors, but also as π-acceptors. This synergic effect is dependent to a large extent on the substituents on the phosphorus ligating atom, as well as on the environment at the metal centre. Electron-withdrawing groups bound to phosphorus are expected to promote the M→P π-bonding. However, electron-withdrawing ligands bound to the metal centre should favour P→M σ-bonding.

It should be mentioned that these synergic effects in the bonding of trivalent phosphorus ligands, have been exploited in the formation of many very stable and active transition-metal phosphine complexes used as catalysts. This stability has enabled these complexes to be fully characterised, many by X-ray diffraction and nuclear magnetic resonance spectroscopies' studies.

Catalysis has been described as an art.[6] The definition of the word "art" in the *Shorter Oxford English Dictionary* is "skill as the result of knowledge and practice" and "an occupation in which skill is employed to gratify taste or produce what is beautiful". This emphasises that, in order to achieve a beautiful product, in this case a "catalyst", the artist, in this case "the chemist", needs to have an understanding of the elements that construct his product, i.e., in order to prepare suitable catalysts, it is required that a coordination chemist understands the factors that affect and participate in the formation of these catalysts.

In this thesis, the first chapter concentrates on introducing the common feature of this work, the metal-phosphine complexes. It describes common routes for the preparation of transition-metal phosphine complexes, some of which are implicated in this work, followed by an analysis of the metal-phosphine bonding and the different factors contributing to its stability. In addition, the coordination chemistry of hybrid multidentate phosphine ligands is introduced because of the fact that the investigated *ortho*-substituted triarylphosphine ligands act this way. The final section describes a few applications of the metal phosphine complexes. It should be noted that all the phosphine ligands investigated in this work have already been prepared and characterised in the literature. However, all the related metal complexes prepared and characterised in this work are new.

Chapter Two highlights the coordination chemistry of the *para*-substituted triarylphosphine ligands: *tris*-(*para*-methoxyphenyl)phosphine $P(4\text{-}CH_3OC_6H_4)_3$ and *tris*-(*para*-hydroxyphenyl)phosphine $P(4\text{-}HOC_6H_4)_3$. A large amount of coordination chemistry has already been carried out on the methoxy-substituted ligand, however, this chapter describes the preparation of new complexes derived from both ligands and a comparison is made.

Chapter Three concentrates on the influence of the methoxy substituent on the coordination chemistry of these ligands: *tris*-(*ortho*-methoxyphenyl)phosphine $P(2\text{-}CH_3OC_6H_4)_3$ and *ortho*-methoxyphenyldiphenylphosphine $PPh_2(2\text{-}CH_3OC_6H_4)$. The electronic and steric effects of this substituent are discussed.

Chapter Four investigates the behaviour of the hybrid multidentate phosphine ligand: *tris*-(*ortho*-hydroxyphenyl)phosphine $P(2\text{-}HOC_6H_4)_3$. Metal chelates are prepared, whithin which the chelate effect is highlighted.

Chapter Five describes the coordination chemistry of the *ortho*-styrylphenyldiphenylphosphine $PPh_2(2\text{-}C_2H_3C_6H_4)$ which is a potential chelating agent. The metal chelates prepared are compared to those in the previous chapter.

Chapter Six describes the preparation of a set of low-valent late transition-metal triarylphosphine fluoride complexes, in which the influence of the phosphine substituents on the metal-fluoride bond is discussed. The metals incorporated therein are: platinum(II), osmium(II) and ruthenium(II).

Chapter Seven concerns the reactivity of metal fluoride complexes with the hybrid mutidentate phosphine ligands already described in Chapters Four and Five.

Finally, Chapter Eight delineates the experimental procedures followed throughout this work and the characterisation data for all the compounds prepared.

1.2 Preparation and Reactivity of Transition-Metal Phosphine Complexes:

Phosphine complexes can be simply prepared by mixing stoichiometric amounts of both the metal complex and the phosphine ligand (Scheme 1.1):

Scheme 1.1

$$[PtCl_2] + 2\,PPh_3 \longrightarrow [PtCl_2(PPh_3)_2]$$

An alternative route is by ligand displacement. The displacement can take place either simply in one step (Scheme 1.2a) or in several successive steps (Scheme 1.2b).

Scheme 1.2

a) $[PtCl_2(CH_3CN)_2] + 2\,PPh_3 \longrightarrow [PtCl_2(PPh_3)_2] + 2CH_3CN$

b) $[Cr(CO)_6] \xrightarrow[-CO]{+PPh_3} [Cr(CO)_5(PPh_3)] \xrightarrow[-CO]{+PPh_3} [Cr(CO)_4(PPh_3)_2]$ etc.

The organic substituents on the phosphorus atom play an important role in determining the strength of the phosphorus-metal bond. These substituents are capable of tuning the electronic and steric characteristics of the phosphine ligand thereby tuning the reactivity of the metal phosphine complex as a whole. For example, the six coordinate complex $[RuCl_2(PPh_3)_4]$, upon dissolution in dichloromethane, loses a PPh_3 group yielding a highly reactive 5-coordinate complex $[RuCl_2(PPh_3)_3]$. The dichloro-*tris*-(triphenylphosphine)ruthenium complex undergoes displacement reactions in which either the PPh_3 groups (Scheme 1.3a) or the chloride ligands are displaced (Scheme 1.3b).[7]

Scheme 1.3
PPh_3 (a) or chloride (b) ligand substitution reactions of $RuCl_2(PPh_3)_3$

a)

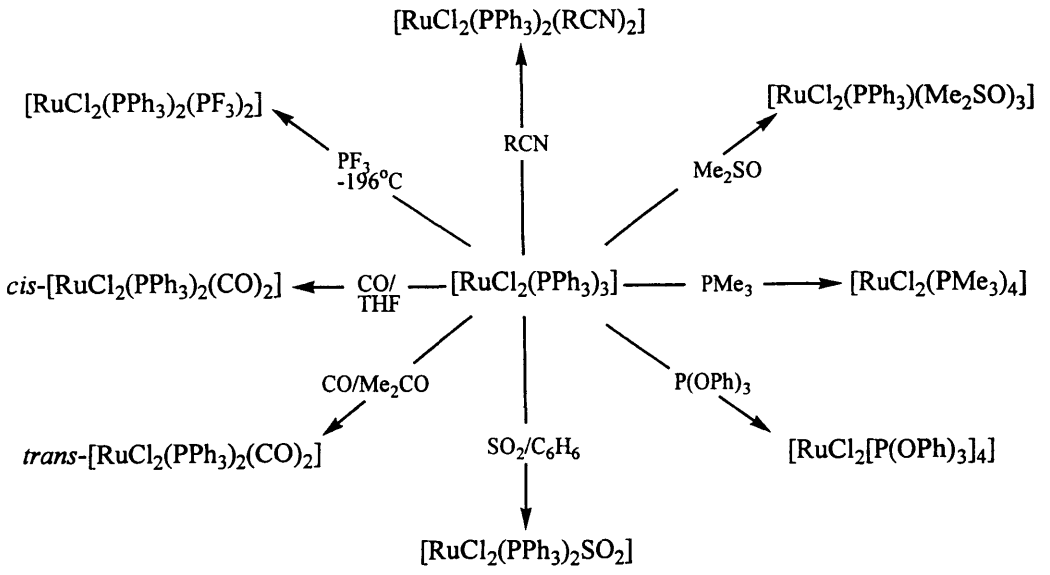

b)

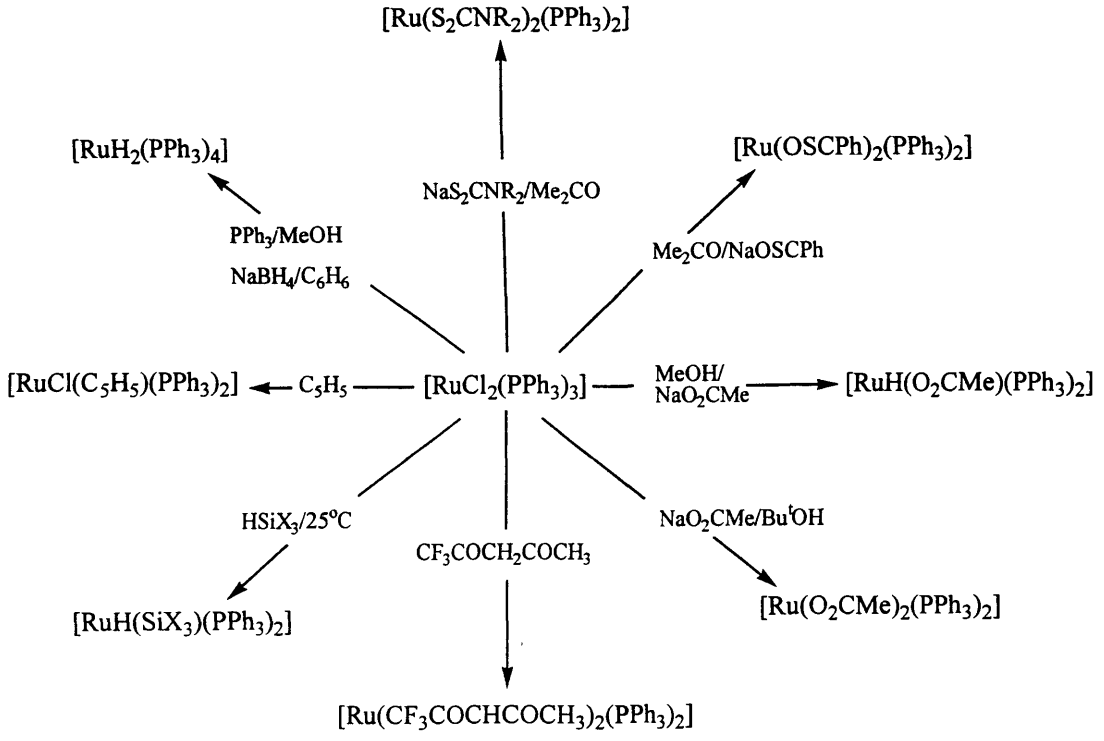

1.3 The Metal-Phosphine Bond:

The nature of metal-ligand interactions is a principal concern of coordination chemists. Three factors coexist in the metal-phosphine bonding interaction; σ-component, π-component and steric effect.

1.3.1 σ-Component:

The amount of σ-component in the metal-phosphine bond is influenced by the Lewis basicity of the phosphine ligand, which is measured by the pKa constant.[5] In the case of tertiary phosphine ligands, pKa = 7.85 - 2.67 $\sum\sigma^*$ where σ^* is called the *Taft Value* which is a measure of the inductive effect of substituents at phosphorus.[8,9]

Table 1.1 Basicities of Phosphines

	PH_3	$MePH_2$	Me_2PH	Me_3P	PPh_3	$P(2,4,6\text{-}(CH_3O)_3C_6H_2)_3$
pKa	-14.0	-3.2	3.9	8.6	2.7	11.2

The σ-interaction was thought to be the only type of bonding present in metal-phosphine ligand complexes and several authors[10-12] have used coupling constants from NMR spectroscopy to make a strong case for σ-only effects. Coupling constants obtained from ^{31}P NMR spectroscopy offer coordination chemists valuable hints into the nature and strength of bonding between phosphine ligands and the metal centre, and about any interactions with other ligating groups.[13,14] In many cases, phosphorus chemical shift and coupling constant data on their own have been used to establish the structures of many metal phosphine complexes. It has been shown that the coupling constant $^1J_{Pt\text{-}P}$ derives essentially from the *Fermi Contact Term* (Equation 1.1),[15,16]

Equation 1.1

$$^1J_{Pt\text{-}P} \propto k\,\alpha^2_{Pt}\,\alpha^2_{P}\,|\psi_{(6s)}(0)|^2\,|\psi_{(3s)}(0)|^2 \;..\;..$$

where "k" is constant for the set of examined compounds, the α^2_X-term represents the s-character of the donor orbital (when X = P) or of the acceptor orbital (when X = M) in the Pt-P bond, and the $|\psi_X(0)|^2$-term represents the electron density of the orbital indicated, evaluated at the nucleus of atom X.

The s-character of a bond formed by platinum(II) in a square planar complex is approximately 1/4 as the metal atom makes use of dsp^2-hybrids, whilst in the corresponding octahedral complex of platinum(IV), it is approximately 1/6 as the metal atom makes use of d^2sp^3-hybrids. Thus, the ratio between the s-character in Pt(II) complexes and the s-character in Pt(IV) complexes is expected to be approximately 0.67.

Table1.2
^{195}Pt-^{31}P Coupling Constants (in $CDCl_3$)/Hz

Complex	$^1J_{Pt\text{-}P}$
trans-$[PtCl_2(PBu_3)_2]$	2380 ± 4
cis-$[PtCl_2(PBu_3)_2]$	3508 ± 6
trans-$[PtCl_4(PBu_3)_2]$	1462 ± 4
cis-$[PtCl_4(PBu_3)_2]$	2070 ± 2

From the data in Table 1.2, the $J_{Pt(IV)}/J_{Pt(II)}$ ratio is approximately 0.60, supporting the concept of the *Fermi Contact Term,*[16] and confirming that changes in coupling constants reflect mainly changes in s-electron wave functions.

1.3.2 π-Component:

On comparing the promotional energies 3s→3d for phosphorus and nitrogen, it can be seen that the promotional energy in the phosphorus atom is relatively small allowing the possible participation of vacant d orbitals in bonding (Figure 1.1).

Figure 1.1
Promotional Energies 3s→3d for Phosphorus and Nitrogen

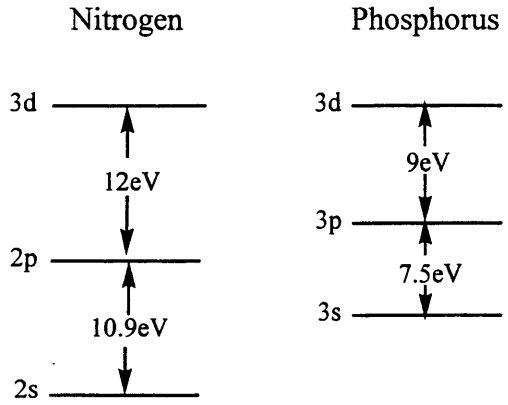

The greater contribution of the higher-energy d levels in the case of phosphorus compared to that of nitrogen leads to a larger atom, a reduced electronegativity and to a greater polarisability.

Early theories suggest that the σ-component and the π-component reinforce each other in the, so-called, "synergic effect".[17] To explain the particularly good bonding capabilities of PX_3 ligands, Chatt[18] proposed that the donor σ-component, which uses the lone pair of electrons on P(III) and a suitable vacant orbital on the metal, is reinforced by donor M→P synergic π back-bonding from the metal to phosphorus.[19] Accordingly, phosphorus (III) ligands are seen as members of a group of ligands, collectively called π-acceptor ligands, which includes carbonyl, nitrosyl and isocyanide, etc. A representation of the synergic effect is shown in Figure 1.2 for the M-CO bond.[20]

Figure 1.2

a) represents the formation of the metal ← carbon σ-bond using an unshared pair of electrons on the carbon atom.

b) represents the formation of the metal → carbon π-bond using the nd metal electrons.

a)

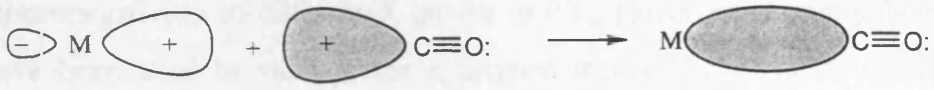

b)

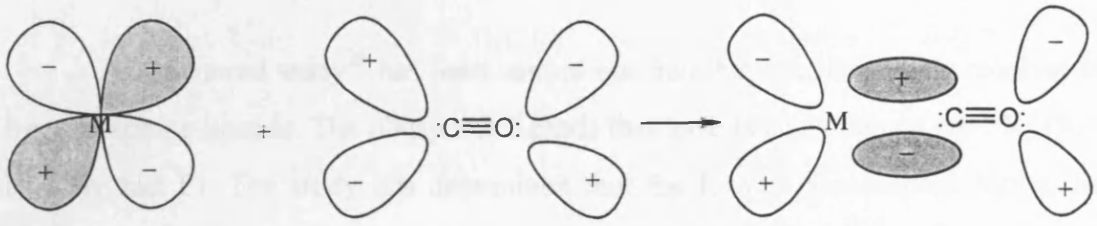

The amount of back donation from the filled metal d orbital depends on the identity of the metal, on the electronegativity of the ligands, other than the phosphine, coordinated to it, and on the electronegativity of the substituents attached to phosphorus.[9] The influence of the electronegativity of these substituents can be illustrated using the ν_{CO} data in Table 1.3.[21]

Table 1.3
The Variation of CO Frequency in $[Mo(CO)_3L_3]$

L	ν_{CO} cm^{-1}	
$(C_2H_5)_3P$	1937	1841
$(C_6H_5O)_3P$	1994	1922
$Cl_2(C_2H_5O)P$	2027	1969
Cl_3P	2040	1991
F_3P	2090	2055

Increasing the electronegativity of the substituents on the phosphorus atom strengthens the π-bonding between the metal and the phosphine, which leads to a reduction in the electron density at the metal centre as detected by an increase in the frequency value of the CO stretching. There have been several attempts [8,22-25] to attribute the variation in the CO stretching frequencies solely to the variation in the σ-bond between the metal and the phosphorus, caused by variations in the electronegativites of different X groups in PX_3. However, several publications[23,26,27] have been used to validate the synergism theory and to study qualitatively and quantitatively the π-component in the metal phosphine bond.

An advanced study[28] has been carried out into the π-back bonding receiver in free phosphine ligands. The phosphine ligands that have been examined are PX_3 (X = H, CH_3 and F). The study has determined that the Lowest Unoccupied Molecular Orbital of PX_3 is the orbital 3e, which is a hybrid orbital and mostly composed of 3p character from the phosphorus (Table 1.4).

Table 1.4
The 3e hybrid composition in the corresponding phosphine ligands.

Phosphine ligand	%3p character on phosphorus	%3d character on phosphorus
PH_3	36	23
$P(CH_3)_3$	14	10
PF_3	44	23

The ligand with the highest 3p character of those in Table 1.4 is PF_3. This observation could be used to account for the greater stability of some metal-PF_3 complexes as compared to similar metal-PX_3 complexes. More recently, "Potential Retention of Diatomic Differential Overlap" (PRDDO) calculations have been employed in order to investigate further the type of π-back bonding, M→P, in complexes containing phosphine ligands.[29] The examination was focused on the d^{10} complex

$[Ni(NH_3)_3(PH_3)]$. The calculations were executed with a double basis set, with and without including the phosphorus d orbitals. If the phosphine ligand position is considered on the z-axis, the inclusion of the phosphorus d-orbitals in the calculations should lead to a result where the d_{xz} and d_{yz} Ni orbitals appear depopulated as compared to d_{xy} and d_{x2-y2} orbitals (Table 1.5).

Table 1.5
Ni d Orbital Populations with and without Inclusion of the Phosphorus d Orbitals in the Basis Set.

Ni d orbitals	Including P_d (e)	Without including P_d (e)
d_{xz}, d_{yz}	1.60	1.57
d_{xy}, d_{x2-y2}	1.74	1.76

This suggests that including phosphorus d orbitals has very little effect. However, additional calculations[29a] appear to substantiate the conclusion that the π-accepting orbital of the phosphine has σ^*-symmetry;[29b,c] the P-H overlap populations of the free and complexed phosphine ligand in $[Cr(NH_3)_5(PH_3)]$ are 0.61 and 0.51 respectively, which indicates the considerable population of the P-H σ^* orbital in the complex. Moreover, endorsing the fact that PF_3 complexes are more stable than those of PH_3,[29a] the high polar P-F bond is characterised by a low-lying σ^* orbital and thus is a better π-acceptor. In addition, it is well known that the σ P-F bond is highly polar towards F, which means that the σ^* P-F bond is highly polar towards P, which increases the σ^*-metal d_π overlap.

Fig 1.2
The π-bonding Formed by Overlap of d-σ* Hybrid Orbitals on PX_3 Ligands with d Orbitals on the Metal[30]

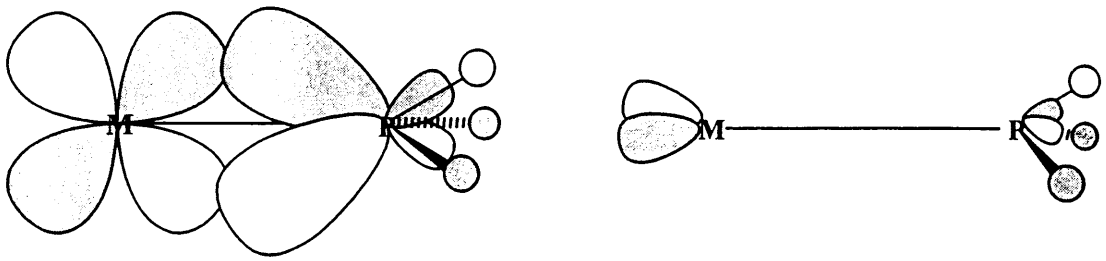

1.3.3. Steric Effect:

The steric effect is defined as "changes in molecular properties as a result of forces (usually nonbonding) between parts of a molecule", for example changing from $P(4\text{-}CH_3C_6H_4)_3$ to $P(2\text{-}CH_3C_6H_4)_3$. Special cases involve bonding between parts of a molecule, as in going from $P(OEt)_3$ to $P(OCH_2)_3CMe$ or on changing "n" in a chelate complex $[M\{Ph_2P(CH_2)_nPPh_2\}]$.[31]

After realising that competition between different phosphine ligands for coordination positions at the metal centre could not be explained solely by the electronic effect,[32] Tolman measured the "size" of a ligand using a steric parameter, which is now known as the Tolman's cone angle.[33] It is defined as "the angle at the metal atom of the cone swept out by the van der Waals radii of the groups attached to the phosphorus atom". This is illustrated in Figure 1.3.

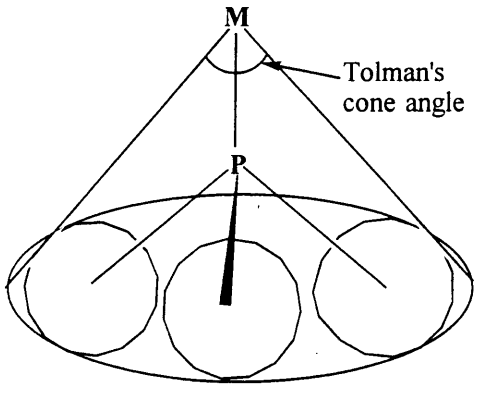

Figure 1.3

The coordination of the phosphine ligand to the metal centre is associated with a variation in the C-P-C angle on the phosphorus atom. Upon coordination, an increase in the C-P-C angle takes place. This increase is less pronounced for bulkier ligands,[31] which explains the reason why smaller coordination chemical shifts $\Delta^{31}P$ are associated with bulkier ligands. It is worth mentioning that an increase in the C-P-C angle is related to an increase in the s-character in the phosphorus-carbon bond. Indeed, this variation affects the bonding between the phosphorus and the metal.

The significant influence of the steric effect on the metal-phosphine ligand bond, particularly with bulky ligands, may affect the course of many reactions involving coordination complexes. The strain caused by this effect will tend to lengthen the metal-phosphorus bond which, in turn, will have a disproportionately large effect on any π-supplement to the bonding.[34] It is noteworthy that the steric bulk of triphenylphosphine and other aromatic phosphines classifies them as weakly bound ligands when attached to metal centres. This is highly ideal and relevant to catalysis.[7] Similar complexes are usually highly dissociable in organic solvents, inducing free sites on the metal centre susceptible to activate reactant molecules.

1.4 Coordination Chemistry of Hybrid Multidentate Phosphine Ligands:

A considerable part of this work concerns the synthesis and coordination chemistry of hybrid multidentate phosphine ligands. The ligands highlighted are the *tris*-(*ortho*-hydroxyphenyl)phosphine and the *ortho*-styryldiphenylphosphine which can chelate to metal centres.

In general, chelation forms a distinct topic area in chemistry. It spans inorganic, organic, and physical chemistry and is of great significance in analytical chemistry. It contributes largely to biological processes and has many applications in the field of medicine. The word *chelation* describes the process of ring formation as a result of the coordination of a multidentate ligand to a metal. It was the caliperlike

mode of attachment of the molecules to the metal atom that led Morgan and Drew (1920) to suggest the name *chelate*. The word *chelate* is derived from the Greek word "chele" meaning a lobster's claw. Ligands like *o*-hydroxyphenyl*bis*-(phenyl)phosphine, which act in this way, are referred to as *chelating agents*, and the complexes they form as *metal chelates*.

In general, metal complexes containing bidentate ligands are easier to prepare and more difficult to decompose than those containing comparable unidentate ligands. For a chelating ligand that contains z donor atoms, all capable of coordination to a metal ion, (z-1) chelate rings will be formed. The larger the value of z, the greater the stability of the resulting complex. The enhanced entropic stability associated with chelation is called the *chelate effect* and will be discussed in Chapter Four.

In 1893, Werner discovered the chelate behaviour of ethylenediamine in the complex bis-(ethylenediamine)platinum(II) chloride, $[Pt(en)_2]Cl_2$ (Figure 1.4). Werner's insight into the formation of this complex led him unerringly to the concept of ring formation. The nitrogen atoms of each ethylenediamine molecule occupy two coordination sites in the coordination shell of the platinum atom. The environment of the platinum atom is exactly the same as that in the tetrammine analogue, $[Pt(NH_3)_4]Cl_2$ (Figure 1.4).

Figure 1.4

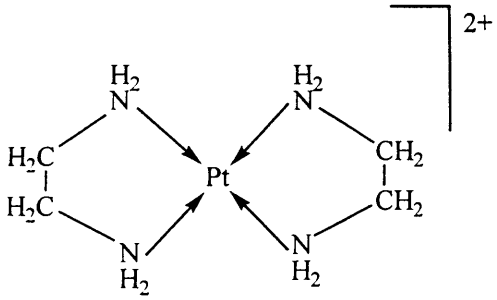

bis-(ethylenediamine)platinum(II)

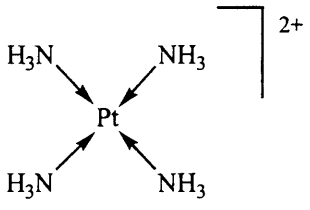

tetrammineplatinum(II)

1.5 Applications of Metal Phosphine Complexes:

Metal-phosphine complexes have significant applications in catalysis reactions. They catalyse carbonylations, hydrogenations, hydration reactions, in addition to other reactions.[35] Below, examples of catalytic reactions are outlined.

1.5.1 Carbonylation Reactions:

Group (VIII) metal complexes catalyse carboalkoxylation, carboxylation, and carboamidation of olefins and alkyl halides to generate organic esters, acids, amides and are well-known reactions.[36] For example, $[PdCl_2(PPh_3)_2]$ has been receiving increasing attention in the carboxylation of olefins due to its effectiveness at lower pressures and temperatures.[37,38]

Scheme 1.4

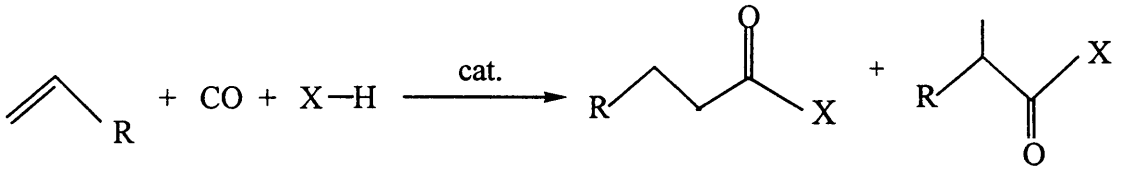

Where X = OR, NR'$_2$; R = H, alkyl, aryl, alkenyl.

1.5.2 Hydrogenation Reactions:

Metal-phosphine complexes follow a homogeneous catalysation in the hydrogenation of carbon monoxide, ketones, aldehydes, and olefins. [39-41] One of the best studied soluble catalysts for olefin hydrogenation is Wilkinson's catalyst, $[RhCl(PPh_3)_3]$ (Scheme 1.5). [41]

Scheme 1.5
A Major Mechanistic Pathway for Olefin Hydrogenation by Wilkinson's Catalyst. (S = Solvent or possibly loosely bonded tertiary phosphine)

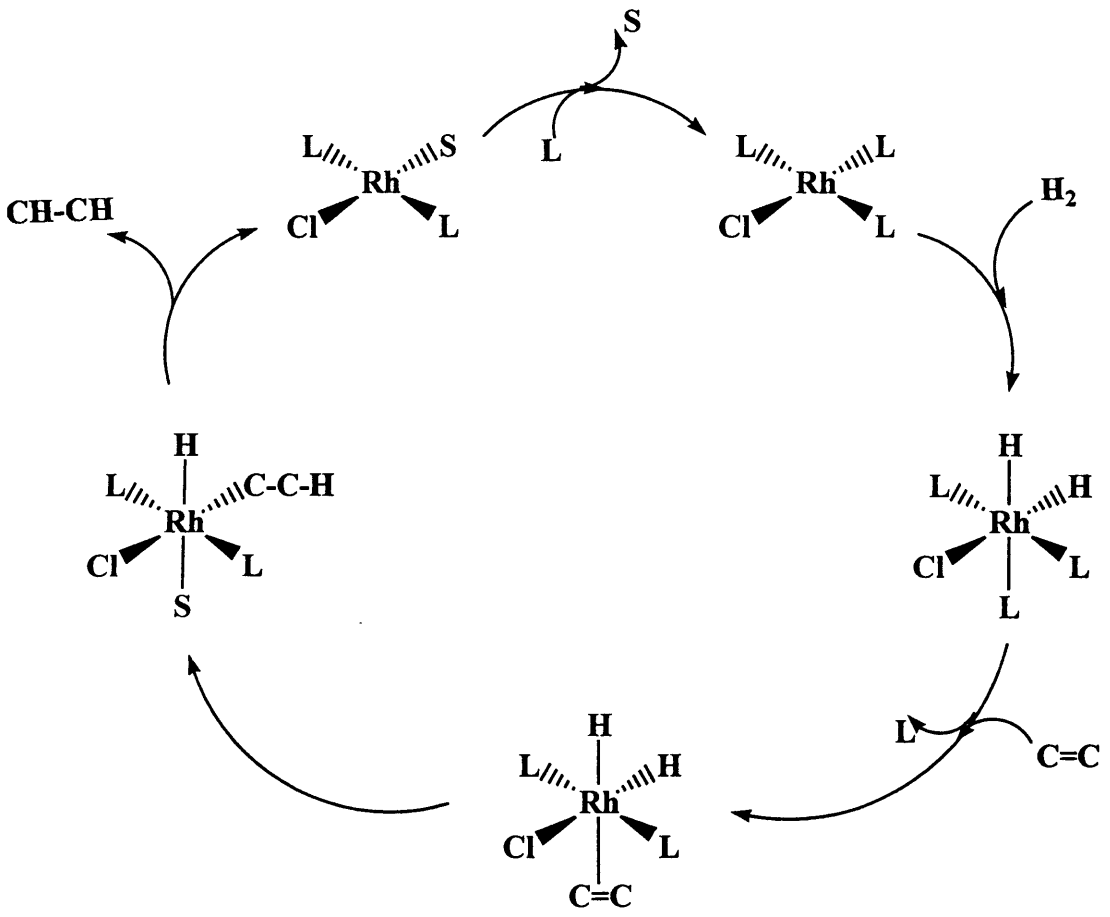

1.5.3 Hydration Reactions:

The platinum catalyst in Scheme 1.6 is called Trogler's catalyst: $[PtH(OH)(PMe_3)_2]$.[42] It hydrates simple unhindered linear olefins.[43]

Scheme 1.6

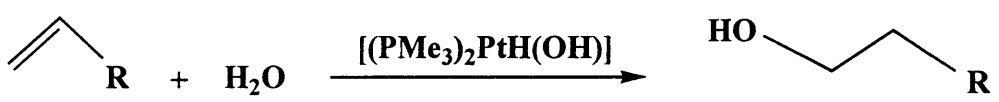

1.6 Summary:

The present study throws light on the coordination chemistry of substituted triarylphosphine ligands to late transition-metals. The bonding between the metal and the phosphine ligand is a synergic one, highly affected by the nature of the substituents at the phosphorus from electronic and steric approaches. This bonding is further stabilised by the *chelate effect* in the case of phosphine ligands acting as chelating agents.

Chapter One References

[1] G. Booth, *Complexes of the Transition Metals With Phosphines, Arsines and Stibines,* in *Advanced inorganic chemistry and radiochemistry*, volume 6, H. J. Emeleus and A. G. Sharpe (eds), New York: Academic Press, 1964.

[2] J. E. Brady, *General chemistry, Principles & stucture*, John Wiley & sons, Inc, 1990, 320.

[3] R. G. Pearson, *J. Am. Chem. Soc.*, 1963, **85**, 3533.

[4] R. G. Pearson, *Chem. Brit.*, 1967, **3**, 103.

[5] H. Goldwhite, *Introduction to Phosphorus Chemistry*, Cambridge texts in chemistry and biochemistry, 1981.

[6] C. Masters, *Homogeneous Transition-metal Catalysis - a gentle art*, 1981, Chapman and Hall.

[7] F. H. Jardine, *Prog. Inorg. Chem.*, 1984, **31**, 265.

[8] M. Bigorgne, *J. Inorg. Nucl. Chem.*, 1964, **26,** 107.

[9] C. A. Tolman, *J. Am. Chem. Soc.*, 1970, **92,** 2953.

[10] A. Pidcock, R. T. Richards, L. M. Venanzi, *J. Chem. Soc. (A)*, 1966, 1707.

[11] F. H. Allen and A. Pidcock, *J. Chem. Soc. (A)*, 1968, 2700.

[12] L. M. Venanzi, *Chem. Brit.*, 1968, 162.

[13] a) B. Jacobson, *Ph.D. Thesis*, Sussex, Brighton, U.K., 1977.
b) P. B. Hitchcock, B. Jacobson and A. Pidcock, *J. Chem. Soc., Dalton Trans.*, 1977, 2038.

[14] a) E. Shustorovich, *J. Am. Chem. Soc.*, 1979, **101**, 792.
b) E. Shustorovich, *Inorg. Chem.*, 1979, **18**, 1039.

[15] a) A. D. Pidcock, *Ph.L. Thesis*, Oxford, 1963.
b) G. W. Schneider and A. D. Buchingham, *Discuss. Faraday Soc.*, 1962, **34**, 147.

[16] J. A. Pople and D. P. Santry, *Mol. Phys.*, 1964, **8**, 1.

[17] R. W. Taft and J. W. Rakshys, *J. Am. Chem. Soc.*, 1965, **87,** 4387, and references cited therein.

[18] a) J. Chatt, *Nature* (London), 1950, **165,** 637.
b) A. A. Williams, *J. Chem. Soc.*, 1951, 3061.

[19] A. J. Carty, N. J. Taylor, A. W. Coleman and M. F. Lappert, *J. Chem. Soc., Chem. Commun.*, 1979, 639.

[20] F. A. Cotton and G. Wilkinson, *Advanced Inorganic Chemistry*, John Wiley & Sons, Inc., New York, N.Y., 1972, section 22.2.

[21] F. A. Cotton and G. Wilkinson, *Advanced Inorganic Chemistry*, John Wiley & Sons, Inc., New York, N.Y., 1972, section 22.13.

[22] R. J. Angelici and M. D. Malone, *Inorg. Chem.*, 1967, **6**, 1731.

[23] L. M. Venanzi, *Chem. Brit.*, 1968, **4**, 162.

[24] R. J. P. Williams, *Chem. Brit.*, 1968, **4**, 277.

[25] S. O. Grim and D. A. Wheatland, *Inorg. Chem.*, 1969, **8**, 1716.

[26] H. J. Plastas, J. M. Stewart and S. O. Grim, *J. Am. Chem. Soc.*, 1969, **91**, 4326.

[27] M. G. Hogben, R. S. Gay and W. A. G. Graham, *J. Am. Chem. Soc.*, 1966, **88**, 3457.

[28] S.-X. Xiao, W. C. Trogler, D. E. Ellis and Z. Berkovitch-Yellin, *J. Am. Chem. Soc.*, 1983, **105**, 7033.

[29] a) D. S. Marynick, *J. Am. Chem. Soc.*, 1984, **106**, 4064.

b) A. Crispini, K. N. Harrison, A. G. Orpen, P. G. Pringle and J. R. Wheatcroft, *J. Chem. Soc., Dalton Trans.*, 1996, 1069, and references cited therein.

c) B. J. Dunne, R. B. Morris and A. G. Orpen, *J. Chem. Soc., Dalton Trans.*, 1991, 653.

[30] C. J. Cobley and P. G. Pringle, *Inorg. Chim. Acta.*, 1997, **265**, 107.

[31] C. A. Tolman, *Chem. Rev.*, 1977, **77**, 313.

[32] C. A. Tolman, *J. Am. Chem. Soc.*, 1970, **92**, 2956.

[33] N. N. Greenwood and A. Earnshaw, *Chemistry of the Elements*, Preganon Press, Oxford, 1984.

[34] J. Emsley and D. Hall, *The Chemistry of Phosphorus*, Harpen & Row Ltd., 1976.

[35] R. J. P Corriu, C. Hoarau, A. Mehdi and C. Reyé, J. Chem. Soc., *Chem. Commun.*, 2000, 71.

[36] a) S. B. Ferguson and H. Alper, *J. Mol. Catal.*, 1986, **34**, 381.

b) H. Alper and D. Leonard, *J. Chem. Soc., Chem. Commun.*, 1985, 511.

[37] K. Bittler, N. Von Kutepow, D. Neubauer and H. Reis, *Angew. Chem. Int. Ed.*, 1968, **7**, 329.

[38] D. M. Fenton, *J. Org. Chem.*, 1973, **38**, 3192.

[39] M. Graziani, M. Lenarda, R. Ros and U. Belluco, *Coord. Chem. Rev.*, 1975, **16**, 35.

[40] H. Alper, F. Urso, D. J. H. Smith, *J. Am. Chem. Soc.*, 1983, **105**, 6737.

[41] J. A. Osborn, F. H. Jardine, J. F. Young and G. Wilkinson, *J. Chem. Soc.*, 1966, **A**, 1711.

[42] C. M. Jensen and W. C. Trogler, *J. Am. Chem. Soc.*, 1986, **108**, 723.

[43] C. M. Jensen and W. C. Trogler, *Science (Washington, D.C.)*, 1986, **233**, 1069.

CHAPTER TWO

COORDINATION CHEMISTRY OF SOME PARA-SUBSTITUTED ARYL PHOSPHINE LIGANDS

CHAPTER TWO

COORDINATION CHEMISTRY OF SOME *PARA*-SUBSTITUTED ARYL PHOSPHINE LIGANDS

2.1 Introduction:

This chapter covers the synthesis and characterisation of two *para*-substituted aryl phosphine ligands and the products from reactions of these ligands with some platinum group metal starting materials. The ligands are *tris*-(*para*-methoxyphenyl)phosphine, $P(4\text{-}CH_3OC_6H_4)_3$, and *tris*-(*para*-hydroxyphenyl)phosphine, $P(4\text{-}HOC_6H_4)_3$. These have been allowed to react with platinum(II), palladium(II), rhodium(I) and rhodium(III) complexes.

The coordination chemistry of the *tris*-(*para*-methoxyphenyl)phosphine ligand is well established in the literature, in contrast to that of the *tris*-(*para*-hydroxyphenyl)phosphine ligand. The methoxy group contribution to the coordination of the former phosphine ligand to late transition metal complexes, such as rhodium(I) carbonyl complexes[1] and platinum(II) chloride complexes,[2-5] has been already investigated. Despite the large distance between the *para*-substituents and the metal centres in these complexes, the coordination chemistry at the metal is largely dependent on the electronic character of these substituents.[4] The methoxy groups on the *para*-positions of the aryl rings induce an increase in the Lewis basicity of the phosphine ligand when comparing the *tris*-(*para*-methoxyphenyl)phosphine ligand to the triphenyl phosphine ligand. This is revealed when examining the Pt-Cl vibrational frequencies and Pt-P coupling constants in the platinum(II) phosphine chloride complexes and carbonyl stretching frequencies in rhodium(I) phosphine carbonyl complexes.

In addition to the preparation and characterisation of new late transition-metal phosphine complexes incorporating $P(4\text{-}CH_3OC_6H_4)_3$ and $P(4\text{-}HOC_6H_4)_3$ ligands, the

present chapter compares these two phosphine ligands in terms of substituent influence on the coordination chemistry taking place at the metal centres. This is highlighted by comparing relevant characterisation data. This comparison is extended to already known *para*-substituted triarylphosphine ligands.

2.2 Synthesis and Characterisation of $P(4\text{-}CH_3OC_6H_4)_3$ (3) and $P(4\text{-}HOC_6H_4)_3$ (5):

The phosphine ligands have been previously described and have been prepared here according to a slightly modified literature route.[6]

A convenient laboratory method for preparing tertiary aryl phosphines is by the reaction of a phosphorus halide with a suitable Grignard reagent. In this case, the Grignard reagent is the *para*-methoxyphenylmagnesiumbromide (**2**). This is formed from the reaction of 4-bromoanisole with an excess of magnesium turnings in THF (Scheme 2.1).

Scheme 2.1

(**1**) (**2**)

Treatment of the Grignard reagent, *in situ,* with trichlorophosphine gives the *tris*-(*p*-methoxyphenyl)phosphine (**3**) (Scheme 2.2):

Scheme 2.2

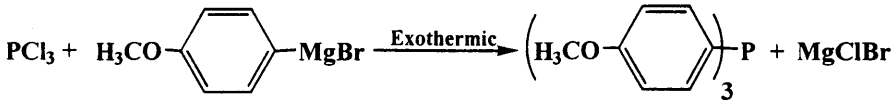

(**2**) (**3**)

Any excess of the Grignard reagent is destroyed by reaction with an aqueous solution of ammonium chloride (Scheme 2.3).

Scheme 2.3

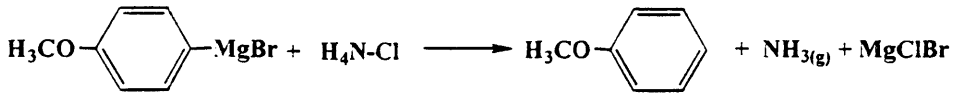

(2) **Anisole**

The phosphine ligand (**3**) is a white air-stable powder which has been characterised by ^{1}H and $^{31}P\{^{1}H\}$ NMR spectroscopies, mass spectrometry and elemental analysis (see Chapter Eight). Recrystallisation from methanol at high temperature affords clear translucent crystals suitable for X-ray structural analysis (Figure 2.1). The single crystal structure for this compound has been reported previously,[7] and the data from the two analyses are essentially identical. Of note is the geometry around the phosphorus atom which is approximatly pyramidal, the average angle C-P-C of 101.29° is close to that of the triphenylphosphine (102.99°)[8] and the aryl rings are arranged in a staggered configuration and perpendicular to the base of the phosphorus pyramid.

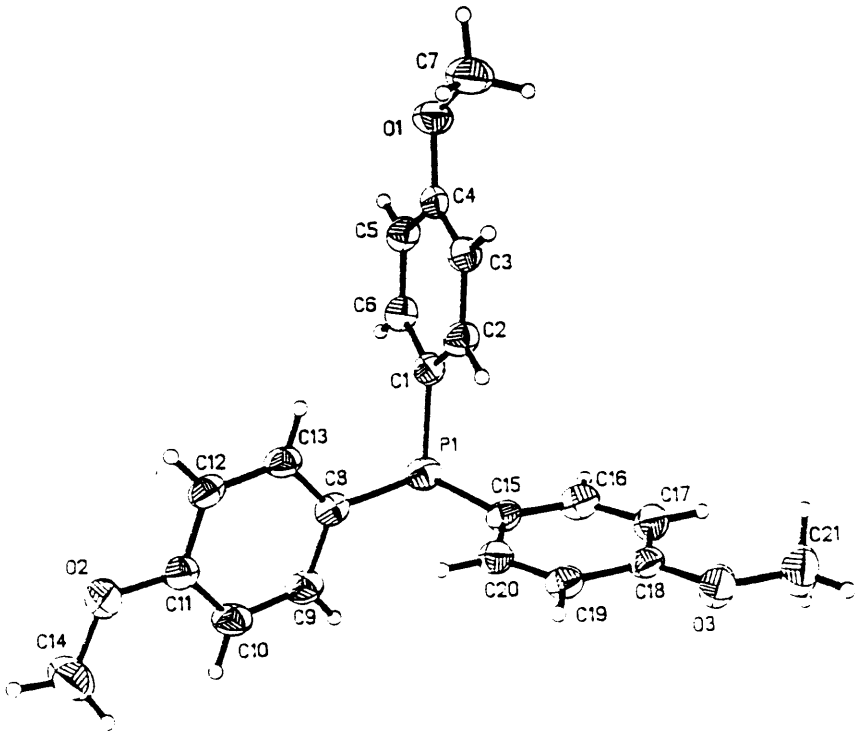

Figure 2.1:
Crystal Structure of
$P(4\text{-}CH_3OC_6H_4)_3$ (3)

The next step is demethylation using hydrobromic acid (Scheme 2.4).

Scheme 2.4

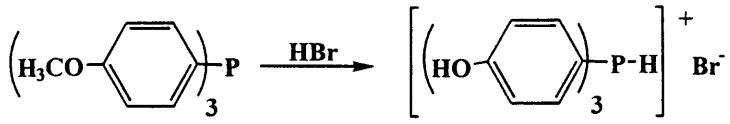

(3) **(4)**

The dissolution of the *tris*-(*p*-hydroxyphenyl)phosphinehydrobromide salt (**4**) in an aqueous solution of sodium hydroxide generates the second free phosphine ligand (**5**) which precipitates out of the solution after addition of acetic acid according to Scheme 2.5. The *tris*-(*p*-hydroxyphenyl)phosphine ligand (**5**) has been characterised by ^{1}H, $^{31}P\{^{1}H\}$ and $^{13}C\{^{1}H\}$ NMR spectroscopies and mass spectrometry (see experimental chapter).

Scheme 2.5

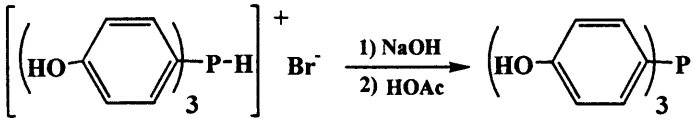

(4) **(5)**

In order to establish the Lewis basicity of ligands (**3**) and (**5**), which will affect their ability to coordinate to metal centres, their ^{31}P NMR chemical shifts may be compared with those of related triarylphosphine ligands (Table 2.1).[9-11]

Table 2.1
^{31}P Chemical Shifts of
Triarylphosphines P(4-RC_6H_4)$_3$

[a] Ref. (10). Recorded in $CDCl_3$. [b] This work. Recorded in $CDCl_3$. [c] This work. Recorded in d^6 acetone. [d] Ref. (12). Recorded in $CDCl_3$.

R	$\delta(^{31}P)$ /ppm
NMe_2	-10.2[a]
OMe	-9.9[b]
OH	-9.8[c]
CH_3	-6.8[d]
H	-4.7[a]
F	-8.4[a]
Cl	-7.8[a]

According to Table 2.1, $\delta(^{31}P)$ shifts to lower frequency when the R groups in the *para*-position to phosphorus on the aryl rings are replaced with more electron-donating groups. The opposite trend is observed for electron-withdrawing groups. From this observation, a polarisation pattern is proposed in Figure 2.2 to help understand the different mechanisms and effects taking place in related *para*-aryl substituted phosphine ligands.

Figure 2.2
Polarisation Pattern of Ar-P-Z

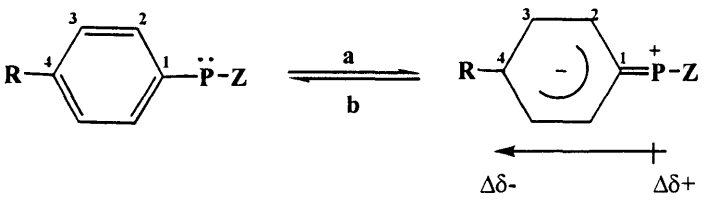

The a:b ratio in the polarisation pattern (Figure 2.2) depends on the nature of the group R. An electron-withdrawing group R causes a partial positive charge on C4 (in the *para*-position to phosphorus) which induces an electron-delocalisation from the

lone pair on phosphorus toward this carbon atom. Such a delocalisation should increase the P-C1 electron overlap population. Indeed, $|^1J_{P\text{-}C1}|$ increases proportionally to the electron-withdrawing affinity on the *para*-position (Table 2.2).[10]

Table 2.2
$|^1J_{P\text{-}C1}|$ in $P(Ar)_3$ Ligands with Different *para*-Substituents.

Substituent	$\|^1J_{P\text{-}C1}\|$ /Hz
NMe_2	4.4
OMe	5.6
OH	8.4
Me	10.3
H	10.8
F	10.9
Cl	12.1

According to the pattern in Figure 2.2, for systems of the type RC_6H_4PZ, if the lone pair of electrons at the phosphorus is free, better electron-withdrawing groups R will induce an increase in $|^1J_{P\text{-}C1}|$. The opposite trend is observed for electron-donating groups R. In contrast, if the lone pair of electrons at the phosphorus is engaged in bonding, better electron-donating groups R will induce an increase in $|^1J_{P\text{-}C1}|$. The opposite trend is observed for electron-withdrawing groups R. The NMR chemical shifts of the aryl carbon atoms and that of the phosphorus atom depend on both resonance and inductive effects. It should be noted that the ^{13}C NMR data for C1 reveal that the resonance effect is 4-5 times more important than the inductive one (it is only 0.45 to 2.3 times more important in the case of the other aryl carbon atoms).

To conclude, the substituent on the aryl ring attached to phosphorus has a significant influence on the basicity of phosphine ligand. According to the data in

Table 2.1, the methoxy and hydroxy groups on the *para*-positions on the aryl rings of the triarylphosphine ligands are good electron-donor groups. This is due to the appearance of the corresponding ^{31}P signals at lower frequencies when compared to related phosphine ligands. However, according to the data included in Table 2.2, the relatively low $|^{1}J_{P\text{-}Cl}|$ value related to the methoxy-substituted ligand is a clear hint of the electron-donating property of the methoxy group. The relatively high $|^{1}J_{P\text{-}Cl}|$ value related to the hydroxy-substituted ligand suggests a certain phenomenon impeding the electron-donating property of the hydroxy group.

2.3 Synthesis and Characterisation of Platinum(II) Derivatives:

A set of platinum(II) complexes have been prepared incorporating both of the *para*-substituted aryl phosphine ligands, $P(4\text{-}CH_3OC_6H_4)_3$ (**3**) and $P(4\text{-}HOC_6H_4)_3$ (**5**). The complexes are of the type $[PtX_2L_2]$ where X = Cl, Me and L = (**3**) or (**5**) and $[PtClL_3]^+Cl^-$ where L = (**3**) or (**5**) and $[PtCl_2(PEt_3)\{P(4\text{-}CH_3OC_6H_4)_3\}]$. Common features of complexes of these types are the square planar geometry around the platinum(II) centre, which uses dsp^2-hybrids, and the different possible arrangements of the ligands around the metal resulting in different isomers, *cis*- or *trans*-isomers or a mixture of both. It is relatively straightforward to assign the phosphorus signals in ^{31}P NMR experiments to a particular isomer from the coupling between the phosphorus and platinum nuclei. Thus, the ^{31}P NMR signal of a phosphorus atom bound to a platinum atom is expected to be flanked by what are called "satellites" defining a doublet.

2.3.1 Synthesis and Characterisation of Platinum(II) Complexes incorporating $P(4\text{-}HOC_6H_4)_3$:

When *cis*-$[PtCl_2(CH_3CN)_2]$ is treated with two equivalents of the phosphine ligand (**5**) in acetone, a mixture of three square planar[13] complexes *cis*-[*tris*-(*p*-hydroxyphenyl)phosphine]dichloroplatinum(II) (**6**), *trans*-[*tris*-(*p*-hydroxyphenyl)-phosphine]dichloroplatinum(II) (**7**), and *tris*-[*tris*-(*p*-hydroxyphenyl)phosphine]-chloroplatinum(II) chloride (**8**) results (Scheme 2.6).

Scheme 2.6

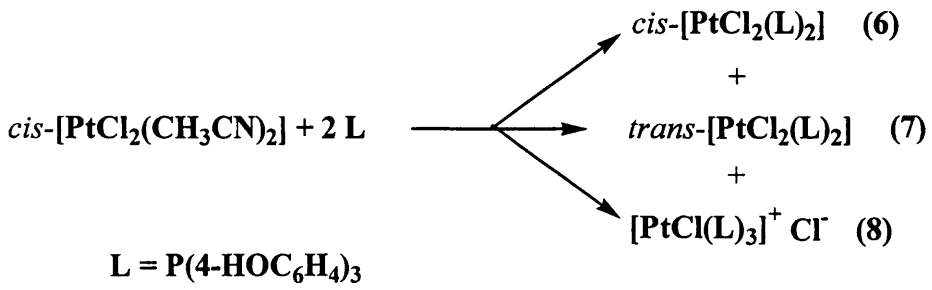

The three products have been separated by fractional recrystallisation as indicated by the $^{31}P\{^{1}H\}$ NMR spectra in Figures 2.3, 2.4 and 2.5. (**6**), (**7**) and (**8**) and have been characterised by ^{1}H NMR, $^{31}P\{^{1}H\}$ NMR spectroscopies, mass spectrometry, IR spectroscopy and elemental analysis. In addition, single crystals have been isolated for the *cis*-isomer (**6**) by slow evaporation from the solvent acetone, and for the *trans*-isomer by slow precipitation from acetone:hexane. Stirring a mixture of (**6**) and (**7**) in acetone at room temperature favours the *trans*→*cis* conversion. Adding an excess of the phosphine ligand to the mixture of isomers favours the formation of solely the *tris*-phosphine platinum(II) cationic complex (**8**).

Figure 2.3
$^{31}P\{^{1}H\}$ NMR Spectrum of *cis*-[*tris*-(*p*-hydroxyphenyl)phosphine]dichloroplatinum(II) (6)

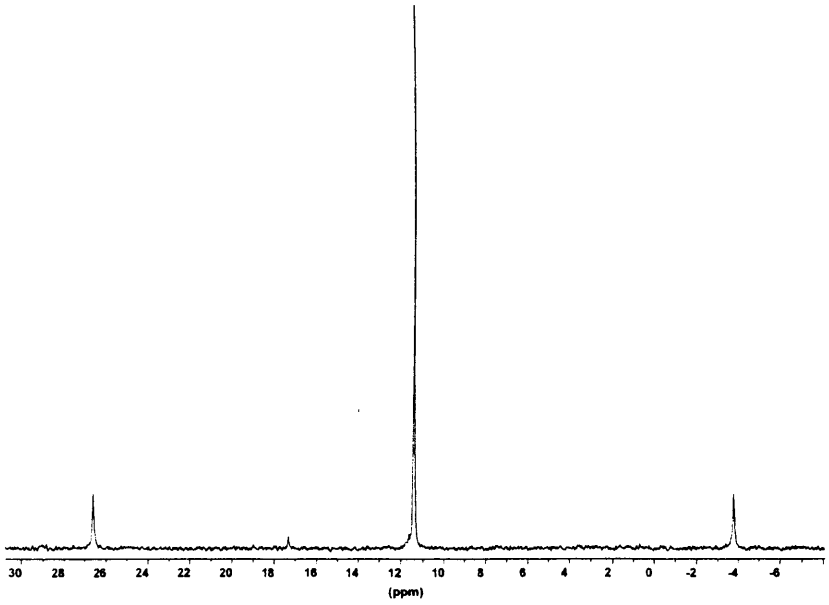

Figure 2.4
$^{31}P\{^{1}H\}$ NMR Spectrum of *trans*-[*tris*-(*p*-hydroxyphenyl)phosphine]dichloroplatinum(II) (7)

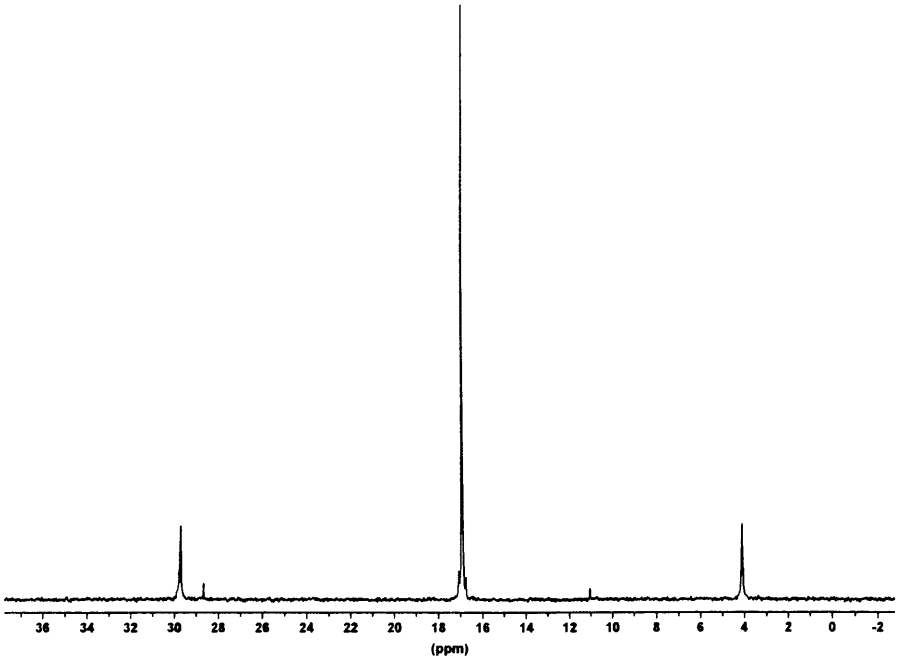

Figure 2.5
$^{31}P\{^{1}H\}$ NMR Spectrum of *tris*-[*tris*-(*p*-hydroxyphenyl)phosphine]chloroplatinum(II) chloride (8) (The arrow points out the impurity).

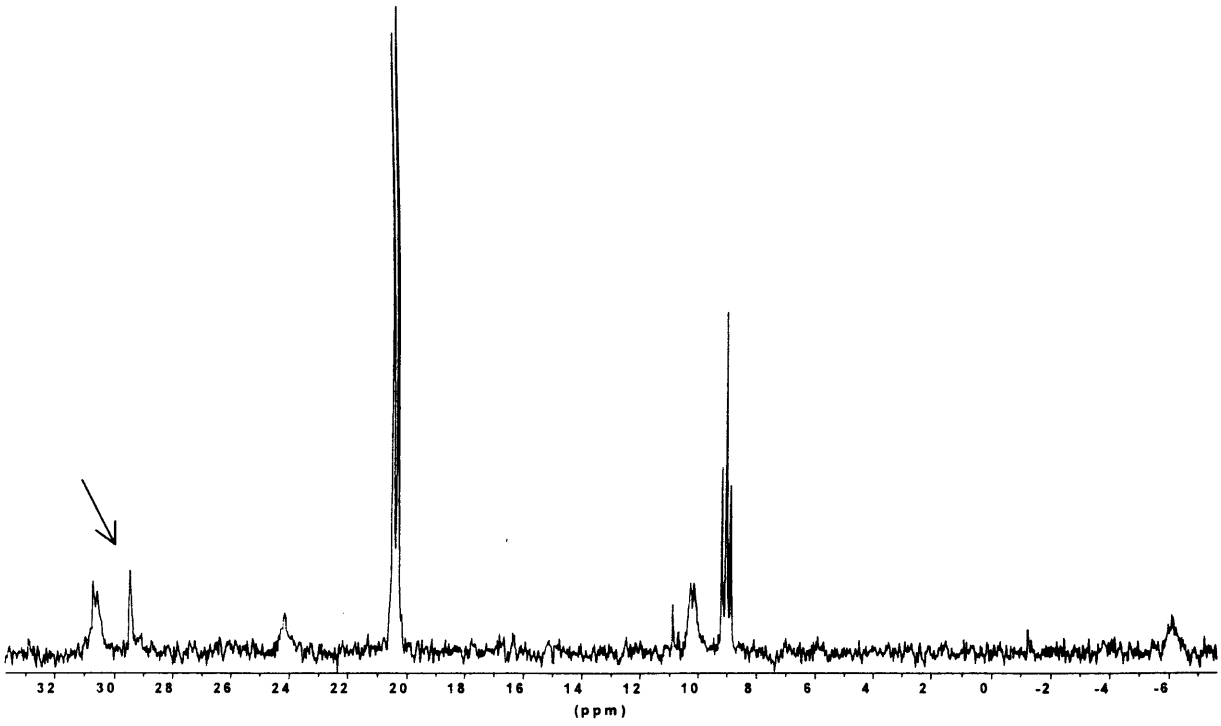

Characterisation of *cis*-[$PtCl_2\{P(4\text{-}HOC_6H_4)_3\}_2$] (6):

The ^{31}P NMR data of various *cis*-[$PtCl_2(L)_2$] complexes are compared in Table 2.3 as a function of the aryl substituent in the *para*-position to phosphorus. It can be seen that there is no significant variation in the phosphorus coordination chemical shift (Δ) when changing the nature of the substituent.

Table 2.3
^{31}P-{^1H} NMR Data for Complexes of Type *cis*-[$PtCl_2L_2$].

Complexes	Δ/ppm[f]	$^1J_{Pt\text{-}P}$/Hz
cis-[$PtCl_2\{P(4\text{-}HOC_6H_4)_3\}_2$] (**6**)[a]	21.2	3700
cis-[$PtCl_2\{P(4\text{-}CH_3OC_6H_4)_3\}_2$][b]	20.9	3703
cis-[$PtCl_2\{P(4\text{-}CH_3C_6H_4)_3\}_2$][c]	20.1	3691
cis-[$PtCl_2\{P(C_6H_5)_3\}_2$][d]	18.6[e]	3676
cis-[$PtCl_2\{P(4\text{-}ClC_6H_4)_3\}_2$][c]	18.3[e]	3648
cis-[$PtCl_2\{P(4\text{-}CF_3C_6H_4)_3\}_2$][c]	20.5	3611
cis-[$PtCl_2\{P(4\text{-}C_6F_{13}C_6H_4)_3\}_2$][g]	21.5	3631

[a] This work. Recorded in d^6acetone. [b] This work. Recorded in $CDCl_3$. [c] Ref. 9. Recorded in $CDCl_3$. [d] Ref. 14. Recorded in CH_2Cl_2 containing 10%C_6D_6. [e] Ref. 10. Recorded in $CDCl_3$. [f] $\Delta = \delta_{P(complex)} - \delta_{P(free\ ligand)}$. [g] Ref. 15.

On comparing the Pt-P coupling constants, however, a slight variation is observed which reflects the nature of the *para*-substituent. The more electron-withdrawing the *para*-substituent is, the smaller is the $^1J_{Pt\text{-}P}$ value. Referring to the *Fermi Contact Term* (Section 1.3.1), the decrease in the $^1J_{Pt\text{-}P}$ values in Table 2.3 could be attributed to a decrease in the s-character in the Pt-P σ-bond. Varying the substituents on the aryl rings affects mainly the two values α^2_P and $|\psi_{(3s)}(0)|^2$ in the *Fermi Contact Term*

equation. Both values are expected to increase upon increasing the electronegativity on the phosphorus. The rehybridisation of the phosphorus orbitals according to Bent's rule[16] affects the α^2_P value and the contraction of the phosphorus 3s orbital affects the $|\psi_{(3s)}(0)|^2$ value. It might be expected that these trends would be reflected in the structural data for (**6**). Single crystals suitable for X-ray diffraction were grown by slow evaporation from the acetone (Figure 2.6), the data for which are included in Table 2.4. To be noted that the largest difference peak and hole data for (**6**) are +3.45 e at 1.58 Å from O(1) and –2.33 e at 1.19 Å from Pt(1).

Figure 2.6
Crystal Structure of *cis*-$[PtCl_2\{P(4\text{-}HOC_6H_4)_3\}_2].2C_3H_6O$ (6)

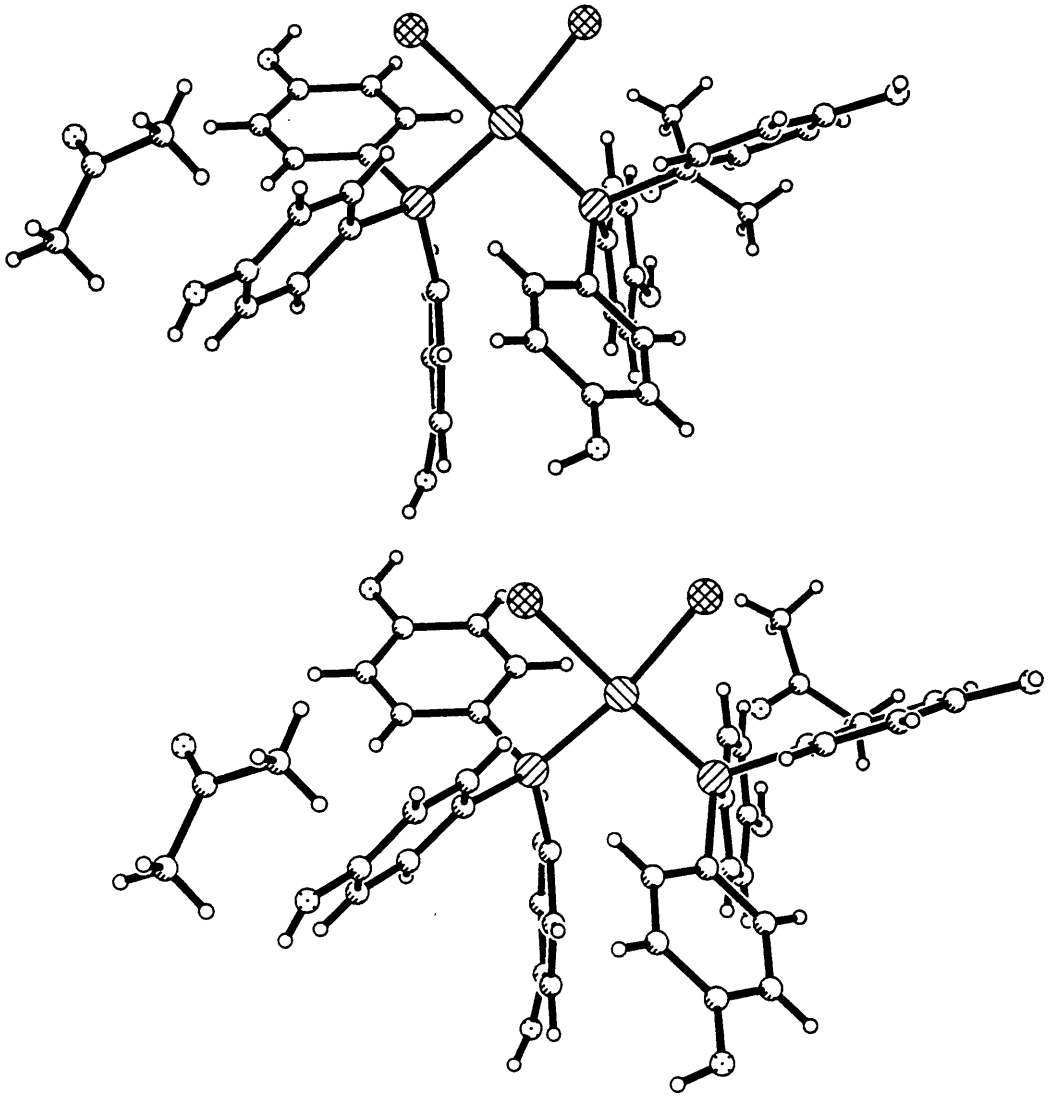

Figure 2.6 (Continued)
Crystal Structure of *cis*-$[PtCl_2\{P(4\text{-}HOC_6H_4)_3\}_2].2C_3H_6O$ (6)

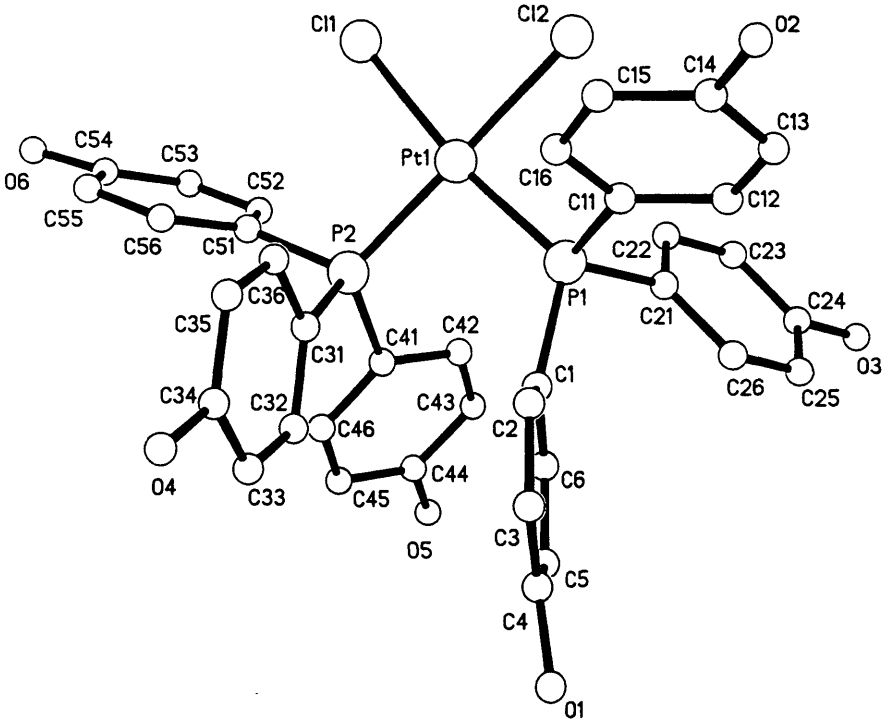

Table 2.4

Selected Bond Distances (Å) and Angles (°) with e.s.d. in Parentheses about Pt(II) for *cis*-$[PtCl_2\{P(4\text{-}HOC_6H_4)_3\}_2]$ (6)

Pt-P(1)	2.268(4)	Pt-P(2)	2.243(4)
Pt-Cl(1)	2.362(4)	Pt-Cl(2)	2.376(4)
P(1)-Pt-P(2)	95.68(14)	P(2)-Pt-Cl(1)	92.45(14)
P(1)-Pt-Cl(1)	171.52(14)	P(2)-Pt-Cl(2)	178.30(15)
P(1)-Pt-Cl(2)	85.96(14)	Cl(1)-Pt-Cl(2)	85.90(14)
C(11)-P(1)-Pt	106.3(4)	C(21)-P(1)-Pt	113.6(4)
C(1)-P(1)-Pt	124.0(4)		
C(31)-P(2)-Pt	109.9(4)	C(51)-P(2)-Pt	114.6(4)
C(41)-P(2)-Pt	115.6(3)		

An asymmetric arrangement exists at the platinum centre in terms of Pt-P or Pt-Cl bond lengths and in terms of the angles between the different ligating groups at the metal, i.e. P(2) atom is closer to platinum than P(1) atom. Consequently, Cl(2), which is *trans* to P(2), is further from the platinum than Cl(1). These differences in Pt-P lengths are in line with differences in the P-Pt-Cl angles; P(2)-Pt-Cl(1) [92.45(14)°] is larger than P(1)-Pt-Cl(2) [85.96(14)°]. These asymmetric Pt-Cl bond lengths and P-Pt-Cl bond angles have been identified in related *cis*-[$PtCl_2$(phosphine)$_2$] crystal structures.[15] Likewise, the Pt-P bond lengths and their asymmetry [2.243(4) and 2.268(4) Å] in complex (**6**) are very similar to those in *cis*-[$PtCl_2(PPh_3)_2$] [2.251(2) and 2.265(2) Å], which indicates that the *para*-hydroxy groups have an insignificant influence on the platinum-phosphorus bond lengths. However, this does not correlate with the ^{31}P NMR results, which revealed an influence of the *para*-substituent on the $^1J_{Pt\text{-}P}$ value. Thus, changes in Pt-P bond lengths and $^1J_{Pt\text{-}P}$ values are not linked. However, the increase in $^1J_{Pt\text{-}P}$ coupling constants and the decrease in Pt-P bond lengths are both proportional to an increase in the s-character in the platinum-phosphorus bond. It seems, according to this work, that the $^1J_{Pt\text{-}P}$ coupling constants are more sensitive to s-character in the Pt-P bonds then to the bond lengths.

This crystal structure reveals a more interesting effect in the phosphine ligands themselves. An intermolecular hydrogen bond is observed between the hydroxy groups on adjacent molecules and between hydroxy groups and chloride atoms (Figure 2.6). This intermolecular hydrogen bond O(1)...H...O'(2) [2.672(17) Å] is relatively strong and is comparable to values from the literature [2.455 (5) Å].[17] It occurs solely on one corner of the molecule causing a large distortion in one of the aryl rings. The remarkably distorted angle is C(1)-P(1)-Pt [124.0(4)°] which is much larger than a normal C(phenyl)-P-Pt angle such as C(11)-P(1)-Pt [106.3(4)°] and C(21)-P(1)-Pt [113.6(4)°] (from the same molecule). This may be compared with the largest C-P-Pt angle in *cis*-[$PtCl_2(PPh_3)_2$] which is 116.5°.[15] The second distorted angle is directly related to the first one. It is the angle between the bond P(1)-C(1) and the aryl ring plane attached to O(1). Its value is 165.0° (Figure 2.6). According to the Cambridge Crystallographic Data Base,[18] only thirteen aryl phosphine complexes, out of the many thousands of structurally characterised metal-aryl phosphine complexes, exhibit larger distortions with an angle smaller than 165.0°. The common feature in these complexes

is a steric effect forcing the molecules to adopt unusual configurations. However, the distorsion in complex (**6**) is likely to be due to the hydrogen bond O(1)...H...O'(2) tilting an aryl ring [incorporating O(1)] away from the centre of the complex and tilting another aryl ring [incorporating O'(2)] toward the metal centre [C(11)-P(1)-Pt: 106°.3(4)]. This distortion affects one phosphine ligand [P(1)] without affecting the second [P(2)]. The angles around the second phosphorus [P(2)] are relatively similar and conform with data for comparable platinum-phosphine complexes.[15]

Two molecules of acetone occur in the region beyond the hydroxy-groups [O(3)H and O(4)H] and are likely to be involved in weak hydrogen bonding with these substituents.

Characterisation of *trans*-[$PtCl_2${$P(4\text{-}HOC_6H_4)_3$}$_2$] (7):

Leaving a mixture of the neutral isomers stirring in solution at room temperature leads to a *trans*→*cis* conversion. It is possible to isolate the *trans*-isomer, in a pure state (according to the $^{31}P\{^1H\}$ NMR spectrum in Figure 2.4), by fractional recrystallisation. The *trans*-isomer is much more soluble in acetone than the *cis*-isomer, which is in accord with previous observations reported in the literature.[19] This makes it difficult to isolate the *trans*-isomer in high yield.

The $^1J_{Pt\text{-}P}$ coupling constant of the *cis*-isomer (**6**) is larger than that of the *trans*-isomer (**7**) due to the difference in the *trans*-influence between the chloride and the phosphine ligands. In Table 2.5, $^1J_{Pt\text{-}P}$ values corresponding to a set of *trans*-isomers are included which, when compared with the data for the related *cis*-isomers in Table 2.3, illustrate clearly the link between the geometry and the characterisation data.

Table 2.5
Platinum-Phosphorus coupling constants for *trans*-Platinum(II) Phosphine Complexes

Complexes	$^1J_{Pt-P}$/Hz
trans-$[PtCl_2\{P(4\text{-}HOC_6H_4)_3\}_2]$ (7) [a]	2598
trans -$[PtCl_2\{P(C_6H_5)_3\}_2]$ [b]	2605
trans -$[PtCl_2\{PPh_2(C_4H_9)\}_2]$ [c]	2531
trans -$[PtCl_2\{PPh(C_4H_9)_2\}_2]$ [c]	2462
trans -$[PtCl_2\{P(C_4H_9)_3\}_2]$ [c]	2392
trans-$[PtCl_2\{P(4\text{-}C_6F_{13}C_6H_4)_3\}_2]$ [d]	2719

[a] This work. Recorded in d^6acetone. [b] Ref. 20. Recorded in CH_2Cl_2. . [c] Ref. 13. Recorded in CH_2Cl_2. [d] Ref. 15.

From Table 2.5 it can be seen that the $^1J_{Pt-P}$ coupling constant increases when replacing alkyl phosphine with aryl phosphine ligands.[21] This is due to an increase in the π-accepting capability of the phosphine in the platinum(II)-phosphine bonding. Thus, in this set of complexes, the non-contact terms could be taken in consideration in order to interpret the metal-phosphorus coupling constant values. It seems, to a certain extent, that the $^1J_{Pt-P}$ is proportional to the π-character in the Pt-P bonding.

In contrast to the *cis*-isomer (**6**), when comparing complex (**7**) to the triphenylphosphine analogue, the hydroxyl group in the *para*-position does not significantly affect the Pt-P coupling. From the NMR data, it can be concluded that in the *cis*-isomer (**6**), the dominant bond component between the metal and the phosphorus is the σ-bond. The chloride *trans* to the phosphorus causes electron-density to flow through the σ-bond, from the phosphorus atom towards the chloride, strengthening the σ-bond. Thus an electron-donating group in the *para*-position enhances the σ-bond and consequently increases the $^1J_{Pt-P}$ coupling value. However, in

the *trans*-isomer type of complexes, the σ-bond is not as dominant as in the *cis*-isomer type of complexes. This is due to the high *trans*-influence of the phosphine ligands and having the two phosphine ligands mutually *trans*. In other terms, two good electron-donating groups mutually *trans*, would increase the contribution of π-character to the metal-phosphine bond. Therefore, the metal-phosphine synergism in the *trans*-isomer is more pronounced than in the *cis*-isomer. Hence, the influence of electron-donating groups on the aryl rings of the phosphine ligand is concealed by the relatively significant π-back-bonding in the metal-phosphine bond. Adding a fluorous chain in the *para*-position of the aryl ring of the phosphine ligand in *trans*-$[PtCl_2\{P(4\text{-}C_6F_{13}C_6H_4)_3\}_2]$ complex[15] (Table 2.5) induces a partial positive charge δ^+ on the metal centre due to an increase in the π-back-bonding. However, according to the synergic nature of the metal-phosphine bond, the σ-component is strengthened as detected by an increase in the corresponding $^1J_{Pt\text{-}P}$ value.

Single crystals of (7) suitable for X-ray structural analysis have been grown by slow precipitation from acetone:hexane (Figure 2.7). Some related bond distances and angles for complex (7) are listed in Table 2.6.

Figure 2.7
Crystal Structure of *trans*-$[PtCl_2\{P(4\text{-}HOC_6H_4)_3\}_2].6C_3H_6O$ (7)

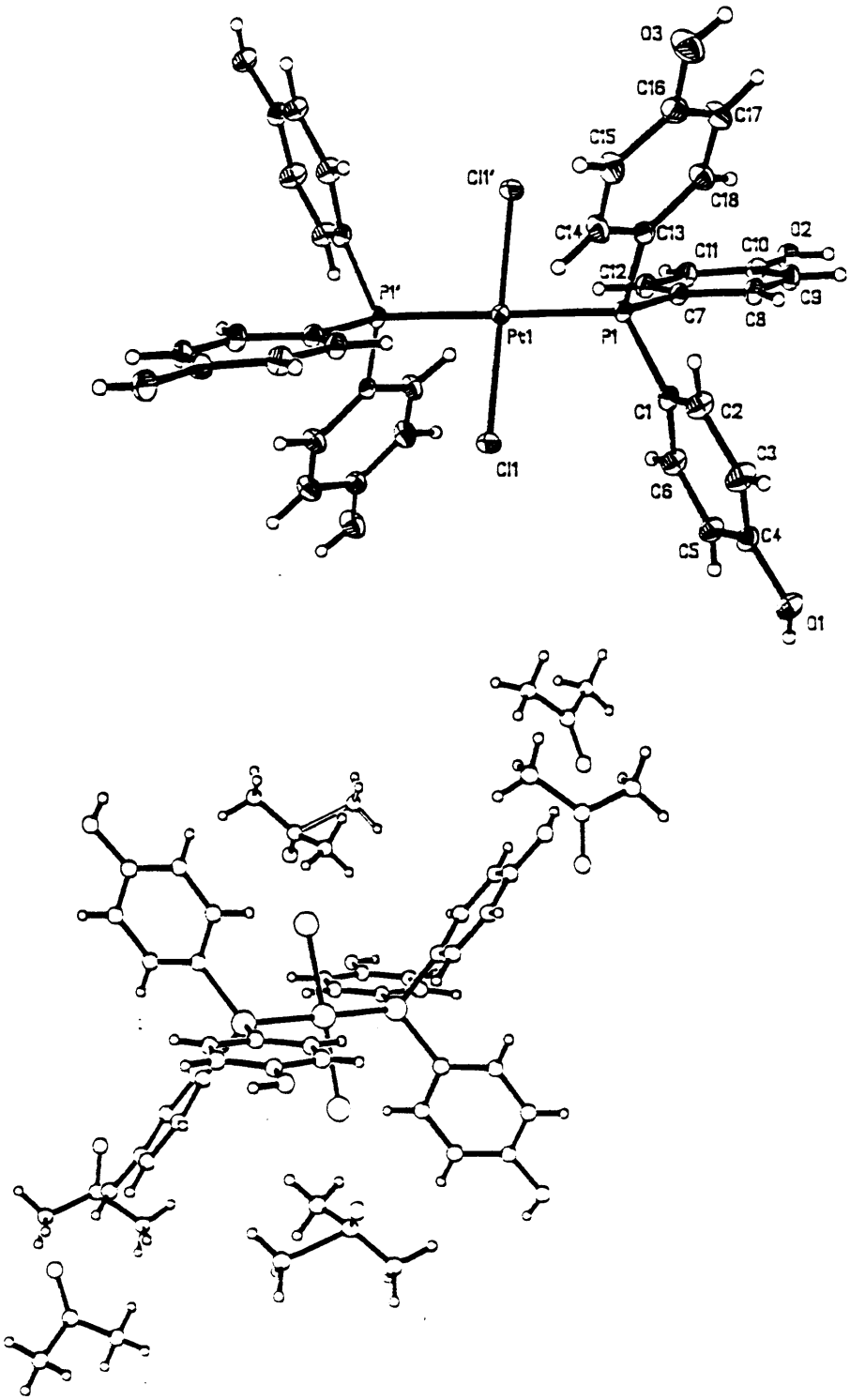

Table 2.6
Selected Bond Distances (Å) and Angles (°) with e.s.d. in Parentheses about Pt(II) for *trans*-[$PtCl_2\{P(4\text{-}HOC_6H_4)_3\}_2$] (7)

Pt-P(1)	2.3109(13)	Pt-P(1')	2.3109(13)
Pt-Cl(1)	2.3014(11)	Pt-Cl(1')	2.3014(11)
P(1)-Pt-P(1')	180.0	Cl(1)-Pt-Cl(1')	180.0
P(1)-Pt-Cl(1')	87.36(4)	P(1)-Pt-Cl(1)	92.64(4)
C(13)-P(1)-Pt	109.29(11)	C(1)-P(1)-Pt	118.88(11)
C(7)-P(1)-Pt	113.55(11)		

In complex (**7**) the platinum atom is located on a crystallographic centre of symmetry and hence it adopts a symmetrical *trans* square planar geometry in which the P-Pt-P and Cl-Pt-Cl angles are 180.0° and the P-Pt-Cl axes are slightly offset from orthogonal. The Pt-P bond lengths in the *trans*-isomer are longer than those of the *cis*-isomer, which is consistent with the difference in the $^1J_{Pt\text{-}P}$ values in the two isomers. The opposite trend is observed for the Pt-Cl bond lengths. Due to the relatively large phosphine *trans*-influence, each phosphine is inducing an elongation in the bond *trans* to itself. Unlike the *cis*-isomer, complex (**7**) does not exhibit any remarkable distortion in the phosphine ligands or more specifically in the aryl rings. Six molecules of acetone surround each platinum complex in the region beyond the hydroxy-groups and are likely to be involved in weak hydrogen bonding with these substituents. Comparing the X-ray crystallographic data of complex (**7**) to those of *trans*-[$PtCl_2\{P(4\text{-}C_6F_{13}C_6H_4)_3\}_2$] complex,[15] the Pt-P bond length in the former [2.3109(13) Å] is shorter than that in the latter [2.331(2) Å] which is not consistent with the spectroscopic data listed in Table 2.5. Similarly to the *cis*-isomer (**6**) case, this observation confirms that the platinum-phosphorus bond length is not proportional to the $^1J_{Pt\text{-}P}$ coupling constant.

Characterisation of $[PtCl\{P(4\text{-}HOC_6H_4)_3\}_3]^+Cl^-$ (8):

Addition of an excess of the free ligand (**5**) to the mixture of products in Scheme 2.6 leads to the formation of the *tris*-[*tris*-(*p*-hydroxyphenyl)phosphine]-chloroplatinum(II) chloride (**8**) (Scheme 2.7). The nature of the counterion has been confirmed as chloride by gravimetric analysis using 0.1M $AgNO_3$ aqueous solution (see experimental chapter).

Scheme 2.7

cis-$[PtCl_2(L)_2]$ (6)
\+ + **excess of L** ⟶ $[PtCl(L)_3]^+ Cl^-$ (8)
trans-$[PtCl_2(L)_2]$ (7)

L = $P(4\text{-}HOC_6H_4)_3$

In the ^1H NMR spectrum of (**8**), in addition to the signals attributable to the hydroxyl groups, are two signals assigned to *ortho*-aryl hydrogen atoms in a 1:2 intensity ratio corresponding to the aryl groups on the phosphine ligands *trans*- and *cis*-Cl respectively. Similar features are evident for the *meta*-aryl hydrogen atoms. The $^{31}P\{^1H\}$ NMR data are shown in Table 2.7 using the labelling indicated in Figure 2.8.

Figure 2.8
The structure of $[PtCl(L)_3]^+Cl^-$.[14]
P1 = P2 = L = aryl phosphine ligand.

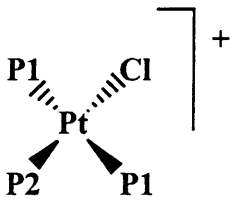

Table 2.7
$^{31}P\{^{1}H\}$ NMR Data for *tris*-Phosphine Platinum(II) Cationic Complexes.

Cations	δ_{P1} /ppm	δ_{P2} /ppm	$^{2}J_{P1-P2}$ /Hz	$^{1}J_{Pt-P1}$ /Hz	$^{1}J_{Pt-P2}$ /Hz
$[PtCl\{P(4\text{-}HOC_6H_4)_3\}_3]^+$ (**8**)[a]	20.3	9.0	18	2483	3701
$[PtCl\{P(4\text{-}CH_3OC_6H_4)_3\}_3]^+$ (**9**)[b]	21.4	10.1	18	2469	3676
$[PtCl(PPh_3)_3]^+$ [c]	23.8	13.1	19	2482	3638

[a] This work. Recorded in d^6 acetone. [b] This work. Recorded in $CDCl_3$. [c] Ref. 22, 23. Recorded in CD_2Cl_2.

The two mutually *trans* phosphine ligands' signal is detected as a high frequency doublet at 20.3 ppm compared to that for the phosphine *trans* to Cl which gave a lower frequency triplet at 9.0 ppm. The 18 Hz coupling is characteristic of a $P_{cis\text{-}P}$ coupling at a Pt(II) centre.[24] The $^{1}J_{Pt\text{-}P}$ coupling constant assigned to phosphorus *trans* phosphorus (2483Hz) is smaller than that for phosphorus *trans* to Cl (3701Hz), which mirrors the data for *cis*- and *trans*- neutral platinum(II) complexes (**6**) and (**7**) and is due to the increased *trans*-influence of the triarylphosphine compared to that for Cl. In fact, one of the routes to prepare *cis*-$[PtX_2(phosphine)_2]$ is by abstracting one phosphine ligand (usually triarylphosphine only) from complexes similar to (**8**) and (**9**).[25] The phosphine ligand removed is *trans* to another phosphine ligand, the resulting product being *cis*-$[PtX_2(phosphine)_2]$.

Interestingly, although the $^{1}J_{Pt\text{-}P}$ coupling constants ($P_{trans\text{-}Cl}$) are actually quite similar to those for the neutral *cis*-$[PtCl_2(phosphine)_2]$ species, the $^{1}J_{Pt\text{-}P}$ coupling constants (P_{transP}) are more than 100 Hz smaller than those for the *trans*-$[PtCl_2(phosphine)_2]$ species, which could be associated with the cationic charge here.

Comparing the $^{31}P\{^{1}H\}$ NMR data of complexes (**8**) and (**9**) to those of the triphenylphosphine analogue, no significant differences in the data are observed,

except those corresponding to $^1J_{Pt-P}$ coupling *trans* to Cl. This observation is in line with what has already been established on comparing the data for the *cis*- and *trans*-isomers of $[PtCl_2\{P(4\text{-}HOC_6H_4)_3\}_2]$. Once more, the effect of the *para*-substituent is more evident on the $^1J_{Pt-P}$ *trans*-Cl when compared to $^1J_{Pt-P}$ *trans*-P.

2.3.2 Synthesis and Characterisation of Platinum(II) Complexes of P(4-$CH_3OC_6H_4)_3$ (3):

Reaction of $[PtCl_2(CH_3CN)_2]$ With $P(4\text{-}CH_3OC_6H_4)_3$ (3):

Reaction of $[PtCl_2(CH_3CN)_2]$ with three equivalents of the ligand (**3**) affords a mixture of two species, the *bis*- and *tris*-phosphine platinum(II) complexes (Scheme 2.8). In the *bis*-phosphine complex, the geometry around the metal centre is *cis*. The *trans* configuration is not observed in this preparation which is reminiscent of the difference between the reaction described in Section 2.3.1 (Scheme 2.6) and that described in this section (Scheme 2.8). The *trans* configuration in complex (**7**) in Scheme 2.6 is the result of a driving force favoured by the existence of the hydroxy groups instead of the methoxy groups as *para*-substituents in the aryl rings of the phosphine ligands.

Scheme 2.8

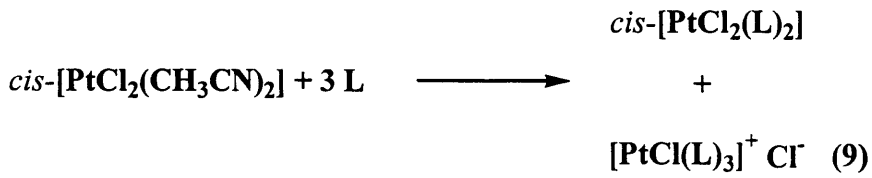

L = $P(4\text{-}CH_3OC_6H_4)_3$

The solubility of both products in Scheme 2.8 is very similar. Therefore, it is almost impossible to separate pure *tris*-phosphine platinum(II) complex (**9**). However, the three products (**6**), (**7**) and (**8**) (Scheme 2.8) are easily separated by fractional recrystallisation from acetone:hexane.

The *cis*-$[PtCl_2\{P(4\text{-}CH_3OC_6H_4)_3\}_2]$ complex has been previously prepared and characterised.[2-5] Therefore, it was easy to identify the corresponding characterisation data in a mixture of products. The ^1H NMR spectrum of complex (**9**) exhibits a multiplet in the aryl proton region (7.54-6.47 ppm), in addition to two singlets at 3.77 and 3.74 ppm in a 1:2 intensity ratio corresponding to the aryl methoxy groups of phosphine ligands *trans*- and *cis*-Cl respectively. The $^{31}P\{^1H\}$ NMR data for complex (**9**) are included in Table 2.7 (Section 2.3.1).

Reaction of $[PtCl(\mu\text{-}Cl)(PEt_3)\}_2]$ With $P(4\text{-}CH_3OC_6H_4)_3$ (3):

The reaction of the sym-*trans*-$[\{PtCl(\mu\text{-}Cl)(PEt_3)\}_2]$ dimer with two equivalents of the phosphine (**3**) affords a mixed phosphine platinum(II) monomer (Scheme 2.9) (Figure 2.9).[26]

Scheme 2.9

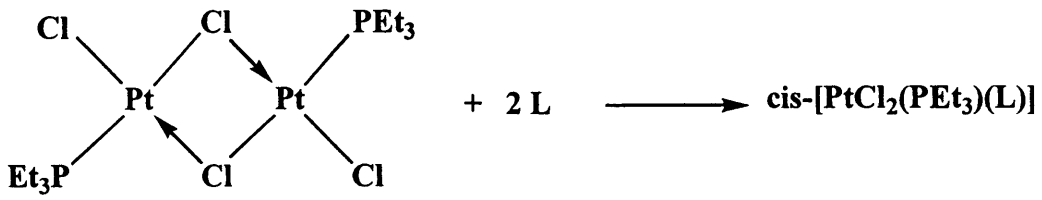

(10)

L = $P(4\text{-}CH_3OC_6H_4)_3$

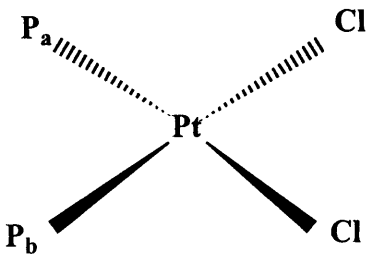

Fig. 2.9
Stucture of *cis*-$[PtCl_2(PEt_3)(L)]$ (10)

P_a = L, P_b = PEt_3.
δ_{Pa} 9.0 (d, $^1J_{Pt\text{-}Pa}$ = 3798 Hz, $^2J_{Pa\text{-}Pb}$ = 16 Hz) and δ_{Pb} 5.9 (d, $^1J_{Pt\text{-}Pb}$ = 3430 Hz, $^2J_{Pa\text{-}Pb}$ = 16 Hz) (Recorded in $CDCl_3$)

The $^{31}P\{^{1}H\}$ NMR spectrum is comparable to those of related mixed phosphine platinum(II) monomers.[15] It exhibits a doublet at 9.0 ppm ($^{2}J_{Pa\text{-}Pb}$ = 16 Hz) assigned to the ligand (**3**) coordinated to platinum, in addition to a lower frequency doublet, at 5.9 ppm having the same phosphorus-phosphorus coupling, assigned to the coordinated PEt_3. The signals are assigned mainly according to the $^{1}J_{Pt\text{-}P}$ coupling constants. The larger $^{1}J_{Pt\text{-}P}$ corresponds to the triarylphosphine ligand and the smaller one to the trialkylphosphine ligand. The difference between the $^{1}J_{Pt\text{-}P}$ values is due to the difference in π-acceptor character which is larger for aryl phosphines compared to alkyl ones.

The product of the reaction in Scheme 2.9 is not pure. The complex (**10**) is mixed with a by-product *cis*-$[PtCl_2\{P(4\text{-}CH_3OC_6H_4\}_3\}_2]$ (δ_P 11.0 ppm, $^{1}J_{Pt\text{-}P}$ = 3703 Hz).[13] The only plausible explanation for the existence of the latter product is that the ligand (**3**) has reacted with some unreacted $PtCl_2$ which is one of the starting materials used in the preparation of the $[\{PtCl(\mu\text{-}Cl)(PEt_3)\}_2]$ dimer. The possibility that an excess of the ligand (**3**) has reacted with the complex (**10**) has been excluded because of the difference in the *trans*-influence between Cl and phosphine. Attempts to separate the two products have been unsuccessful.

Synthesis and Characterisation of *cis*-$[PtMe_2\{P(4\text{-}CH_3OC_6H_4)_3\}_2]$ (11):

Complex (**11**) has been prepared by two routes. The methylation of *cis*-$[PtCl_2\{P(4\text{-}CH_3OC_6H_4)_3\}_2]$ with MeLi (Scheme 2.10) and displacement of the weakly coordinated diene from $[(COD)PtMe_2]$ (COD = η^4-1,5-cyclooctadiene) with two equivalents of the free ligand (**3**).[27a]

Scheme 2.10

$cis\text{-}[PtCl_2(L)_2]$ + excess of MeLi $\rightarrow$ $cis\text{-}[PtMe_2(L)_2]$ + 2LiCl

$L = P(4\text{-}CH_3OC_6H_4)_3$ **(11)**

The *cis*-$[PtCl_2(L)_2]$ complex in Scheme 2.10 is prepared by stirring *cis*-$[PtCl_2(CH_3CN)_2]$ with two equivalents of the corresponding phosphine ligand in dichloromethane.

The excess of methyl lithium from the reaction depicted in Scheme 2.10 is neutralised by the dropwise addition of a concentrated aqueous solution of NH_4Cl, the neutralisation reaction follows the equation described in Scheme 2.11.

Scheme 2.11

$$NH_4Cl + MeLi \rightarrow LiCl + NH_3 + CH_4$$

Mass spectrometry of the white square planar complex (**11**) shows two main signals assigned to the parent ion minus the methyl group and the parent ion minus both methyl groups. The ^1H NMR spectrum, in addition to the signals assigned to the ligand, gives rise to a low-frequency second-order doublet of doublets, flanked by satellites. The corresponding ^1H NMR data along with the $^{31}P\{^1H\}$ NMR data are shown in Table 2.8.

Table 2.8
NMR Parameters for *cis*-$[PtMe_2(L)_2]$ Complexes.

L	$\delta_{H\,(Me)}$ /ppm	$^2J_{Pt\text{-}H}$ /Hz	$^3J_{P1\text{-}H\,(Me)}$ /Hz[c]	$^3J_{P2\text{-}H\,(Me)}$ /Hz[c]	δ_P /ppm	$^1J_{Pt\text{-}P}$ /Hz
$P(4\text{-}MeOC_6H_4)_3\}$[a]	0.12	69	6.5	6.7	24.4	1932
PPh_3[d]	0.34	69	-[e]	-[e]	27.7	1900
PEt_3[b]	0.4	68	6.0	7.0	9.7	1856

[a] This work. Recorded in CD_2Cl_2. [b] Ref. 28,29. Recorded in CH_2Cl_2
[c] P_1 or P_2 could be the phosphorus *cis* or *trans* to the methyl. [d] Ref. 27. Recorded in CD_2Cl_2. [e] Not reported.

When the data in Table 2.8 are compared, it can be seen that the ^{1}H NMR values associated with the methyl groups do not differ significantly when the substituents on the phosphine ligand are changed. As discussed earlier for the *cis*-$[PtCl_2(phosphine)_2]$ complexes, introduction of the *para*-methoxy substituents into these platinum dimethyl *bis*-triarylphosphine complexes causes an increase in the $^{1}J_{Pt\text{-}P}$ coupling constant associated with the increase in basicity of the phosphine ligand $[P(4\text{-}CH_3OC_6H_4)_3$ *versus* $PPh_3]$.

An important conclusion may be derived from these observations; the substituents on the phosphorus atom affect the ^{31}P NMR chemical shift as well as the $^{1}J_{Pt\text{-}P}$ value. However, this influence is not transferred across the platinum centre to the methyl groups.

Table 2.9
$^{31}P\{^{1}H\}$ NMR Data of $[PtX_2L_2]$ Complexes (X = Cl, Me) (L = (3), PEt_3)

Complex	δ_P/ppm	$^{1}J_{Pt\text{-}P}$/Hz
cis-$[PtCl_2\{P(4\text{-}MeOC_6H_4)_3\}_2]$ **(A)**[a]	11.0	3703
cis-$[PtMe_2\{P(4\text{-}MeOC_6H_4)_3\}_2]$ **(B)**[b]	24.4	1932
cis-$[PtCl_2(PEt_3)_2]$ **(C)**[c]	8.4	3507
cis-$[PtMe_2(PEt_3)_2]$ **(D)**[d]	9.7	1856

[a] This work. Recorded in $CDCl_3$. [b] This work. Recorded in CD_2Cl_2
[c] Ref. 30. Recorded in CH_2Cl_2. [d] Ref. 28. Recorded in CH_2Cl_2.

In Table 2.9, NMR data for the related *cis*-$[PtCl_2(phosphine)_2]$ and *cis*-$[PtMe_2(phosphine)_2]$ complexes are summarised. Here, the $^{1}J_{Pt\text{-}P}$ for the phosphine ligands *trans* to Cl (complexes **A** and **C**) are significantly larger than those for the phosphine ligands *trans* to Me (complexes **B** and **D**) which is due to the large difference in the *trans*-influence between a chloride and a methyl group.

2.4 Reaction of $[PdCl_2(CH_3CN)_2]$ with $P(4\text{-}HOC_6H_4)_3$ (5):

In the coordination chemistry of palladium metal, the coordination chemist lacks an important tool in characterising and probing palladium phosphine bonding, due to the fact that no coupling is observed between the phosphorus and palladium nuclei. However, palladium chemistry has many interesting applications of which some examples have been outlined in Chapter One. Therefore, attempts have been made to synthesise some palladium(II) derivatives. *Cis*-$[PdCl_2(CH_3CN)_2]$ was allowed to react with two equivalents of $P(4\text{-}HOC_6H_4)_3$ (**5**) to give a yellow-orange product which precipitated out of solution in a relatively high yield on addition of hexane. The far-IR spectrum of the product was inconclusive due to the absence of the Pd-Cl stretch.[31] The $^{31}P\{^1H\}$ NMR spectrum exhibited a singlet at 20.1 ppm as the major resonance, and two smaller, slightly broadened resonances at 30.8 ppm and 29.1 ppm. As described in the synthesis of $[(Ph_3P)_3PdCl][BF_4]$ and $[(Ph_3P)_3PdCl][OSO_2CF_3]$,[32] the $^{31}P\{^1H\}$ NMR spectrum corresponds to that of the dimer $[\{P(4\text{-}HOC_6H_4)_3\}_4Pd_2(\mu\text{-}Cl)_2]^{2+}$ (**12**).

The yellow-orange product was dissolved in acetone, and an excess of the phosphine ligand was added. After stirring for two hours, the resulting product revealed the presence of $[PdCl\{P(4\text{-}HOC_6H_4)_3\}_3]^+$ (**13**). The $^{31}P\{^1H\}$ NMR results are summarised in Table 2.10. The structure of the tertiary phosphine palladium complex is shown in Figure 2.10.

Scheme 2.12

$$cis\text{-}[PdCl_2(CH_3CN)_2] + 2\,L \longrightarrow [(L)_4Pd_2(\mu\text{-}Cl)_2]^{2+} \text{ (12)} + [PdCl(L)_3]^+ \text{ (13)}$$

$L = P(4\text{-}HOC_6H_4)_3$

Figure 2.10
The structure of $[PdCl(L)_3]^+Cl^-$ (13).
P1 = P2 = L = arylphosphine ligand.

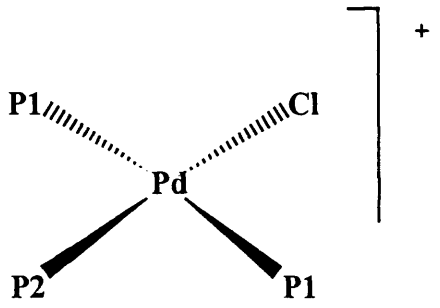

Table 2.10
$^{31}P\{^1H\}$ NMR Data for Arylphosphine Pd(II) Complexes.

Complex	δ_{P1}/ppm	δ_{P2}/ppm	$^2J_{P1\text{-}P2}$/Hz
$[(L)_4Pd_2(\mu\text{-}Cl)_2]^{2+}$ (12)[a]	20.1	-	-
$[PdCl(L)_3]^+$ (13)[a]	26.6 (d)	30.5 (t)	14
$[(PPh_3)_4Pd_2(\mu\text{-}Cl)_2]^{2+}$ [b].	23.9	-	-
$[PdCl(PPh_3)_3]^+$ [b]	30.8 (d)	34.2 (t)	16

[a] This work. Recorded in d^6 acetone. [b] Ref. 32. Recorded in CH_3NO_2.

Adding an excess of the phosphine ligand to complex (**12**) leads to the formation of the *tris*-phosphine palladium(II) complex (**13**) as evidenced by a doublet and a triplet signal in the $^{31}P\{^1H\}$ NMR spectrum. This reaction suggests that complex (**12**) is actually a dimer. The small coupling values (14 and 16 Hz) are attributed to the P_{cisP} coupling which is well described in the literature.[32] The slight low-frequency shifting of the phosphorus signal when comparing complex (**13**) to its triphenylphosphine analogue mirrors that seen for the analogous platinum(II) cationic complex (**8**) which is caused by the electronic enhancement as a result of the mesomeric-donating effect induced by the hydroxy groups.

2.5 Synthesis and Characterisation of Rh(I) and Rh(III) Phosphine Complexes:

The complexes of the noble metal are well known to exhibit a rich chemistry especially in the catalytic field.[33] Complexes of d^8-metal [Rh(I)] or d^6-metal [Rh(III)] can be coordinatively unsaturated e.g. $[Rh(CO)Cl(PPh_3)_2]$ (d^8, 4-coordinate) and $[H_2RhCl(PPh_3)_2]$ (d^6, 5-coordinate)[34] and, as such, these types of complexes are susceptible to substrate fixation via either nucleophilic attack using the vacant metal orbitals or electrophilic attack using the filled metal orbitals which can be influenced by the electronic and steric properties of the ancillary ligands.

In the following sections, 2.5.1 and 2.5.2, the preparation and characterisation of both Rh(I) and Rh(III) complexes of the *para*-substituted triarylphosphine ligands are described.

2.5.1 Synthesis and Characterisation of *trans*-$[Rh(CO)Cl\{P(4\text{-}HOC_6H_4)_3\}_2]$ (14):

Treatment of the dinuclear rhodium(I) complex $[\{Rh(CO)_2(\mu\text{-}Cl)\}_2]$ with four equivalents of the ligand $P(4\text{-}HOC_6H_4)_3$ (**5**) in refluxing acetone, leads to the formation of the yellow air-sensitive square planar Rh(I) complex (**14**) (Scheme 2.13). The ^1H NMR spectrum exhibits the ligand signals. The mass spectrum reveals two main signals assigned to the parent ion minus carbonyl group and the parent ion minus carbonyl and chlorine. The $^{31}P\{^1H\}$ NMR spectral results are shown in Table 2.11.

Scheme 2.13

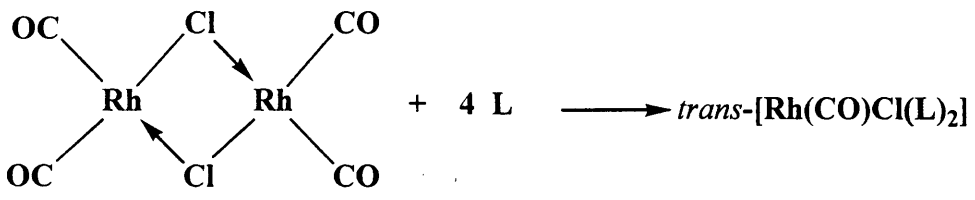

(**14**)

L = $P(4\text{-}HOC_6H_4)_3$

Table 2.11
$^{31}P\{^{1}H\}$ NMR Data for *trans*-[Rh(CO)Cl(L)$_2$] Complexes

L	Δ/ppm[f]	$^{1}J_{Rh-P}$/Hz
$P(4\text{-}HOC_6H_4)_3$ (**14**)[a]	34.7	123
$P(4\text{-}CH_3OC_6H_4)_3$[b]	34.9	125
$P(4\text{-}CH_3C_6H_4)_3$[c]	34.1	124
PPh_3[d]	29.5	124
$PEtPh_2$[e]	39.6	123
PEt_2Ph[e]	41.9	120
PEt_3[e]	43.8	116

[a] This work. Recorded in d^6 acetone. [b] This work. Recorded in $CDCl_3$. [c] Ref. 12. Recorded in toluene. [d] Ref. 15. Recorded in CH_2Cl_2 at 224K. [e] Ref. 35. Recorded in CH_2Cl_2. [f] $\Delta = \delta_{P(complex)} - \delta_{P(free\ ligand)}$.

The complex *trans*-[Rh(CO)Cl{P(4-$CH_3OC_6H_4)_3$}] has been prepared in this work following a similar route to that of complex (**14**), for the purpose of comparison with the latter complex. Its characterisation data are very similar to those already published.[36] Δ values (Table 2.11) describe the difference in phosphorus chemical shift upon coordination. The addition of electron-donating groups, such as methyl, methoxyl or hydroxyl in the *para*-position of the aryl rings in the phosphine ligands, induces an increase in the coordination chemical shift value compared to that of the non-substituted triphenylphosphine ligand. The variations in the Δ values are more pronounced when replacing the aryl groups with alkyl groups. Reducing the number of aryl groups in the phosphine ligand results in a reduction of the π-acceptor character in the phosphine ligand which is reflected in an increase in the Δ values. Variations in the $^{1}J_{Rh-P}$ values are negligible except when replacing the aryl groups with alkyl groups.

A very important class of noble metal complexes is the rhodium(I) carbonyl type. The rhodium-carbonyl mutually reinforcing bonding involves both σ- and π-components. As described in Chapter One, the σ-component is formed as a result of an interaction between a filled sp carbon orbital and a vacant metal σ-orbital. The π-component is formed as a result of an interaction between a filled metal dπ- or a hybrid dpπ-orbital and a vacant anti-bonding pπ*-orbital of the carbon monoxide. The synergic bonding between the metal and the carbonyl group is detected by the C≡O stretching frequency which can be used to monitor any variations in electron density at the metal centre. The stretching frequency of free carbon monoxide ν_{CO} is 2148 cm^{-1}. A high electron density at the metal enhances the π-component, accommodating electrons in antibonding CO orbitals. Consequently, the C≡O bond is weakened and its stretching frequency decreases. The opposite trend is observed when low electron density at the metal enhances the σ-component, leading to a strengthening in C≡O bond and to an increase in the corresponding frequency.

Table 2.12
Carbonyl Stretching Frequencies in *trans*-[Rh(CO)Cl(L)] Complexes.

L	ν_{CO}/cm^{-1}
$P(4\text{-}HOC_6H_4)_3$ **(14)**[a]	1980
$P(4\text{-}CH_3OC_6H_4)_3$[a]	1958
PPh_3[b]	1980
$P(4\text{-}CF_3C_6H_4)_3$[c]	1990

[a] This work. [b] Ref. 37,38. [c] Ref. 15. Recorded in CH_2Cl_2.

The Nujol mull IR spectrum of the *trans*-[Rh(CO)Cl($P(4\text{-}CH_3OC_6H_4)_3$)] complex (Table 2.12) reveals one ν_{CO} stretching vibration at 1958 cm^{-1} as expected for the *trans*-structure. Removing the *para*-methoxy substituent induces an increase in

the carbonyl stretching frequency value. It is 1980 cm^{-1} in the triphenyl phosphine analogue. While the electron-withdrawing group CF_3 in the *para*-position induces an increase in the carbonyl stretching frequency value when comparing the relevant complex to the one incorporating the triphenylphosphine analogue. Hence, an electron-withdrawing group in the *para*-position induces a C≡O bond strengthening, while an electron-donating group in the same position induces a C≡O bond weakening. The complexes incorporating alkyl groups exhibit stretching frequencies at (typically) 1961cm^{-1} in chloroform solution.[37,38]

According to the $^{31}P\{^1H\}$ NMR data, the hydroxyl group in complex (**14**) is expected to induce a similar influence on the carbonyl group as the methoxy group does due to their comparable electron-donating capability. However, a marked increase in the ν_{CO} value is observed when replacing the methoxyl by the hydroxyl in the *para*-position. This observation mirrors previous unexpected behaviour, such as in the case of platinum(II) complexes (**6**), (**7**) and (**8**), and could be linked to the same characteristic, i.e. the hydroxy group could engage itself in hydrogen bonding reducing its electronic contribution to the aryl ring of the phosphine ligand. Therefore, the ν_{CO} value of complex (**14**) is very similar to that of the triphenylphosphine analogue.

2.5.2 Synthesis and Characterisation of $[(\eta^5\text{-}C_5Me_5)Rh(L)Cl_2]$ Complexes:

Treatment of the dinuclear rhodium(III) complex $[\{(\eta^5\text{-}C_5Me_5)Rh(\mu\text{-}Cl)Cl\}_2]$ with two equivalents of $P(4\text{-}CH_3OC_6H_4)_3$ (**3**) or $P(4\text{-}HOC_6H_4)_3$ (**5**) leads to the formation of monomeric Rh(III) complexes: $[(\eta^5\text{-}C_5Me_5)Rh(L)Cl_2]$ (**15**) when L = (**3**) and (**16**) when L = (**5**) (Scheme 2.14).

Scheme 2.14

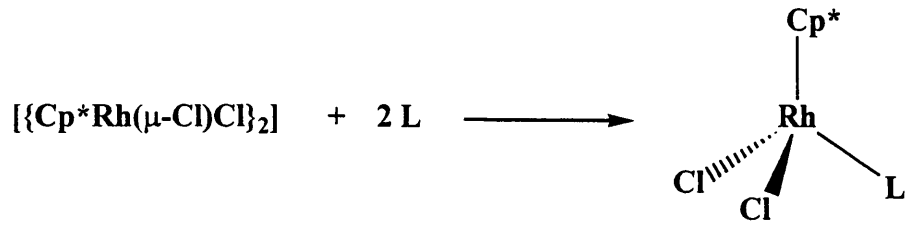

Cp* = η^5-C_5Me_5

(15) when L = P(4-$CH_3OC_6H_4$)$_3$
(16) when L = P(4-HOC_6H_4)$_3$

In the ^1H NMR spectra, in addition to the signals associated with the phosphine ligands, a doublet at δ 1.29 [15H, J_{P-H} ca. 4Hz, complex (**15**)] and a doublet at δ 1.08 [15H, J_{P-H} ca. 3Hz, complex (**16**)] are assigned to the Cp* protons coupling to the phosphorus atoms. There are no significant differences in J_{P-H} or δ_H values or the proton chemical shifts corresponding to the Cp* protons between complexes (**15**) and (**16**) or related [(η^5-C_5Me_5)Rh(L)Cl_2] (L = triarylphosphine) complexes.

According to the $^{31}P\{^1H\}$ NMR data shown in Table 2.13, the introduction of either a methoxy or an hydroxy group in the *para*-position of the phenyl rings in these phosphine ligands does not affect the coupling constant $^1J_{Rh-P}$, indicating that the introduction of such groups does not induce significant variations in the rhodium-phosphorus bonding.

Table 2.13
$^{31}P\{^1H\}$ NMR Data of [Cp*Rh(L)Cl_2] Complexes.

L	Δ/ppm [e]	$^1J_{Rh-P}$/Hz
P(4-$CH_3OC_6H_4$)$_3$ (**15**)[a]	38.8	144
P(4-HOC_6H_4)$_3$ (**16**)[b]	37.2	143
PPh_3[c]	35.2	144
P(4-$C_6F_{13}C_6H_4$)$_3$[d]	34.9	146

[a] This work. Recorded in $CDCl_3$. [b] This work. Recorded in DMSO. [c] Ref. 39. [d] Ref. 15. [e] Δ = $\delta_{P(complex)} - \delta_{P(free\ ligand)}$.

A single crystal of $[(\eta^5\text{-}C_5Me_5)Rh\{P(4\text{-}CH_3OC_6H_4)_3\}Cl_2]$ (**15**) has been isolated and characterised by X-ray diffraction (Figure 2.12). The complex (**15**) has recrystallised in a monoclinic crystal system and adopts a piano stool geometry around the metal centre.[40] Selected bond lengths and angles are included in Table 2.14 along with those of $[(\eta^5\text{-}C_5Me_5)Rh\{P(4\text{-}C_6F_{13}C_6H_4)_3\}Cl_2]$.[15] This comparison indicates that there are no significant differences in the geometry of the Cp* ring or the base of the piano stool structure. The Rh-P and Rh-C(Cp*) bond lengths are virtually identical indicating that the electron-donating methoxy group and the electron-withdrawing perfluoroalkyl group have negligible effect on the first coordination sphere of this type of metal complex.

Figure 2.11
Crystal Structure of $[(\eta^5\text{-}C_5Me_5)Rh\{P(4\text{-}CH_3OC_6H_4)_3\}Cl_2].2CH_2Cl_2$ (15)

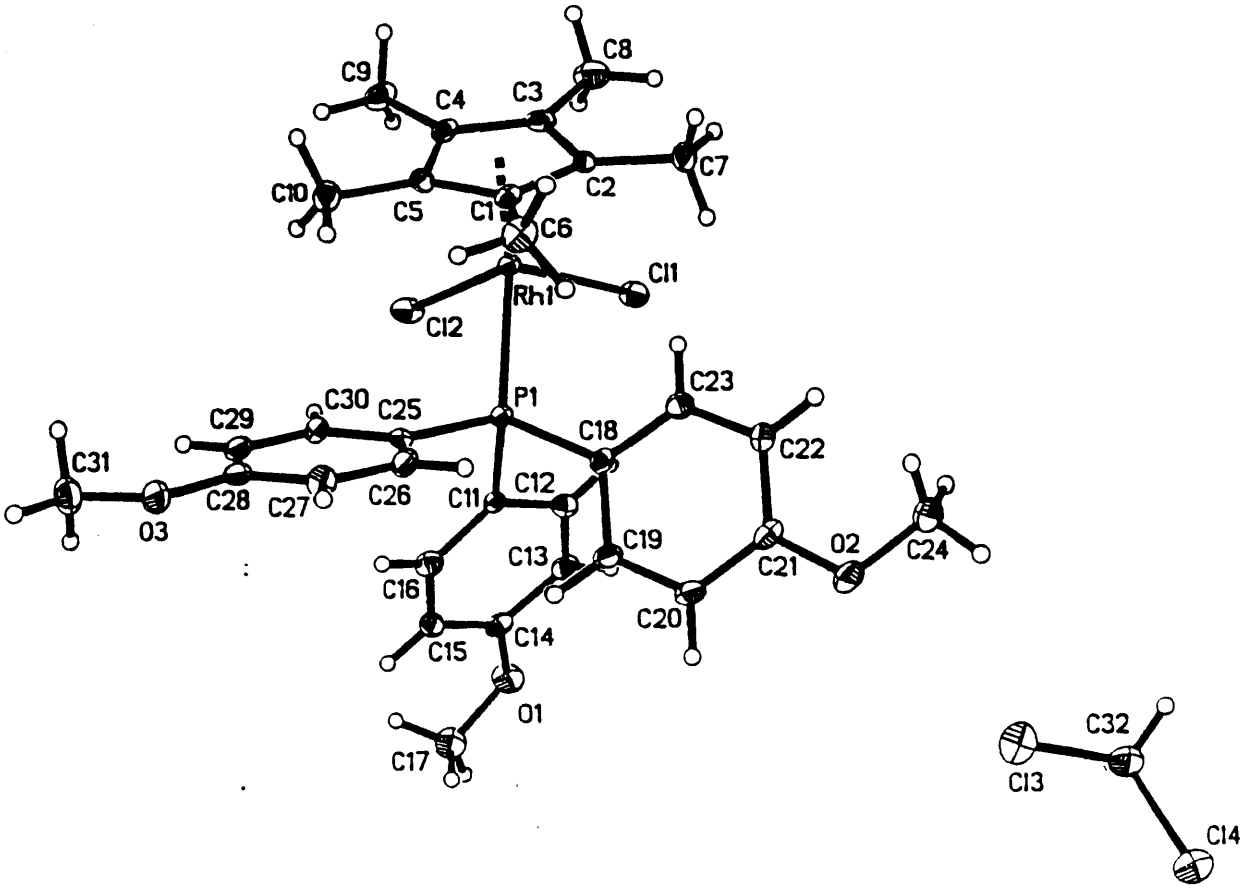

Table 2.14
Selected Bond Distances (Å) and Angles (°) with Estimated Standard Deviation in Parentheses about Rhodium for [Cp*Rh(L)Cl_2] Complexes.

	L = P(4-$CH_3OC_6H_4$)$_3$ (15)	L = P(4-$C_6F_{13}C_6H_4$)$_3$[a]
Rh(1)-Cl(1)	2.417(2)	2.393(2)
Rh(1)-Cl(2)	2.400(2)	2.398(3)
Rh(1)-C(1)	2.194(6)	2.215(9)
Rh(1)-C(2)	2.184(6)	2.204(9)
Rh(1)-C(3)	2.213(6)	2.164(9)
Rh(1)-C(4)	2.222(5)	2.201(8)
Rh(1)-C(5)	2.158(6)	2.179(9)
Rh(1)-P(1)	2.328(2)	2.332(3)
av.C(Cp*)-C(Cp*)	1.438	1.438
av.C(Cp*)-C(Me)	1.478	1.478
P-Rh-Cl(1)	93.01(6)	88.28(9)
P-Rh-Cl(2)	84.80(5)	86.00(9)
Cl(1)-Rh-Cl(2)	93.08(6)	93.95(9)

[a] **Ref. 15.**

Table 2.15
C(Cp*)-Rh-P Angles in [(η^5-C_5Me_5)Rh{P(4-$CH_3OC_6H_4$)$_3$}Cl_2] (15)

C(5)-Rh-P	109.0(2)	C(2)-Rh-P	120.6(2)
C(1)-Rh-P	98.0(2)	C(3)-Rh-P	158.9(2)
C(4)-Rh1-P1	145.3(2)		
C(5)-Rh-Cl(2)	100.9(2)	C(2)-Rh-Cl(2)	153.3(2)
C(1)-Rh-Cl(2)	138.4(2)	C(3)-Rh-Cl(2)	115.7(2)
C(4)-Rh-Cl(2)	90.8(2)		

In addition, on comparison of the C(Cp*)-Rh-P angles (Table 2.15), it can be seen that the smallest angle C-Rh-P is 98.0(2)°, it corresponds to the carbon atom straight above the phosphine ligand. However, the smallest two angles among the C(Cp*)-Rh-Cl angles are [C(3)-Rh-Cl(1) 91.0(2)° and C(4)-Rh-Cl(2) 90.8(2)°]. Therefore, the steric effect caused by the proximity of the Cp* ring to the phosphine ligand causes a tilting of the planar Cp* ring away from the phosphine ligand.

2.6 Summary:

Both the *tris*-(*para*-methoxyphenyl)phosphine and the *tris*-(*para*-hydroxyphenyl)phosphine ligands coordinate readily to a series of late transition-metal centres to give analogues of well-established triphenylphosphine metal complexes. Both methoxy and hydroxy *para*-substituents induce an electron-donating effect towards the phosphorus atom, enhancing its nucleophilicity towards the metal centre. However, It should be noted that the influence of the former substituent is larger than that of the latter substituent. The hydroxy group is capable of engaging in hydrogen bonds that reduce its electronic contribution to the aryl ring of the phosphine ligand. Additionally, these hydrogen bonds are capable of affecting the structure of the phosphine ligand such as inducing distortions in the substituted aryl rings and favouring the formation of unexpected configurations as detected in the coordination chemistry of the ligand $P(4\text{-}HOC_6H_4)_3$ (**5**) to platinum(II) and rhodium(I) complexes.

Chapter Two References

[1] V. Garcia, M. A. Garralda and E. Zugasti, *J. Organomet. Chem.*, 1987, **322**, 249.

[2] H. G. Alt, R. Baumgärtner and H. A. Brune, *Chem. Ber.*, 1986, **119**, 1694.

[3] H. A. Brune, M. Falck, R. Hemmer, G. Schmidtberg and H. G. Alt, *Chem. Ber.*, 1984, **117**, 2791.

[4] H. A. Brune, M. Falck, R. Hemmer and H. G. Alt, *Chem. Ber.*, 1984, **117**, 2803.

[5] R. McCrindle, G. J. Arsenault, A. Gupta, M. J. Hampden-Smith, R. E. Rice and A. J. McAlees, *J. Chem. Soc., Dalton Trans.*, 1991, 949.

[6] A. E. Sinear, W. Valient and J. Wirth, *J. Org. Chem.*, 1960, **25**, 2001.

[7] a) T. Alman, R. G. Goel and A. L. Beauchamp, *Acta Crystallogr., Sect. C*, 1986, **42**, 603.

b) J. Bruckmann, C. Kruger and F. Lutz, *Z. Naturforsch., Teil B*, 1995, **50**, 351.

[8] J. J. Daly, *J. Chem. Soc.*, 1964, 3799.

[9] C. Cobley and P. G. Pringle, *Inorg. Chim. Acta.*, 1997, **265**, 107

[10] a) W.-N. Chou and M. Pomerantz, *J. Org. Chem.*, 1991, **56**, 2762.

b) M. Pamerantz., B. T. Ziemnicka, Z. M. Merchant, W.-N. Chou, W. B. Perkins and S. Bittner, *J. Org. Chem.*, 1985, **50**, 1757.

[11] S. O. Grim and W. Yankowsky, *Phosphorus and Sulfur*, 1977, **3**, 191.

[12] C. A. Tolman, P. R. Meakin, D. L. Linder and P. J. Jesson, *J. Am. Chem. Soc.*, 1974, **96**, 2762.

[13] S. O. Grim, R. L. Keiter and W. McFarlane, W., *Inorg. Chem.*, 1967, **6**, 1133.

[14] R. G. Goel, *Inorg. Nucl .Chem. lett.*, 1979, **15**, 437.

[15] J. Fawcett, E. G. Hope, R. D. W. Kemmitt, D. R. Paige, D. R. Russell and A. M. Stuart, *J. Chem. Soc., Dalton Trans.*, 1998, 3751.

[16] H. A. Bent, *Chem. Rev.*, 1961, **61**, 275.

[17] D. Steinborn, M. Gerisch, C. Bruhn and J. A. Davies, *Inorg. Chem.*, 1999, **38**, 680.

[18] F. H. Allen and O. Kennard, *3D Search and Research Using the Cambridge Structural Database, Chemical Design Automations News*, 1993.

[19] M. Fushimi, M. Suzuki and A. Uehara, *Bull. Chem. Soc. Jpn.*, 1988, **61**, 1809.

[20] M. Gómez, G. Muller, D. Sainz and J. Sales, *Organometallics*, 1991, **10**, 4036.

[21] P. S. Pregosin, R. W. Kunz, *^{31}P and ^{13}C NMR Of Transition Metal Complexes*, Springer, New York, 1979.

[22] C. Scheffknecht, A. Rhomberg, E. P. Müller, P. Peringer, *J. Organomet. Chem.*, 1993, **463,** 245.

[23] P. S. Pregosin, R. Favez, R. Roulet, T. Boschi, R. A. Michelin and R. Ros, *Inorg. Chim. Acta*, 1980, **45**, L7.

[24] P. S. Pregosin and R. W. Zunz, *NMR, Basic Principles and Progress*, P. Diehl, E. Fluck and R. Kosfeld (eds), Springer, NewYork, 1979.

[25] F. De Jong, J. J. Bour and P. P. J. Schlebos, *Inorg. Chim. Acta*, 1988, **154**, 89.

[26] M. J. Atherton, J. Fawcett, A. P. Hill, J. H. Holloway, E. G. Hope, D. R. Russell, G. C. Saunders and R. M. J. Stead, *J. Chem. Soc., Dalton Trans.*, 1997, 1137.

[27] a) C. M. Haar, S. P. Nolan, W. J. Marshall, K. G. Moloy, A. Prock and W. P. Giering, *Organometallics*, 1999, **18**, 474.

b) R. H. Reamy and G. M. Whitesides, *J. Am. Chem. Soc.*, 1984, **106**, 81.

[28] F. H. Allen and A. Pidcock, *J. Chem. Soc. (A)*, 1968, 2700.

[29] K. R. Dixon and D. J. Hawke, *Can. J. Chem.*, 1971, **49**, 3252 and references cited therein.

[30] P. S. Pregosin, *Coord. Chem. Rev.*, 1982, **44**, 247.

[31] G. Balimann, H. Motschi and P. S. Pregosin, *Inorg. Chim. Acta*, 1977, **23**, 191.

[32] M. R. Masson and J. G. Verkade, *Organometallics*, 1992, **11**, 2212.

[33] J. P. Collman and L. S. Hegedus, *Principles and Applications of Organo-transition Metal Chemistry*, University Science Books, Calif., 1980.

[34] C. A. Tolman, *Chem. Soc. Rev.*, 1972, **1**, 337.

[35] B. E. Mann, C. Masters and B. L. Shaw, *J. Chem. Soc. (A)*, 1971, 1104.

[36] a) M. A. Bennett, R. J. H. Clark and D. L. Milner, *Inorg. Chem.*, 1967, **6**, 1647.

b) D. Evans, J. A. Osborn and G. Wilkinson, *J. Chem. Soc. (A),* 1968, 3133.

c) I. C. Douek and G. Wilkinson, *J. Chem. Soc. (A)*, 1969, 2604.

d) S. Serron, S. P. Nolan and K. G. Moloy, *Organometallics*, 1996, **15**, 4301.

[37] S. O. Grim and R. A. Ference, *Inorg. Nuclear Chem. Letters*, 1966, **2**, 205.

[38] L. Vaska and J. Peone, *J. Chem. Soc., Chem. Commun.*, 1971, 418.

[39] J. H. Holloway, E. G. Hope and G. C. Saunders, unpublished work.

[40] R. D. Brost, G. C. Bruce, S. L. Grundy and S. R. Stobart, *Inorg. Chem.*, 1993, **32**, 5195.

CHAPTER THREE

COORDINATION CHEMISTRY OF MONODENTATE ORTHO-SUBSTITUTED ARYL PHOSPHINE LIGANDS

CHAPTER THREE

COORDINATION CHEMISTRY OF MONODENTATE *ORTHO*-SUBSTITUTED ARYL PHOSPHINE LIGANDS

3.1 Introduction:

This chapter is concerned with the coordination chemistry of two closely related *ortho*-substituted triarylphosphine ligands, *tris*-(*ortho*-methoxyphenyl)-phosphine (**17**) and (*ortho*-methoxyphenyl)diphenylphosphine (**18**). Both ligands bear the same type of substituents in the *ortho*-position of the aryl ring. However, in the latter ligand, only one phenyl ring is substituted, whilst in the former ligand, all the three rings are mono-substituted.

In Chapter Two, it was shown that *para*-substituents affect the coordination chemistry of phosphine ligands mainly from an electronic influence. Their position at the back of the aryl rings insulate the ligating atom from any steric effect. However, the coordination chemistry of triarylphosphine ligands incorporating substituents in the *ortho*-positions can be considerably influenced by the nature of these substituents from a steric as well as from an electronic effect since these substituents are close enough to the phosphorus to induce variations in its coordination to metal centres. In the literature, the *tris*-(*ortho*-methoxyphenyl)phosphine ligand is classified as a hemilabile bi-dentate ether-phosphine ligand.[1] It is capable of coordinating to metal centre through both, oxygen and phosphorus. The oxygen, considered as a "hard" Lewis base has been shown to form a labile bond upon coordination to a low-valent late transition-metal centre.[2] This sort of lability would be of interest in the area of homogeneous catalysis since cleavage of the metal-oxygen bond could be used to generate a vacant site at the metal centre for catalysis. The oxygen coordination usually occurs after one of the methoxy groups has been demethylated. In contrast, the mono-substituted aryl phosphine ligand forms relatively stable complexes in which

the ligand acts as a monodentate ligand *via* phosphorus only. A chelation could be achieved with demethylation acting as the driving force.[3]

The concept of hemilability of ether-phosphine ligands will be discussed in details in Chapter Four. However, delineating the behaviour of the ligand P(2-$CH_3OC_6H_4)_3$ (**17**) will be mentioned briefly here. Recently, it has been described that the reaction of the dirhodium tetraacetate $[Rh_2(O_2CCH_3)_4]$ with (**17**) yields the following metal chelates $[Rh_2(\mu\text{-}OAc)_3\{\mu\text{-}(2\text{-}OC_6H_4)P(2\text{-}MeOC_6H_4)_2\}(HOAc)]$ and $[Rh_2(\mu\text{-}OAc)_3\{\mu\text{-}(2\text{-}OC_6H_4)P(2\text{-}MeOC_6H_4)_2\}(NCMe)]$.[1] The latter complex is obtained by the recrystallisation of the former from MeCN:H_2O. An exchange process is detected in the former complex, where both methoxy groups are competing on the same coordination site on one rhodium(II) centre. This methoxy-rhodium bond is labile enough to be substituted by another more strongly coordinating ligand such as acetonitrile or CO under a carbon monoxide atmosphere, in $CDCl_3$. This substitution is highly dependent on the concentration of the substituting ligand.

The *ortho*-methoxyphenyldiphenylphosphine (**18**) has been shown to act in both mono- and bi-dentate modes.[3] It was the first ligand to be called "hemilabile".[4] Rauchfuss and Jeffrey noticed that phosphine-ether ligands bind well enough to allow isolation and purification, and readily dissociate the "hard" ligating atom, thus generating a vacant site allowing the substrate binding. A single crystal for $[RuCl_2\{PPh_2(2\text{-}CH_3OC_6H_4)_3\}_2].CH_2Cl_2$ complex (Figure 3.1) was studied by X-ray diffraction.[4]

Figure 3.1

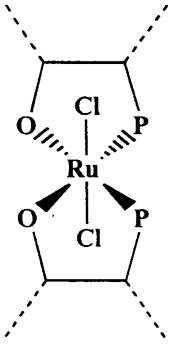

The coordination plane containing the two chelating phosphine ligands in a *cis* arrangement around the ruthenium(II) centre, is well defined. The Ru-O distances [2.299(3) and 2.257(3) Å] are much longer than the sum of the covalent radii (1.99 Å), which suggests that the oxygen atoms are weakly coordinated to the ruthenium(II) centre. This state is confirmed by the experimental observation that the oxygen atoms are readily displaced by a variety of ligands in solution. Ru-P distances are 2.217(1) Å and 2.219(1) Å compared with Ru-P distances in six-coordinate Ru(II) complexes with mutually *trans* phosphine ligands where values commonly range between 2.41 and 2.44 Å.[5] The shortness of Ru-P distances are in line with the fact that the long Ru-O distances are decreasing the oxygen *trans*-influence. The weak Ru-O bond does not affect the stability of the complex. Despite the aforementioned reactivity with a variety of ligands, the Ru(II) complex revealed a remarkably oxygen and heat stability.

In this chapter, the coordination of both phosphine ligands, (**17**) and (**18**), acting as monodentate ligands to platinum(II) and rhodium(III) metal centres, will be described. It is of interest to investigate how the methoxy groups affect the chemistry at the phosphorus centre without themselves being involved in any bonding to the metal centre.

3.2 Synthesis and Characterisation of $P(2\text{-}CH_3OC_6H_4)_3$ (17) and $PPh_2(2\text{-}CH_3OC_6H_4)$ (18):

The *ortho*-substituted phosphine ligands (**17**) and (**18**) have been previously reported.[3,6] Their synthesis is by the same general route[7] described for the *para*-substituted phosphine ligands (Chapter Two). Here, the starting material for both ligands is the *o*-bromoanisole which, on reaction with magnesium turnings in THF, yields the corresponding Grignard reagent (Scheme 3.1).

Scheme 3.1

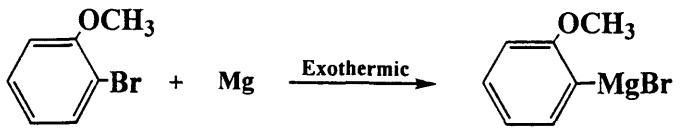

The *in situ* treatment of the Grignard reagent with trichlorophosphine or chlorodiphenylphosphine leads to the formation of the ligands (**17**) or (**18**) respectively (Scheme 3.2). The excess of Grignard reagent is removed on treatment with an aqueous solution of ammonium chloride.

Scheme 3.2

(17) when x=0
(18) when x=2

The singlet phosphorus chemical shift for (**17**) is at -39.3 ppm and that for (**18**) is at -16.9 ppm (both NMR experiments were run in $CDCl_3$). The ^1H NMR of the ligand (**17**) gives rise to a set of multiplets in the 7.20-6.70 ppm range, in addition to a singlet at 3.70 ppm that corresponds to the methoxy groups. However, the ^1H NMR of the ligand (**18**) exhibits more complicated signals in the aryl region (7.30-6.66 ppm) due to the existence of two different types of aryl rings. Its methoxy signal appears at 3.75 ppm. On comparing the *tris*-(*p*-methoxyphenyl)phosphine (**3**) to the *tris*-(*o*-methoxyphenyl)phosphine (**17**), it can be seen that moving the methoxy-groups from *para*- to *ortho*-position induces a shift to lower frequency in the phosphorus signal of ca. 30 ppm (from -9.9 ppm to -39.3 ppm). In general, the phosphorus chemical shift is closely related to the electronegativity of the groups attached to the phosphorus atom although it is also related to the steric effect.[8,9] Each methoxy group and the phosphorus are positioned *cis* to each other on adjacent atoms of the aryl ring, which allows the methoxy groups to be in close proximity to the phosphorus lone-pair, enhancing the electron density on the ligating atom and at the same time increasing the bulkiness of the ligand.[10] It is valuable to consider the link between the ligating ability of a substituted aryl phosphine ligand and the nature and position of the

corresponding substituent. Stemming from this idea, Grim *et al.*[11] published phosphorus chemical shift Group Contributions for aryl groups in phosphine ligands. A series is included in Table 3.1 allowing a comparison to be made between the ligands described in this work with similar triaryl substituted phosphine ligands.

Table 3.1
Phosphorus Chemical Shift Group Contributions for Aryl Groups in Tertiary Phosphines

Substituent	Group contribution
4-$CF_3C_6H_4$	-2.0
4-$CH_3OC_6H_4$	-3.4
3-$CF_3C_6H_4$	-1.7
3-$CH_3OC_6H_4$	-0.7
2-$CF_3C_6H_4$	-6.2
2-$CH_3OC_6H_4$	-12.8

In Table 3.1, the lowest Group Contribution is that corresponding to *meta*-substituted aryl phosphine ligands followed by the *para*-substituted type. The highest Group Contribution is that corresponding to *ortho*-substituted type. Moreover, the *ortho*-methoxyphenyl substituent has one of the highest Group Contributions and this is mainly due to its mesomeric and inductive donating effect. In addition, the position of the oxygen in close proximity to the lone-pair of electrons on the phosphorus causes a through-space electronic enhancement to the nucleophilicity of the latter atom. The Group Contributions, included in Table 3.1, account for the difference between the phosphorus chemical shift of ligand (**17**) and that of ligand (**18**). The two additional methoxy-groups in the former ligand shift the corresponding phosphorus signal to a lower frequency, compared to that of the latter.

The increase in the nucleophilicity of the phosphine ligand, caused by the *ortho*-methoxy groups, has been rationalised in terms of an anchimeric effect involving overlap of the empty 3d phosphorus orbital with the filled 2p orbital of the *ortho*-methoxy oxygen.[12] For example, kinetic studies carried out in acetone on the addition of triarylphosphine ligands $P(XC_6H_4)_3$ to the dienyl ring of $[(1\text{-}5\text{-}\eta^5\text{-}C_6H_7)Fe(CO)_3]^+$ revealed the following rate variation X: 2-MeO > 4-MeO > 4-Me > H >> 2-Me (relative rates $90/9/4/1/10^{-3}$).[12]

In general, 2-methoxyphenylphosphine ligands attract special interest in catalysis due to their capability to increase the rates of some oxidative addition reactions.[13] This characteristic is highly dependent on the direct interaction of the oxygen with the metal. The phosphorus, strongly bound to the metal centre, brings the methoxy groups in proximity to the metal centre, thus favouring an interaction. The oxidative addition reactions of the complexes: *trans*-$[Ir(CO)Cl\{PMe_2(2\text{-}CH_3OC_6H_4)\}_2]$, *trans*-$[Ir(CO)Cl\{PMe_2(4\text{-}CH_3OC_6H_4)\}_2]$ and *trans*-$[Ir(CO)Cl(PMe_2Ph)_2]$ towards a selection of electrophiles (X-Y) such as MeI, MeCOCl and PhCOCl, have been investigated.[13] From the rate of disappearance of the starting material, it was noticed that the iridium complex incorporating the $PMe_2(2\text{-}CH_3OC_6H_4)$ ligand reacted much faster than the iridium complex incorporating the PMe_2Ph ligand. In both cases, the readily formed product was exclusively the *trans*-$[Ir(CO)ClXY(L)_2]$ complex, where L is a relevant phosphine ligand (Figure 3.2). In contrast, the reaction of the *trans*-$[Ir(CO)Cl\{PMe_2(4\text{-}CH_3OC_6H_4)\}_2]$ complex afforded a mixture of products identified as different isomers for the configuration depicted in Figure 3.2.

Figure 3.2

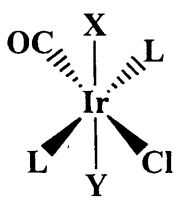

L = $PMe_2(2\text{-}CH_3OC_6H_4)$, PMe_2Ph.

The authors[13] suggested that, in the case of the $PMe_2(2\text{-}CH_3OC_6H_4)$ ligand, the direct electron donation from the ether oxygen towards the iridium metal would lower the activation energy required for the oxidative addition reaction. This donation is shown schematically in Figure 3.3. The ether oxygen and iridium(I) interaction is expected to be weak. However, it should become stronger upon the formation of the highly polar intermediates.[14]

Figure 3.3

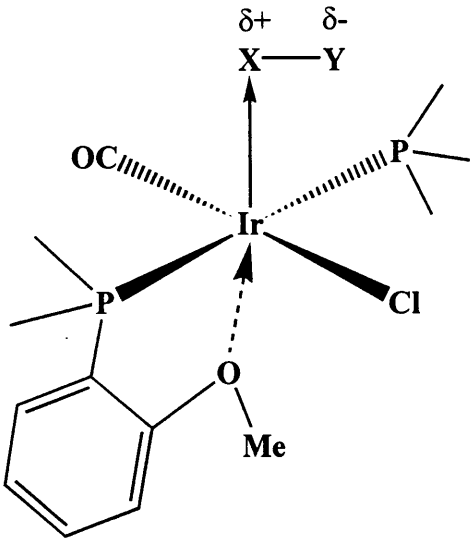

3.3 Preparation and Characterisation of Unsym.*cis*-[$Pt_2(\mu\text{-}Cl)_2Cl_2\{P(2\text{-}CH_3OC_6H_4)_3\}_2$] (19):

A crude phosphorus NMR experiment suggested that the reaction of the platinum(II) complex $[PtCl_2(CH_3CN)_2]$ with the ligand (**17**), in dichloromethane, afforded one platinum phosphine complex as a major product, in addition to a mixture of unidentified products (Scheme 3.3). Crystals suitable for X-ray diffraction studies precipitated out of the solution. A $^{31}P\{^1H\}$ NMR experiment, run on the dissolved crystals, confirmed that they correspond to the main product. The structural studies revealed an unsymmetrical *cis* platinum(II) dimer, unsym.*cis*-$[Pt_2(\mu\text{-}Cl)_2Cl_2\{P(2\text{-}CH_3OC_6H_4)_3\}_2]$ (**19**). Doubly-halogen bridged platinum(II) dimers are well known to

be synthetically important starting materials for the preparation of platinum(II) monomers, following the cleavage of the halogen bridge by nucleophiles such as amines, phosphines, olefins and carbonyl.[15,16] However, an unsymmetrical *cis* geometry around the two platinum centres is a relatively unusual arrangement, in comparison with the well established symmetrical geometry.[17]

Scheme 3.3

$$[PtCl_2(CH_3CN)_2] + L \rightarrow \textbf{Unsym.}\textit{cis}\textbf{-}[Pt_2(\mu\text{-}Cl)_2Cl_2L_2]\ \textbf{(19)}$$

$$+$$

Unidentified products

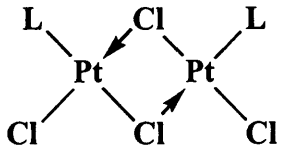

(19)

L = $P(2\text{-}CH_3OC_6H_4)_3$

The mass spectrum revealed the successive loss of two chlorine atoms from the platinum dimer (**19**) [m/z 1199 ($[M - Cl]^+$) and 1164 ($[M - 2Cl]^+$)]. The ^1H NMR spectrum was inconclusive, as the experiment solution contained a mixture of products. However, aryl protons gave rise to a set of multiplets in the expected region, 8.00-6.50 ppm. In the range 3.60-3.20 ppm, the spectrum exhibited singlets attributed to methoxy groups. The ^{31}P NMR spectrum was more informative as it was easy to identify one main product at 11.0 ppm flanked by satellites ($^1J_{Pt\text{-}P} = 2814$ Hz) assigned to the phosphorus atom in the platinum(II) dimer (**19**).

It has been suggested in the literature[18] that dinuclear platinum(II) phosphine complexes are actually intermediate complexes formed before bridge cleavage affords mononuclear platinum(II) phosphine complexes. This bridge cleavage is more rapid in the case of less sterically demanding phosphine ligands as compared to bulkier phosphine ligands. Therefore, the latter type of ligands should favour the formation of more stable dinuclear species than the former. Indeed, this hypothesis has been

confirmed following the preparation of a large set of doubly-halogen bridged platinum(II) dimers.[18] However, extremely bulky phosphine ligands, such as P(*o*-tolyl)$_3$, have been excluded from the hypothesis. In fact, the authors[18] were not able to isolate any platinum(II) species incorporating this ligand. In contrast, when using P(*m*-tolyl)$_3$ and P(*p*-tolyl)$_3$, they were able to isolate platinum(II) phosphine monomers. Interestingly, in this work, *cis*-[$Pt_2(\mu\text{-}Cl)_2Cl_2L_2$] (**19**) dimer [L = $P(2\text{-}CH_3OC_6H_4)_3$] has been prepared in which the phosphine ligand is considered as a highly bulky ligand,[19] especially when compared to the phosphine ligands that had been investigated in the literature.[18] It should be noted that there is a paucity of characterisation data for unsymmetrical *cis*-dinuclear platinum(II) phosphine complexes. However, the $^{31}P\{^1H\}$ NMR data of the complex (**19**) may be compared to those of unsym.*cis*-[$Pt_2(\mu\text{-}Cl)_2Cl_2(PPh_2C_6F_5)_2$].[18]

Table 3.2
$^{31}P\{^1H\}$ NMR Data of Unsym.*cis*-[$Pt_2Cl_4L_2$] Dimers

Complexes	Solvent	$^1J_{Pt\text{-}P}$/Hz
unsym.*cis*-[$Pt_2(\mu\text{-}Cl)_2Cl_2\{P(2\text{-}CH_3OC_6H_4)_3\}_2$] (**19**)[a]	$CDCl_3$	2814
unsym.*cis*-[$Pt_2(\mu\text{-}Cl)_2Cl_2(PPh_2C_6F_5)_2$].[10]	$CDCl_3$	2793

[a]. This work.

Since $P(2\text{-}CH_3OC_6H_4)_3$ is bulkier than the fluorinated phosphine ligand, the cone angle is larger and, hence, the s-character in the P-C bonds is expected to be larger. This should lead to a smaller Pt-P coupling constant in complex (**19**) but this is not observed. On the other hand, when a comparison between these complexes is based solely on the electronic factor, the ligand incorporating electron-donor substituents would be expected to induce an increase in the $^1J_{Pt\text{-}P}$ value when compared to that for the ligand incorporating electron-withdrawing substituents which correlates with the data in Table 3.2.

It has been observed that the dinuclear platinum(II) phosphine complexes of the type $[Pt_2(\mu\text{-}Cl)_2Cl_2(phosphine)_2]$ exist in solution as both *cis* and *trans*-isomers. In most of the cases, the major isomer, i.e. the *trans* one, is favoured by a bulkier phosphine ligand and by a more polar solvent. Since the *trans* configuration is the favoured one, it would be expected that its concentration should be larger than that of the *cis* isomer. This is of interest with respect to the isomerisation of complex unsym.*cis*-$[Pt_2(\mu\text{-}Cl)_2Cl_2\{P(2\text{-}CH_3OC_6H_4)_3\}_2]$ (**19**) that will be outlined subsequently in this chapter.

Figure 3.4
Crystal Structure of Unsym.*cis*-$[Pt_2(\mu\text{-}Cl)_2Cl_2\{P(2\text{-}CH_3OC_6H_4)_3\}_2]$ (19)

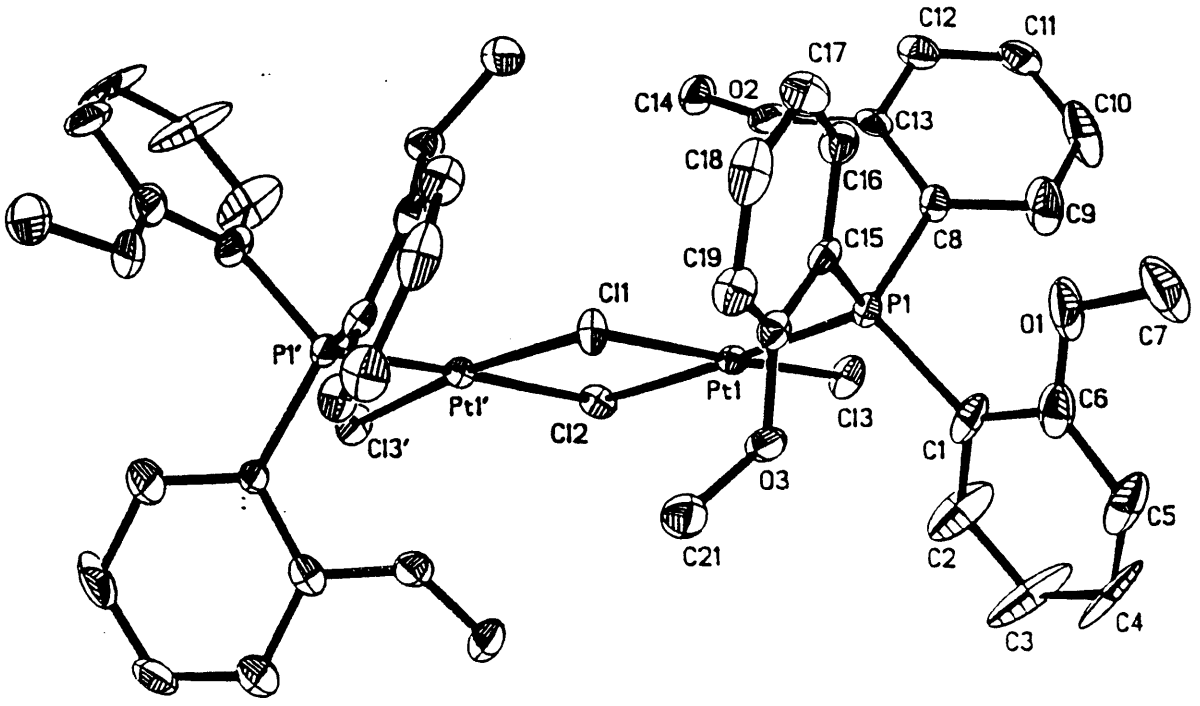

Table 3.3
Selected Bond Distances (Å) and Angles (°) with e.s.d. in Parentheses about Pt(II) for Unsym.*cis*-$[Pt_2(\mu\text{-}Cl)_2Cl_2\{P(2\text{-}CH_3OC_6H_4)_3\}_2]$ (19) complex.

Pt(1)-P(1)	2.233(4)	Pt(1)-Cl(3)	2.286(4)
Pt(1)-Cl(1)	2.322(3)	Pt(1)-Cl(2)	2.410(3)
Cl(1)-Pt(1')	2.322(3)	Cl(2)-Pt(1')	2.410(3)
P(1)-Pt(1)-Cl(3)	90.81(13)	P(1)-Pt(1)-Cl(1)	95.02(12)
Cl(3)-Pt(1)-Cl(1)	172.53(13)	P(1)-Pt(1)-Cl(2)	177.25(10)
Cl(3)-Pt(1)-Cl(2)	90.06(13)	Cl(1)-Pt(1)-Cl(2)	83.90(11)
Pt(1)-Cl(1)-Pt(1')	98.5(2)	Pt(1')-Cl(2)-Pt(1)	93.7(2)

The solid state structure of complex (**19**) (Figure 3.4) reveals a distorted square planar geometry around the metal centres, due to the large divergence of the inter-ligand angles from the theoretical 90 and 180°. The platinum-phosphine bond lengths are short compared to values from the literature such as those found in [PtCl(P(*t*-Bu)$_2$CHCH$_2$CH$_2$)]$_2$(μ-Cl)$_2$] [2.255(3) Å].[20,21] This observation explains the relatively large Pt-P coupling as a result of a certain correlation between the $^1J_{Pt\text{-}P}$ value and the Pt-P bond length. The other plausible explanation for this observation is that each platinum centre is coordinated only to one phosphine ligand. Thus, the steric bulkiness is reduced, inducing a decrease in the Pt-P bond length. The large *trans*-influence of the phosphine ligands induces a lengthening in the platinum-bridging chloride Cl(2) bonds *trans* to themselves compared to those *trans* to terminal chlorides. Moreover, the Pt(1)-Cl(1) [Cl(1) is *trans* to terminal chloride atoms] bond length [2.322(3) Å] is smaller than that of Pt(1)-Cl(2) [Cl(2) is *trans* to phosphine ligands] [2.410(3)Å], which is rationalised in terms of the difference in *trans*-influence between phosphine and chloride ligands. To be noted that the largest difference peak and hole data for (**19**) are +2.55 e at 1.58 Å from C(16) and –3.87 e at 0.58 Å from Pt(1).

After dissolving the crystals of complex (**19**) in dichloromethane, the $^{31}P\{^1H\}$ NMR spectrum revealed the existence of a different species in which the phosphorus environment is different to that in complex (**19**). The correspondent chemical shift of the phosphorus signal is at -10.4 ppm, split further by coupling to platinum(II) with a

value $^{1}J_{Pt\text{-}P}$ = 4240 Hz. The new complex has been characterised as the sym.*trans*-$[Pt_2(\mu\text{-}Cl)_2Cl_2\{P(2\text{-}CH_3OC_6H_4)_3\}_2]$ (**20**). The solvent has considerable influence on the configuration of this type of dimer, as well as on its final yield.[17] The more polar solvent favours the isomerisation of the complex (**19**) to give the *trans* geometry in complex (**20**).

It is also possible to prepare the dimer (**20**) by allowing Zeise's dimer' sym.*trans*-$[Pt_2(\mu\text{-}Cl)_2Cl_2(C_2H_4)_2]$ to react with two equivalents of the ligand (**17**) in refluxing 1,1,2,2-tetrachloroethane (Scheme 3.4). However, the resulting complex (**20**) is the major product but, mixed with a number of other unidentified products, it is hard to purify.

Scheme 3.4

sym.*trans*-$[Pt_2(\mu\text{-}Cl)_2Cl_2(C_2H_4)_2]$ + 2 L → sym.*trans*-$[Pt_2(\mu\text{-}Cl)_2Cl_2L_2]$ (**20**)

+

Unidentified products

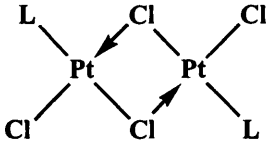

(**20**)

L = $P(2\text{-}CH_3OC_6H_4)_3$

Table 3.4
$^{31}P\{^{1}H\}$ NMR Data of Sym.*trans*-$[Pt_2Cl_4L_2]$ Dimers

Complexes	Solvent	$^{1}J_{Pt\text{-}P}$/Hz
sym.*trans*-$[Pt_2(\mu\text{-}Cl)_2Cl_2\{P(2\text{-}CH_3OC_6H_4)_3\}_2]$ (**20**) [a]	CD_2Cl_2	4240
sym.*trans*-$[Pt_2(\mu\text{-}Cl)_2Cl_2(PPh_3)_2]$[17]	$C_2H_2Cl_4$-$CDCl_3$ [b]	4100
sym.*trans*-$[Pt_2(\mu\text{-}Cl)_2Cl_2(PPh_2C_6F_5)_2]$[18]	$CDCl_3$	3740

[a]. This work. [b]. The NMR experiment was carried out at 55°C.

It is evident from data in Tables 3.2 and 3.4 that the $^{1}J_{Pt\text{-}P}$ for the *trans* isomer is larger than that for the *cis* isomer. In the unsym.*cis* isomer, both phosphine ligands are *trans* to the same chloride atom. Therefore, the *trans*-influence exerted by one of the phosphine ligands could be transmitted through the chloride bridge, weakening the Pt-P bond and thus, decreasing the $^{1}J_{Pt\text{-}P}$ value. This phenomenon does not exist in the sym.*trans* type of dimers, as each phosphine ligand is *trans* to a different chloride atom.

According to the data in Table 3.4, electron-donating substituents on the aryl rings of the phosphine ligand in complex (**20**) enhance the Pt-P bonding by increasing the $^{1}J_{Pt\text{-}P}$ value compared to that of the triphenyl phosphine analogue. An opposite trend has been observed with the complex incorporating an electron-withdrawing group on an aryl ring in the phosphine ligand. These data correlate with those included in Table 3.2 and are attributed to the strong electronic influence of the substituents on the phosphorus on the coordination of the phosphine ligand to the metal centre.

Comparing the two dimers in Table 3.2, the difference between the two coupling constants of the unsym.*cis* complexes is $\Delta J = 21$ Hz. However, the difference between the two coupling constants of the sym.*trans* complexes, included in Table 3.4, is $\Delta J = 500$ Hz. There is a large difference between the two ΔJ values, which is due to the fact that the σ-component is more dominant in the Pt-P bond when the phosphine ligands are *trans* to two different chloride bridges, compared to unsym.*cis* complexes. In the former case, electron-donating substituents on the aryl phosphine ligands would enhance the Pt-P bonding inducing a significant increase in the $^{1}J_{Pt\text{-}P}$ value. However, when the phosphine ligands are *trans* to the same chloride atom, they exert a *trans*-influence on each other through the same bridge. Therefore, in this case the π-component is more intense than in the sym.*trans* case and, consequently, the electron-donor groups will induce a smaller influence on the Pt-P bond.

Comparing the coordination chemical shift values for the dimers unsym.*cis*-$[Pt_2(\mu\text{-}Cl)_2Cl_2\{P(2\text{-}CH_3OC_6H_4)_3\}_2]$ (**19**) and sym.*trans*-$[Pt_2(\mu\text{-}Cl)_2Cl_2\{P(2\text{-}CH_3OC_6H_4)_3\}_2]$ (**20**) (50.3 and 28.9 ppm respectively), a large difference is detected

that could be attributed to an enhanced methoxy oxygen-platinum interaction in the former dimer. The difference in the intensity of oxygen-platinum interaction could be linked to the difference in steric requirements between both dimers.

3.4 Preparation and Characterisation of *trans*-[$PtCl_2${$P(2\text{-}CH_3OC_6H_4)Ph_2$}$_2$] (21):

The reaction of [$PtCl_2(CH_3CN)_2$] with two equivalents of $PPh_2(2\text{-}CH_3OC_6H_4)$ (**18**), at room temperature, afforded an air-stable platinum(II) phosphine monomer, *trans*-[$PtCl_2${$P(2\text{-}CH_3OC_6H_4)Ph_2$}$_2$] (**21**). This was the only isomer obtained from this reaction (Scheme 3.5).

Scheme 3.5

$$[PtCl_2(CH_3CN)_2] + 2\,L \rightarrow \textit{trans}\text{-}[PtCl_2L_2]\ (21).$$

L = $PPh_2(2\text{-}CH_3OC_6H_4)$

The *trans*-geometry was confirmed by a single band in the far IR spectrum at 340 cm^{-1}, assigned to a Pt-Cl stretching in a *trans*-square planar structure [$PtCl_2$(phosphine)$_2$]. The mass spectrum exhibited, in addition to the parent ion, the loss of two chlorine atoms successively [m/z 850 ($[M]^+$), 815 ($[M - Cl]^+$) and 779 ($[M - 2Cl]^+$)]. The ^1H NMR gave rise to a set of multiplets in the range 7.80-6.80 ppm assigned to the aromatic protons in different environments. It also exhibited a singlet at 3.70 ppm assigned to the methoxy group protons. The $^{31}P\{^1H\}$ NMR spectrum was more useful as it provided additional evidence that the geometry is *trans* around the metal centre. The $^1J_{Pt\text{-}P}$ value, 2716 Hz, falls in the range of those for similar *trans*-[$PtCl_2$(phosphine)$_2$] complexes. The formation of solely the *trans* isomer suggested a relative increase in the electron-donating properties of the ligand and/or on a steric effect forcing the resulting product to adopt a less sterically demanding geometry. $^{31}P\{^1H\}$ NMR data are included in Table 3.5 and compared to closely related platinum(II) phosphine complexes.

Table 3.5
Platinum-Phosphorus Coupling Constants for *trans* Platinum(II) Phosphine Complexes

Complexes	$^1J_{Pt\text{-}P}$/Hz
trans-[$PtCl_2\{P(2\text{-}CH_3OC_6H_4)Ph_2\}_2$] (**21**)[a]	2716
trans-[$PtCl_2\{P(4\text{-}HOC_6H_4)_3\}_2$] (**7**)[b]	2598
trans -[$PtCl_2\{P(C_6H_4)_3\}_2$][c]	2605

[a] This work. Recorded in CD_2Cl_2. [b] This work. Recorded in d^6acetone. [c] Ref. 22. Recorded in CH_2Cl_2.

In Chapter Two, it was noticed, while interpreting the NMR data of a set of *trans*-[$PtCl_2$(phosphine)$_2$] complexes, that the electron-donating substituents in the *para*-positions of the aryl rings had little effect on the platinum-phosphorus bonding. This observation was sustained by the fact that in the *trans*-isomers' case, the σ-component is not as dominant as in the *cis*-isomers' case. However, in Table 3.5, a clear increase in the $^1J_{Pt\text{-}P}$ value is observed when comparing complex (**21**) to its triphenylphosphine analogue and that is due to the large methoxy-group contribution enhancing the σ-character in the platinum-phosphorus bond.

The ligand (**18**) bearing one substituted aryl ring is less bulky than that bearing three substituted aryl rings (**19**). Therefore, it was possible to accommodate two phosphine ligands on the same metal centre. However, the adopted configuration is *trans*, as the ligands prefered to take mutually *trans* positions, decreasing steric interactions. In both types of complexes (**19**)/(**20**) and (**21**), the low steric interactions favoured the dominance of electronic factors on the metal-phosphine coordination.

The recrystallisation of the complex (**21**) from dichloromethane:hexane solution, afforded clear translucent crystals suitable for single crystal X-ray diffraction studies (Figure 3.5). Selected bond distances and angles for (**21**) are shown in Table

3.6. To be noted that the largest difference peak and hole data for (**21**) are +4.13 e at 0.89 Å from Pt(2) and –2.58 e at 0.90 Å from Pt(2).

Figure 3.5
Crystal Structure of *trans*-[$PtCl_2${$P(2\text{-}CH_3OC_6H_4)Ph_2$}] (21)

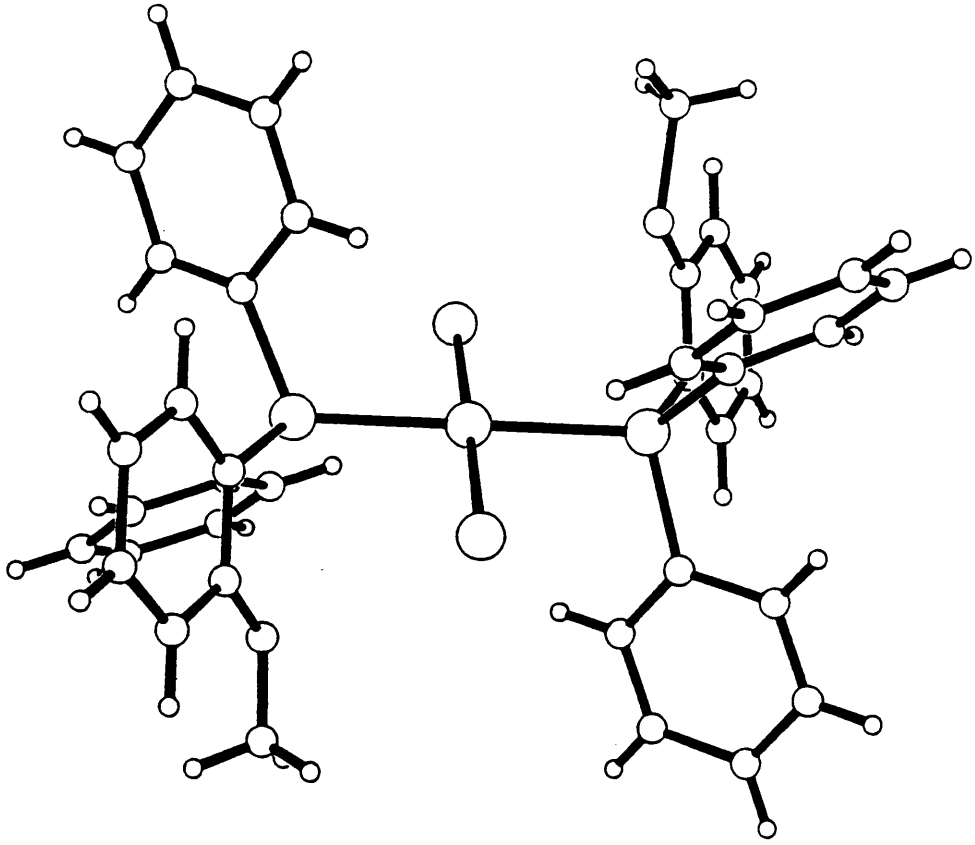

Table 3.6
Selected Bond Distances (Å) and Angles (°) with e.s.d. in Parentheses about Platinum(II) for *trans*-[$PtCl_2${$P(2\text{-}CH_3OC_6H_4)Ph_2$}$_2$] (21).

Pt-P(1)	2.306(11)	Pt-P(1')	2.306(11)
Pt-Cl(1)	2.326(10)	Pt-Cl(1')	2.326(10)
P(1)-Pt-P(1')	180.0(8)	Cl(1)-Pt-Cl(1')	180.0(5)
P(1)-Pt-Cl(1')	90.4(4)	P(1)-Pt-Cl(1)	89.6(4)
P(1')-Pt-Cl(1')	89.6(4)	Cl(1)-Pt-P(1')	90.4(4)

The crystal structure of the complex (**21**) (Figure 3.5) reveals an approximate symmetry around the platinum(II) centre. Comparing the Pt-P and Pt-Cl bond lengths

in complex (**21**) to those of *trans*-[$PtCl_2\{P(4\text{-}HOC_6H_4)_3\}_2$] (**7**) (Table 2.6), no significant difference is observed. Thus, the steric bulk of the ligand (**18**) is not inducing the expected elongation in the Pt-P bond. Therefore the electronic factor is dominant, confirming the conclusion drawn from the NMR data. Moreover, when comparing the angles around the platinum centre in complex (**21**) to those in complex (**7**), the angles in the former are closer to the theoretical values in a square planar complex (90°). This difference could be due to steric strain induced by certain hydrogen bonding in complex (**7**) causing a deviation from the theoretical values.

3.5 Preparation and Characterisation of $[(\eta^5\text{-}C_5Me_5)Rh\{P(2\text{-}CH_3OC_6H_4)Ph_2\}Cl_2]$ (22):

Treatment of the dinuclear rhodium(III) complex $[\{(\eta^5\text{-}C_5Me_5)Rh(\mu\text{-}Cl)Cl\}_2]$ with two equivalents of $P(2\text{-}CH_3OC_6H_4)Ph_2$ (**18**) affords the monomeric rhodium(III) complex $[(\eta^5\text{-}C_5Me_5)Rh\{P(2\text{-}CH_3OC_6H_4)Ph_2\}Cl_2]$ (**22**) (Scheme 3.6).

Scheme 3.6

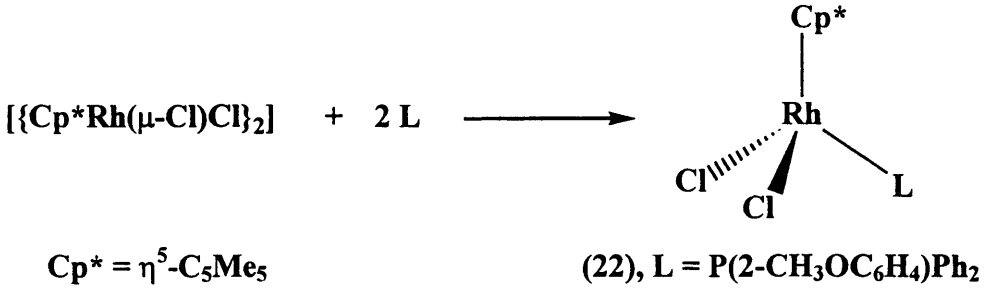

The mass spectrum reveals successive loss of two chlorine atoms [m/z 565 ($[M - Cl]^+$) and 530 ($[M - 2Cl]^+$)]. The ^1H NMR spectrum exhibits a doublet at 1.34 ppm ($J_{P\text{-}H}$ ca. 3 Hz) assigned to the Cp* protons coupling to the phosphorus atom. The methoxy-group signal is a singlet at 3.30 ppm and the aryl protons give rise to a set of multiplets in the 8.15-6.83 ppm range. There are twice as many multiplets in the aryl proton region of the complex (**22**) compared to the free phosphine ligand (**18**). This observation indicates the existence of inequivalent aryl protons in the phosphine ligand bound to the metal centre, that are equivalent in the free ligand. The high steric effect induced by the bulkiness of the phosphine ligand is the main factor in causing

hindered rotation around the rhodium-phosphorus bond.[23] The $^{31}P\{^{1}H\}$ NMR data shown in Table 2.13 (Chapter Two) confirm that the introduction of either a methoxy or a hydroxy group in the *para*-position of the phenyl ring in the triarylphosphine ligand does not significantly affect the coupling constant $^{1}J_{Rh-P}$. The same conclusion could be derived from complex (**22**) (Table 3.7).

Table 3.7
$^{31}P\{^{1}H\}$ NMR data for [Cp*Rh(L)Cl$_2$]

L	Δ/ppm [d]	$^{1}J_{Rh-P}$/Hz
P(*p*-$CH_3OC_6H_4)_3$ (**15**)[a]	38.8	144
P(*p*-$HOC_6H_4)_3$ (**16**)[b]	37.2	143
PPh_3 [c]	35.2	144
P(2-$CH_3OC_6H_4)Ph_2$ (**22**)[a]	45.3	142

[a] This work. Recorded in $CDCl_3$. [b] This work. Recorded in DMSO. [c] Ref. 24. [d]
$\Delta = \delta_{P(complex)} - \delta_{P(free\ ligand)}$.

From Table 3.7, there is a large increase in the phosphorus coordination chemical shift Δ for complex (**22**) compared to that for the other rhodium complexes, and comparable to that observed for the unsym.*cis*-[$Pt_2(\mu\text{-}Cl)_2Cl_2\{P(2\text{-}CH_3OC_6H_4)_3\}_2$] (**19**) dimer. The most plausible explanation for this increase is a direct interaction between the metal and the methoxy group. This type of interaction has been observed in the literature[13] and considered an important factor in facilitating the oxidative addition reactions of similar metal phosphine complexes. The same direct interaction could be an additional argument for a hindered rotation around Rh-P deduced from the ^{1}H NMR spectrum.

The dinuclear rhodium(III) complex [$\{(\eta^5\text{-}C_5Me_5)Rh(\mu\text{-}Cl)Cl\}_2$] did not react with the ligand P(2-$CH_3OC_6H_4)_3$ (**17**). The experiment was carried out under different conditions: both dichloromethane and acetone were used as solvents and the reactions

were done both in aerobic and anaerobic conditions. Moreover, the reactions were carried out either at room temperature or under refluxing conditions. The $^{31}P\{^{1}H\}$NMR spectrum did not exhibit any rhodium-phosphorus coupling. The steric effect in this type of complex could be hindering the reaction of the mentioned dinuclear rhodium(III) complex with the *tris*-substituted triarylphosphine ligand (**17**).

3.6 Summary:

According to this work, both phosphine ligands $P(2\text{-}CH_3OC_6H_4)_3$ (**17**) and $PPh_2(2\text{-}CH_3OC_6H_4)$ (**18**) acted solely as mono-dentate ligands, making use of the phosphorus lone pair. This is despite the plausible methoxy oxygen-metal interaction detected in the complexes prepared.

The unsym.*cis*-$[Pt_2(\mu\text{-}Cl)_2Cl_2\{P(2\text{-}CH_3OC_6H_4)_3\}_2]$ (**19**) dimer was prepared. It isomerised to sym.*trans*-$[Pt_2(\mu\text{-}Cl)_2Cl_2\{P(2\text{-}CH_3OC_6H_4)_3\}_2]$ (**20**) in dichloromethane. In both complexes (**19**) and (**20**), each platinum centre was bound to only one phosphine ligand. Thus, the reduction of the steric bulkiness around the metal gave advantage to the electronic factor over the steric one in manipulating the phosphine bonding to the metal centre. The same conclusion was derived from the characterisation of the *trans*-$[PtCl_2\{P(2\text{-}CH_3OC_6H_4)Ph_2\}_2]$ (**21**) complex, where the two phosphine ligands were mutually *trans* on the platinum(II) centre. This arrangement favoured a decrease in the steric interactions between both ligands. However, the steric effect was the dominant factor in the $[(\eta^5\text{-}C_5Me_5)Rh\{P(2\text{-}CH_3OC_6H_4)Ph_2\}Cl_2]$ (**22**) complex and it has clearly affected the rhodium-phosphorus bonding. This was mainly due to the bulkiness of the ligating groups to Rh(III) and to the general steric hindrance in the whole structure of $[Cp^*Rh(L)Cl_2]$ complexes.

Chapter Three References

[1] F. P. Prucknik, R. Starosta, M. W. Kowalska, E. Galdecka, Z. Galdecki and A. Kowalski, *J. Organomet. Chem.*, 2000, **597**, 20.

[2] I. Le Gall, P. Laurent, E. Soulier, J.-Y. Salaün and H. des Abbayes, *J. Organomet. Chem.*, 1998, **567**, 13.

[3] C. E. Jones, B. L. Shaw and B. L. Turtle, *J. Chem. Soc. Dalton Trans.*, 1974, 992.

[4] J. C. Jeffrey and T. B. Rauchfuss, *Inorg. Chem.*, 1979, **18**, 2658.

[5] B. L. Haymore and J. A. Ibers, *J. Am. Chem. Soc.*, 1975, **97**, 5369.

[6] B. B. Jarvis and B. A. Marien, *J. Org. Chem.*, 1976, **41**, 2182.

[7] A. E. Sinear, W. Valient and J. Wirth, *J. Org. Chem.*, 1960, **25**, 2001.

[8] J. M. Jenkins and B. L. Shaw, *J. Chem. Soc. (A)*, 1966, 770.

[9] A. Pidcock, *J. Chem. Soc., Chem. Commun.*, 1968, 92.

[10] a) J. H. Letcher and J. R. Vanwazer, *J. Chem. Phys.*, 1966, **44**, 815.
b) H. S. Gutowski and J. Larmann, *J. Am. Chem. Soc.*, 1965, **87**, 3815.

[11] S. O. Grim and A. W. Yankowsky, *Phosphorus and Sulfur*, 1977, **3**, 191.

[12] J. G. Atton and L. A. P. Kane-Maguire, *J. Organomet. Chem.*, 1982, **226**, C43 and references cited therein.

[13] E. M. Miller and B. L. Shaw, *J. Chem. Soc., Dalton Trans.*, 1974, 480.

[14] P. B. Chock and J. Halpern, *J. Am. Chem. Soc.*, 1966, **88**, 3511.

[15] N. M. Boag and M. S. Ravetz, *J. Chem. Soc., Dalton Trans.*, 1995, **21**, 3473.

[16] K. R. Dixon and D. J. Hawke, *Can. J. Chem.*, 1971, **49**, 3252.

[17] W. Baratta and P. S. Pregosin, *Inorg. Chim. Acta*, 1993, **209**, 85.

[18] I. M. Al-Najjar, *Inorg. Chim. Acta*, 1987, **128**, 93.

[19] a) C. A. Tolman, *Chem. Rev.*, 1977, **77**, 313 and references cited therein.
b) G. K. Anderson, H. C. Clark and J. A. Davies, *Inorg. Chem.*, 1981, **20**, 3607 and references cited therein.

[20] B. L. Simms, M. Shang, J. Lu, W. J. Youngs and J. A. Ibers, *Organometallics*, 1987, **6**, 1118.

[21] A. G. Orpen, L. Brammer, F. H. Allen, O. Kennard, D. G. Watson and R. Taylor, *J. Chem. Soc., Dalton Trans.*, 1989, S56 and S67.

[22] M. Gómez, G. Muller, D. Sainz and J. Sales, *Organometallics*, 1991, **10**, 4036.

[23] W. D. Jones and F. J. Feher, *Inorg. Chem.*, 1984, **23**, 2376.

[24] J. H. Holloway, E. G. Hope and G. C. Saunders, unpublished work.

CHAPTER FOUR

COORDINATION CHEMISTRY OF THE TRIS-(ORTHO-HYDROXYPHENYL)PHOSPHINE LIGAND

CHAPTER FOUR

COORDINATION CHEMISTRY OF THE *TRIS-(ORTHO-*HYDROXYPHENYL)PHOSPHINE LIGAND

4.1 Introduction:

In Chapter One, the concept of chelation was introduced and a very interesting topic in this type of chemistry is related to the coordination of chelating agents bearing mixed ligating functionalities. To investigate this area further, the preparation and coordination chemistry of the *tris*-(*o*-hydroxyphenyl)phosphine (**23**) (Figure 4.1) is described in the present chapter.

Figure 4.1
***tris*-(*o*-hydroxyphenyl)phosphine (23)**

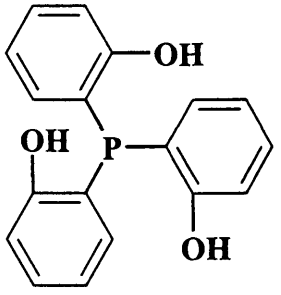

In 1961, Neunhoeffer and Lamza[1] were the first to synthesise the *tris*-(*o*-hydroxyphenyl)phosphine ligand which they were able to isolate and characterise, by elemental analysis, as a monohydrate: $C_{18}H_{15}O_3P.H_2O$ (Molecular Weight 328.3). It should be noted that the two ligating groups are different according to the Lewis classification, i.e. the phosphorus is a "soft" Lewis base while the oxygen is a "hard" Lewis base. Thus, these two atoms are expected to bind differently to the transition metals. The phosphine ligand (**23**) exhibits several interesting characteristics; in addition to its chelating capabilities, the position of the hydroxy groups in the *ortho*-positions of the aryl rings imposes significant electronic and steric requirements.[2-4]

This chapter includes general introductions to the main aspects of chelation, such as the thermodynamic aspects and the ring contributions, to the specific class of chelating agents, the phosphorus-oxygen based ligands, and to the concept of hemilability. In addition, examples from the application of metal chelates are described. Subsequently, the coordination chemistry of the *tris*-(*o*-hydroxyphenyl)phosphine ligand to late transition-metals such as platinum(II), rhodium(I) and rhodium(III), is discussed.

4.2 Thermodynamic Aspects, the "*CHELATE EFFECT*":

For a system in equilibrium, the standard free energy change $\Delta G°$ is related to the equilibrium constant K^T according to the Equation 4.1:

$$\Delta G° = -RTLnK^T \qquad \textbf{Equation 4.1}$$

$\Delta G°$ is related to the *enthalpy* change $\Delta H°$ and to the *entropy* change of the system according to the Equation 4.2:

$$\Delta G° = \Delta H° - T\,\Delta S° \qquad \textbf{Equation 4.2}$$

Schwarzenbach[5] proposed the term "chelate effect" to describe the increased stability brought to the complex by the formation of a metal chelate. He related this effect to changes in thermodynamic quantities accompanying the complex formation. A more stable complex features a higher equilibrium constant K^T, which implies a more negative standard free energy change, according to Equation 4.1. A more negative standard free energy change implies a more negative *enthalpy* change or a more positive *entropy* change or the combination of both these changes according to Equation 4.2. On the assumption that *enthalpy* changes associated with the formation of metal-ligand bonds are the same, whether the ligands were unidentate or chelating, Schwarzenbach concluded that the special stability attributed to chelation is mainly due to the favourable *entropy* changes, which accompany the complexation reaction.

Thermodynamic data are available for many chelation reactions. Herein, an example is illustrated:

Thermodynamic data for the reactions of aqueous ions Mn^{2+}, Fe^{2+} and Ni^{2+} with 2,2',2''-triaminoethylamine {tren= $N(CH_2CH_2NH_2)_3$} and with ethylenediamine (en), according to Schemes 4.1 and 4.2, are listed in Table 4.1.[6]

Scheme 4.1

$$\mathbf{M(H_2O)_6^{2+}(aq) + tren\ (aq) \rightarrow M(tren)\ (H_2O)_2^{2+}(aq) + 4H_2O\ (l)}$$

Scheme 4.2

$$\mathbf{M(H_2O)_6^{2+}(aq) + 2en(aq) \rightarrow\ M(en)_2(H_2O)_2^{2+}\ (aq) + 4H_2O\ (l)}$$

These data establish that the *enthalpy* changes for the formation of the tren complexes are less exothermic than those for the formation of en complexes by 13 to 17 $kJmol^{-1}$, and this has been attributed,[7] partly, to the steric strain resulting from the presence of three chelate rings {as opposed to only two in the (en) complexes}, and partly to the inherently lower strength of the M-N bond when N is a tertiary nitrogen atom {as opposed to the primary nitrogen atom in (en)}.

Table 4.1 (a and b) Thermodynamic Data for the Formation of Some Complex Ions in Aqueous Solution. $\Delta G^{\varnothing}$, $\Delta H^{\varnothing}$, and $T\Delta S^{\varnothing}$ in $kJmol^{-1}$; $\Delta S^{\varnothing}$ in $kJK^{-1}mol^{-1}$

(a) $[M(H_2O)_6]^{2+}$ (aq) + tren (aq) → $[M(tren)(H_2O)_2]^{2+}$ (aq) + $4H_2O$ (l)

Metal	$\Delta H^{\varnothing}_{298}$	$\Delta S^{\varnothing}_{298}$	$T\Delta S^{\varnothing}_{298}$	$\Delta G^{\varnothing}_{298}$
Mn	-12.6	69	20.7	-33.3
Fe	-26.4	77	23.1	-49.5
Ni	-63.4	92	27.5	-90.9

(b) $[M(H_2O)_6]^{2+}$ (aq) + 2en (aq) → $[M(en)_2(H_2O)_2]^{2+}$ (aq) + $4H_2O$ (l)

Metal	$\Delta H^{\varnothing}_{298}$	$\Delta S^{\varnothing}_{298}$	$T\Delta S^{\varnothing}_{298}$	$\Delta G^{\varnothing}_{298}$
Mn	-25.2	8	2.5	-27.7
Fe	-43.5	0	0	-43.5
Ni	-76.4	13	3.8	-80.2

However, the *entropy* changes for the formation of the tren complexes are more positive compared to those for the formation of the en complexes. This difference stems from the fact that in Scheme 4.1 there are only two species as starting materials and five as products, whereas, in Scheme 4.2 there are three species as starting materials and five as products. Thus, there is a relative increase in the number of species resulting from chelation in Scheme 4.1, which does not occur in Scheme 4.2. The greater the number of chelate rings which one ligand can form, the greater the relative increase in the number of species produced in a reaction and, hence, the more favourable the "disorder" within the system, in other terms, the more favourable the change in *entropy*.

4.3 Δ_R Ring Contributions To ^{31}P NMR Parameters of Transition-Metal-Phosphorus Chelates:

In 1972, Shaw *et al.*[8] proclaimed a linear correlation between the ^{31}P chemical shifts for the free tertiary phosphine (δF) and the change in chemical shift on coordination "Δ". From the relationship, $\Delta = \mathbf{A}\ \delta\mathbf{F} + \mathbf{B}$, coordination shifts of phosphines can be predicted, once enough analogues are known for calculations of the two constants A and B. About ten years later, Garrou[9] reported in a review that such a correlation does not exist in the case of chelating agents for which the chemical shifts fall outside the range predicted by the $\Delta = A\ \delta F + B$ relationship. However, he postulated that the mode of bonding in bidentate ligands could be determined through knowledge of the empirical relationship between ring chelation and the δP values (δP = chemical shift of the phosphorus atom under study). In order to sustain such a discussion, a new parameter, Δ_R, was introduced and defined as the difference between the coordination chemical shift, Δ, of a *cis*-disubstituted phosphine complex and the coordination chemical shift of an equivalent phosphorus atom in a chelate complex. Δ_R is called the "ring contribution" to a ^{31}P chemical shift. However, an approximation is almost always required since it is difficult to find an exact match of chelate and bis-monodentate ligand complexes and the best calculations are made for molecules which allow internal comparisons such as in the complex **A** (Figure 4.2). Here, the phosphorus atom P_C is *ortho*-metalated triphenylphosphite and *trans* to a triphenylphosphite ligand and it can be compared with P_A which is an unmetalated triphenylphosphite ligand and *trans* to a triphenylphosphite ligand. Similarly, the phosphorus atom P_D is *ortho*-metalated triphenylphosphite and occupies a position *trans* to a σ-bound phenyl group and it can be directly compared with P_B which is an unmetalated triphenylphosphite ligand *trans* to a σ-bound phenyl group. In this system, the Δ_R values for the five-membered rings are in good agreement.

Figure 4.2. Complex A

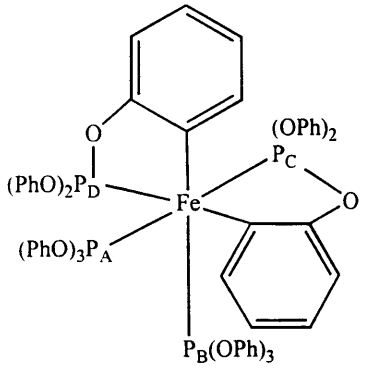

Table 4.2. ^{31}P NMR Data of Complex A

δP	Δ_R
+144.2 (A)	
+149.5 (B)	
+176.4 (C)	+33.2
+180.8 (D)	+31.1

Although the theoretical aspects of the Δ_R are not yet clear, knowledge of its contribution to the δP value is invaluable in making structural assignments in phosphine transition metal complexes. In 1961, Merriwether[10] examined the phosphorus chemical shifts of a set of nickel carbonyl phosphine complexes (Figure 4.3).

Figure 4.3

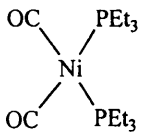

δP = +20.7

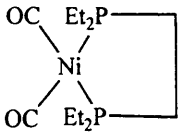

δP = +48.6

The author noticed the shift to higher frequency of the phosphorus signal in the metal chelate $[Ni(CO)_2(Et_2PCH_2CH_2PEt_2)]$ compared to that in $[Ni(CO)_2(PEt_3)_2]$. Hence, the following conclusion was postulated, "it might be possible to use this unusually large resonance shift as a diagnostic test for the presence of phosphorus in a 4- or 5-membered ring." In 1980, Mazanec *et al.*[11] published interesting phosphorus NMR data for a set of rhodium poly(phosphine) nitrosyl complexes (Figure 4.4).

Figure 4.4
δP in ppm. P_B and P_C are bound to two phenyl rings.
P_A is bound to one only. These phenyl rings have been omitted for clarity.

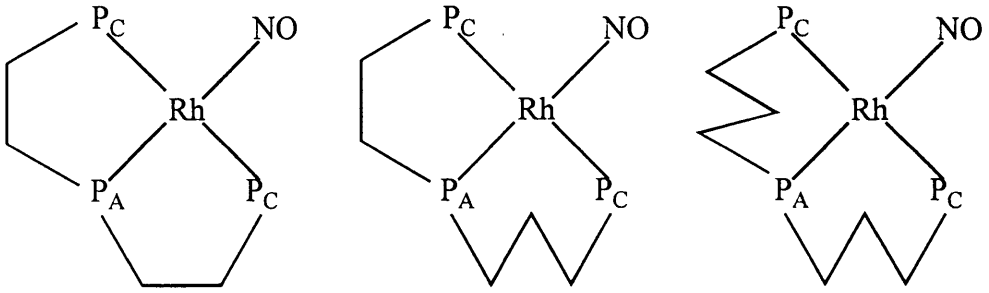

A	B	C
$\delta P_A = +89.3$	$\delta P_A = +56.0$	$\delta P_A = +18.8$
$\delta P_B = +69.7$	$\delta P_B = +68.9$	$\delta P_C = +29.2$
	$\delta P_C = +30.2$	

The δP_B values of +69.7 and +68.9 in complexes **A** and **B** for a phosphorus in a 5-membered ring occur at about 40 ppm to higher frequency to that of P_C in complexes **B** and **C** where 6-membered rings are present. The differences between these chemical shifts reflect the influence of the size of the ring. The much larger high frequency shift in δP_A between complexes A and C arises from the same effect, except that P_A exists at the bridgehead of two chelate rings. If δP_A resonances have equal contributions from both rings, that for P_A in complex B should appear midway between the δP_A resonance in **A** (+89.3) and that in **C** (+18.8); i.e. ca. +54 ppm. The good agreement between the experimental data and this calculated chemical shift is proof that an additive effect in Δ_R occurs.

4.4 Phosphorus-Oxygen Based Ligands:

Hybrid bidentate ligands incorporating phosphorus as the substitutionally inert ligating atom, and oxygen as the substitutionally labile ligating atom, have been extensively studied. This interest stems from the fact that these ligands feature characteristics enabling them to be useful in various catalytic processes,[12,13-15] small

molecule activation,[16,17] and the stabilisation of unusual ligand bonding modes in transition metal complexes in comparison to their non-chelated analogues.[18,19] The first ligand in this class to be called "hemilabile" was the *ortho*-methoxyphenyldiphenyl-phosphine (**18**).[20] Recently, the preparation of a set of Rh(I) bidentate phosphine complexes have been published (Schemes 4.3, 4.4, and 4.5).[21]

Scheme 4.3. R = Et, iPr.

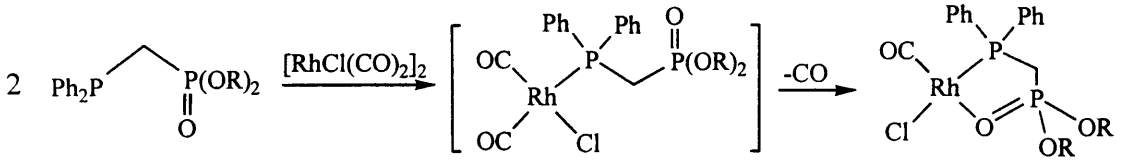

A

Scheme 4.4

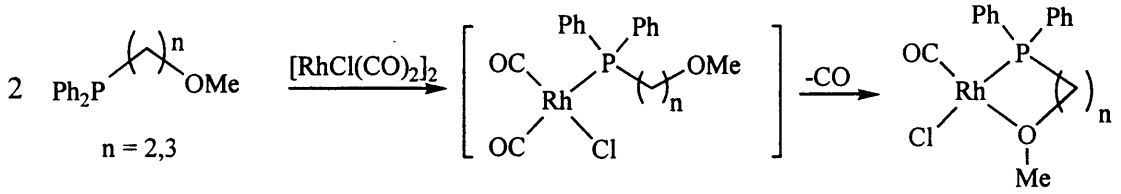

B

Scheme 4.5

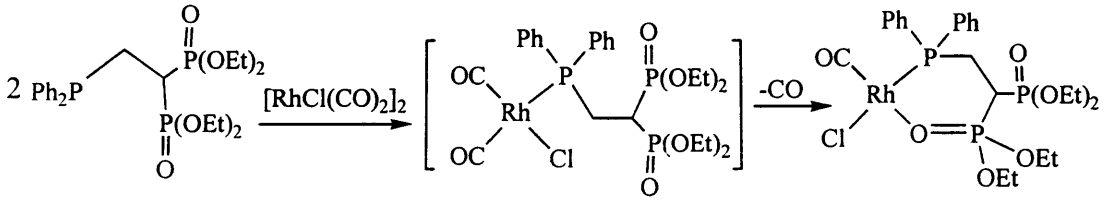

C

The crystal structure of complex **A** reveals a P=O bond length [1.490(7) Å] longer than the P=O bond length in an uncoordinated phosphonate group,[22] confirming the presence of a rhodium-oxygen interaction. In order to show the hemilabile behaviour of the bidentate ligands at the Rh(I) centre, CO gas was bubbled, at room temperature,

through a dichloromethane solution of complexes **A** and **B** under nitrogen. The result was that the chelate ring was broken according to Scheme 4.6.

Scheme 4.6

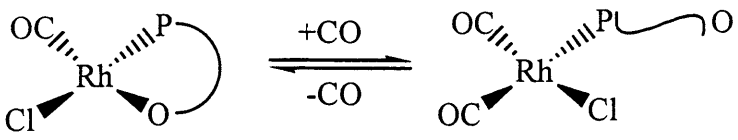

The phosphorus NMR spectrum of complex **C** (Scheme 4.5), at 0°C, reveals the lability of the phosphonate function. It shows three signals at 42.9, 27.1 and 19.0 ppm, ascribed to the phosphine, free phosphonate, and the coordinated phosphonate groups respectively. Increasing the temperature results in a coalescence of the last two signals, which are replaced by only one signal at 22.4 ppm (60°C).

4.5 Hemilability:

The coordination chemistry of ligands incorporating mixed functionalities to transition metal centres has been receiving increased attention recently.[12,23,24] More specifically, attention has concentrated on homogeneous transition metal catalysis, metal complex small molecule activation, chemical sensing, and the stabilisation of reactive, unsaturated transition metal species.

In 1979, Jeffrey and Rauchfuss[20] were the first to introduce the concept of hemilability to coordination chemistry. Hemilabile ligands contain both substitutionally inert and substitutionally labile groups. The ligands are called hemilabile ligands because they incorporate weakly chelating groups (substitutionally labile groups) that are capable of, temporarily, holding coordination sites at reactive transition-metal centres, in the absence of substrates. However, in the presence of substrates, such weak temporary bonds are easy to dissociate from the transition metal centre allowing the formation of a free coordination site (Figure 4.5). The other group of the chelating agent is the substitutionally inert group. The main advantage of this

arrangement is that the labile group is kept in close proximity to the transition metal centre such that recoordination can occur in the absence of a substrate (Figure 4.5). At this stage, the chelate effect of the bidentate ligand confers stability to the catalyst precursor.

Figure 4.5

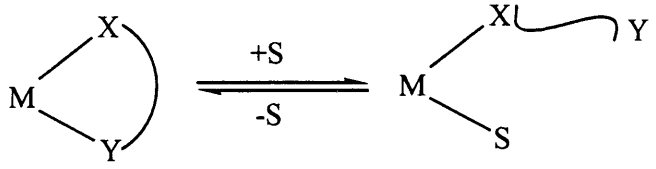

The hemilability of a chelate could be observed *via* a study of the fluxionality of the substitutionally labile groups. Several exchange reactions involving fluxional ligands have been studied. Herein, three examples are briefly illustrated.

- Lindner and co-workers[25] have studied the behaviour of two ether-phosphine bidentate ligands coordinated to ruthenium (Scheme 4.7):

Scheme 4.7

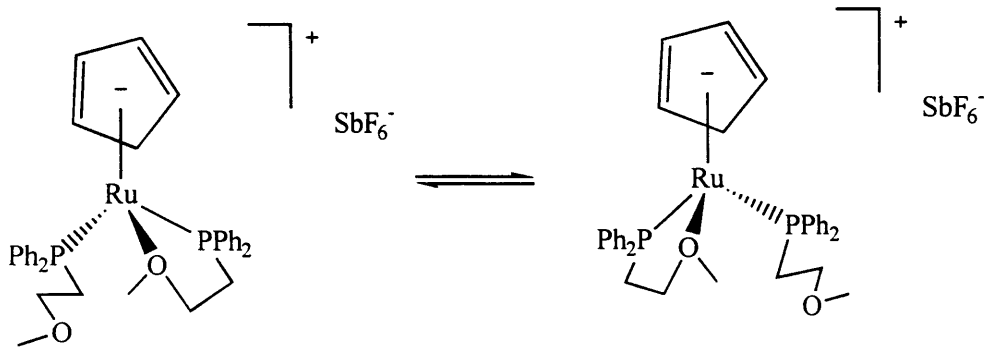

Such fluxional processes have been called an "opening and closing" reaction or a "wind screen wiper" reaction.[26]

- Orrell *et al.*[27] have studied the behaviour of the 2,6-diacetylpyridine (DAP) ligand in *fac*-[ReCl(CO)$_3$(DAP)] (Scheme 4.8), and have called this fluxional process, a "tick-tock" reaction.

Scheme 4.8

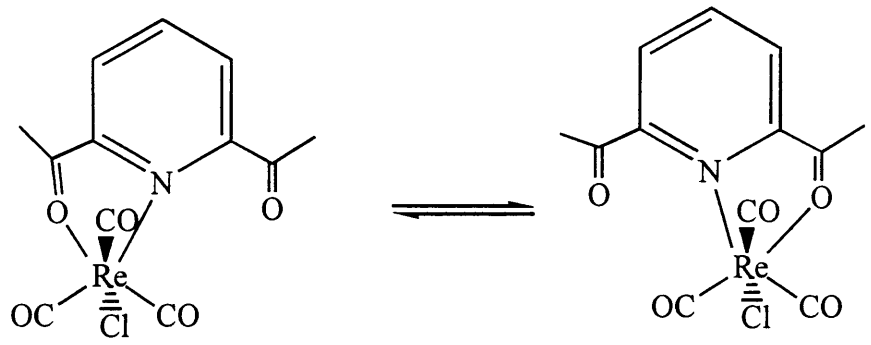

- Others[28] have observed hemilability *via* ligand "interchange" reactions. Such kinds of reactions involve equilibrium between weakly bound groups of hemilabile ligands and coordinating counterions. For example, interchange between two pendant ether groups and two triflate counterions was observed by Chadwell *et al.* (Scheme 4.9).[28a]

Scheme 4.9

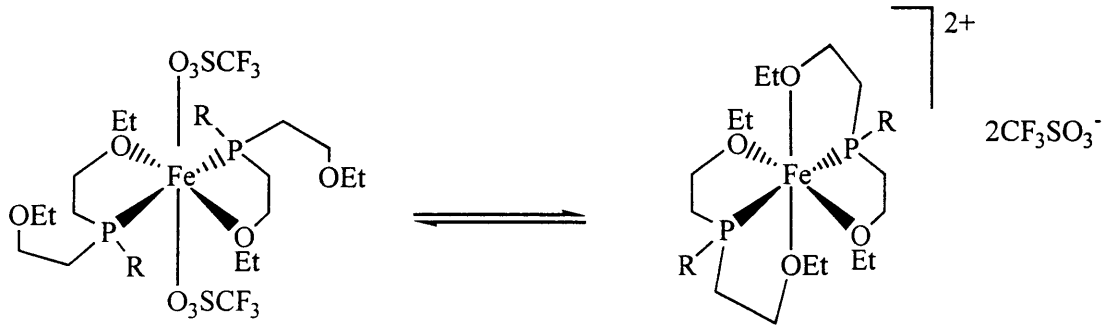

R = CH_2Ph

4.6 Applications:

There have been widespread application of the chelate effect industrially and medically (for example, in chelation therapy, chemotherapeutic agents and metal sequestration, extraction and separation), this has included commercialisation of processes incorporating hemilability. Dunbar *et al.*[29,30] revealed the ability of the Rh(I) complex $[Rh(TMPP)_2(CO)][BF_4]$ [TMPP = *tris*-(2,4,6-trimethoxyphenyl)phosphine] as an *optical-based CO sensor*. They were able to show that this complex could be used to reversibly and selectively sense CO in the presence of O_2, CO_2, N_2 and H_2 under atmospheric conditions (Scheme 4.10)

Scheme 4.10. Ar = TMPP.

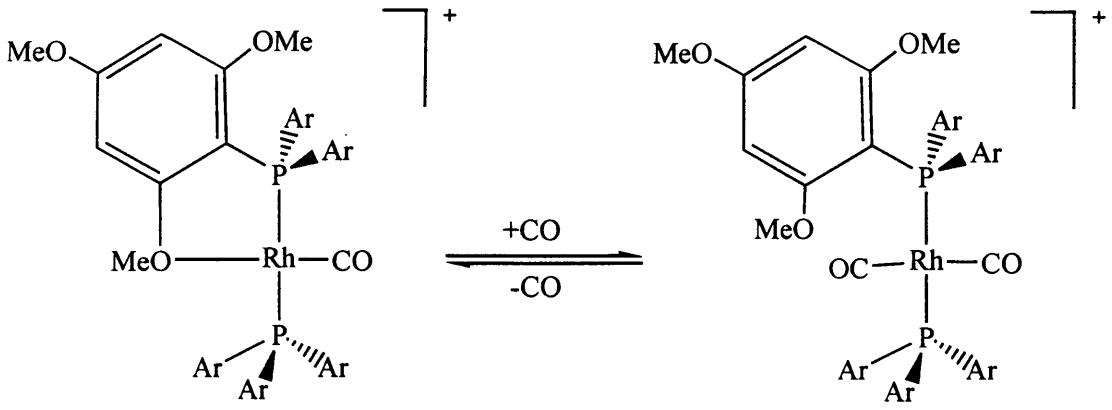

The uptake of a CO molecule by rhodium(I) occurs following breakage of the bond between the rhodium(I) centre and the substitutionally labile methoxy group.

4.7 Synthesis of $P(2\text{-}HOC_6H_4)_3$ (23):

The synthesis of the *ortho*-substituted triarylphosphine ligand (**23**) follows the slightly modified literature route[6] already described in the synthesis of the *para*-substituted triarylphosphine ligand (**5**).

The *tris*-(*o*-methoxyphenyl)phosphine ligand (**7**), the preparation of which was described in Chapter Three, was demethylated by reaction with hydrobromic acid

overnight under nitrogen, to yield the *tris*-(*o*-hydroxyphenyl)phosphine hydrobromide salt (Scheme 4.11):

Scheme 4.11

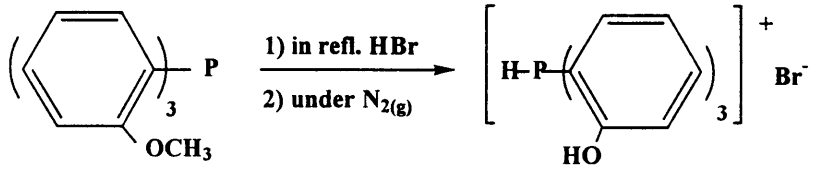

(7)

The hydrobromide salt is a white solid. Following dissolution in an aqueous solution of sodium hydroxide, the addition of acetic acid allows the precipitation of the free phosphine (Scheme 4.12):

Scheme 4.12

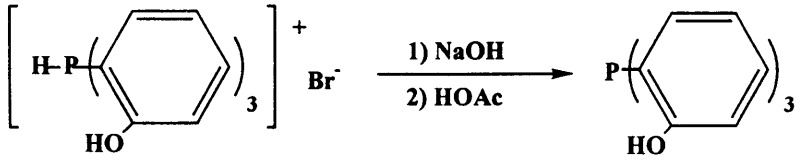

(23)

The *tris*-(*o*-hydroxyphenyl)phosphine is white and air-stable as a solid but air-sensitive in solution. It has been characterised by ^{1}H and $^{31}P\{^{1}H\}$ NMR spectroscopies and mass spectrometry. Moreover, X-ray diffraction studies have been carried out on a single crystal from the ligand (**23**), isolated from ether:hexane solution (Figure 4.6). However, the recrystallisation from methanol afforded crystals assigned to the phosphine oxide $OP(2\text{-}HOC_6H_4)_3$ hydrogen bound to this solvent through the hydroxy groups (Figure 4.7).

Figure 4.6
Crystal Structure of *tris*-(*o*-hydroxyphenyl)phosphine (23)

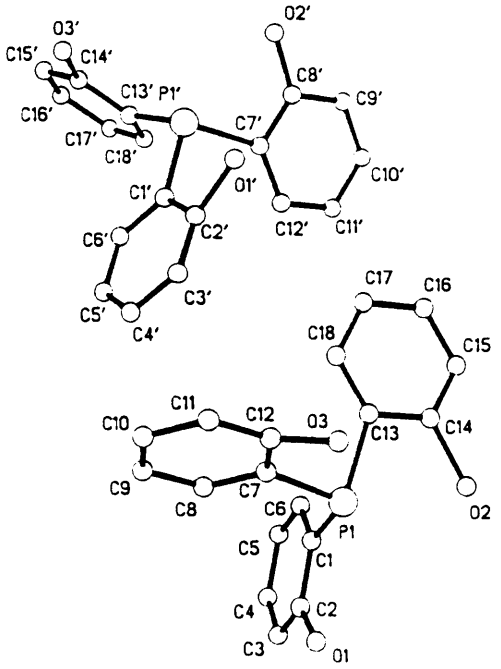

Figure 4.7
Crystal Structure of *tris*-(*o*-hydroxyphenyl)phosphineoxide.methanol

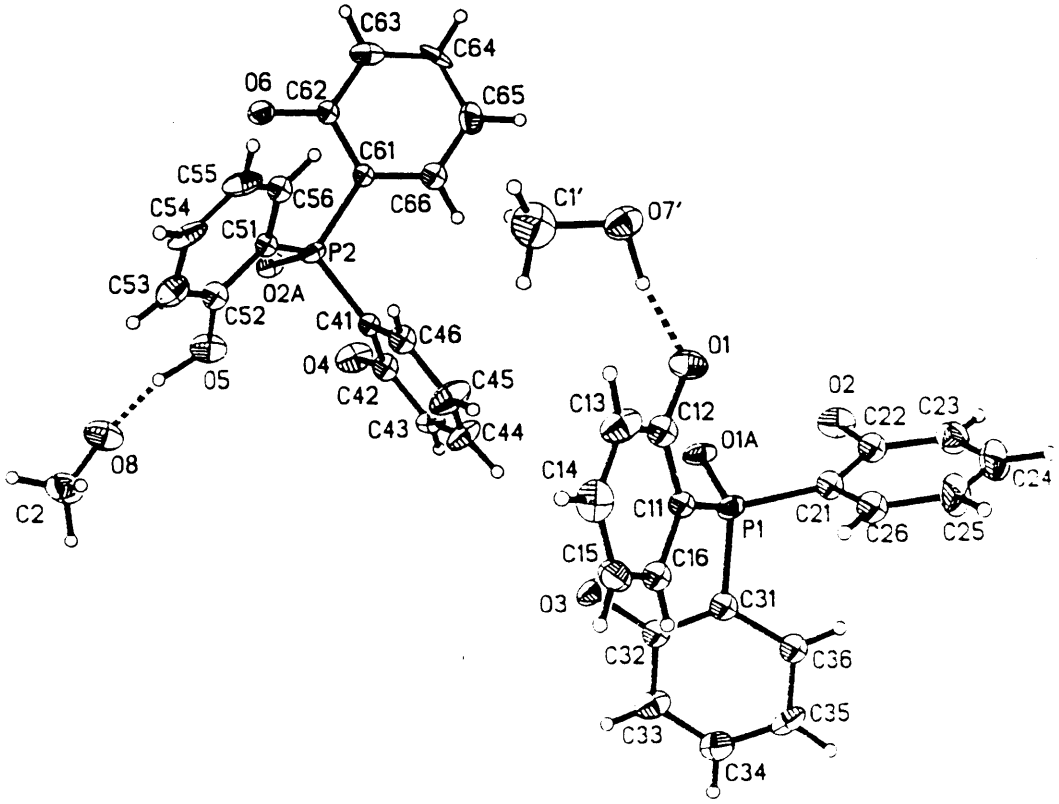

Only few *o*-phosphanyl-phenols have been synthesised,[4f] and the most extensively studied ligand is the *o*-hydroxyphenyldiphenylphosphine.[4b,31] Following the work on the *o*-methoxyphenyldiphenylphosphine,[32] Shaw *et al.* investigated the coordination chemistry of the *o*-hydroxyphenyldiphenylphosphine ligand.[4a] This was allowed to react with $K_2[PtCl_4]$ to yield *trans*-$[PtCl_2\{PPh_2(2\text{-}HOC_6H_4)\}_2]$ which was impossible to isolate analytically pure. They believed that it was due to the "ease of ring closure of the complex and the uptake of solvents" that was detected by proton NMR spectroscopy. Treatment of the platinum phosphine complex with sodium acetate in refluxing ethanol afforded the metal chelate, *cis*-$[Pt(2\text{-}OC_6H_4PPh_2)_2]$. The authors noticed the ease of ring opening of this metal chelate when it reacted, in benzene, with reagents such as methyl lithium in diethyl ether, affording $[PtMe(2\text{-}OC_6H_4PPh_2)\{PPh_2(2\text{-}HOC_6H_4)\}].C_6H_6$. More recent work was carried out by Chaudret *et al.*[33] on the same bidentate phosphine ligand when it was allowed to react with a reduced solution of $[\{Ru(\eta^5\text{-}C_5Me_5)Cl_2\}_n]$ by zinc in methanol and afforded the metal chelate, $[Ru(\eta^5\text{-}C_5Me_5)(2\text{-}OC_6H_4PPh_2)\{PPh_2(2\text{-}HOC_6H_4)\}]$. The crystal structure of this complex revealed a short hydrogen bond between the free hydroxy group and the metalated oxygen atom and it has proved to be unreactive towards molecules such as H_2 and MeI.

It was anticipated that the *tris*-(*o*-hydroxyphenyl)phosphine ligand (**17**) would act as a chelating agent. However, it was also hoped that other factors; the steric effect arising from hydroxy groups in the *ortho*-position of each aryl ring and the electronic effect generated by the hydroxy groups, might contribute to the overall behaviour of this ligand.

4.8 Preparation of Platinum(II) Derivatives:

The *bis*-(acetonitrile)platinumdichloride $[PtCl_2(CH_3CN)_2]$ complex was treated, at room temperature, with two molar equivalents of *tris*-(*o*-hydroxyphenyl)phosphine (**17**), in dichloromethane and under nitrogen. Before any purification, the $^{31}P\{^1H\}$ NMR spectrum, in wet DMSO, of the resulting white

product revealed the presence of a single peak at 23.6 ppm (vbs, $^{1}J_{Pt\text{-}P}$ = 2887 Hz) (Figure 4.8).

Figure 4.8
$^{31}P\{^{1}H\}$ NMR Spectrum Recorded, in Wet DMSO, on the Product from the Reaction of $[PtCl_2(CH_3CN)_2]$ with (17).

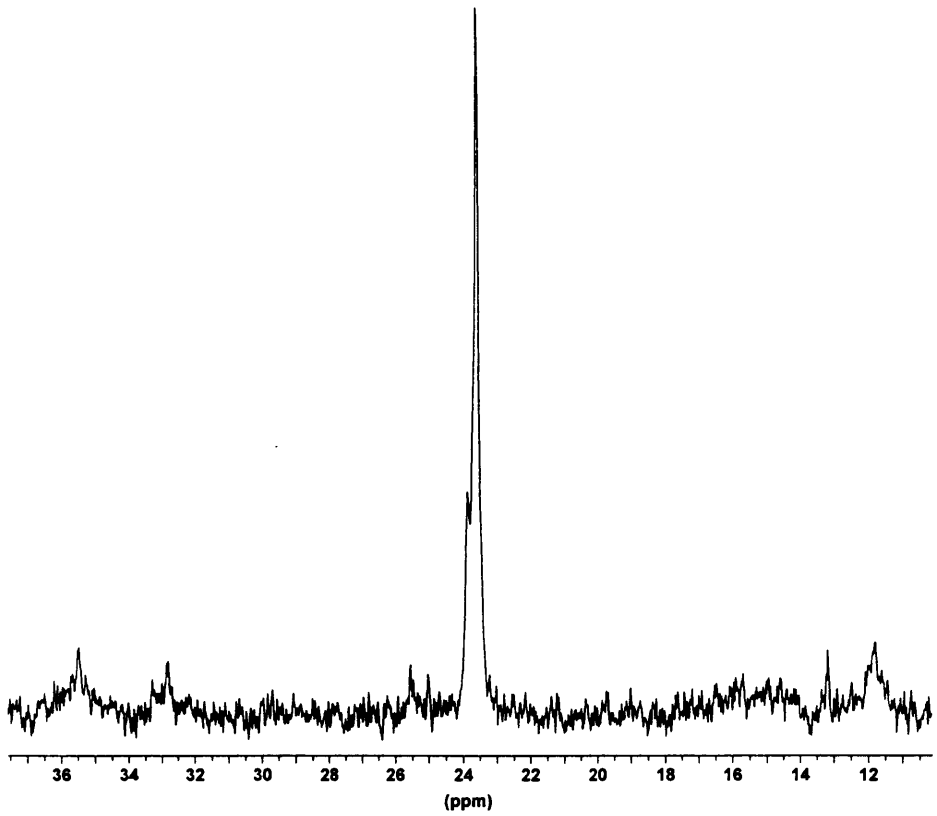

A single crystal was isolated from the NMR experiment solution of complex (**24**). The X-ray diffraction studies on this crystal confirmed the presence of the novel platinum *bis*-chelate complex (**24**) with two phenoxy-phosphine ligands (Figure 4.9).

Figure 4.9
Crystal Structure of $[Pt\{\kappa^2\text{-}P(2\text{-}OC_6H_4)(2\text{-}HOC_6H_4)_2\}_2].4DMSO$ (24)

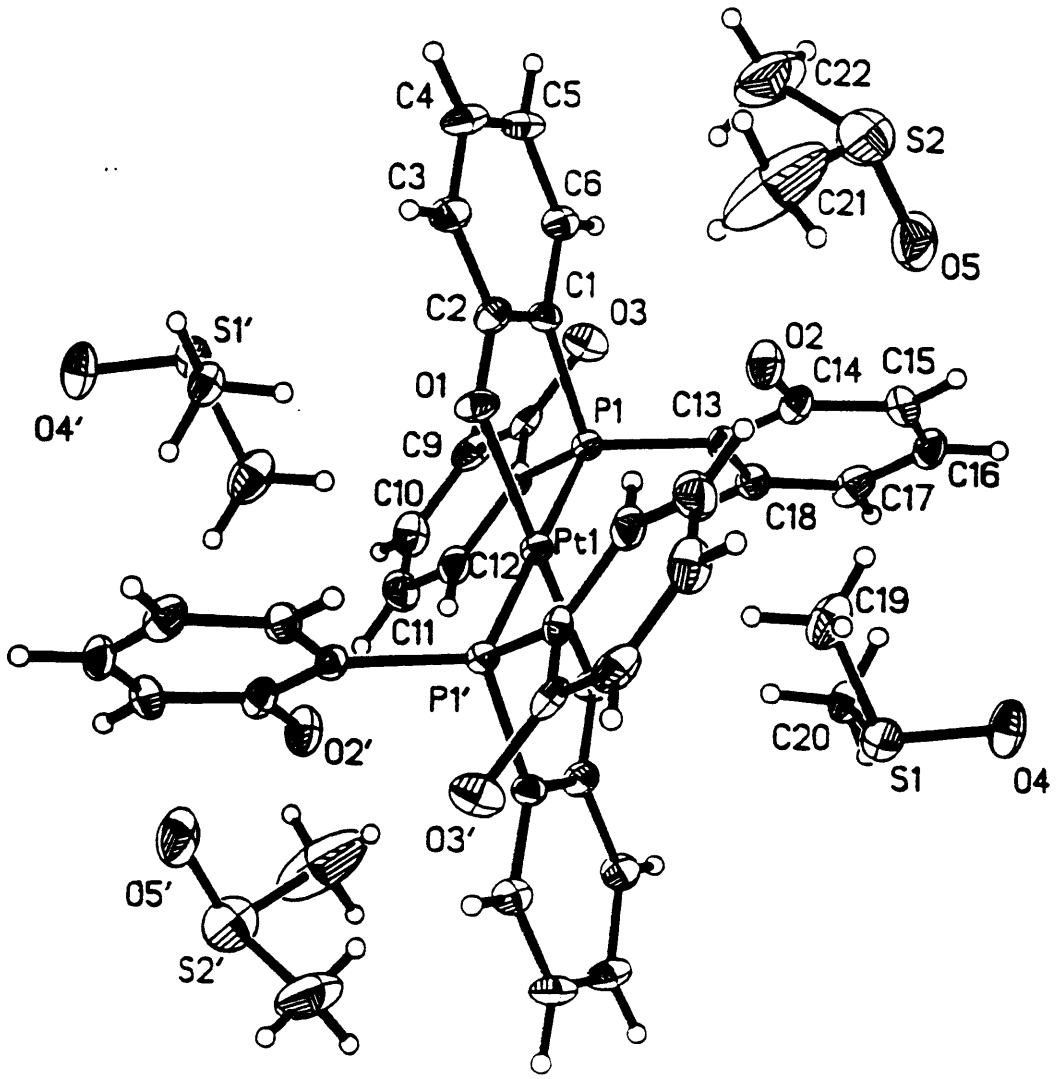

Hitherto, phosphorus ligands containing alcohol functions are rare compared to those containing ester, ether, or ketone groups.[4a,29c,33-37] However, the phosphino-alcohol chelating agents that have been investigated tend to undergo a deprotonation to yield phosphine-phenoxy-metal chelates.[4a,38] In most of the cases, in order to achieve chelation, the complex containing the P/OH ligand system, acting as monodentate, has to undergo a reaction with a base in order to liberate the proton of the hydroxy group and then has to react with an acid to liberate the halide (in general, when halogeno metal complexes are used as starting materials) from a second coordination site on the metal, in order to achieve ring closure.[36] According to other procedures, the starting material had to be induced to react, at high temperature (e.g. refluxing $CHCl_3$), for more than twenty four hours in order to achieve chelation.[38] Thus, from the literature, it appears that a driving force is almost indispensable for the formation of phosphine-phenoxy-metal complexes, using phosphine-alcohols as the chelating agents. For example, Willis *et al.*,[36] after allowing K_2PtCl_4 to react with $PPh_2CH_2C(CF_3)_2OH$, had to add KOH, and then separate the KCl byproduct, in order to obtain $[Pt\{O(CF_3)_2CCH_2PPh_2\}_2]$.

In marked contrast, here, the *bis*-acetonitrileplatinumdichloride complex has reacted with $P(2\text{-}HOC_6H_4)_3$ to yield a platinum-phenoxy chelate (**24**) without the application of an external driving force. The reaction occurs at room temperature but raising the reaction temperature dramatically accelerates the reaction. The complete conversion of the starting materials occurs in two to three hours at room temperature and in ten to fifteen minutes in boiling acetone.

The resulting metal chelate (**24**) is air- and moisture-stable. Moreover, it is relatively stable in refluxing acetone under air. The platinum(II)-chelate (**24**) recrystallised in the monoclinic crystal system with an approximate centre of symmetry on the platinum(II) ion and surrounded by four molecules of dimethylsulfoxide (DMSO). The platinum(II) centre has square-planar geometry and the two phosphine chelating agents are mutually *trans*. The two phosphorus atoms and the two oxygen atoms form a square.

Table 4.3
Selected Bond Distances (Å) and Angles (°) with e.s.d. in Parentheses about Pt(II) for[Pt{κ^2-P(2-OC_6H_4)(2-HOC_6H_4)$_2$}$_2$].4DMSO (24)

Pt(1)-O(1)	2.016(5)	Pt(1)-O(1')	2.016(5)
Pt(1)-P(1)	2.298(2)	Pt(1)-P(1')	2.298(2)
P(1)-Pt(1)-P(1')	180.0	O(1)-Pt(1)-O(1')	180.000(1)
P(1)-Pt(1)-O(1)	85.40(16)	P(1)-Pt(1)-O(1')	94.60(17)

The platinum-oxygen bond length is 2.016(5) Å (Table 4.3) which is shorter than the sum of the respective covalent radii and is consistent with a stable platinum(II)-oxygen bond. The platinum-phosphorus bond length is 2.298(2) Å which is shorter than that in the *trans*-[$PtCl_2${$P(4\text{-}HOC_6H_4)_3$}$_2$] (**7**), 2.3109(13) Å (Chapter Two). This difference is attributed to a strengthening of both the σ- and π-bonding between Pt and P. The electronic enhancement on the phosphorus atoms is caused by their proximity to the oxygen atoms, which induce a higher percentage s-character in the σ Pt-P bond. Moreover, the oxygen ligating atoms increase the electronic density on the platinum centre, strengthening the π-back donation toward the 3e hybrid orbital of the phosphorus atom.[39] The constraints imposed by the five-membered ring and the steric requirements of the substituents at the phosphorus, especially incorporating *ortho*-substituted aryl rings, cause the ring O-Pt-P angles to be narrowed from 90° (the ideal interligand angle) to 85.40(16)°, and the O-Pt-P' angle (or the O'-Pt-P angle) to be widened from 90° to 94.60(17)°. However, the mutually *trans* atoms define 180.000° angles as required by the crystallographic symmetry.

In an attempt to recrystallise the clear-yellow crystals, they were dissolved in deuterated chloroform and the $^{31}P\{^1H\}$ NMR spectrum was recorded for the resulting solution. Since its colour had changed, instantly, to dark orange, the $^{31}P\{^1H\}$ NMR spectrum, this time, showed three different new resonances (Figure 4.10):

- 15.6 ppm (bs, $^1J_{Pt\text{-}P}$ = 2742 Hz).
- 21.3 ppm (bd, $^2J_{P\text{-}P}$ = 387 Hz).

- 10.7 ppm (bd, $^{2}J_{P\text{-}P}$ = 387 Hz).

The two doublets are mutually coupled but the noisy baseline precluded the identification of any satellites.

Figure 4.10
$^{31}P\{^{1}H\}$ NMR Spectrum of the Crystals of (24) Dissolved in $CDCl_3$ (Figure 4.9)

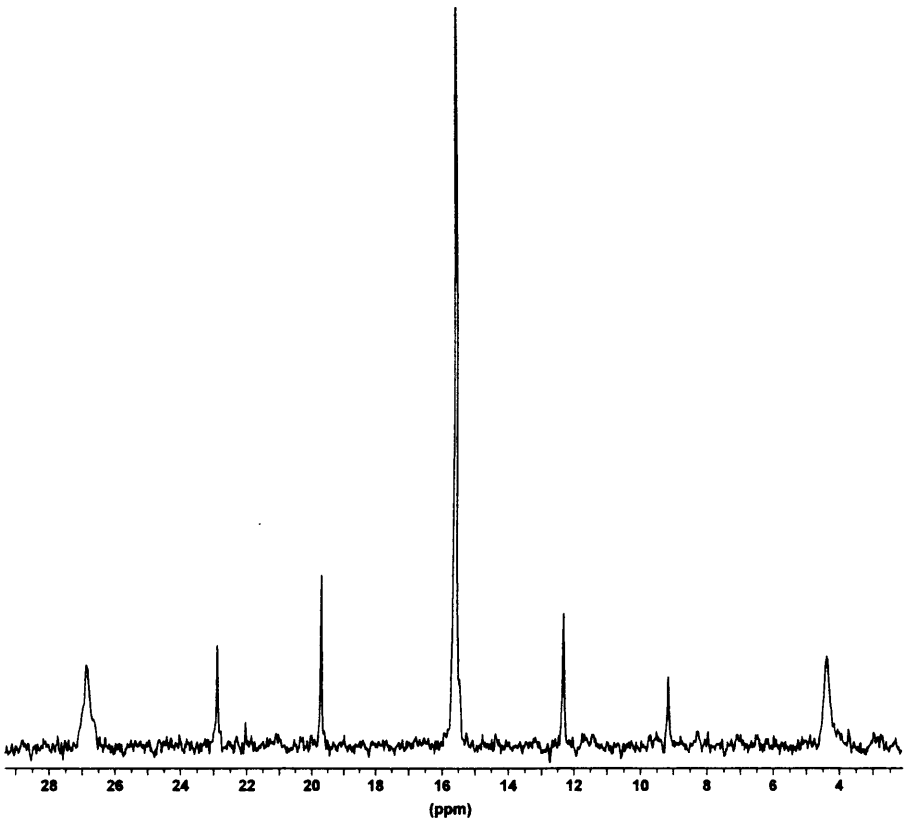

Variation of results was observed when NMR spectra of complex (**24**) were recorded in different solvents, indicating that the structure of this complex is solvent dependent. Therefore, a further investigation into this dependence was required. After preparing complex (**24**) using dichloromethane as the reaction solvent, the corresponding $^{31}P\{^{1}H\}$ NMR experiment was recorded in dry DMSO and under nitrogen. The resulting spectrum revealed a major broad singlet at 15.2 ppm and a smaller broad one at ca. 25.0 ppm. When this NMR solution was opened to the air, the high frequency signal intensity increased. On the other hand, when the $^{31}P\{^{1}H\}$ NMR experiment of the same complex was run in $CDCl_3$, the corresponding spectrum

revealed solely a singlet at 14.0 ppm, which was replaced by a singlet at 23.4 ppm after adding two drops of wet DMSO. The related ^{1}H NMR spectrum exhibited the appearance of a singlet at 3.46 ppm assigned to DMSO coordinated to a platinum(II) centre.[40] It seems that the DMSO is ligating the platinum and that the water is acting as a medium, accelerating this ligation. This phenomenon has already been observed in the literature where aqueous medium is favoured in the process of preparing platinum complexes such as $[PtCl_2(DMSO)_2]$.[40]

Figure 4.11

Structures and $^{31}P\{^{1}H\}$ NMR Data for the Platinum Phosphine Complexes (24), (25) and (26). Recorded in $CDCl_3$.

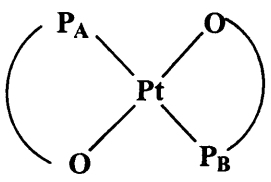

(24)

δ 14.0

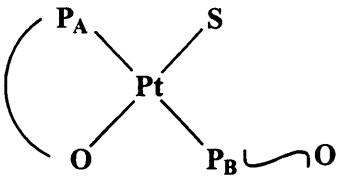

(25)

δ 21.3 (P_B)

δ 10.7 (P_A)

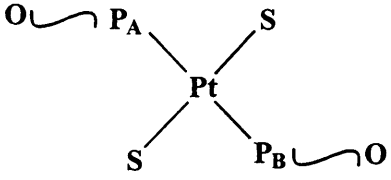

(26)

δ 23.1

P/O system corresponds to $P(2\text{-}HOC_6H_4)_3$ and S = DMSO

The $^{31}P\{^{1}H\}$ NMR spectrum, recorded in $CDCl_3$, on the dissolved crystals of (**24**) revealed signals assigned to both complexes (**24**) and (**25**). It seems that, in solution, the DMSO molecules that have crystallised with complex (**24**) were starting to ligate the metal centre, yielding complex (**25**). In some cases, the NMR spectrum, recorded in wet DMSO, exhibited two singlets assigned to both complexes (**24**) and (**26**). These observations hint at a possible fluxionality in which the hydroxy groups compete with DMSO molecules for coordination sites at the metal centre. This competition might be favoured by hydrogen bonds between the hydroxy groups and DMSO, keeping the latter group in close proximity to the metal centre. However, variable-temperature $^{31}P\{^{1}H\}$ NMR spectroscopy, up to 80°C, run on a wet DMSO

solution of (**24**) and (**26**), results in just sharpening of broad, room temperature, NMR signals indicating that there is no exchange between these complexes at the observed temperatures. It could be added that an additional fluxionality arises from the fact that three hydroxy groups compete for one coordination site at the metal centre.

These remarkable results differ from the usual observations for similar systems. For example, Pringle *et al.*[41] have investigated the fluxionality in $[PtCl_2(Ph_2PCH_2CMe_2OH)_2]$ and they have found an interchange between the unchelated and the monochelated ligand where the chloride and the hydroxy group are competing for the same coordination site at the metal centre. However, the formation of the *bis*-chelate required the addition of a base and this *bis*-chelate was not interchanging with the other two previously mentioned structures. The platinum-oxygen bond exhibited a remarkable stability in solution and at high temperatures such as in boiling ethanolic KOH. The fluxionality in the system (**24**)/(**25**)/(**26**) is very important since *trans*-$[Pt(P\cap O)_2]$ is relatively stable in the solid state, but the Pt-O bond can be dissociated in solution, allowing the formation of a free coordination site at the metal centre. This observation, thus, fulfils the requirements for a hemilabile ligand where the phosphorus atom is strongly bound to the metal centre whilst the oxygen is not and acts as a substitutionally labile group that is capable of temporarily holding a coordination site at the platinum(II) centre in the absence of a substrate.

In the subsequent discussions, different solvents were used in the NMR experiments in order to obtain as much as possible relevant data on the complexes (**24**), (**25**) and (**26**). Therefore, the solvent will be mentioned with the related data.

Table 4.4
$^{31}P\{^{1}H\}$ NMR Data for the Platinum Phosphine Complexes (24), (25) and (26)

Complexes	δP/ ppm	Δ/ ppm[c]	$^{1}J_{Pt\text{-}P}$/ Hz	$^{2}J_{P\text{-}transP}$/ Hz
$[Pt(P\cap O)_2]$ (**24**)[a]	15.2 (s)	64.6	2742	
trans-[Pt(P∩O)(P~O)(S)] (**25**)[b]	δP_A 10.7 (d)	59.7	-	387
	δP_B 21.3 (d)	70.3	-	387
trans-$[Pt(P\sim O)_2(S)_2]$ (**26**)[b]	23.6 (s)	72.6	2887	

[a] This work. Recorded in d^6-DMSO. [b] This work. Recorded in $CDCl_3$. S = DMSO. [c] Coordination chemical shift. δP of the free phosphine ligand is -49.0 ppm (Recorded in diethylether. The lock solvent is $CDCl_3$). [d] Ring contribution. [e] Compared to complex (26). [f] Comparing P_A and P_B in complex (25).

From the data in Table 4.4, the phosphorus chemical shift values of the chelating and non-chelating phosphine ligands in (**25**) are quite similar to those in (**24**) and (**26**) respectively. The coordination chemical shift values 64.6 and 59.7 ppm for the phosphorus atoms engaged in chelation in complexes (**24**) and (**25**), could be used as a diagnostic sign for the presence of the phosphorus atom in a five-membered ring.[9] The difference between the chemical shift values of P_A and P_B could be assigned to the ring contribution Δ_R. However, this difference is only -10.6 ppm, which is a low value for a five-membered ring.[9] This might offer an argument for the fluxional behaviour in this complex where the state of the phosphine ligand is interchanging between the monodentate and bidentate modes. Both $^{1}J_{Pt\text{-}P}$ values, 2742 Hz for (**24**) and 2887 Hz for (**26**), are relatively low, confirming the *trans* phosphorus arrangement around the platinum centre.[42] Comparing (**24**) and (**26**), the increase in the platinum-phosphorus coupling and the shift of the phosphorus signal to a higher frequency could be assigned to the electronic deficiency at the metal centre in the Zwitterionic (**26**) compared to the neutral (**24**). The 387 Hz value is comparable to other P_{transP} coupling values from the literature.[43]

A comparison in the $^{31}P\{^1H\}$ NMR data between the platinum(II) bis-chelate (**24**) and *trans*-$[PtCl_2\{P(2\text{-}HOC_6H_4)_3\}_2]$ (**7**) is illustrated in Table 4.5.

Table 4.5
$^{31}P\{^1H\}$ NMR Data for *trans*-$[Pt\{\kappa^2\text{-}P(2\text{-}OC_6H_4)(2\text{-}HOC_6H_4)_2\}_2]$ (24) and *trans*-$[PtCl_2\{P(4\text{-}HOC_6H_4)_3\}_2]$ (7)

Complex	δF/ppm[a]	δP/ppm	Δ/ppm[b]	$^1J_{Pt\text{-}P}$/Hz	Δ_R/ppm[c]
trans-$[PtCl_2(L)_2]$ (7)[d]	-9.8	16.9	26.7	2598	
trans-$[Pt(P\cap O)_2]$ (**24**)	-49.0[e]	15.6[f]	64.6	2742[f]	37.9

[a] δF = chemical shift of the respective free ligands. [b] Coordination chemical shift. [c] Ring contribution comparing *trans*-$[PtCl_2(L)_2]$ to *trans*-$[Pt(P\cap O)_2]$. [d] This work. Recorded in d^6 acetone. L = $P(4\text{-}HOC_6H_4)_3$. [e] This work. Recorded in diethylether, the lock solvent is $CDCl_3$. [f] This work. Recorded in d^6 DMSO.

The increase in the coupling constant (Table 4.5) is related to the electronic enhancement on the phosphorus atoms caused by the *ortho*-hydroxy groups. This electronic enhancement increases the percentage s-character in the platinum-phosphorus bond which, according to *Fermi Contact Term*, is manifested by an increase in the Pt-P coupling value. The variation in $^1J_{Pt\text{-}P}$ values correlates with the variation in the platinum-phosphorus bond lengths when comparing the crystal structures of the same complexes. The ring contribution value "Δ_R" (37.9 ppm) is approximate, because of the difference in the *trans*-influence between the chloride and the phenoxy groups. However, it is quite similar to values from the literature.[44]

4.9 Preparation of a Rhodium(III) Derivative:

The dinuclear rhodium(III) complex $[\{Rh(\eta^5\text{-}C_5Me_5)Cl(\mu\text{-}Cl)\}_2]$ was treated with two equivalents of $P(2\text{-}HOC_6H_4)_3$ (**23**) in dichloromethane, at room temperature and under nitrogen. NMR experiments were run on a sample taken from the resulting dichloromethane solution. The ^1H NMR spectrum revealed a broad singlet at a relatively high frequency (8.29 ppm) assigned to the hydroxy protons, the aryl

protons' signals at the usual chemical shift values (7.54-6.67 ppm), and a doublet at 1.28 ppm (J_{P-H} = 3.5 Hz) assigned to the phosphorus-proton (Cp*) coupling (Cp* = η^5-C_5Me_5). The $^{31}P\{^1H\}$ NMR spectrum exhibited a noisy baseline, and a broad doublet at 19.5 ppm ($^1J_{Rh-P}$ = 137 Hz). The proposed reaction route is illustrated in Scheme 4.13.

Scheme 4.13

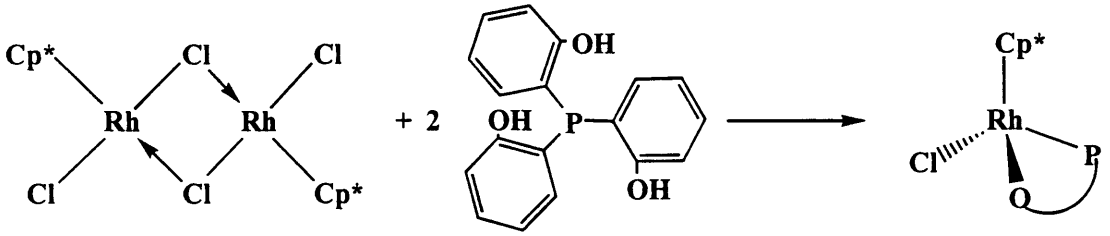

Cp* = C_5Me_5 **(29)**

The steric effect appears to be very important in [Cp*Rh(PR_3)X_2] complexes in general. In 1994, Jones *et al.*[45] published the preparation of a set of [(C_5Me_5)Rh(PR'_3)RX] complexes (X = Cl, Br, I; R = Me, n-C_3H_7, 2-MeC_6H_4, etc; R' = Me, 4-MeC_6H_4, etc). Using conformation dynamics, they were able to show that hindered rotation about the rhodium-phosphorus bond occurs. The pentamethylcyclopentadienyl ring and the substituents on the phosphine ligand are the main rotational barriers in this type of compound.[46]

Here, where P(2-$HOC_6H_4)_3$ is used, an increase in the coordination chemical shift of the phosphorus signal upon chelation has been observed, compared to analoguous monodentate and to less sterically demanding ligands. In such a genuinely bulky complex, [Cp*Rh(PR_3)X_2], the steric effect has a large influence on the phosphorus NMR data.

Table 4.6
$^{31}P\{^1H\}$ NMR Data of $[Cp^*Rh(PAr_3)Cl_2]$ and $[Cp^*Rh(\kappa^2\text{-}(2\text{-}OC_6H_4)P(2\text{-}HOC_6H_4)_2)Cl]$ Complexes

Complex	δP/ppm	Δ/ppm	$^1J_{Rh\text{-}P}$/Hz
$[Cp^*Rh(PPh_3)Cl_2]$[a,i]	28.2	32.9[d]	141
$[Cp^*Rh(P(4\text{-}CH_3OC_6H_4)_3)Cl_2]$ (**15**)[b,h]	27.3	37.2[e]	143
$[Cp^*Rh(P(4\text{-}HOC_6H_4)_3)Cl_2]$ (**16**)[c,h]	28.7	38.5[f]	144
$[Cp^*Rh(\kappa^2\text{-}(2\text{-}OC_6H_4)P(2\text{-}HOC_6H_4)_2)Cl]$ (**29**)[a,h]	19.5	68.5[g]	137

[a] Recorded in $CDCl_3$. [b] Recorded in CD_2Cl_2. [c] Recorded in d^6 acetone. [d] Compared to $\delta_{P\ (free\ ligand)}$ = -4.7 ppm. [e] Compared to $\delta_{P\ (free\ ligand)}$ = -9.9 ppm. [f] Compared to $\delta_{P\ (free\ ligand)}$ = -9.8 ppm. [g] Compared to $\delta_{P\ (free\ ligand)}$ = -49.0 ppm. [h] This work. [i] Ref. 47.

Comparing the coordination chemical shift values in Table 4.6, the large value (68.5 ppm) of the latter complex compared to the former three, confirms chelation. The inclusion of the phosphorus in a five-membered ring affects the electronic properties of the phosphine ligand in terms of σ-donation and π-acceptance which influence the $^1J_{Rh\text{-}P}$ coupling value. From a steric approach, the *tris*-(*ortho*-hydroxyphenyl)phosphine ligand (**23**) is bulkier than the PPh_3, $P(4\text{-}CH_3OC_6H_4)_3$ and $P(4\text{-}HOC_6H_4)_3$ ligands.[48] As a result of this steric effect, a lengthening in the rhodium-phosphorus bond in the $[Cp^*Rh(\kappa^2\text{-}(2\text{-}OC_6H_4)P(2\text{-}HOC_6H_4)_2)Cl]$ (**29**) complex occurs. This lengthening reduces the electronic contribution of the phosphorus in the rhodium-phosphorus bond, decreasing the $^1J_{Rh\text{-}P}$ value and shifting the phosphorus signal relatively to a lower frequency.

This coordination reaction will be compared to that for the *ortho*-vinylphenyldiphenylphosphine ligand in Chapter Five.

4.10 Preparation of a Rhodium(I) Derivative:

The dinuclear rhodium(I) complex $[\{Rh(\mu\text{-}Cl)(CO)_2\}_2]$ was treated with two equivalents of $P(2\text{-}HOC_6H_4)_3$ in dichloromethane, at room temperature and under nitrogen. The ^1H NMR spectrum revealed a set of singlets at high and low frequencies (11.72-9.21 and 2.77 ppm) assigned to the hydroxy protons and multiplets in the aryl proton region (7.64-6.29 ppm). The $^{31}P\{^1H\}$ NMR spectrum of the resulting product exhibited a noisy baseline and two broad mutually coupled doublet of doublets having an ABX spin system (Figure 4.13). The simulated values[49] are shown in Table 4.12. The Nujol mull IR spectrum of the resulting product revealed a relatively high stretching frequency for the carbonyl group (2082 cm^{-1}). The suggested product is $[Rh(CO)\{\kappa^2\text{-}P(2\text{-}OC_6H_4)(2\text{-}HOC_6H_4)_2\}\{P(2\text{-}HOC_6H_4)_3\}]$ (**30**) depicted in Figure 4.12. The rhodium(I) is bound to two phosphine ligands, one is acting in a monodentate fashion whilst the other is acting in a bidentate fashion. The carbonyl group is *trans* to the oxygen of the chelating agent.

Figure 4.12
$[Rh(CO)\{\kappa^2\text{-}P(2\text{-}OC_6H_4)(2\text{-}HOC_6H_4)_2\}\{P(2\text{-}HOC_6H_4)_3\}]$ (30)

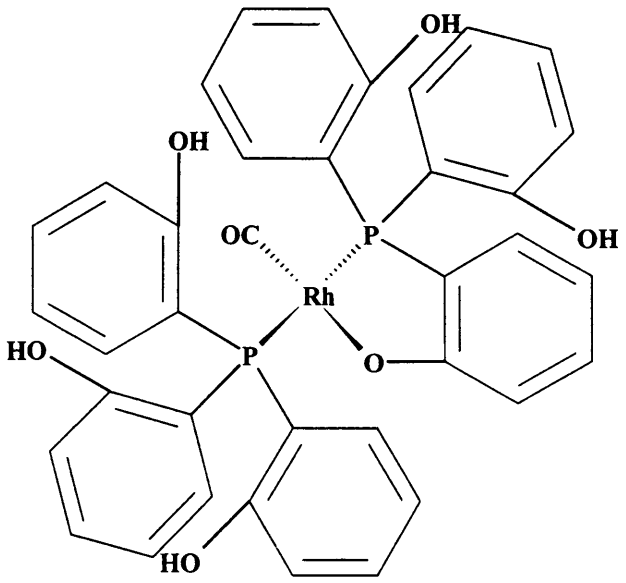

Similar complexes have been previously prepared, such as $[Rh(CO)\{\kappa^2\text{-}P(2\text{-}OC_6H_4)Bu^t_2\}\{P(2\text{-}CH_3OC_6H_4)Bu^t_2\}]$[50] and its iridium analogue,[35] and it has been

concluded that similar complexes exhibit interesting reactivity such as SO_2 fixation and reversible oxidative addition of H_2.

Table 4.7
$^{31}P\{^1H\}$ NMR (δ in ppm and J in Hz) and IR (ν in cm^{-1}) Data of Rhodium Carbonyl Phosphine Chelates

Complex	δ_{PA}[a]	Δ_{PA}	δ_{PB}[b]	Δ_{PB}	$\lvert^1J_{Rh-P}\rvert$	$^2J_{P-P}$	ν_{CO}
trans-[Rh(CO)(P∩O)(P~O)] (**30**)	41.6	90.6[d]	34.7	83.7[d]	93 (P∩O) 94 (P~O)	472	2082
trans-[Rh(CO)(PPh_3){(2-OC_6H_4)PPh_2}][c]	45.0	73.2[e]	24.4	52.6[e]	133 (PA)[a] 139 (PB)[b]	307	1956

[a] Chelating ligand. [b] Monodentate ligand. [c] Ref. 51. [d] $\delta_{P\ (free\ ligand)}$ = -49.0 ppm. [e] $\delta_{P\ (free\ ligand)}$ = -28.2 ppm (Ref. 52).

The small rhodium(I)-phosphorus coupling constants, the large phosphorus-*trans*-phosphorus coupling constant and the high carbonyl streching frequency are rare for this type of complex.[35] The small $^1J_{Rh-P}$ value is due to a weak P→Rh bond resulting in a reduction in electron density at the metal centre which translates into less Rh→CO π-back donation and a high frequency CO stretch. This suggests a weak O→Rh π-back bonding which confers a labile character to this specific bond. The coordination chemical shift values for both phosphorus signals in complex (**30**) (Table 4.7) are remarkably large and very similar, which might suggest some interchanging between the ligands at the metal centre. The variable temperature $^{31}P\{^1H\}$ NMR experiments conducted between -50 and +50°C revealed no changes from the spectrum observed at room temperature.

Figure 4.13
Experimental and Simulated $^{31}P\{^{1}H\}$ NMR Spectra of the Reaction Product of $[\{Rh(\mu\text{-}Cl)(CO)_2\}_2]$ with $P(2\text{-}HOC_6H_4)_3$

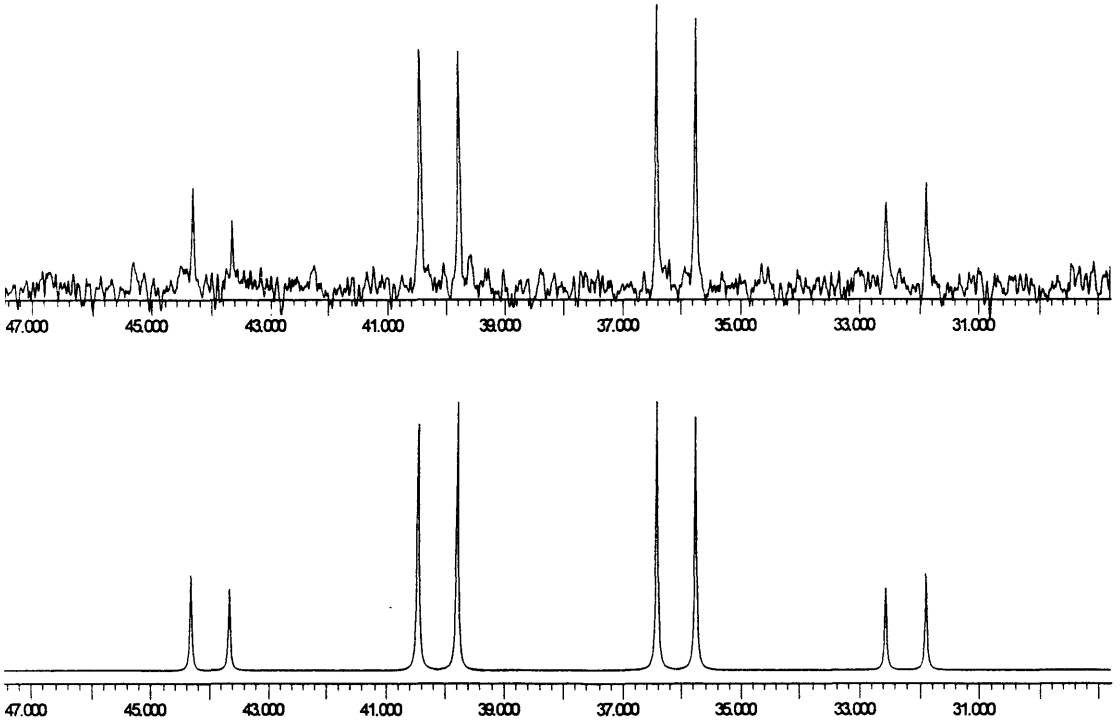

4.11 Summary:

This chapter describes the preparation and coordination chemistry of the *tris*-(*ortho*-hydroxyphenyl)phosphine (**23**) ligand to late transition metals. The *chelate effect* and the *ring contribution* (Δ_R) are introduced and highlighted within the discussion of the characterisation of these complexes. In this system, one of the ligating atoms, the phosphorus, is a "soft" Lewis base, whilst the other ligating atom, the oxygen, is a "hard" Lewis base. Upon coordination to low-valent late transition-metals, the former group acts as a substitutionally inert ligating atom, and the latter group acts as a substitutionally labile ligating atom. The complex $[Pt\{\kappa^2\text{-}P(2\text{-}OC_6H_4)(2\text{-}HOC_6H_4)_2\}_2]$ (**24**) exhibits an increased metal-phosphine bond strength compared to the monodentate phosphine complexe *trans*-$[PtCl_2\{P(4\text{-}HOC_6H_4)_3\}_2]$ (**7**) described in this work (Chapter Two). The crystal structure of (**24**) reveals a relatively short platinum-oxygen bond length, however this bond is readily dissociated in solution and this is highly dependent on the solvent used.

Chapter Four References

[1] O. Neunhoeffer and L. Lamza, *Chem. Ber.*, 1961, **94**, 2514.

[2] C. A. Willoughby, R. R. Duff, Jr., W. M. Davies and S. L. Buchwald, *Organometallics*, 1996, **15**, 472.

[3] a) I. M. Lorkovic, M. S. Wrighton and W. M. Davies, *J. Am. Chem. Soc*, 1994, **116**, 6220.

b) A. L. Casalnuovo, T. V. RajanBabu, T. A. Ayers and T. H. Warren, *J. Am. Chem. Soc.*, 1994, **116**, 9869.

c) K.-Y. Shih, K. Totland, S. W. Seidel and R. R. Schrock, *J. Ar. Chem. Soc.*, 1994, **116**, 12103.

[4] a) H. D. Empsall, B. L. Shaw and B. L. Turtle, *J. Chem. Soc., Dalton Trans.*, 1976, 1500.

b) E. F. Landvatter and T. B. Rauchfuss, *Organometallics*, 1982, **1**, 506.

c) K. R. Dunbar, J. H. Matonic and V. P. Saharan, *Inorg. Chem.*, 1994, **33**, 25.

d) S. B. Sembering, S. B. Colbran and D. C. Craig, *Inorg. Chem.*, 1995, **34**, 761.

e) R. Schmutzler, D. Schomburg, R. Bartsch and O. Stelzer, *Z. Naturforsch*, 1984, **B39**, 1177.

f) J. Heinicke, R. Kadyrov, M. K. Kindermann, M. Koesling and P. G. Jones, *Chem. Ber.*, 1996, **129**, 1547.

[5] C. F. Bell, *Principles and Applications of Metal Chelation*, Clarendon Press Oxford, 1977.

[6] A. E. Sinear, W. Valient and J. Wirth, *J. Org. Chem.*, 1960, **25**, 2001.

[7] P. Paoletti, M. Ciampolini and L. Socconi, *J. Chem. Soc.*, 1963, 3589.

[8] B. E. Mann, C. Masters and B. L. Shaw, *J. Chem. Soc. (A)*, 1971, 1104.

[9] P. E. Garrou, *Chem. Rev.*, 1981, **81**, 229.

[10] L. S. Merriwether and J. R. Leto, *J. Am. Chem. Soc.*, 1961, **83**, 3192.

[11] T. J. Mazanec, K. D. Tau and D. W. Meek, *Inorg. Chem.*, 1980, **19**, 85.

[12] A. Bader and E. Lindner, *Coord. Chem. Rev.*, 1991, **108**, 27.

[13] E. Lindner, B. Keppeler and P. Wagner, *Inorg. Chim. Acta*, 1997, **97**, 258.

[14] G. J. P. Britovsek, K. J. Cavell and W. Keim, *J. Mol. Catal.*, 1996, **110**, 77.

[15] S. Mecking and W. Keim, *Organometallics*, 1996, **15**, 2650.

[16] M. Martin, O. Gevert and H. Werner, *J. Chem. Soc., Dalton Trans.*, 1996, 2275.

[17] E. Lindner, B. Keppleter, H. A. Mayer, K. Gierling, R. Fawzi and M. Steimann, *J. Organomet. Chem.*, 1996, **526**, 175.

[18] J.-C. Shi, D.-X. Wu, T.-B. Weng, M.-C. Hong, Q.-T. Liu, B.-S. S.-J. Lu and H.-Q. Wang, *J. Chem. Soc., Dalton Trans.*, 1996, 2911.

[19] K. R. Dunbar, J.-S. Sun and A. Quillevéré, *Inorg. Chem.*, 1994, **33**, 3598.

[20] J. C. Jeffrey and T. B. Rauchfuss, *Inorg. Chem.*, 1979, **18**, 2658.

[21] I. Le Gall, P. Laurent, E. Soulier, J.-Y. Salaün and H. des Abbayes, *J. Organomet. Chem.*, 1998, **567**, 13.

[22] S. Ganguly, J. T. Mague and D. M. Roundhill, *Inorg. Chem.*, 1992, **31**, 3500.

[23] E. Lindner, R. Speidel, R. Fawzi and W. Hiller, *Chem. Ber.*, 1990, **123**, 2255.

[24] J. Okuda, *Comments Inorg. Chem.*, 1994, **16**, 185.

[25] B. De Klerk-Engles, J. H. Groen, K. Vrieze, A. Mockel, E. Lindner and K. Coubitz, *Inorg. Chim. Acta*, 1992, **195**, 237.

[26] L. Horner and G. Simons, *Z. Naturforsch., B: Anorg. Chem. Org. Chem.*, 1984, **39**, 497.

[27] K. G. Orrell, A. G. Osborne, V. Sik and M. W. Da Silva, *Polyhedron*, 1995, **14**, 2797.

[28] a) S. J. Chadwell, S. J. Coles, P. G. Edwards and M. B. Hursthouse, *J. Chem. Soc., Dalton Trans.*, 1996, 1105.

b) R. Jaouhari and P. G. Edwards, *Rech. Trav. Chim. Pays-Bas*, 1988, **107**, 511.

c) N. W. Alcock, A. W. G. Platt and P. Pringle, *J. Chem. Soc., Dalton Trans.*, 1987, 2273.

d) J. P. Farr, P. E. Wood and A. L. Balch, *Inorg. Chem.*, 1983, **22**, 3387.

e) A. R. Sanger, *Can. J. Chem.*, 1983, **61**, 2214.

[29] K. R. Dunbar, *Comments Inorg. Chem.*, 1992, **13**, 313.

[30] J. I. Dulebohn, S. C. Haefner, K. A. Berglund and K. R. Dunbar, *Chem. Mater.*, 1992, **4**, 506.

[31] M. K. Cooper, J. M. Downes, P. A. Duckworth and E. R. T. Tiekink *Aust. J. Chem.*, 1992, **45**, 595

[32] C. E. Jones, B. L. Shaw and B. L. Turtle, *J. Chem. Soc., Dalton Trans.*, 1974, 992.

[33] M. Canestrari, B. Chaudret, F. Dahan, Y.-S. Huang, R. Poilblanc, T.-C. Kim and M. Sanchez, *J. Chem. Soc., Dalton Trans.*, 1990, 1179.

[34] C. D. Montgomery, N. C. Payne and C. J. Willis, *Inorg. Chim. Acta*, 1986, **117**, 103.

[35] H. D. Empsall, E. M. Hyde and B. L. Shaw, *J. Chem. Soc., Dalton Trans.*, 1975, 1690.

[36] R. T. Boeré, C. D. Montgomery, N. C. Payne and C. J. Willis, *Inorg. Chem.*, 1985, **24**, 3680.

[37] J. Heinicke, R. Kadyrov, M. K. Kindermann, M. Kloss, A. Fischer and P. G. Jones, *Chem. Ber.*, 1996, **129**, 1061.

[38] T. B. Rauchfuss, *Inorg. Chem.*, 1977, **16**, 2966.

[39] S.-X. Xiao, W.-C. Trogler, D. E. Ellis and Z. Berkovitch-Yellin, *J. Am. Chem. Soc.*, 1983, **105**, 7033.

[40] W. Kitching, C. J. Moore and D. Doddrell, *Inorg. Chem.*, 1970, **9**, 541.

[41] N. W. Alcock, A. W. G. Platt and P. G. Pringle, *Inorg. Chim. Acta*, 1987, **128**, 215.

[42] a) S. O. Grim, R. L. Keiter and W. McFarlane, *Inorg. Chem.*, 1967, **6**, 1133.
b) P. S. Pregosin and R. W. Kunz, *31P and 13C NMR of Transition Metal Complexes*, Springer, New York, 1979.

[43] J. M. Jenkins and B. L. Shaw, *Proc. Chem. Soc.*, 1963, 279.

[44] J.-S. Sun, C. E. Uzelmeier, D. L. Ward and K. R. Dunbar, *Polyhedron*, 1998, **17**, 2049.

[45] W. D. Jones and F. J. Feher, *Inorg. Chem.*, 1984, **23**, 2376.

[46] W. D. Jones and V. L. Kuykendall, *Inorg. Chem.*, 1991, **30**, 2615.

[47] B. L. Haymore and J. A. Ibers, *J. Am. Chem. Soc.*, 1975, **97**, 5369.

[48] a) C. A. Tolman, *Chem. Rev.*, 1977, **177**, 313.
b) C. A. Tolman, *J. Am. Chem. Soc.*, 1970, **92**, 2956.

[49] gNMR, version 3.6, Cherwell Scientific Publishing Ltd., Oxford, 1995.

[50] H. D. Empsall, C. E. Jones, E. M. Hyde and B. L. Shaw, *J. Chem. Soc., Dalton,* 1974, 1980.

[51] L. Dahlenburg, K. Herbst and M. Kühnlein, *Z. Anorg. Allg. Chem.*, 1997, **623**, 250.

[52] S. O. Grim and A. W. Yankowsky, *Phosphorus and Sulfur*, 1977, **3**, 191.

CHAPTER FIVE

COORDINATION CHEMISTRY OF ORTHO-VINYLPHENYLDIPHENYLPHOSPHINE LIGAND

CHAPTER FIVE

COORDINATION CHEMISTRY OF *ORTHO*-VINYLPHENYLDIPHENYLPHOSPHINE LIGAND

5.1 Introduction:

The previous chapters cover the coordination chemistry of aryl phosphine ligands bearing differing substituents in the *para*-positions as well as in the *ortho*-positions in the aryl rings. In the latter case, the *ortho*-substituents incorporate oxygen atoms, which could act as a second ligating atom, in addition to the phosphorus. The oxygen is well known to be a harder Lewis base when compared to the phosphorus. As a result of this, the nature of the oxygen bonding to late transition-metals confers specific characteristics to the ligand such as hemilability.

In this chapter, the discussion will be concerned with details of the coordination chemistry of a different *ortho*-substituted aryl phosphine ligand: *ortho*-vinylphenyldiphenylphosphine, also called *ortho*-styryldiphenylphosphine and abbreviated **SP**. This ligand is expected to act in a different manner upon its coordination to metals when compared to the P,O chelating agent. This is mainly due to the exceptional features of the olefin ligating group (see Section 5.2). In addition to comparing the phosphorus/vinyl system and the phosphorus/oxygen system, this chapter describes the preparation of new transition-metal phosphine complexes comparable to other complexes prepared in this work, incorporating either the chloride (Present Chapter) or the fluoride (Chapter Seven) as the halide ligand. Moreover, it was planned to prepare a platinum(II) fluoride SP complex starting from the complex $[PtCl_2(SP)]$ (**32**) (see Section 5.5) and following the route described in Chapter Six (Scheme 6.2). However, due to time constraints, this last synthesis was not carried out. It should be noted that many stable transition-metal olefin complexes incorporating the SP ligand have been already reported (see Section 5.3).[1,2]

5.2 Metal-Olefin Bonding:

The coordination of transition-metals to ligands allows the formation of stable metal-ligand bonds as a result of the σ-donor/π-acceptor synergism. The Dewar-Chatt-Duncanson model[3] of metal-olefin bonding is well known to organometallic chemists and it beautifully illustrates the synergism that is taking place between the two components of coordination (Figure 5.1).

Figure 5.1
The Dewar-Chatt-Duncanson Model on Metal-Olefin Bonding

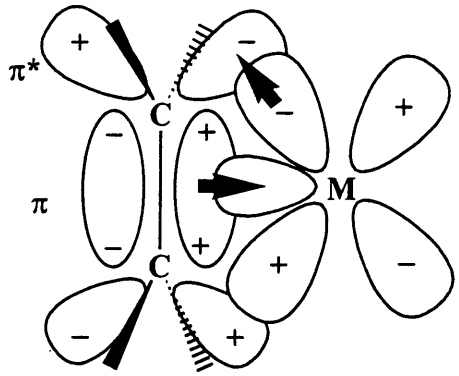

- **σ-donation out of the filled olefin π orbital**
- **π-back-donation out of the filled metal d orbital**

Complexes incorporating mutually reinforcing metal-olefin bonding belong to a class called **π-complexes**. This nomination refers to the fact that the olefin ligand uses orbitals having π-symmetry in the L→M donor as well as the L←M acceptor interaction with the metal. The qualitative bonding between the transition-metal and the olefin resembles that of the transition-metal to CO group in terms of donor acceptor synergism. Like CO, olefins are considered to be weak σ-donors and both groups possess empty orbitals of low energy, which can accept electrons from filled d-orbitals of transition metals. Both removing electrons from the bonding molecular orbitals of the olefin group and donating electrons into its antibonding molecular orbitals tend to weaken the C=C bonding. This is confirmed by a decrease in the $\nu_{C=C}$

vibrational frequencies, of 60-150 cm^{-1}, between a free olefin and a coordinated one. In addition, an increase in the C=C bond length is observed.

One of the best understood olefin-metal complexes is the platinum-ethene complex $K[PtCl_3(C_2H_4)].H_2O$, which was first prepared by the Danish pharmacist, Zeise, in the 19th century (1827). However, its true structure was discovered in the following century (1950). The ethene group is bound perpendicular with respect to the platinum(II)-chlorine plane, and the midpoint of the C=C bond is on the line formed by the platinum centre and the *trans* chloride ion (Figure 5.2).

Figure 5.2
Zeise's Salt

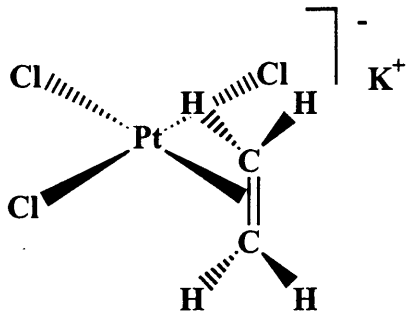

The C=C bond distance is 1.375(4) Å whilst that of free ethene is only 1.34 Å. The C=C stretching frequency in Zeise's salt is 1520 cm^{-1} whilst that of free ethene is 1623 cm^{-1}. The Pt-Cl bond length *trans* to the ethene group (2.34 Å) is longer than that *cis* to it (2.30 Å) because of the larger *trans*-influence of the ethene group compared to that of the chloride ligand.

The electron affinity (EA) of the metal correlates with the L→M σ-bonding, so that a high EA favours σ-bonding. On the other hand, the promotion energy (PE) of the metal correlates with the L←M π-bonding, in a way that a low PE favours π-bonding.[4] Moreover, the electron density around the metal has a large influence on the nature of the metal-olefin bonding. In Zeise's salt, where the other three ligating groups are chlorides, electron withdrawal from the metal orbitals is enhancing the σ-component in the metal-olefin bond. The substituents (X) on the olefin group can have

similar effect, i.e. substituents such as F, CN or COOH on the olefin generate a poorer σ-donor and a better π-acceptor ligand. Stemming from this and according to Bent's rule,[5] a bending back of the olefin substituents away from the metal-olefin bond results from a high degree of π-back donation from the metal. In extreme cases, the structure of the complex approaches that of a metallacyclopropane (Figure 5.3).

Figure 5.3
Limiting Structures:

a) metal-olefin complex **b) metallacyclopropane**

The deviation from planarity of coordinated ethylene should, therefore, correlate with the tendency of carbon to use hybrid orbitals with higher p character in the C-X bond. This tendency grows with increasing electronegativity of the substituents[6] (e.g. the $H_3C\cdot$ radical is planar and $F_3C\cdot$ radical is pyramidal[5]).

Figure 5.4
Structure of $[(\eta^5\text{-}C_5H_5)Rh(C_2F_4)(C_2H_4)]$

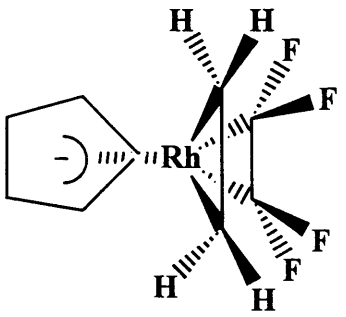

A study of the structure of η^5-cyclopentadienylethylenetetrafluoroethylene-rhodium, $[(\eta^5\text{-}C_5H_5)Rh(C_2F_4)(C_2H_4)]$ (Figure 5.4) was undertaken in order to

establish the deformation induced by substituents on the ethylene group.[7,8] This structure was determined by X-ray diffraction studies, revealing an overall trigonal ligand geometry about the Rh atom. The bending back of the substituents on the olefin group is described according to Ibers and co-workers convention,[9] where they have used a number of interatomic angles and dihedral angles (Figure 5.5).

Figure 5.5
Relevant Angles Describing the Bending Back of Substituents on Olefin Bound to Metal Centre.

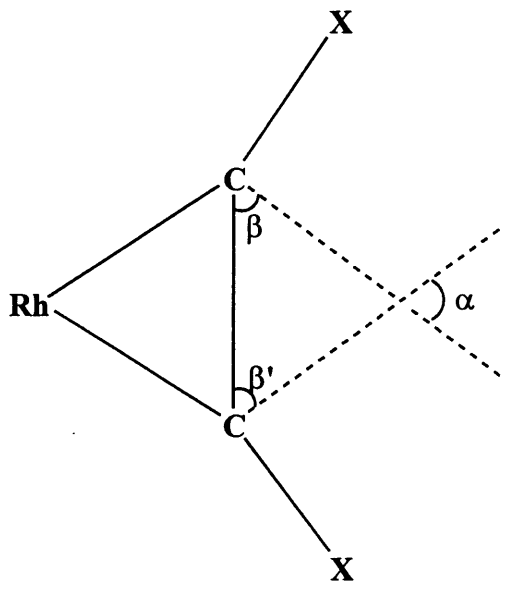

α is the angle between the two plane normals perpendicular to the olefin carbon-substituent planes (X-C-X). β and β' are the angles between C=C bond and the plane normals mentioned. The increase in the bending back is related to an increase of α from 0° (sp^2 carbon) and to a decrease of β from 90° (sp^2 carbon).

Table 5.1
α and β Values in Some Metal-Olefin Complexes (According to Ibers and Co-workers Convention)[9]

Complex	Ligand	α	β
$K[PtCl_3(C_2H_4)].H_2O$[a]	C_2H_4	34.7	72.7
$[(\eta^5\text{-}C_5H_5)Rh(C_2F_4)(C_2H_4)]$	C_2H_4	42.4	69.1
$[(C_4H_9NC)_2Ni\{C_2(CN)_4\}]$[b]	$C_2(CN)_4$	56.8	61.6
$[(\eta^5\text{-}C_5H_5)Rh(C_2F_4)(C_2H_4)]$	C_2F_4	74.3	52.8

[a] Ref. 10. [b]. Ref. 9.

From Table 5.1, it can be seen that all the coordinated olefins exhibit some bending back and the amount of back-bending is both metal and olefin-substituent X dependent. As predicted, increasing the electronegativity of X increases the bending back which prompts discussion of the nature of the metal-olefin bonding and whether it is rather a "metallacyclopropane" type. Because of the steric and electronic constraints, it is almost impossible to have a carbon atom surrounded by perfect tetrahedral geometry in a metal-coordinated olefin complex. Therefore, the authors decided to carry out approximate calculations where they have placed fluorine atoms on carbon atoms in an approximate tetrahedral fashion. The resulting α and β simulated values were close to the experimental ones ($\Delta\alpha = 4.6°$ and $\Delta\beta = 2.3°$) which are consistent with the "rhodiacyclopropane" model.[11,12]

5.3 Introduction to the Coordination Chemistry of *ortho*-styryldiphenylphosphine (SP):

The SP ligand was first prepared in 1967 by Bennett *et al.*[13] It was a second generation ligand following coordination work carried out on the (*o*-allylphenyl)diphenylphosphine (AP) ligand (Figure 5.6). The authors[13] were faced by

the isomerisation of (**AP**) to (*o-cis*-propenylphenyl)diphenylphosphine (**PP**) during the coordination wherein the Lewis acidity of the double bond is reduced, having a methyl group attached to the alkene.

Figure 5.6

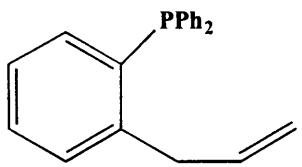

(AP)

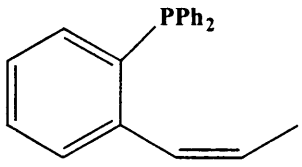

(PP)

The coordination chemistry of olefinic tertiary phosphine ligands is a very interesting area in chemistry because of the coexistence of two very different ligating groups in the same ligand, the phosphorus atom, which is mainly a σ-donor and the olefin group, which is mainly a π-acceptor. The combination of these two effects increases the probability of the olefinic phosphine ligand stabilising the metal centre upon coordination.[14-16] Bennett and co-workers managed to establish a rich literature describing the coordination chemistry of the SP ligand. Their investigation focused on the preparation of a considerable set of metal SP complexes covering a wide variety of transition-metals, such as Cr(0), Mo(0), W(0), Mn(I), Re(I),[13,17] Fe(0),[18] Ru(0)[18] and (II),[19] Rh(I)[20] and Ni,[21,22] Pd[23,24] and Pt[21,23,25] in both oxidation states (0) and (II). The SP ligand has been used to stabilise metal-olefin bonding by the chelate effect. For example, [Pd(olefin)L_2] type of complexes where L is a tertiary phosphine, have not been extensively studied due to their low thermal stability.[1] Therefore, SP ligand was put forward and the authors[23] managed to separate single crystals for a relatively stable complex [Pd$(SP)_2$] (Figure 5.7) and to characterise it using X-ray diffraction.

Figure 5.7
Structure of $[Pd(SP)_2]$

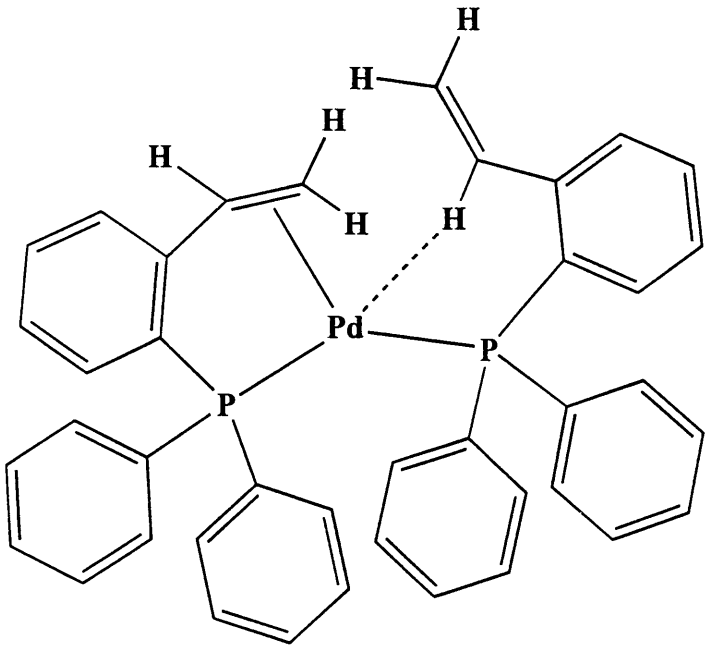

In this palladium *bis*phosphine complex, one of the phosphine ligands is acting as a bidentate ligand while the other is acting as a monodentate phosphorus-bound ligand. If the coordination centres are considered to be the two phosphorus atoms and the midpoint of the coordinated vinyl group, the geometry around the palladium atom is approximately trigonal. In addition, a close interaction is observed between the palladium atom and the α-hydrogen atom of the uncoordinated vinyl group, thus the palladium atom has a tendency to tetrahedral coordination. It is noteworthy that the crystal structures of the complexes $[M(SP)_2]$ (M = Pt, Ni) have been determined and both of the phosphine ligands are bound in a bidentate fashion to the metal centre which is coordinated in a distorted tetrahedron.[21] According to structural, spectroscopic and chemical evidence, palladium has the lowest affinity for olefins out of the three zerovalent metals, Ni, Pd and Pt. The reactivity of the vinyl group in this type of complex has been investigated. For example, the palladium complex (Figure 5.7) has been allowed to react with an excess of SP ligand to yield $[Pd(SP)_3]$ where all the vinyl groups are free. The addition of an aqueous HBF_4 to $[Pd(SP)_2]$ resulted in the formation of a five-membered ring chelate (σ-alkyl)palladium(II) salt (Figure 5.8) where the metal is surrounded by a *trans* geometry.[23] However, the reaction of

$[Pt(SP)_2]$ with aqueous HBF_4 or HPF_6 resulted in the formation of a mixture of *cis*- and *trans*-$[Pt\{\kappa^2(2\text{-}CH_3CHC_6H_4PPh_2)\}(SP)][Y]$ ($Y = BF_4$, PF_6).[21]

Figure 5.8
Structure of *trans*-$[Pd\{\kappa^2(2\text{-}CH_3CHC_6H_4PPh_2)\}(SP)][BF_4]$

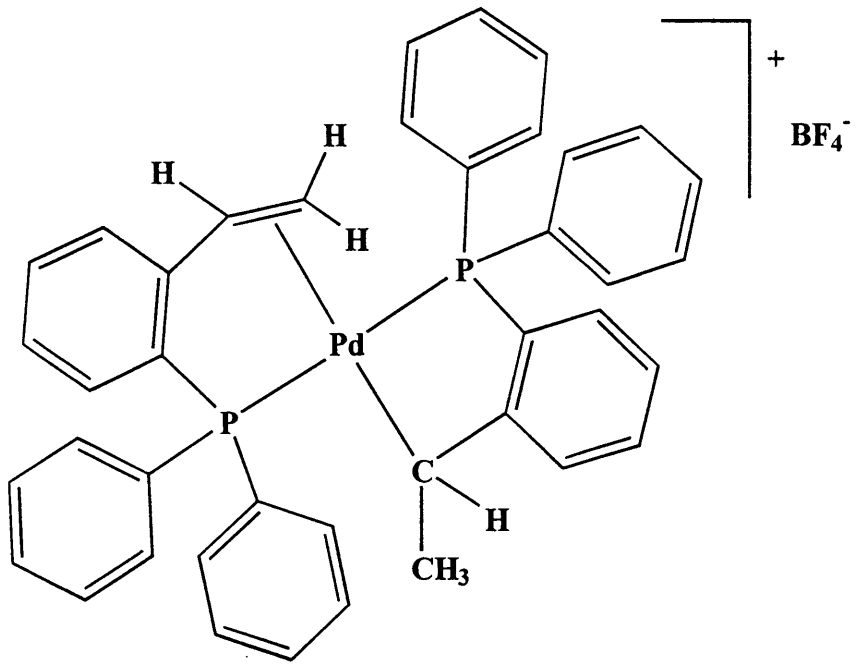

5.4 Preparation and Characterisation of $PPh_2(2\text{-}C_2H_3C_6H_4)$ (SP):

The ligand has been prepared following a similar route to the other *ortho*-substituted aryl phosphine ligands already described in this work (Chapters Three and Four). The starting material is *o*-bromostyrene which, on treatment with magnesium turnings, yields the corresponding Grignard reagent and this then reacts with chlorodiphenylphosphine to yield the desired product (SP) (Figure 5.9).

Figure 5.9
Structure of *ortho*-styryldiphenylphosphine (31)

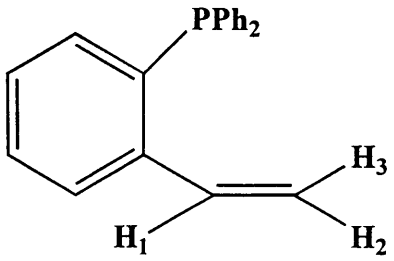

(SP)

The characterisation data obtained on this ligand are in good agreement with the data already published in the literature[13,19] and some of the data for this ligand are important for later discussions on the coordination chemistry and are drawn to the attention of the reader here.

The $^{31}P\{^{1}H\}$ NMR spectrum exhibits a singlet at -13.8 ppm. In the ^{1}H NMR spectrum, the assignment of the H_3 signal is based on its relatively large vicinal coupling to H_1 (17 Hz). The H_3 signal is also subject to a long-range coupling to phosphorus (ca. 1 Hz)[26] which is detected by a proton-phosphorus spin decoupled NMR experiment [$^{1}H\{^{31}P\}$]. It has been postulated that this long-range coupling is induced by a direct overlap between the lone pair of the phosphorus atom and the σ-electrons of H_3, comparable to hydrogen bonding. This could be one of the reasons for the H_3 signal appearing at a higher frequency relative to that of H_2. The signal of the proton H_1 is usually masked by the aromatic protons' signals.

The un-coordinated vinyl group is characterised by a very weak C=C stretching frequency in the IR spectrum, usually at 1625-1630 cm^{-1}, and by out-of-plane deformation olefinic C-H bands at 990 and 920 cm^{-1}.

5.5 Preparation and Characterisation of the chelate [$PtCl_2$(SP)] (32):

One equivalent of the phosphine ligand SP was allowed to react with [$PtCl_2(CH_3CN)_2$] in dichloromethane. The resulting product is the platinum chelate

$[PtCl_2(SP)]$ (**32**) (Scheme 5.1) confirmed by different spectroscopic methods in addition to X-ray diffraction studies.

Scheme 5.1

$$[PtCl_2(CH_3CN)_2] + (o\text{-}C_2H_3C_6H_4)PPh_2 \rightarrow [Pt\{\kappa^2\text{-}(C_2H_3C_6H_4)PPh_2\}Cl_2]$$

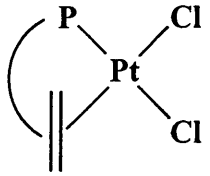

(**32**)

Aromatic protons gave rise to multiplets in the range 7.92-7.25 ppm in the ^1H NMR spectrum. The vinyl protons' signals are shifted to lower frequencies compared to those of the free ligand due to changes in the shielding effects of the π-electrons, except the one corresponding to the H_2 proton. The three signals are now flanked by satellites due to the coupling to ^{195}Pt. The results are summarised in Table 5.2 together with those of the free ligand.

Table 5.2
NMR Data of SP and Platinum(II)-SP Complexes
(δ_H in ppm and J_{HH} in Hz)

Compound	δ_{H1}	δ_{H2}	δ_{H3}	$\lvert J_{13} \rvert$	$\lvert J_{12} \rvert$	$\lvert J_{23} \rvert$	$\lvert J_{P\text{-}H3} \rvert$
SP [a]	-[b]	5.13	5.54	17	11	1	1
$[Pt(SP)Cl_2]$ (**32**)[c]	5.98	5.22	3.58	13	8	<0.5	3
$[Pt(SP)_2]$[d]	4.05	3.33	2.47	9.4	8.3	-[e]	-[e]

[a] This work. Recorded in $CDCl_3$. [b] Obscured by the aromatic protons. [c] This work. Recorded in $CDCl_3$. $J_{H1\text{-}Pt}$=62Hz, $J_{H2\text{-}Pt}$=70Hz, $J_{H3\text{-}Pt}$=55Hz. [d] Ref. 21. Recorded in d^8-toluene. [e] Not reported.

The chemical shift of H_3 was affected more by coordination compared to that of H_2. This difference is attributed to the unsymmetrical position of the metal relative to the vinyl protons. The short interaction usually takes place between the metal and the unsubstituted carbon C1 atom of the olefin group. The substituent on the olefin group, specifically on C2, induces an orbital polarisation,[27] which favours an increase in the C1 coefficient, thus strengthening the Pt-C1 interaction. On the other hand, a decrease is observed in both types of spin-spin coupling, the geminal and the vicinal proton coupling values. Nevertheless, these changes are small when compared to those for other coordinated olefin groups.[28] Therefore, the vinyl group retains significant amounts of double bond character.

The Pt-H (vinyl) coupling constants of complex (**32**) (Table 5.2) are similar to values from the literature[25] and their existence confirms the vinyl-metal bonding and, hence, chelation of the phosphine ligand. For example, in the *cis*-[$PtBr_2(\kappa^2$-2-MeOCH=CH-$C_6H_4PPh_2$)] complex, J_{Pt-H} = 75 Hz, where H is the α-proton of the coordinated vinyl group.[25] Additionally, the increase in the J_{P-H3} value in complex (**32**) (Table 5.2) confirms the through-space coupling between the phosphorus and this proton since the formation of the chelation ring brings the H_3 proton in closer proximity to the phosphorus atom.

The $^{31}P\{^1H\}$ NMR spectrum exhibits one signal consistent with the existence of one phosphorus atom environment. It is a singlet at 23.1 ppm with a $^1J_{Pt-P}$ coupling constant of 3234 Hz. This $^1J_{Pt-P}$ coupling constant is typical for a phosphorus *trans* to Cl and, when compared to a coupling in a relevant complex *cis*-[$PtCl_2(\eta$-$C_2H_4)PPh_3$] ($^1J_{Pt-P}$ = 3262 Hz),[29] the chelate effect in the former complex appears to have only a small influence on the bonding nature between Pt and P.

In order to establish a correlation between the electronic environment of the metal centre and the type of the metal-olefin bonding, the NMR data of the [$PtCl_2$(SP)] complex (**32**) prepared in this work were compared to those of the platinum(0) complex [$Pt(SP)_2$] from the literature (Table 5.2).[21] The three protons' chemical shifts moved to lower frequencies when comparing the Pt(II) and Pt(0) complexes, especially that of H_3, and both the geminal and vicinal proton coupling

constants decreased. One would expect a higher electron density at the platinum atom in $[Pt(SP)_2]$ complex compared to that in the $[PtCl_2(SP)]$ complex (**32**) and this difference is translated into a C=C bond weakening revealed in a decrease in the coupling constants and shielding of the vinyl protons' signals. For d^8 metal-olefin complexes, σ-bonding is expected to dominate over π-back-bonding, taking into consideration the relatively high electron affinity (EA) of the metal. On the other hand, for d^{10} metal-olefin complexes, an increase in the π-back-bonding is predicted and related to a relatively high $d^{10} \rightarrow d^9$ ionisation potential (IP).

In the IR spectrum of the $[PtCl_2(SP)]$ complex, a weak signal at 1481 cm^{-1} is assigned to a bound C=C stretching vibration and this decrease is expected upon olefin coordination.[19,25]

A single crystal, suitable for X-ray diffraction, was isolated by slow evaporation from dichloromethane solution (Figure 5.10). To be noted that the largest difference peak and hole data for (**32**) are +6.32e at 0.95 Å from Pt(1) and –2.50 e at 0.86 Å from Pt(1).

Figure 5.10
Crystal Structure of $[PtCl_2(SP)]$ (32)

a)

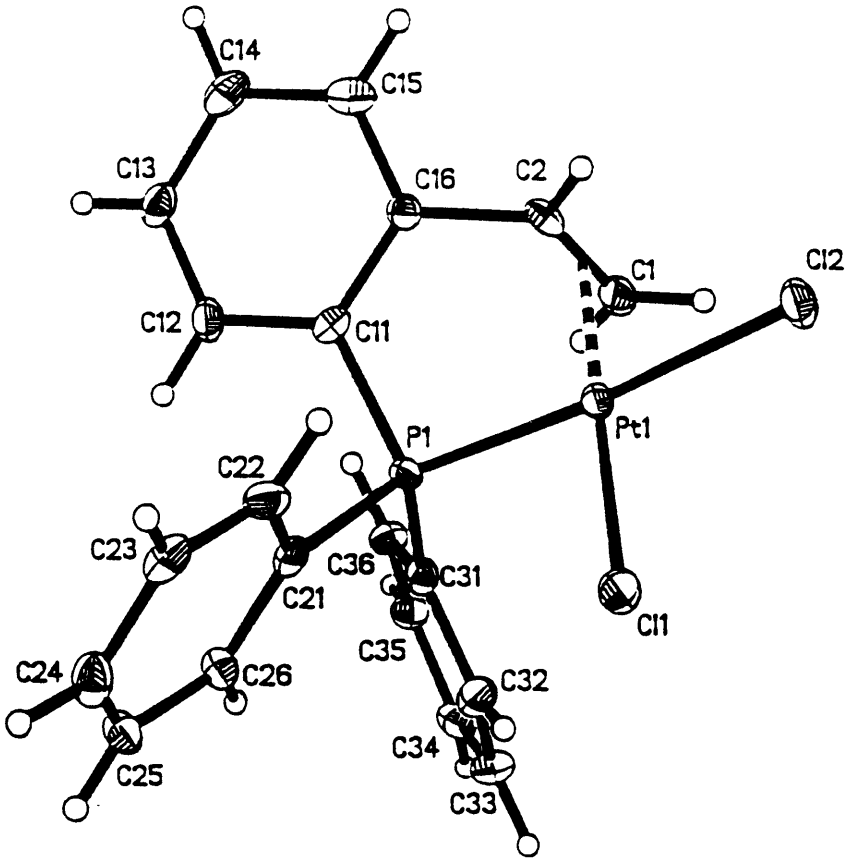

b)

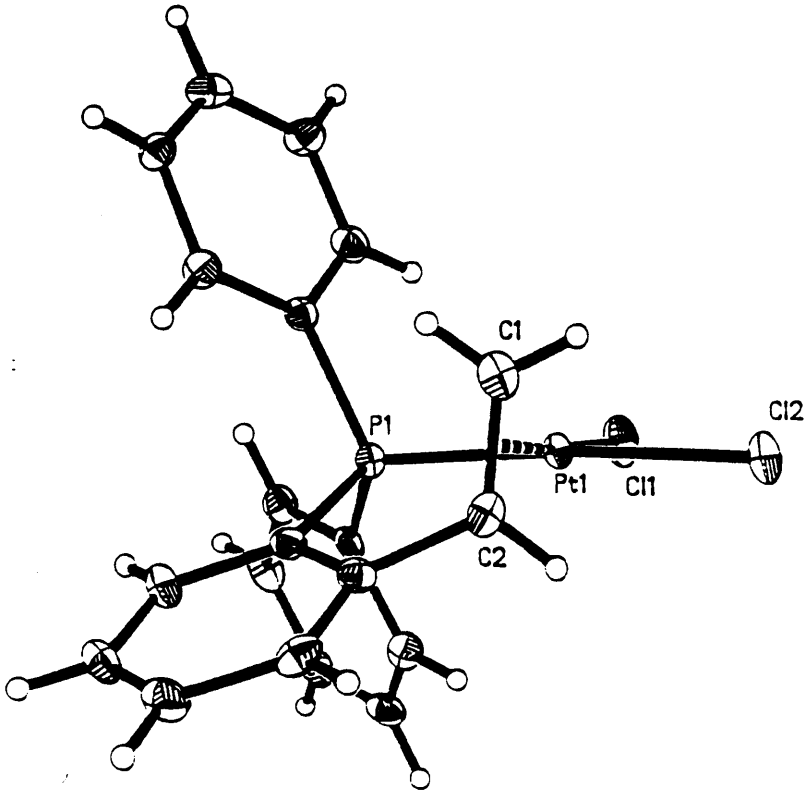

The platinum complex has square planar geometry around the metal centre. The chloride atoms are mutually *cis* and the phosphine ligand is acting as a chelating agent. Relevant data is shown in Table 5.3.

Table 5.3
Selected Bond Distances (Å) and Angles (°) with e.s.d. in Parentheses about Pt(II) for [$PtCl_2$(SP)] Complex (32)

Pt-C1	2.118(10)	C1-Pt-C2	38.5(3)
Pt-C2	2.168(10)	C1-Pt-P	89.6(3)
Pt-P	2.232(2)	C2-Pt-P	84.8(3)
Pt-Cl1	2.299(3)	P-Pt-Cl1	91.80(9)
Pt-Cl2	2.351(2)	P-Pt-Cl2	174.85(9)
C1-C2	1.415(13)	C1-Pt-Cl1	156.2(3)
		C2-Pt-Cl1	165.1(2)
		P-Pt-Cl2	174.85(9)
		Cl1-Pt-Cl2	91.15(9)
		C2-C1-Pt	72.6(5)
		C1-C2-Pt	68.8(6)

From Figure 5.10b, it can be seen that the olefinic double bond is not perfectly perpendicular to the plane formed by the platinum(II) centre and the two chlorides, which might correlate with the difference in the J_{Pt-H} values in the ^1H NMR spectrum. The terminal C1 atom is tilted away from the phosphorus. This type of inclination has been reported before for a variety of metal olefin complexes.[30] The Pt-C1(terminal) bond length is shorter than the Pt-C2 bond, which explains the larger influence of coordination on the chemical shifts of the terminal protons compared to the one neighbouring the aryl ring. This difference in lengths is reflected in the angles C2-C1-Pt and C1-C2-Pt.[30b] The vinyl bond length, C=C, in complex (**32**), 1.415(13) Å, is longer than that of an uncoordinated one and is consistent with its formulation as a π-bonded group. For example, the complex [$Fe(CO)_2(\kappa^2$-SP)(SP)][31] incorporates two SP ligands, one is acting as a chelating agent while the other is bound to the metal centre

solely through the phosphorus atom. The C=C bond length in the former ligand is 1.455(8) Å and in the latter is 1.339(10) Å. Comparing this latter value to the one obtained in complex (**32**), an obvious increase is noticed due to the bonding nature of the vinyl group, which is predominantly a π-acceptor ligand. The Pt-P bond length, 2.232(2) Å, in $[PtCl_2(SP)]$ (**32**) is shorter than that for a comparable complex $[PtMe_2(SP)]$ [2.276(1) Å],[32] which is due to the difference in the *trans*-influence between a methyl group and a chloride. Both distances are shorter than Pt-P distances in complexes incorporating an SP ligand acting as a monodentate ligand[31] because of the chelate effect causing a contraction in the Pt-P bonding. When comparing the Pt-P bond lengths in complex (**32**) to those in complex *cis*-$[PtCl_2\{P(4\text{-}HOC_6H_4)_3\}_2]$ (**6**) (Chapter Two) and complex *cis*-$[PtCl_2(PPh_3)_2]$,[33] the Pt-P bond lengths in complex (**6**), [2.268(4) and 2.243(4) Å] and in the triphenylphosphine analogue, [2.251(2) and 2.265(2) Å], are longer than that of complex (**32**), this difference could be assigned to the chelate effect in the latter.

It was originally planned to prepare the $[PtMe_2(SP)]$ complex by replacing the chloride ligands in complex (**32**) with methyl ligands following the same route described in Section 2.3.2 where *cis*-$[PtMe_2\{P(4\text{-}CH_3OC_6H_4)_3\}_2]$ (**11**) was prepared from *cis*-$[PtCl_2\{P(4\text{-}CH_3OC_6H_4)_3\}_2]$ (Scheme 2.10). The plan extended to the fluorination of the methylated complex $[PtMe_2(SP)]$ using aHF similarly to the route described in Chapter Six, that resulted in the preparation of the doubly fluoride bridged platinum(II) dimer $[Pt_2(\mu\text{-}F)_2\{P(4\text{-}CH_3OC_6H_4)_3\}_4]^{2+}$ $2HF_2^-$ (**35**) starting from *cis*-$[PtMe_2\{P(4\text{-}CH_3OC_6H_4)_3\}_2]$ (**11**) (Scheme 6.2). However, due to time constraints, these reactions were not carried out. It should be noted that the $[PtMe_2(SP)]$ complex has already been prepared by the displacement of the weakly coordinated diene from $[(COD)PtMe_2]$ (COD = η^4-1,5-cyclooctadiene) with one equivalent of the SP ligand.[34]

5.6 Preparation of Rhodium(III) Complexes:

The reaction of the ligand SP with $[PtCl_2(CH_3CN)_2]$ complex readily afforded the metal chelate. This is almost certainly due to steric and electronic conditions favouring the formation of the "$5^1/_2$" membered ring. However, in contrast to the behaviour of *tris*-(*o*-hydroxyphenyl)phosphine ligand, when the SP ligand was

allowed to react with the rhodium(III) dimer $[\{(\eta^5\text{-}C_5Me_5)Rh(\mu\text{-}Cl)Cl\}_2]$, it afforded a monomer in which the phosphine ligand is ligated solely by the phosphorus atom while the olefin group is free. In order to obtain a "$5^1/_2$" membered ring compound, in this case, a different driving force is needed.

5.6.1 Synthesis and Characterisation of $[(\eta^5\text{-}C_5Me_5)RhCl_2(SP)]$ (33):

Treatment of the dinuclear rhodium(III) complex $[\{(\eta^5\text{-}C_5Me_5)Rh(\mu\text{-}Cl)Cl\}_2]$ with two equivalents of *ortho*-styryldiphenylphosphine (SP) leads to the formation of a monomeric Rh(III) complex $[(\eta^5\text{-}C_5Me_5)RhCl_2(SP)]$ (**33**) (Scheme 5.2).

The ^1H NMR spectrum of (**33**) exhibits multiplets between 7.69 and 7.27 ppm assigned to the aryl protons of the phosphine ligand. Three doublets of doublets are assigned to the olefinic protons; one at 6.89 ppm assigned to H_1 ($J_{H1\text{-}H2}$ = 11 Hz, $J_{H1\text{-}H3}$ = 17 Hz), the second is at 5.46 ppm assigned to H_3 ($J_{P\text{-}H3}$ < 1Hz, $J_{H1\text{-}H3}$ = 17 Hz), the third is at 4.83 ppm and is assigned to H_2 ($J_{P\text{-}H2}$ < 1Hz, $J_{H1\text{-}H2}$ = 11 Hz). Additionally, the Cp* protons give rise to a doublet, coupling to the phosphorus atom ($J_{P\text{-}H}$ = 1.3 Hz).

Scheme 5.2:

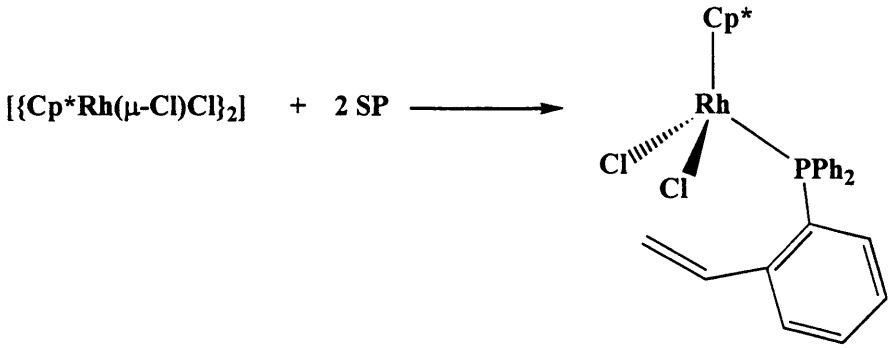

Cp*=η^5-C_5Me_5 **(33)**

The chemical shifts of the olefinic protons of the mono-coordinated phosphine ligand are very similar to those of the free ligand. Moreover, the IR spectrum measured in a Nujol mull, showed a weak absorption at 1623 cm^{-1} assigned to an un-coordinated vinyl group, in addition to signals at 1000 and 915 cm^{-1} assigned to the vinyl

deformation modes. These observations confirm that the vinyl group is not engaged in bonding to the metal centre. Of particular interest is the small J_{P-H} coupling associated with the Cp* protons, when compared to that of similar complexes prepared in this work or in the literature (Typically 2-4 Hz).[35] For this type of complex, the steric effect can exert a considerable influence on the coordination chemistry taking place at the metal centre. The free, un-coordinated vinyl group could be increasing the steric bulkiness of the phosphine ligand, pushing it away from the Cp* ring inducing a decrease in the $J_{P-H(Cp^*)}$ coupling.[36]

Figure 5.11
$^{31}P\{^1H\}$ NMR spectrum of $[(\eta^5\text{-}C_5Me_5)RhCl_2(SP)]$ (33)

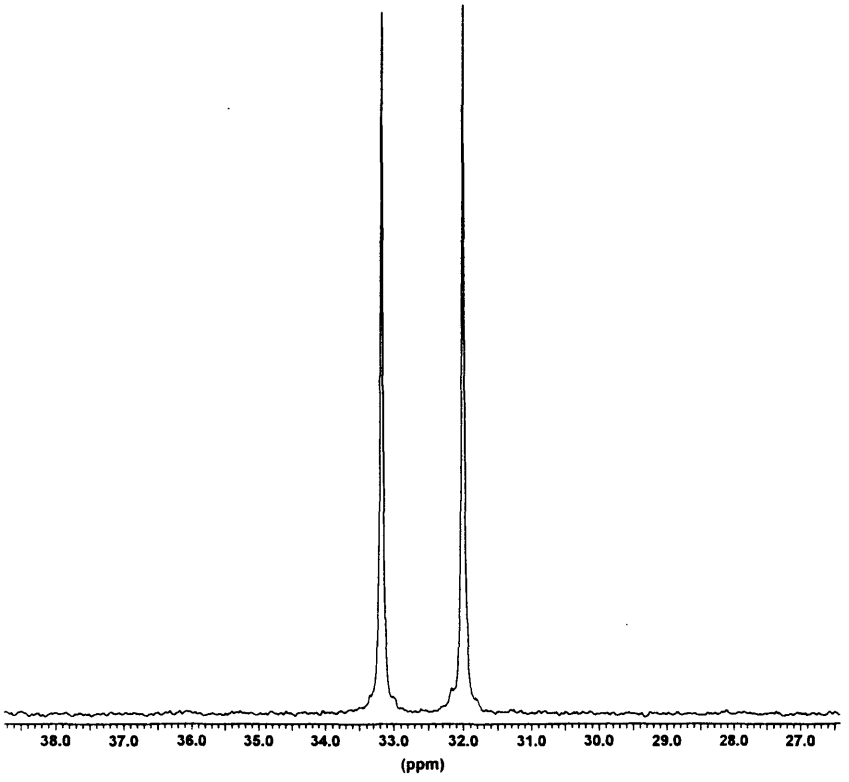

Table 5.4
$^{31}P\{^1H\}$ NMR data for [Cp*RhCl$_2$(L)]

L	$^1J_{Rh-P}$/Hz
P(4-$CH_3OC_6H_4$)$_3$ (**15**) [a]	144
P(4-HOC_6H_4)$_3$ (**16**) [b]	143
PPh_3 [c]	144
P(2-$C_2H_3C_6H_4$)Ph_2 (**33**) [d]	143

[a] This work. Recorded in $CDCl_3$. [b] This work. Recorded in DMSO. [c] Ref. 37. [d] This work. Recorded in CD_2Cl_2.

The $^{31}P\{^1H\}$ NMR experiment (Figure 5.11) reveals a broad doublet at 32.6 ppm. The rhodium-phosphorus coupling is 143 Hz, which is typical and unremarkable (Table 5.4) (Figure 5.11). It has been observed in the previous chapters that the introduction of either a methoxy or a hydroxy group on the *para*-position of the phenyl rings in tertiary aryl phosphine ligands does not significantly affect the coupling constant $^1J_{Rh-P}$ (Table 5.4), indicating that the introduction of such groups does not induce major change in the rhodium-phosphorus bonding. In this section, the SP ligand has an *ortho*-substituent on one of the aryl rings. Once again, the $^1J_{Rh-P}$ value has not been affected by the position of the substituent or by its structure. This value is, therefore, mainly affected by the σ-character in the Rh-P bonding, since the rhodium(III) is not expected to have significant amounts of electron density available for π-back bonding.

5.6.2 Synthesis and Characterisation of [(η^5-C_5Me_5)RhCl{κ^2-($C_2H_3C_6H_4$)PPh_2}][BF_4] (34):

The reaction of the monomer [(η^5-C_5Me_5)$RhCl_2$(SP)] (**33**) with one equivalent of $AgBF_4$ in a dichloromethane solution affords a rhodium chelate as shown in Scheme

5.3. This route has been shown to be successful in similar systems to force the olefin group to bind to the metal centre.[14]

Scheme 5.3:

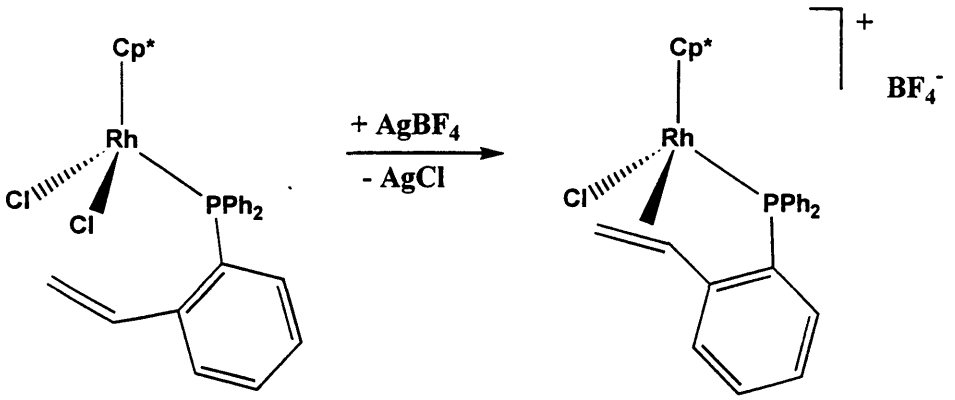

(33) (34)

The formation of the "$5^1/_2$" membered ring upon chelation is clearly detected by the shifting of the phosphorus signal to higher frequency in the $^{31}P(^1H\}$ NMR spectrum (Figure 5.12) (Table 5.5) and of the vinyl protons' signals to lower frequencies in the ^1H NMR spectrum. The IR spectrum did not show any bands assignable to vinyl deformations or C=C stretches.

Figure 5.12
$^{31}P\{^{1}H\}$ NMR spectrum of $[(\eta^5\text{-}C_5Me_5)RhCl\{\kappa^2\text{-}(C_2H_3C_6H_4)PPh_2\}][BF_4]$ (34)

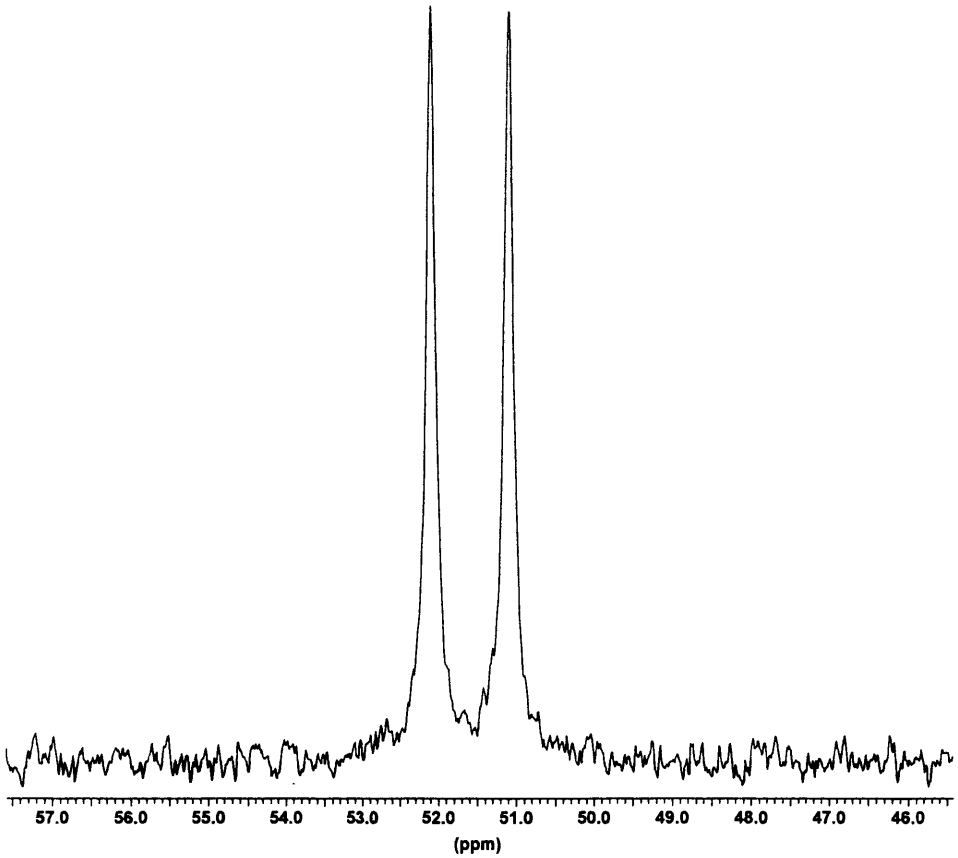

Table 5.5
^{1}H NMR data of SP and $[Cp^*RhCl(X)(Y)]^{n+}$ Complexes
(δ_H in ppm and J in Hz)

Compound	δ_{H1}	δ_{H2}	δ_{H3}	$J_{P\text{-}H(Cp^*)}$	δ_P	Δ^d	$J_{Rh\text{-}P}$
SP[a]	-[b]	5.13	5.54	-	-13.8	-	-
X = Cl, Y = SP, n = 0 (**33**)[c]	6.89	4.83	5.46	1.3	32.6	46.4	143
X, Y = $\{\kappa^2\text{-}(C_2H_3C_6H_4)PPh_2\}$, n = 1 (**34**)[c]	6.38	4.76	4.52	3	50.3	64.1	122

[a] **This work. Recorded in $CDCl_3$.** [b] **Obscured by the aromatic protons.** [c] **This work. Recorded in CD_2Cl_2.** [d] $\Delta = \delta_{complex} - \delta_{free\ ligand}$.

The signals assigned to the two geminal protons H_2 and H_3 in the rhodium chelate are broad, therefore no coupling constants could be deduced. The shifting of these signals towards low frequencies is not significant and this could be accounted for by a small perturbation of the olefin group upon formation of Rh-olefin bond. It is likely that this observation is due to the fact that rhodium(III) is deficient in electron density and would prefer to be ligated by an electron donor group. However the olefin is a weak σ-donor and a strong π-acceptor. It should be noted that the order of the chemical shifts corresponding to vinyl protons in the free ligand as well as in the rhodium complex, where the phosphine is acting as a monodentate ligand, is the following: $\delta_{H1} > \delta_{H3} > \delta_{H2}$. However, in complexes where the olefin is engaged in coordination with the metal centre, the order is different ($\delta_{H1} > \delta_{H2} > \delta_{H3}$). The vinyl group favours a certain coordination position to the metal due to steric and electronic requirements as described previously in Section 5.4.

The difference in the structures between the two rhodium(III) complexes in Table 5.5 is the replacement of a chloride with an olefin group forming a "$5^1/_2$" membered ring. The result is a shifting of the phosphorus signal to higher frequency, an increase in the coordination chemical shift and a decrease in the $^1J_{Rh-P}$ value. These three same observations were noticed in the formation of the rhodium(III) chelate [Cp*Rh{κ^2-(2-OC_6H_4)P(2-HOC_6H_4)$_2$}Cl] (**29**) and described in Chapter Four. Here, the ring contribution Δ_R value is 17.7 ppm (64.1 - 46.4) which is typical for phosphorus-olefin "$5^1/_2$" membered ring species.[38]

The ^{19}F NMR spectrum of the salt (**34**) revealed a singlet at -152.7 ppm assigned to the counterion BF_4^-.

5.7 Summary:

The reaction of $[PtCl_2(CH_3CN)_2]$ complex with the *o*-styryldiphenylphosphine (SP) ligand readily affords the $[PtCl_2(SP)]$ chelate, which is stable in solution. However, it should be noted that the complex resulting from the reaction of $[PtCl_2(CH_3CN)_2]$ with *tris*-(*o*-hydroxyphenyl)phosphine ligand (Chapter Four) exhibits hemilability behaviour. On the other hand, the reaction of $[\{(\eta^5\text{-}C_5Me_5)Rh(\mu\text{-}Cl)Cl\}_2]$ complex with the SP ligand affords the $[(\eta^5\text{-}C_5Me_5)RhCl_2(SP)]$ complex, where the phosphine ligand is acting in a monodentate mode. A further step is needed in order to achieve the chelation. This is achieved by forcing the Rh-Cl bond cleavage by AgCl precipitation, as this vacates a coordination site on the metal centre and, hence, favours the coordination of the vinyl group to the metal. However, the reaction of the same doubly chloride-bridged rhodium dimer with *tris*-(*o*-hydroxyphenyl)phosphine ligand readily affords a stable rhodium chelate.

The oxygen atom is mainly a σ-electron withdrawing ligand whilst the vinyl group is mainly π-electron withdrawing and the vinyl group is larger in size compared to the oxygen atom. Moreover, when comparing the chelation of the ligand SP to that of *tris*-(*o*-hydroxyphenyl)phosphine ligand, the former forms a "$5^1/_2$"-membered ring, whilst the latter forms a more stable five-membered ring.

All of these criteria, put together, make it possible to predict the stability of the resulting metal chelates. Since the rhodium(III) centre is electron deficient, it would not favour any π-back-bonding with a ligand, but the platinum(II) centre is relatively capable of stabilising a π-back-bonding. In this case, it is noteworthy to take into consideration the Lewis basicity of the other ligating groups coordinated to the metal centre. Moreover, the large steric effect around the rhodium(III) centre hinders the formation of the chelate by keeping the vinyl group away from the metal centre.

Chapter Five References

[1] Articles by P. W. Jolly, on Ni, by P. M. Maitlis, P. Espinet, and M. J. H. Russell, on Pd, and by F. R. Hartley, on Pt in: *Comprehensive Organometallic Chemistry*; G. Wilkinson, F. G. A. Stone, E. W. Abel (eds); Pergamon: Oxford, 1982.

[2] E. Uhlig, D. Walther, *Coord. Chem. Rev.*, 1980, **33**, 3.

[3] D. P. M. Mingos, *Bonding of Unsaturated Organic Molecules to Transition Metals; in Comprehensive Organometallic Chemistry*; G. Wilkinson, F. G. A. Stone, E. W. Abel (eds); Pergamon: New York, 1982.

[4] R. S. Nyhlom, *Proc. Chem. Soc.*, 1961, 273.

[5] C. Elschenbroich and A. Salzer, *Organometallics, A Concise Introduction*, 2nd rev. Ed., Weinheim; NewYork; Basel; Cambridge P:VCH, 1992.

[6] a) R. Bau, *Inorg. Chem.*, 1975, **14**, 2653.
b) L. J. Guggenberger, *J. Am. Chem. Soc.*, 1972, **94**, 3779.
c) R. Hoffmann, *J. Am. Chem. Soc.*, 1979, **101**, 3801.

[7] L. J. Guggenberger and R. Cramer, *J. Am. Chem. Soc.*, 1972, **94**, 3780.

[8] R. Cramer, J. B. Kline and J. D. Roberts, *J. Am. Chem. Soc.*, 1969, **91**, 2519.

[9] J. K. Stalick and J. A. Ibers, *J. Am. Chem. Soc.*, 1970, **92**, 5333.

[10] I. M. Al-Najjar, *Inorg. Chim. Acta*, 1987, 128, 93.

[11] C. Panattoni, G. Bombieri, U. Belluco and W. H. Baddley, *J. Am. Chem. Soc.*, 1968, **90**, 798.

[12] G. M. Bodner, B. N. Storhoff, D. Doddrell and L. J. Todd, *J. Chem. Soc., Chem. Commun.*, 1970, 1530.

[13] M. A. Bennett, R. S. Nyholm and D. Saxby, *J. Organomet. Chem.*, 1967, **10**, 301.

[14] M. I. Bruce, M. L. Williams, *J. Organomet. Chem.*, 1986, **314**, 323.

[15] S. J. Dossett, M. Green, M. F. Mahon and J. M. McInnes, *J. Chem. Soc. Chem. Commun.*, 1995, 767.

[16] M. A. Bennett and P. N. Kapoor, *J. Organomet. Chem.*, 1987, **336**, 257.

[17] L. V. Interrante and G. V. Nelson, *Inorg. Chem.*, 1968, **7**, 2059.

[18] M. A. Bannett, G. B. Robertson, I. B. Tomkins and P. O. Whimp, *Chem. Commun.*, 1971, 341.

[19] M. A. Bennett, R. N. Johnson and I. B. Tomkins, *Inorg. Chem.*, 1974, **13**, 346.

[20] M. A. Bennett and L. L. Welling, *Polyhedron*, 1989, **8**, 2193.

[21] M. A. Bennett, C. Chiraratvatana, G. B. Robertson and U. Tooptakong, *Organometallics*, 1988, **7**, 1394.

[22] B. Corain, B. Longato and R. Angeletti, *Inorg. Chim. Acta*, 1985, **104**, 15.

[23] M. A. Bennett, C. Chiraratvatana, G. B. Robertson and U. Tooptakong, *Organometallics*, 1988, **7**, 1403.

[24] T. G. Appleton and M. A. Bennett, *Inorg. Chem.*, 1974, **13**, 3023.

[25] M. A. Bennett, W. R. Kneen and R. S. Nyholm, *J. Organomet. Chem.*, 1971, **26**, 293.

[26] A. G. Moritz, J. D. Saxby, and S. Sternhell, *Aust. J. Chem.*, 1968, **21**, 2565.

[27] L. Libit and R. Hoffmann, *J. Am. Chem. Soc.*, 1974, **96**, 1370.

[28] C. N. Banwell and N. Sheppard, *Mol. Phys.*, 1960, **3**, 351.

[29] I. M. Al-Najjar, *Inorg. Chim. Acta*, 1984, **83**, L53.

[30] a) E. Benedetti and C. Pedone, *J. Organomet. Chem.*, 1971, **29**, 443.
b) S. C. Nyburg, K. Simpson and W. Wong-Ng, *J. Chem. Soc., Dalton Trans.*, 1976, 1865.

[31] G. B. Robertson and P. O. Whimp, *J. Chem. Soc., Dalton Trans.*, 1973, 2454.

[32] M. A. Bennett, H.-K. Chee, J. C. Jeffery and G. B. Robertson, *Inorg. Chem.*, 1979, **18**, 1071.

[33] J. Fawcett, E. G. Hope, R. D. W. Kemmitt, D. R. Paige, D. R. Russell and A. M. Stuart, *J. Chem. Soc., Dalton Trans.*, 1998, 3751.

[34] M. A. Bennett, R. Bramley and I. B. Tomkins, *J. Chem. Soc., Dalton Trans.*, 1973, 166.

[35] W. D. Jones and V. L. Kuykendall, *Inorg. Chem.*, 1991, **30**, 2615.

[36] W. D. Jones and F. J. Feher, *Inorg. Chem.*, 1984, **23**, 2376.

[37] J. H. Holloway, E. G. Hope and G. C. Saunders, unpublished work.

[38] P. E. Garrou, *Chem. Rev.*, 1981, **81**, 229.

CHAPTER SIX

SYNTHESIS AND CHARACTERISATION OF LOW-VALENT PLATINUM GROUP METAL FLUORIDE PHOSPHINE COMPLEXES

CHAPTER SIX

SYNTHESIS AND CHARACTERISATION OF LOW-VALENT PLATINUM GROUP METAL FLUORIDE PHOSPHINE COMPLEXES

6.1 Introduction:

Many low-valent late transition-metal chloride, bromide or iodide phosphine complexes have been prepared. The properties of the components of these complexes, i.e., the metal, the halide, and the phosphine ligand, have been extensively studied and used in the design of catalysts.[1] It has been substantiated in several cases that replacing the halide ion by a smaller one increases the catalytic activity of the resulting complex.[2,3] Nevertheless, there has been little exploration of the chemistry of low-valent late transition-metal fluoride phosphine complexes. This lack of study can be accounted for by the fact that such species would contradict the Hard/Soft Acid/Base Pearson's theory.[4] The fluoride ion is a hard Lewis base. This classification stems from its high electronegativity, small size, in addition to its low polarisability.[5] A ligating atom with such properties would prefer to coordinate to hard Lewis acids such as transition-metals in their high oxidation states. Indeed, the fluoride ion stabilises Rh(VI)[6], Ir(VI),[7] and Pt(VI).[8]

The coordination chemistry of transition metal elements, in general, is a rich area. These elements are considered very "social" entities in that they are capable of coordinating to just about every other element in the Periodic Table. The fluorine should not be an exception. However, the important issue in this matter is finding a suitable fluorinating reagent and the right conditions to prepare the desired low-valent late transition-metal fluoride complexes. Recently, an increasing range of routes to low-valent late transition-metal fluoride complexes using for example, C-F bond activation,[9] aHF,[10] XeF_2,[11] F_2[12] and $Et_3N.3HF$ (TREAT-HF)[13] have been described and, consequently, a broader range of this class of complexes is now appearing in the literature.[14,15]

Despite the commonly held belief that the scarcity of complexes offering a Soft/Hard combination is mainly due to the weak interaction between the mismatching entities, late transition-metal alkoxide or hydroxide complexes have been prepared and characterised. Complexes exhibiting similar combinations have been found to be relevant to catalysis and have started to receive increasing attention.[16]

This chapter considers the preparation and characterisation of platinum group metal fluoride phosphine complexes. The metals used are platinum(II), osmium(II) and ruthenium(II). Various arylphosphine ligands such as $P(4\text{-}CH_3OC_6H_4)_3$, $P(4\text{-}HOC_6H_4)_3$ and PPh_3 have been used, as well as the alkylphosphine ligands, PEt_3 and PCy_3. The discussion will highlight mostly the influence of different phosphine ligands on the metal-fluoride bonding in order to achieve a better understanding of its nature.

6.2 Low-Valent Platinum Group Metal-Fluoride Bond:

According to Pearson's theory, a soft acid such as a low-valent transition metal ought to prefer to coordinate to halides in the order, $F^- < Cl^- < Br^- < I^-$. In contrast to this hypothesis, it has been observed in numerous cases that the most stable halocarbonyl species are the fluoro-derivatives.[17] This phenomenon has been observed while examining the rhodium(I) system depicted in Scheme 6.1. The stability of the complex $[RhX(CO)(PPh_3)_2]$ follows the trend $X^- = F^- > Cl^- > Br^- > I^-$ in dichloromethane solution.[18,19]

Scheme 6.1

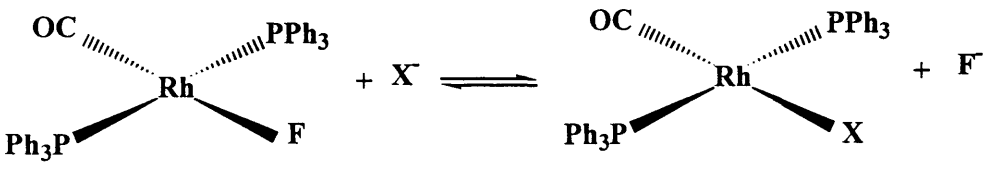

The equilibrium in Scheme 6.1 is shifted to the right upon addition of compounds such as water or methanol. This is explained by the strong hydrogen bonding of the uncomplexed fluoride ion to the hydroxyl groups of these solvents. This specific conclusion is important by itself as it represents an example of a driving force required to prepare a variety of $[RhX(CO)(PPh_3)_2]$ complexes starting from the fluoride analogue by simple fluoride displacement. In addition, it has been noticed that the order of the stretching frequency ν_{CO} in the halocarbonyl complexes, varies with the halogen in the order, $X = I \geq Br \geq Cl > F$ (Table 6.1).[20] This variation, which is inexplicable by the conventional electronegativity concept, could be interpreted in terms of the σ-π dualism theory.

Table 6.1
Carbonyl Stretching Frequencies (cm^{-1})
in *trans*-$[MX(CO)(PPh_3)_2]$.

X	ν_{CO} for M = Ir	ν_{CO} for M = Rh
I	1967	1981
Br	1966	1980
Cl	1965	1980
F	1957	1971

These observations indicate possible π-donation out of the filled p-orbitals at the halides. This type of bonding follows the order, $X = F > Cl > Br > I$. This hypothesis confirms the additional stability of the fluorocarbonyl rhodium complex in Scheme 6.1 compared to that of the other halocarbonyl rhodium complexes. An increase in both, the σ-withdrawing effect and the π-donating effect of the halogen, tends to minimise the competition between the halogen and the carbonyl group for ligating the metal centre.

On the other hand, electronic absorption studies carried out on $[MX(CO)(PPh_3)_2]$ complexes in benzene reveal an increase in λ_{max} following the order X = F < Cl < Br < I.[21] $\lambda_{max} = 1/\Delta E$ is attributed to the transition $a_{1z2} \rightarrow b_{1\pi}$ in a C_{2V} complex (Figure 6.1).[21a] This increase has been assigned to a greater stabilisation of the $b_{1\pi}$ level due to an increase in the π-acceptor capability of the halide, making use of its empty low-lying d_π orbital, following the same trend, i.e. F < Cl < Br < I. A parallel persuasive explanation for the same increase in λ_{max}, is the destabilisation of the a_{1z2} level. This occurs upon increasing the σ-donor ability of the halide, following the trend X = F < Cl < Br < I. The increase in σ-donor ability is linked to a decrease in the electronegativity and an increase in the polarisability of the halogen. The smallest λ_{max} value is assigned to the fluorocarbonyl complex. In other terms, this latter rhodium complex exhibits the most energetic $a_{1z2} \rightarrow b_{1\pi}$ transition compared to the other halocarbonyl complexes.

Figure 6.1
Molecular Orbital Energy Level Correlation Diagram for C_{2V} Complexes

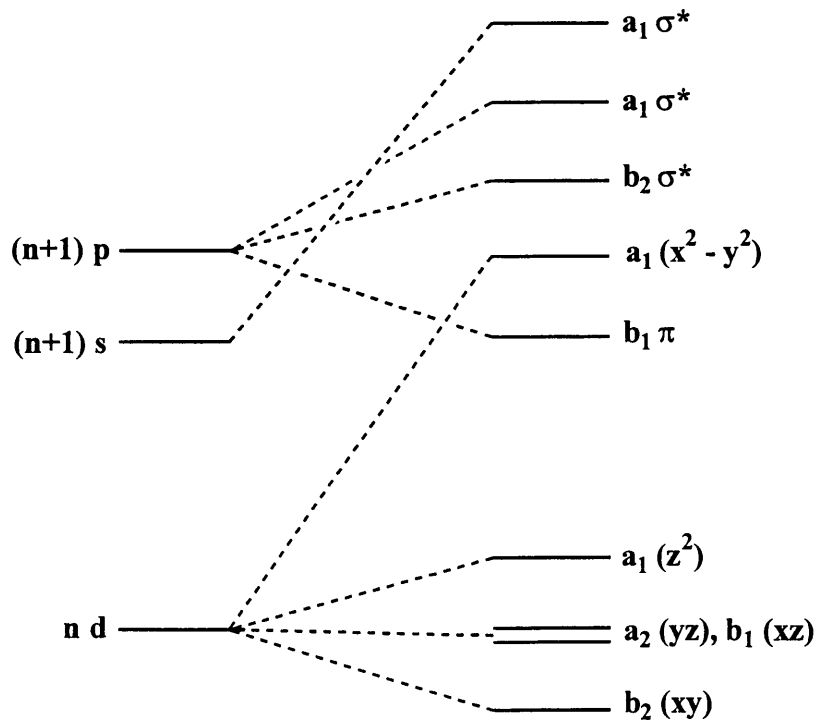

NMR experiments have been carried out on these $[RhX(CO)(PPh_3)_2]$ complexes. The ^{31}P spectra[22] reveal a decrease in the $^1J_{Rh-P}$ value following the order X = F > Cl > Br > I. The large $^1J_{Rh-P}$ value, attributed to the fluoride-containing complex, is consistent with an increase in the σ-donating effect from the phosphorus. The variation in $^1J_{Rh-P}$ is proportional to the variation in the electronegativity of the metal centre which, in turn, is proportional to the electronegativity of the bound halogen.[22a] However, the interpretation of the ^{103}Rh NMR chemical shifts is not as straight forward as that of the previous ^{31}P NMR data. An increase in the shielding of the rhodium signal has been observed following the order X = F (δ 5711) < Cl (δ 5488) < Br (δ 5436) < I (δ 5324).[22a] In general, the NMR chemical shift value is proportional to different factors. The two main factors are the σ_d (diamagnetic shielding) factor and the σ_p (paramagnetic shielding) factor. The increase of the σ_d and σ_p values contributes to the shielding and deshielding of the NMR signal respectively. σ_p is an important factor in the metal NMR experiment as compared to that of the proton. Hence, the importance of σ_p is proportional to the chemical shift range.[23] The paramagnetic shielding factor σ_p is inversely proportional to both "ΔE" and "r" values.[23,24] "ΔE" is the average value of the excitation energy of states having appropriate symmetry. The "r" value is the distance between the metal d-electrons and the nucleus. The observation of a larger deshielding of the ^{103}Rh signal in the case of the fluoride complex compared to the other halogenated complexes, reflects a relatively larger σ_p value. In other terms, it reflects relatively smaller "ΔE" and "r" values. However, according to the electronic absorption studies carried out on the $[RhX(CO)(PPh_3)_2]$ complex and described previously, the smaller λ_{max} value (i.e., the larger "ΔE" value, because $\lambda_{max} = 1/\Delta E$) corresponds to the fluoride-containing complex. On the other hand and according to the nephelauxetic effect, a decrease in the "r" value is related to a decrease in the M-X bond covalency on going up the halide group, which is in line with the observed ^{103}Rh chemical shift variations. Therefore, the observed ^{103}Rh NMR data are more readily interpreted by a variation in the "r" factor rather than changes in "ΔE", bearing in mind that the latter factor confirms the relatively high π-donating effect of the fluoride compared to the other halogen atoms (already shown by IR and electrochemical data). The last observation accounts for the failure of the ^{103}Rh NMR experiment to establish the importance of

the π-donation of the fluoride atom, which has been established by other characterisation techniques mentioned previously. Moreover, electrochemical experiments carried out on $[MX(CO)(PPh_3)_2]$ (M = Rh, Ir and X = halogen)[25] suggest that the fluoro complexes are the most difficult to reduce compared to the other halogeno complexes. Thus, the metal centre in the fluoro complexes is the most electron-rich metal compared to the other complexes.

The ^{19}F NMR experiments appear to be a helpful tool in probing the metal-fluoride bonding. The F→M π-donation depends to a large extent on the electronic behaviour of the other coordinated ligands to the metal centre. To illustrate this dependence, a comparison between two fluoride-containing complexes is taken from the literature and included in Table 6.2.[26]

Table 6.2
^{19}F NMR Data of $[RuHF(CO)P_2]$ vs $[RuHF(X)(CO)P_2]$ where P = P^tBu_2Me.

Complex	δ ^{19}F/ppm
$[RuHF(CO)P_2]$	-311
$[RuHF(py)(CO)P_2]$	-491
$[RuHF(CO)_2P_2]$	-202

Pyridine is predominantly a σ-donor ligand. Its ligation induces a decrease in the electrophilicity of the metal centre. Now that the metal is less electrophilic, F→M π-donation intensity is reduced, which causes a decrease of frequency in the resonance assigned to the fluoride. However, the carbonyl group is predominantly a π-acceptor ligand, therefore it gave a shift to higher frequency.

Overall, the fluoride is the best π-donor halogen. Moreover, the metal-fluoride bonding is characterised by the coexistence of two effects:

- An inductive withdrawing effect through the sigma bond.

- A mesomeric donor effect out of the full p orbitals at the fluoride ion.

However, it is still difficult to establish an exact formula describing the extent of the dualism of σ- and π-bonding between the metal and the fluoride ion. The main reason for this uncertainity is the lack of highly specific characterisation experiments. This characterisation ambiguity is due to a variety of factors, some of which are understood, whilst others are still under investigation.

6.3 Preparation and Characterisation of $[Pt_2(\mu\text{-}F)_2\{P(4\text{-}CH_3OC_6H_4)_3\}_4][HF_2]_2$ (35):

In 1965, the first complex platinum(II) fluoride was reported; $[PtF_2(PPh_3)_2]$.[27] In 1971, this product was reformulated by Kemmitt *et al.*[28] as $[PtF(PPh_3)_3][HF_2]$. The authors[28] noticed that when $[Pt(PPh_3)_3]$ or $[Pt(PPh_3)_4]$ reacted with liquid hydrogen fluoride, only from $[Pt(PPh_3)_4]$ were significant quantities of PPh_3 obtained in addition to a platinum fluoride complex. Detailed chemical analyses carried out on the resulting platinum fluoride complex showed the stoicheiometry $PtF_3(PPh_3)_3$. Moreover, upon reacting this complex with lithium chloride, *cis*-$[PtCl_2(PPh_3)_2]$ was formed in addition to liberation of one molar equivalent of PPh_3. The chemical analyses, and the result from the lithium chloride reaction, were two pieces of evidence for the existence of three triphenylphosphine ligands incorporated in the platinum fluoride complex. Conductivity measurements revealed a 1:1 electrolyte. IR and NMR experiments failed to detect any platinum-hydride bonding. The addition of sodium tetraphenylborate or lithium tetrafluoroborate to the complex afforded $[PtF(PPh_3)_3][BPh_4]$ and $[PtF(PPh_3)_3][BF_4]$ respectively. A weak and broad band at 1410 cm^{-1} in the IR experiment was hesitatingly assigned to HF_2^- anion. Relying mainly on analytical data and conductance measurements, the authors[28] finally concluded that the cation was $[PtF(PPh_3)_3]^+$ and the anion was probably HF_2^-. This structure was later on confirmed by Dixon *et al.*[29] using ^{19}F NMR experiment. The spectrum revealed two sidebands around the main signal, which were assigned to platinum-fluoride coupling. The main signal was a doublet of triplets arising from the fluoride coupling to three phosphorus atoms in two different environments. A singlet at −168 ppm was assigned to HF_2^-.

During the course of investigating the reactivity of the complex $[PtF(PPh_3)_3][HF_2]$, the authors[28] noticed that it reacted with lithium perchlorate in a different way to the way that it reacted with lithium tetrafluoroborate. The product resulting from the former reaction revealed a stoicheiometry $PtF(ClO_4)(PPh_3)_2$, an IR band typical of an ionic perchlorate and a conductivity measurement indicative of a 2:1 electrolyte. The complex was formulated as $[Pt_2(\mu\text{-}F)_2(PPh_3)_4][ClO_4]_2$ (Figure 6.2).

Figure 6.2
Structure of $[Pt_2(\mu\text{-}F)_2(PPh_3)_4][ClO_4]_2$

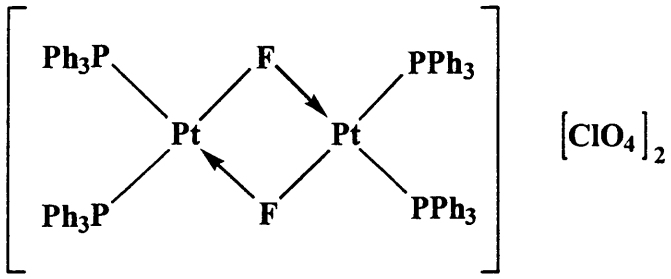

For many years, halogen-bridged dinuclear tertiary phosphine complexes have proven useful as starting materials for the preparation of platinum phosphine monomers. This is due to the ease with which the halogen bridge is cleaved by an incoming nucleophilic entity such as an additional phosphine ligand.[30,31]

The preparation of the platinum(II)-fluoride complex (**35**) which offers an analogous route to a series of platinum-fluoride species, has been carried out using anhydrous HF as the fluorinating agent in a metathesis reaction in which two methyl ligands are replaced by two bridging F^- anions, following the Scheme 6.2.

Scheme 6.2
Preparation of $[Pt_2(\mu\text{-}F)_2\{P(4\text{-}CH_3OC_6H_4)_3\}_4]^{2+}\ 2HF_2^-$ (35)

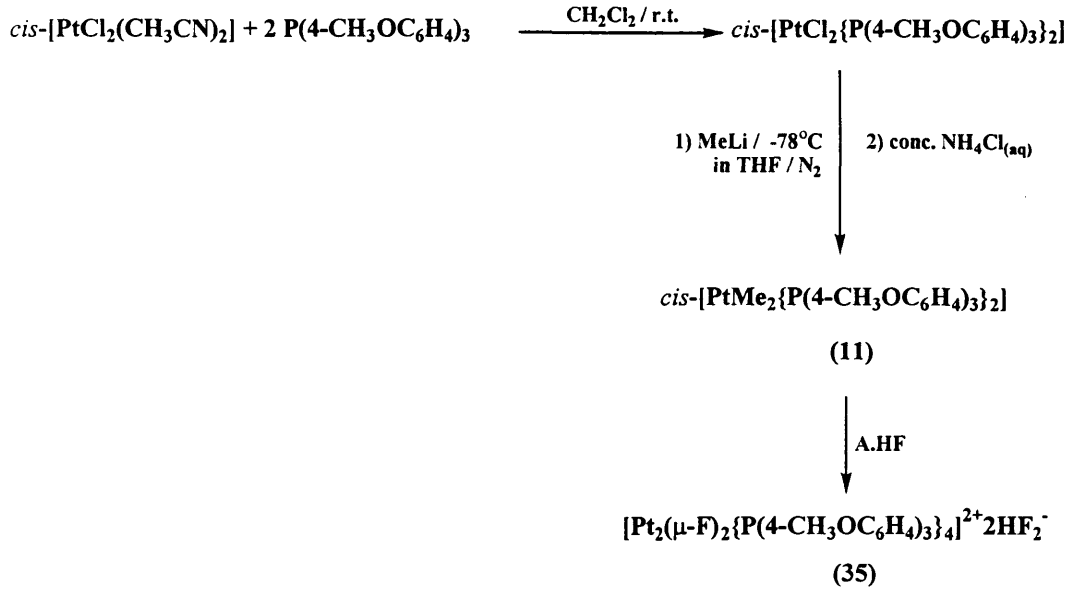

The first step in Scheme 6.2 is the preparation of the platinum dichloride complex, *cis*-$[PtCl_2\{P(4\text{-}CH_3OC_6H_4)_3\}_2]$. The phosphine ligands in platinum(II) phosphine halide complexes bind strongly to the metal and are not readily substituted. The reactivity of these complexes is usually centred at the metal-halide bond. The halide atom is easily substituted by an alkyl group using an organolithium reagent. Accordingly, the chloride ions in *cis*-$[PtCl_2\{P(4\text{-}CH_3OC_6H_4)_3\}_2]$ are displaced by methyl groups following a reaction with methyllithium, at low temperature, under nitrogen. The driving force for this reaction is the formation of lithium chloride. To ensure a complete transformation, a large excess of MeLi is used. The excess of the methylation reagent is neutralised by the addition of concentrated aqueous solution of ammonium chloride. The characterisation of both platinum(II) complexes, the dichloride and dimethyl analogues, has been discussed in Chapter Two. The reactions at the platinum-carbon σ-bond have been extensively studied, for example, the reaction of *cis*-$[Pt(Ph_2)(PEt_3)_2]$ with an excess of HCl in ethanol or benzene resulted in the substitution of the phenyl groups by chloride atoms (Scheme 6.3).[32]

Scheme 6.3

$$cis\text{-}[Pt(Ph_2)(PEt_3)_2] + \text{excess HCl} \longrightarrow trans\text{-}[PtCl_2(PEt_3)_2] + 2\,C_6H_6$$

Following a similar reaction, the resulting methylated platinum(II) complex (**11**), after being dried using the Schlenk line vacuum and transfered to an FEP tube, is reacted with anhydrous HF (The complete procedures are described in Chapter Eight). The result is a high yield of a yellow solid, the doubly fluoride-bridged platinum(II) dimer (**35**). This complex is stable at room temperature and under an inert atmosphere where it has remained intact for two years.

The dimer (**35**) is characterised by ^{1}H, $^{31}P\{^{1}H\}$, $^{19}F\{^{1}H\}$ and ^{195}Pt NMR experiments and the relevant data are in good agreement with previously reported values for platinum(II) fluoride phosphine salts such as $[PtFL_3][BF_4]$ (L = PEt_3, PPh_3).[29,33] The room temperature ^{1}H NMR spectrum of the platinum dimer (**35**) reveals the expected multiplets in the 7.20-6.70 ppm range assigned to the aromatic protons of the arylphosphine ligand, in addition to a singlet at 3.70 ppm assigned to the methoxy groups. Additionally, the spectrum exhibits a broad signal at 10.97 ppm assigned to the HF_2^- counterion. No hydrogen-fluoride coupling could be resolved. The room temperature $^{31}P(^{1}H\}$ NMR spectrum reveals one singlet at 3.8 ppm (Figure 6.3) flanked with two relatively broad satellites in a $^{1}J_{Pt\text{-}P}$ = 3763 Hz coupling value. The room temperature $^{19}F\{^{1}H\}$ NMR experiment reveals a very intense broad singlet at –173 ppm assigned to the HF_2^- counterion and a singlet at –153.7 ppm assigned to BF_4^-. The room temperature ^{195}Pt NMR spectrum exhibits a triplet at –4061 ppm, the coupling is ca. 3778 Hz.

Figure 6.3
$^{31}P\{^{1}H\}$ NMR Spectrum of $[Pt_2(\mu\text{-}F)_2\{P(4\text{-}CH_3OC_6H_4)_3\}_4][HF_2]_2$ (35)

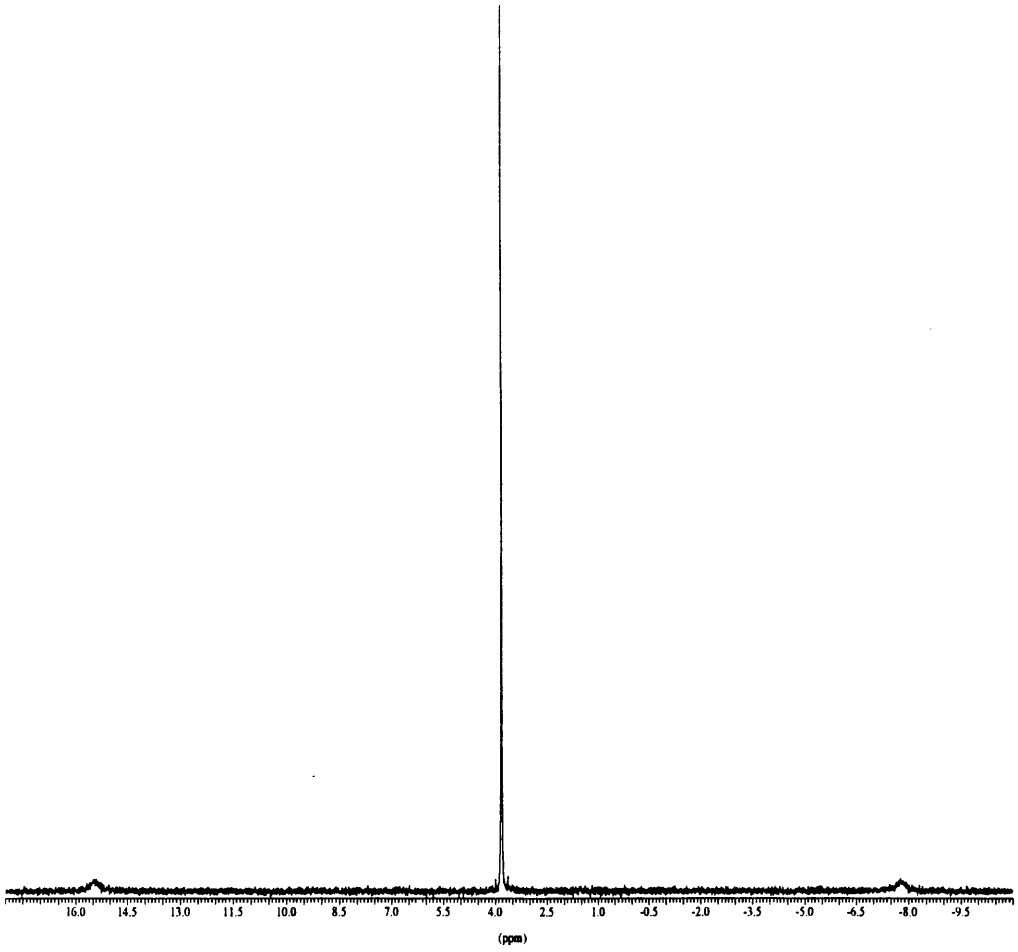

A similar route to that in Scheme 6.2 was followed in the preparation of related dinuclear platinum(II) fluorides, $[Pt_2(\mu\text{-}F)_2(PPh_3)_4][HF_2]_2$ and $[Pt_2(\mu\text{-}F)_2(PEt_3)_4][HF_2]_2$.[34] Methane gas is evolved from this type of reaction and was detected by gas-phase infra-red spectroscopy. The EXAFS studies carried out on these compounds exhibit a relatively short Pt...Pt distance. Throughout the subsequent discussion, the $^{31}P\{^{1}H\}$, $^{19}F\{^{1}H\}$ and ^{195}Pt NMR data of the dimer (**35**) will be compared to those of a well characterised platinum fluoride dimer, $[Pt_2(\mu\text{-}F)_2(PEt_3)_4][HF_2]_2$ (Figure 6.4).[34] The $^{31}P\{^{1}H\}$ NMR spectrum of the latter dimer exhibits a singlet at 17.0 ppm flanked with satellites ($^{1}J_{Pt\text{-}P}$ = 3942 Hz), the $^{19}F\{^{1}H\}$ NMR spectrum exhibits a singlet at -180 ppm assigned to HF and the ^{195}Pt NMR spectrum exhibits a triplet at -4320 ($^{1}J_{Pt\text{-}P}$ = 3941 Hz).

Figure 6.4
Structure of $[Pt_2(\mu\text{-}F)_2(PEt_3)_4]^{2+}$

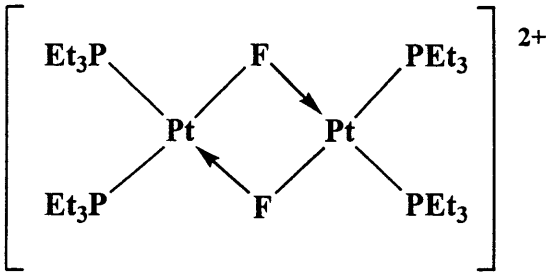

The absence of phosphorus-fluoride coupling suggests that fluxionality is taking place in the dimer (**35**) and its triethylphosphine analogue. Low temperature $^{31}P\{^1H\}$ NMR experiments were therefore conducted on both dimers in dichloromethane solutions. In the case of dimer (**35**), the singlet at 3.8 ppm started broadening at 213 K and then collapsed at 193 K. However, the singlet at 17.0 ppm in the room temperature $^{31}P\{^1H\}$ NMR spectrum of $[Pt_2(\mu\text{-}F)_2(PEt_3)_4][HF_2]_2$ dimer was replaced by a doublet, at 193 K, from which no coupling was resolved.

Figure 6.5
$^{19}F\{^{1}H\}$ NMR Spectra of of $[Pt_2(\mu\text{-}F)_2\{P(4\text{-}CH_3OC_6H_4)_3\}_4][HF_2]_2$ at the Observed Temperatures

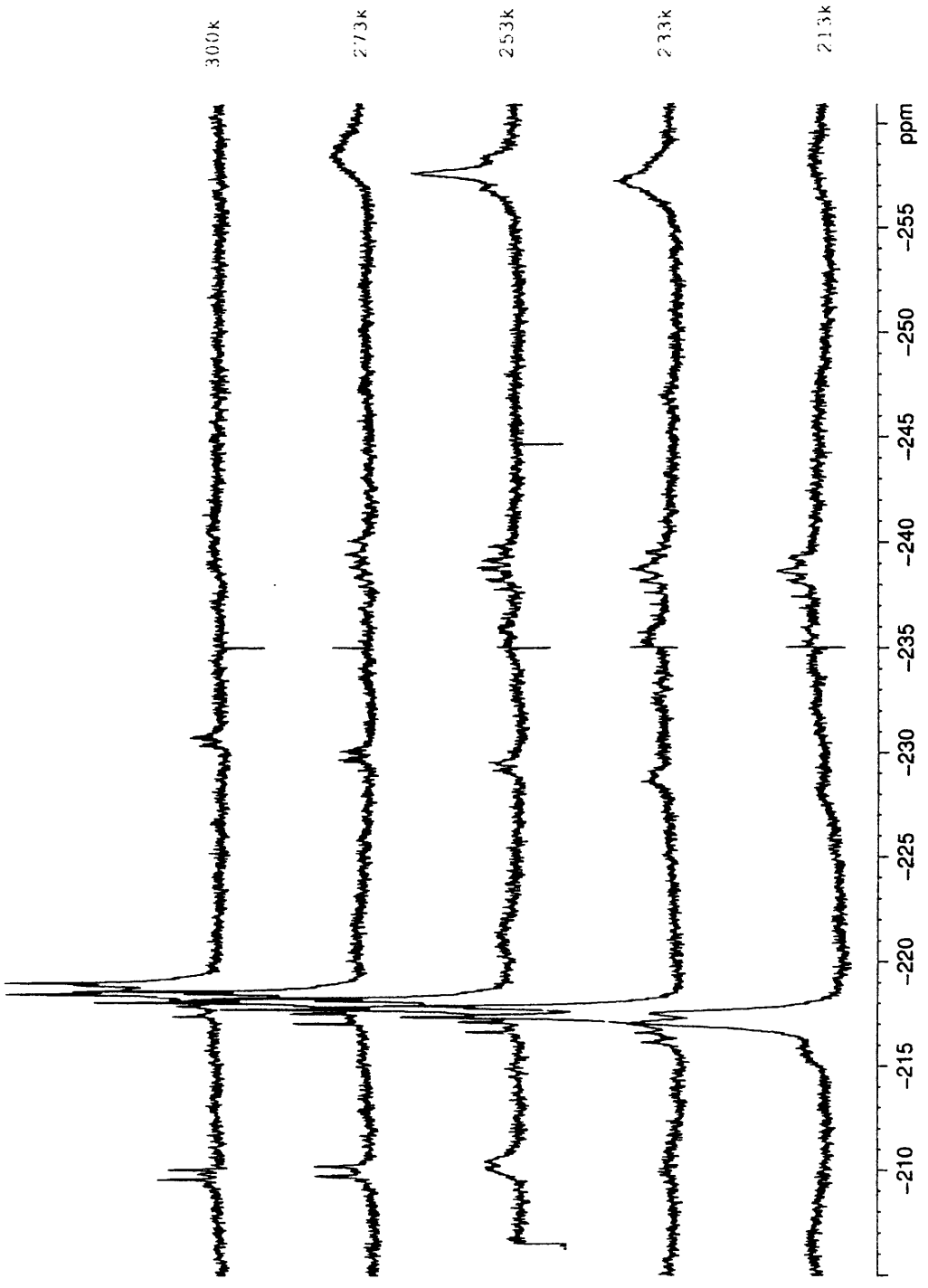

At 253 K, the $^{19}F\{^1H\}$ NMR spectrum of the dimer (**35**) revealed a poorly resolved signal at -256.6 ppm flanked by satellites, $^1J_{Pt\text{-}F}$ = ca. 262 Hz (Figure 6.5). At 193 K, the $^{19}F\{^1H\}$ NMR spectrum of the triethylphosphine analogue also revealed a poorly resolved signal at -265 ppm, $^1J_{Pt\text{-}F}$ = ca. 620 Hz.

No low temperature ^{195}Pt NMR experiment was conducted on the dimer (**35**) due to the related weak room temperature signal. However, at 213 K, the ^{195}Pt NMR spectrum of the triethylphosphine analogue revealed a triplet of triplets at -4367 ppm ($^1J_{Pt\text{-}P}$ = 3870 Hz and $^1J_{Pt\text{-}F}$ = 600 Hz). Since the $^{31}P\{^1H\}$ and $^{19}F\{^1H\}$ NMR data of (**35**) are in agreement with those of $[Pt_2(\mu\text{-}F)_2(PEt_3)_4][HF_2]_2$,[34a] it is reasonable to assume that the ^{195}Pt NMR data will also be similar.

From the NMR data, it is concluded that the platinum(II)-fluoride dimers (**35**) and its triethylphosphine analogue, exhibit fluxional behaviour. These dimers exhibit an AA'A''A'''XX'QQ' spin system, which simplifies by virtue of having $^2J_{P\text{-}cisF}$ too small to be resolved as evidenced by the doublet signal in the $^{31}P\{^1H\}$ NMR spectrum of $[Pt_2(\mu\text{-}F)_2(PEt_3)_4][HF_2]_2$ dimer. This doublet is a result of the phosphorus coupling to the *trans* bridging fluoride.

The substitution of the methyl groups by halide atoms in the dimer (**35**) shifted the phosphorus signal to a lower frequency as compared to its starting material, thus decreased relatively the coordination chemical shift value Δ (Table 6.3).

Table 6.3
Comparison of $^{31}P\{^1H\}$ NMR Data of $[Pt_2(\mu\text{-}F)_2(L)_4][HF_2]_2$ with $[PtCl_2(L)_2]$ and $[PtMe_2(L)_2]$ [L = $P(4\text{-}CH_3OC_6H_4)_3$]

Compound	Δ/ppm[a]
$[Pt_2(\mu\text{-}F)_2(L)_4]^{2+}$ (**35**)	13.7
$[PtCl_2(L)_2]$[b]	20.9
$[PtMe_2(L)_2]$ (**11**)	34.3

[a] $\Delta = \delta_{P\ (complex)} - \delta_{P\ (free\ ligand)}$ = **-9.9 ppm.** [b] **This work.**

Due to the difference in the *trans*-influence between the methyl group and the halogen atoms, an increase in the Δ value is induced when substituting the chloride atoms with methyl groups and a decrease is observed when substituting the methyl with the fluoride ligands.

Table 6.4
Room Temperature $^{31}P\{^1H\}$ NMR Data of $[Pt_2(\mu\text{-}F)_2(L)_4][HF_2]_2$ Dimers

L	$\delta_{P(free\ ligand)}$/ppm	Δ_P/ppm[a]	$^1J_{Pt\text{-}P}$/Hz
$P(4\text{-}CH_3OC_6H_4)_3$	-9.9	13.7	3763
PEt_3	-20.1	37.1	3942

[a] $\Delta_P = \delta_{P\ (complex)} - \delta_{P\ (free\ ligand)}$.

Comparing the room temperature $^{31}P\{^1H\}$ NMR data of $[Pt_2(\mu\text{-}F)_2\{P(4\text{-}CH_3OC_6H_4)_3\}_4][HF_2]_2$ (**35**) to its triethylphosphine analogue (Table 6.4), the variation in the coordination chemical shift values Δ is related to the nature of the phosphine ligand. It is reported that the coordination chemical shift is closely related to the variation in the C-P-C angle at the phosphorus; this angle opens less in bulky phosphine ligands compared to smaller ones upon coordination and its opening is proportional to the coordination chemical shift value.[35,36] In Table 6.4, the arylphosphine ligand is larger than the alkyl one, therefore the coordination chemical shift of the former ligand is smaller than that of the latter. When comparing the platinum-phosphorus coupling constant values, the expected difference between the alkylphosphine containing complex and the arylphosphine analogue is observed and attributed to the higher σ-character in the phosphorus-platinum bond in the trialkylphosphine due to its higher nucleophilicity.

Table 6.5
^{195}Pt and $^{19}F\{^1H\}$ NMR Data of $[Pt_2(\mu\text{-}F)_2(L)_4][HF_2]_2$ Complexes

L	δ_{Pt}/ppm	δ_F/ppm	$^1J_{Pt\text{-}F}$
$P(4\text{-}CH_3OC_6H_4)_3$	-4061[a]	-258[b]	ca. 262
PEt_3[34a]	-4320[a]	-265[c]	ca. 600

[a] At room temperature. [b] At 253 K. [c] At 193 K.

The large platinum-fluoride coupling constant value in the $[Pt_2(\mu\text{-}F)_2(PEt_3)_4][HF_2]_2$ dimer compared to that in the triarylphosphine analogue (Table 6.5) accounts for the greater stability of the platinum-fluoride bond in the former. The relation between the nature of the phosphine ligand and the platinum-fluoride bond stability will be discussed in more detail in Section 6.4.

The bonding between the "soft" Lewis acid, platinum(II), and the "hard" Lewis base, fluoride,[37,38] is interesting enough to be studied in terms of reactivity in order to establish its stability. Thus, the doubly-fluoride bridged platinum(II) dimer (**35**) has been allowed to react with a variety of monodentate phosphine ligands [L = PEt_3, PPh_3, PCy_3, $P(4\text{-}CH_3OC_6H_4)_3$]. The result has been a set of *tris*-phosphine platinum(II)-fluoride monomers, $[PtFL\{P(4\text{-}CH_3OC_6H_4)_3\}_2][HF_2]$.

6.4 Preparation and Characterisation of $[PtFL\{P(4\text{-}CH_3OC_6H_4)_3\}_2][HF_2]$:

Following the preparation of the first *tris*-phosphine platinum(II) fluoride, $[PtF(PPh_3)_3][HF_2]$,[28] a number of similar platinum fluoride monomers were reported,[29] some of which were characterised by X-ray diffraction studies.[39] In 1980, the first crystal structure of this type of complex was solved by Russell *et al.*[39] who showed it corresponded to that of $[PtF(PEt_3)_3][BF_4]$. A marked distortion of the platinum coordination plane towards tetrahedral geometry has been observed due to an

interaction between the fluoride ligand and the protons of two CH_2 groups on the two *cis*-phosphine ligands. This has been assigned to the great electronegativity of the fluoride ligand.

The ^{19}F NMR data offer valuable information on the bonding taking place around the metal centre.[40] In fact, the ^{19}F NMR experiment provided the first reliable proof of platinum(II)-fluoride bonding.[41] When comparing $^2J_{Pt\text{-}F}$ and $^3J_{P\text{-}transF}$ in $[Pt(CF_3)(PMe_2Ph)_3]^+$ cation to $^2J_{Pt\text{-}H}$ and $^3J_{P\text{-}transH}$ in $[Pt(Me)(PMe_2Ph)_3]^+$ cation,[29] the former pair of values are ca. 10 times larger than the latter. These couplings are dominated by *Fermi Contact* interactions and their variation is due to the large difference in the $|\psi_{ns}(0)|^2$-term for hydrogen and fluorine.[42] However, $^1J_{Pt\text{-}H}$ and $^2J_{P\text{-}transH}$ in $[PtH(PR_3)_3]^+$ species are ca. 800 and 160 Hz respectively.[43] Assuming that the related values in the platinum fluoride analogue species are ca. 10 times larger than the observed values in the platinum hydride cations, it would be predicted that $^1J_{Pt\text{-}F}$ and $^2J_{P\text{-}transF}$ values are ca. 8000 and 1600 Hz, which is not the case according to this present work and to literature values. This observation has been refered to the small α^2_{Pt} and α^2_F values in the *Fermi Contact Term*, the former being reduced by bond polarisation towards the fluoride and the latter by the large energy separation between the fluoride 2s and 2p orbitals.[29]

Platinum(II) phosphine fluoro complexes can be prepared by oxidation of the metal(0) complexes,[28,44] such as the reaction of $[Pt(PPh_3)_4]$ with liquid hydrogen fluoride.[28] They can also be prepared by halide metathesis of the corresponding chloro-complexes. For example, *Dixon et al.*[41] managed to prepare a set of $[MF(PR_3)_3][BF_4]$ complexes by the reaction of silver fluoride with the corresponding chloro-complexes. However, in this work, a more convenient method has been used in order to prepare a set of mononuclear platinum(II) phosphine fluoride complexes, starting from the doubly-fluoride bridged platinum dimer (Scheme 6.4).

Scheme 6.4

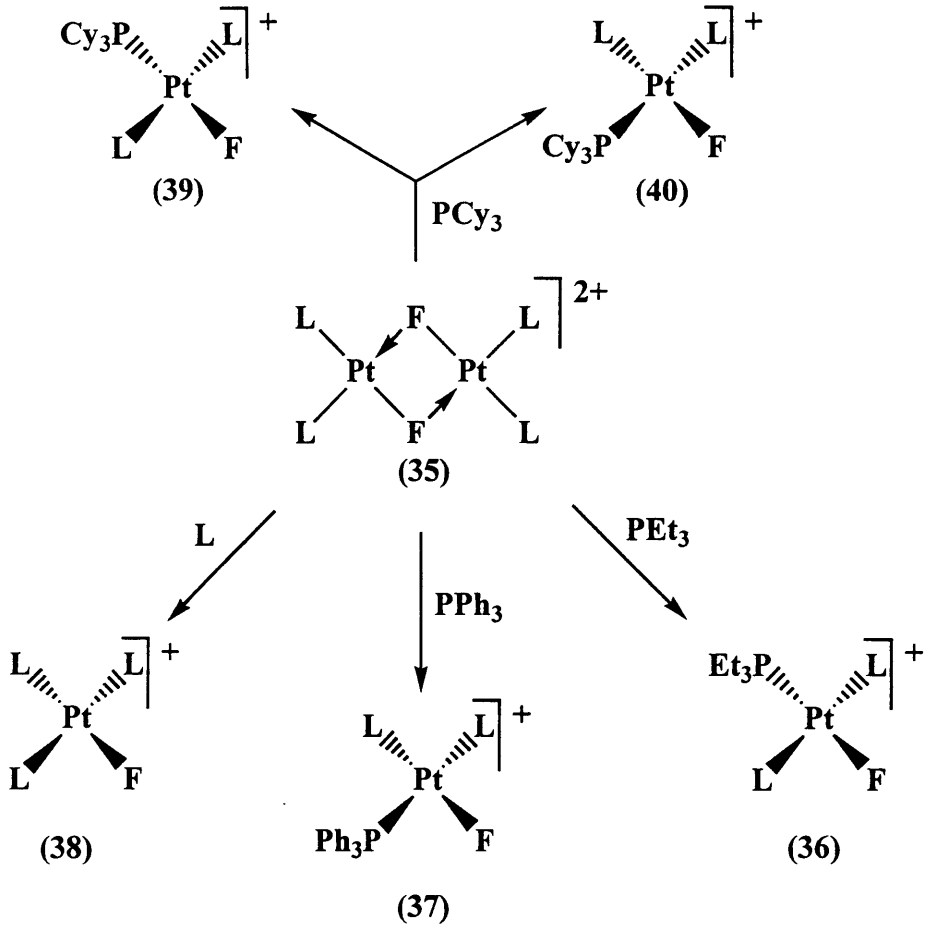

L = P(4-$CH_3OC_6H_4$)$_3$

The reactions described in Scheme 6.4 were carried out in FEP tubes, by simply adding the phosphine starting material to a dichloromethane solution of the platinum(II)-fluoride dimer (**35**) at room temperature. The FEP tube was then heat sealed under vacuum and ^{1}H, $^{31}P\{^{1}H\}$ and $^{19}F\{^{1}H\}$ NMR experiments were carried out on the solutions. Some of these platinum(II)-fluoride complexes are unstable at room temperature in solution and were, therefore, stored in liquid nitrogen prior to the NMR experiments. Since it was impossible to add exactly two molar equivalents of phosphine to the platinum fluoride dimer (**35**), all of the NMR experiments showed the presence of free ligand. In addition, the complexes prepared (**36**)-(**40**) decomposed in solution over a number of hours, which precluded further isolation and purification. This decomposition was unexpected in view of the general stability of

$[PtF(phosphine)_3]^+$ cations reported in the literature,[14] However, since it has been shown that $[PtF(PPh_3)]^+$ cations decompose, in the first instance *via* hydrolysis to $[Pt(OH)(PPh_3)]^+$,[33] the solution instability of (**36**)-(**40**) could arise from traces of water. Although the dichloromethane used as a solvent for these reactions was scrupulously dried and the FEP vessels passivated with fluorine gas, other work from the Fluorine Group at Leicester University has shown that the water can still influence the reactivity of metal fluorides and the decomposition of (**36**)-(**40**) is assigned to the presence of traces of water with the phosphine reagents. Consequently, all the characterisation experiments in this section were undertaken on freshly prepared solutions of the reagents. Examples from these characterisation spectra are depicted in Figures 6.6 and 6.7 assigned to *trans*-$[PtF(PEt_3)L_2][HF_2]$ (**36**).

Figure 6.6 $^{31}P\{^{1}H\}$ NMR Spectrum of *trans*-$[PtF(PEt_3)L_2][HF_2]$ (36). ⌘ Denotes impurity. ☞ Denotes free ligand L.

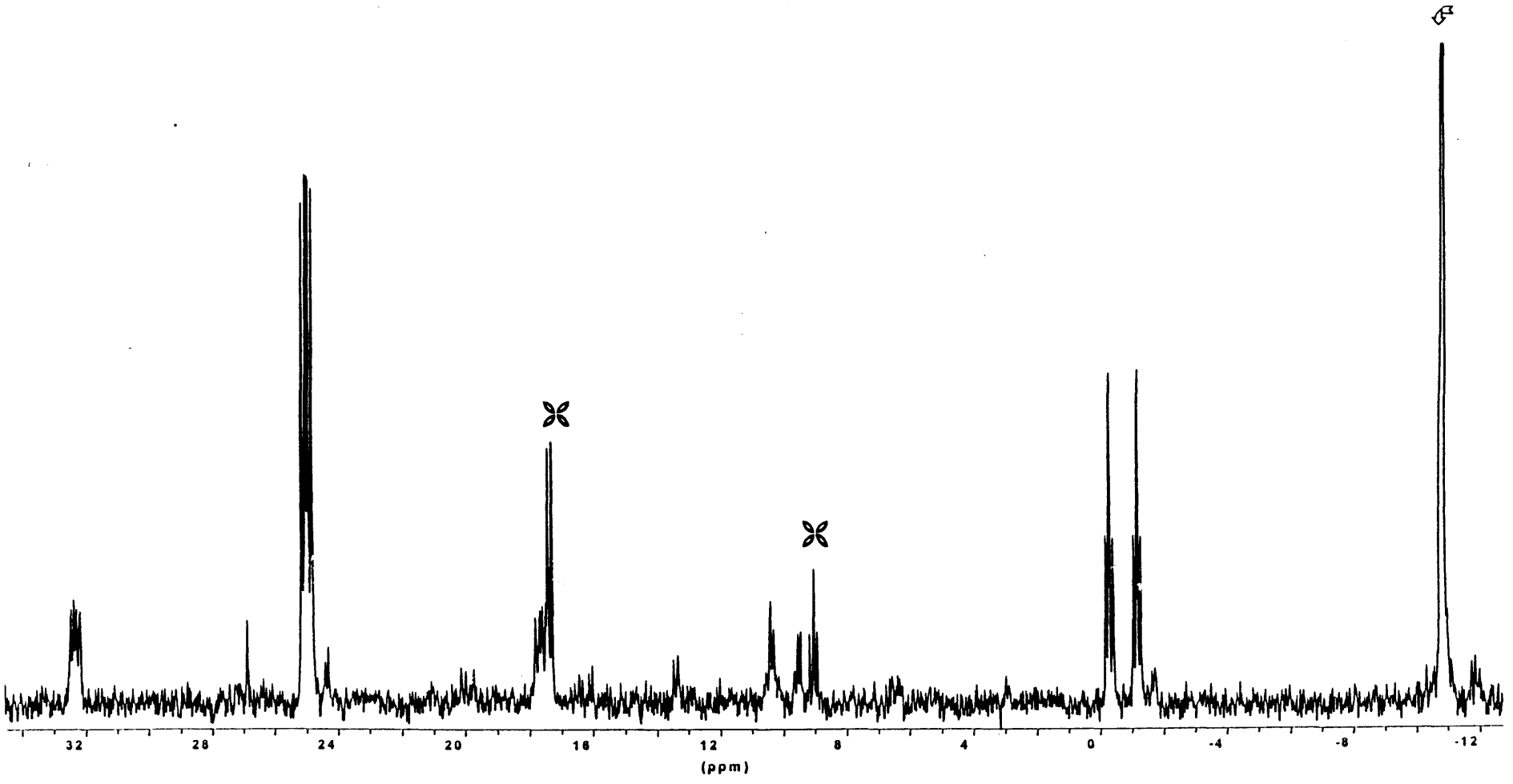

Figure 6.7 $^{19}F\{^{1}H\}$ NMR Spectrum of *trans*-$[PtF(PEt_3)L_2][HF_2]$ (36)

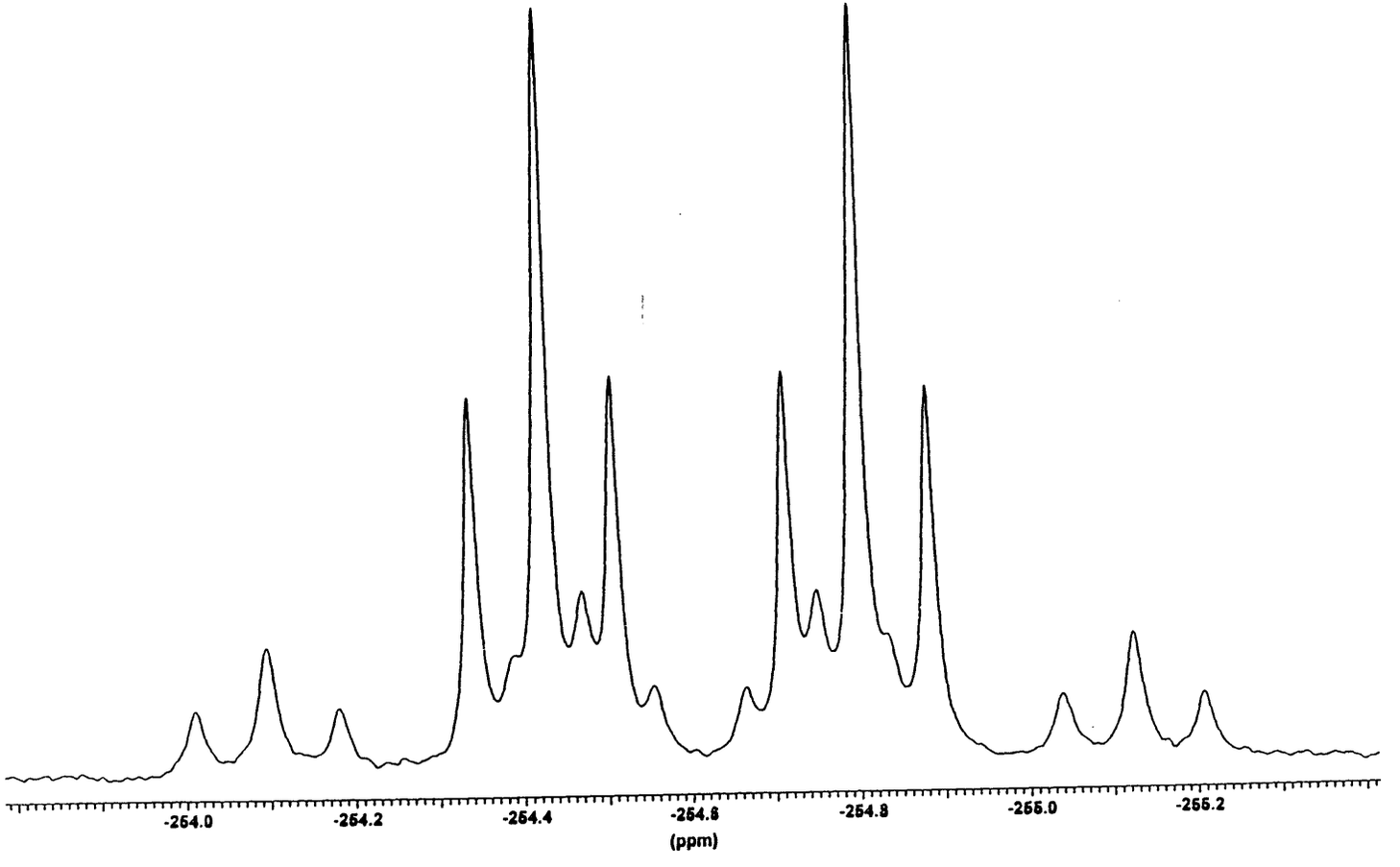

Table 6.6
NMR Data (δ/ppm and J/Hz) for $[PtF(phosphine)_3]^+$ (Pa is *cis* to F and Pb is *trans* to F)

	$[PtF(PEt_3)_3]^+$ [a]	$[PtF(PPh_3)_3]^+$ [a]	*trans*-$[PtF(PEt_3)L_2]^+$ (36)[b]	*cis*-$[PtF(PPh_3)L_2]^+$ (37)[b,c]	$[PtFL_3]^+$ (38)[b]
δ_{Pa} [d]	28.0	26.5	25.0	23.6 (ddd) and 28.3 (ddd)	23.4
δ_{Pb} [d]	3.0	3.0	0.7	-0.8	-1.2
$^2J_{Pa-Pb}$	19	19	20	18	18
$^2J_{Pa-F}$	32	39	32	32	37
$^2J_{Pb-F}$	140	139	141	146	144
$^1J_{Pt-Pa}$	2828	2640	2361	2608[e]	2590
$^1J_{Pt-Pb}$	3455	3701	3391	3693	3729
δ_F [d]	-251.5	-232.0	-254.2	-229.5	-229.8
$^1J_{Pt-F}$	250	67	246	-[f]	ca. 180

[a] Ref. 33. [b] Recorded in d^6 acetone. L = $P(4\text{-}CH_3OC_6H_4)_3$. [c] $^2J_{P\text{-}transP}$ = 405Hz. [d] The multiplicities of the signals of δ_{Pa}, δ_{Pb} and δ_F are dd, dt and dt respectively, unless otherwise stated. [e] Similar values for both *trans* ligands: L and PPh_3. [f] Not resolved.

In Table 6.6, The ^{31}P NMR data related to the platinum fluoride monomers (**36**)-(**38**) are compared to already published data on similar complexes.[33] The $^{1}J_{Pt\text{-}F}$ of complex (**37**) was not resolved. This is most probably due to its relatively small value compared to those of the other complexes included therein, which hints at the relative weakness of the Pt-F bond in complex (**37**). Similar observation has been rationalised in terms of steric effect when comparing $[PtF(PPh_3)_3]^+$ with $[PtF(PEt_3)_3]^+$.[29] However, when comparing $[PtF(PPh_3)(L)_2]^+$ (**37**) and $[PtF(L)_3]^+$ (**38**), the difference between $^{1}J_{Pt\text{-}F}$ values will be due to the electronic-effect while the steric bulkiness of the ligands in both complexes is comparable. Therefore, the inductive and mesomeric electron donation of the methoxy groups in the *para*-positions of one phosphine ligand [complex (**38**)] induced a relative strengthening in the Pt-F bond compared to that of the triphenylphosphine analogue [complex (**37**)].

The chemical shift of the phosphorus signal related to the phosphine ligand in the position *trans* to the fluoride atom is at a lower frequency when compared to that of the phosphine ligand in position *cis* to it. The large difference between both chemical shifts is attributed to the mesomeric donating-effect of the fluoride which affects mainly the *trans* ligating group. The alkyl substituents on the phosphorus in $[PtF(PEt_3)_3]^+$ increase the nucleophilicity of this phosphine ligand, leading to an increase in the electron donation towards the metal centre. This should enhance the inductive withdrawing-effect towards the fluoride, which is reflected in a higher Pt-F coupling constant value and a shifting of the fluoride signal to a lower frequency when compared to the complexes incorporating triarylphosphine ligands. It should be noted that the $^{1}J_{Pt\text{-}Pb}$ (Pb is *trans* to F) values related to $[PtF(PEt_3)_3]^+$ and *trans*-$[PtF(PEt_3)L_2]^+$ (**36**) (Table 6.6) are smaller than those related to the triarylphosphine analogue cations. This reflects an increase in the *trans*-influence of the fluoride in the former two cations compared to the latter set of cations. The *trans*-influence has been highlighted in the literature[29,45] when comparing *tris*-phosphine platinum fluoride to *tris*-phosphine platinum chloride cations where the phosphine ligands incorporated alkyl groups. The authors[29] concluded that the fluoride ligand exhibits a greater *trans*-influence compared to the chloride ligand. However, they have excluded $[PtF(PPh_3)_3]^+$ which exhibited an anomalously low $^{1}J_{Pt\text{-}F}$ value. This phenomenon has been assigned to the steric effect caused by the bulky triphenylphosphine ligand. This explanation is

confirmed by the data in Table 6.7, where the phosphine ligands bound to the platinum(II) are triarylphosphines and the only difference between the two complexes compared therein is the halide atom bound to the metal centre.

Table 6.7
^{31}P NMR (J/Hz) Data of $[PtXL_3]^+$ Cations (Pa is *cis* to X and Pb is *trans* to X).[a]

L, X	$^2J_{Pa-Pb}$	$^1J_{Pt-Pa}$	$^1J_{Pt-Pb}$
L = $P(4\text{-}CH_3OC_6H_4)_3$, X = F (38)	18	2590	3729
L = $P(4\text{-}CH_3OC_6H_4)_3$, X = Cl (9)	18	2467	3671
L = PPh_3, X = F[b]	19	2650	3696
L = PPh_3, X = Cl[b]	19	2482	3643
L = PEt_3, X = F[b]	19	2382	3455
L = PEt_3, X = Cl[b]	19	2261	3474

[a] L = $P(4\text{-}CH_3OC_6H_4)_3$. [b] Ref. 29.

When comparing complexes (**38**) and (**9**) the $^1J_{Pt\text{-}Ptrans F}$ value is slightly larger than that of $^1J_{Pt\text{-}Ptrans Cl}$. Therefore, it could be argued that in this case the *trans*-influence of the chloride is slightly greater than that of the fluoride. Comparing the cations incorporating trialkylphosphine ligands to those incorporating triarylphosphine ligands, two effects, the steric and electronic effects, should be taken in consideration. According to the former, substituting the alkyl groups by aryl groups induces a distortion in the coordination geometry around platinum towards lengthening of the Pt-F bond. This is confirmed by the reduction in the $^1J_{Pt\text{-}F}$ value (Table 6.6), in accordance with the fact that this is very sensitive to bond length.[29,46] According to the latter effect, the larger electron donation of the trialkylphosphine compared to that of the triarylphosphine, enhances the inductive withdrawing effect in the platinum fluoride bond towards the fluoride ligand which, together with an increase in the mesomeric donating effect of the fluoride, increases the *trans*-influence of the fluoride compared to the chloride ligand.

Figure 6.8

$^{31}P\{^{1}H\}$ NMR Spectrum of $[PtFL_3][HF_2]$ (38). The singlet at ca. 3.0 ppm is assigned to the starting material (35).

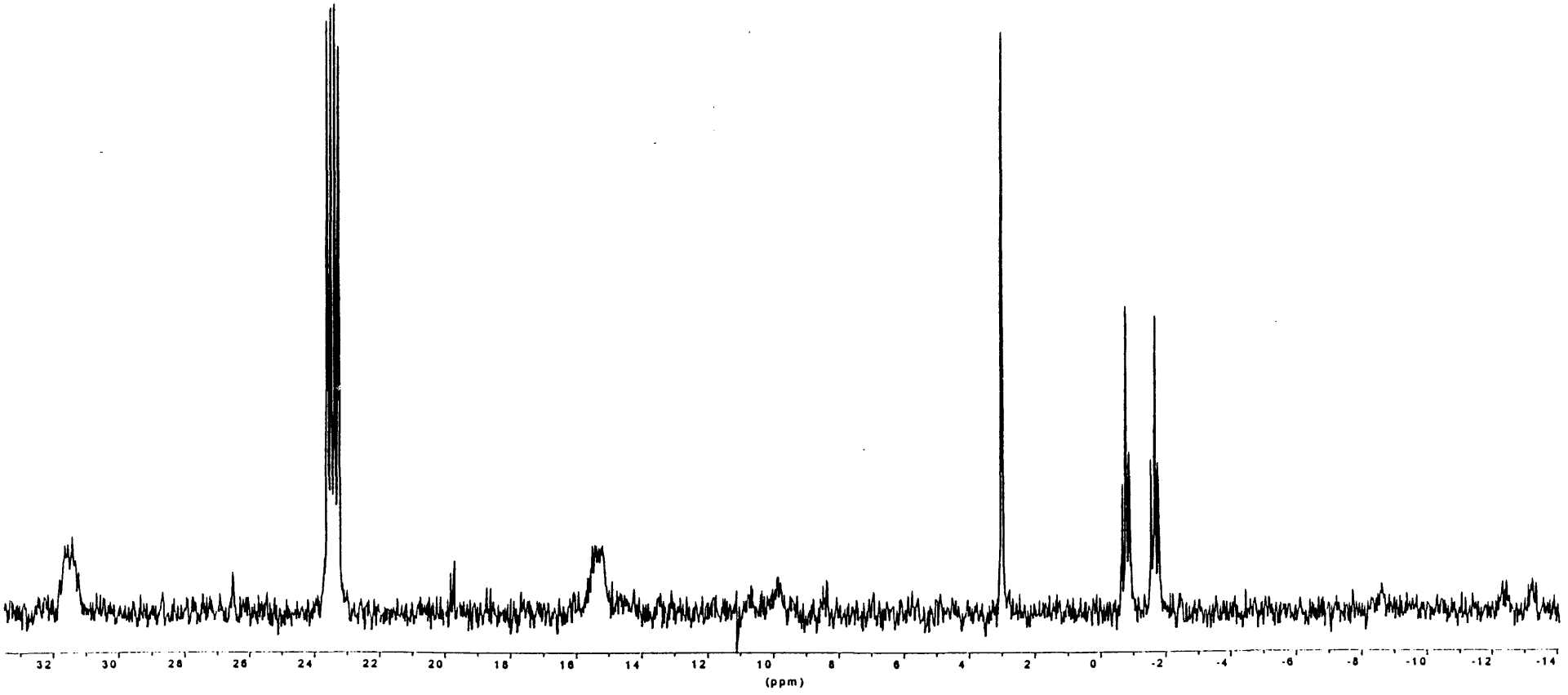

Figure 6.9 $^{19}F\{^{1}H\}$ NMR Spectrum of $[PtFL_3][HF_2]$ (38)

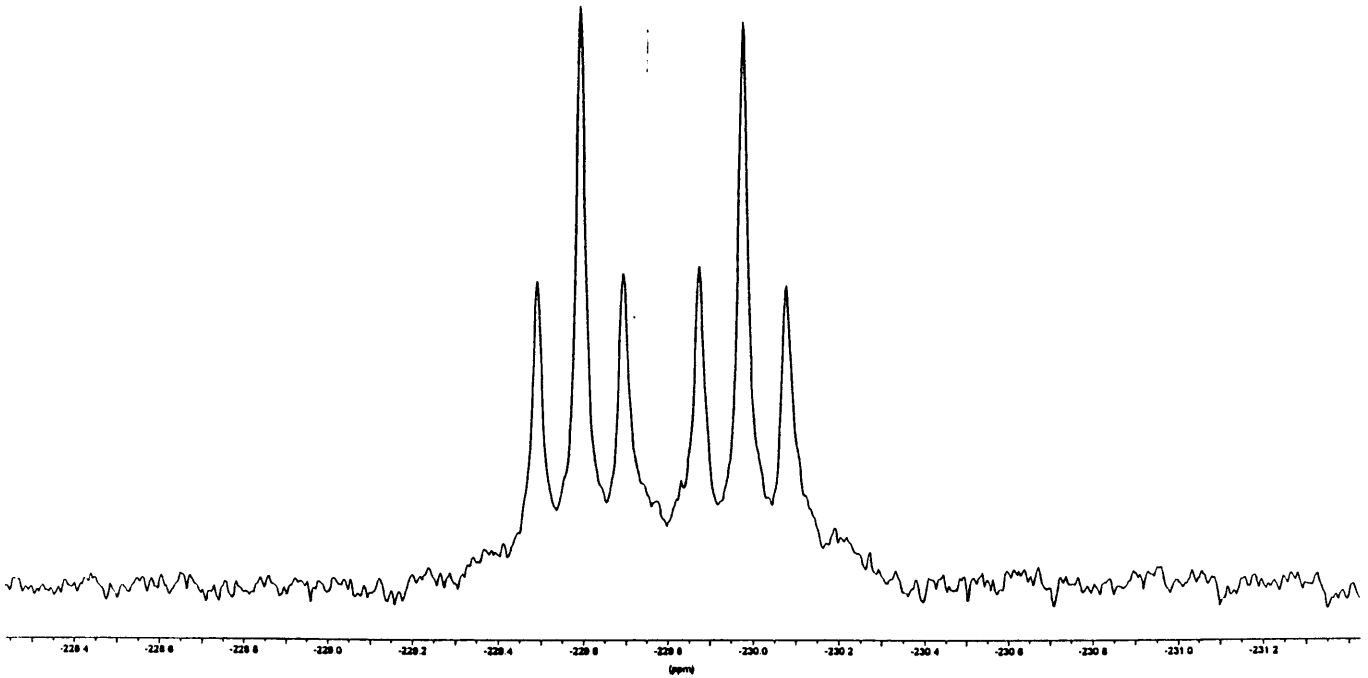

It can be argued that the electronic effect has a considerable influence on determining the configuration of the resulting *tris*-phosphine platinum fluoride products. In other terms, when comparing the preparations of complexes (**36**) and (**37**), the triethylphosphine ligand, which is more nucleophilic compared to the triphenylphosphine ligand, positions itself *trans* to the fluoride which is mainly a σ-electron withdrawing ligand. However, the triphenylphosphine ligand is less nucleophilic compared to the tris(*p*-methoxyphenyl)phosphine one, thus it takes the position *cis* to the fluoride ligand.

The reaction of the platinum(II) fluoride dimer (**35**) with tricyclohexylphosphine ligand afforded a mixture of both *cis* and *trans* isomers. The mixture was in an approximate 1:1 ratio. The assignment of the related signals in the $^{19}F\{^{1}H\}$ NMR spectrum was straight forward, as it exhibited two signals assigned to both isomers, a signal at a high frequency, -229.8 ppm, assigned to the *trans*-isomer and a signal at a low frequency, -250.0 ppm, assigned to the *cis*-isomer.

Table 6.8
NMR Data (δ/ppm and J/Hz) for *cis*- and *trans*-[PtF(PCy$_3$)L$_2$] (Pa is *cis* to F and Pb is *trans* to F) Compared to Complex (38)[a]

	[PtFL$_3$]$^+$ (38)	*trans*-[PtF(PCy$_3$)L$_2$] (39)	*cis*-[PtF(PCy$_3$)L$_2$][b] (40)	
δ_{Pa}	23.4 (dd)	23.4(dd)	PCy$_3$ L	31.0 (dt) 20.5 (ddd)
δ_{Pb} (dt)	-1.2	-1.2	-2.0	
$^2J_{Pa-Pb}$	18	18	18	
$^2J_{Pa-F}$	37	38	PCy$_3$ L	17 44
$^2J_{Pb-F}$	144	145	140	
$^1J_{Pt-Pa}$	2590	2590	-[c]	
$^1J_{Pt-Pb}$	3729	-[c]	-[c]	
δ_F	-229.8 (dt)	-229.8(dt)	-250.0(ddd)	
$^1J_{Pt-F}$	ca. 180	ca. 175	ca. 175	

[a] Recorded in d^6 acetone. L = P(4-CH$_3$OC$_6$H$_4$)$_3$. [b] $^2J_{P\text{-}trans\ P}$ = 363Hz. [c] Not resolved.

The $^{19}F\{^1H\}$ NMR spectrum (Figure 6.10) helped in understanding the more complicated $^{31}P\{^1H\}$ NMR spectrum which is due to the closeness of PCy$_3$-F coupling value to that of PCy$_3$-P(4-CH$_3$OC$_6$H$_4$)$_3$.

Figure 6.10 $^{19}F\{^{1}H\}$ NMR Spectrum of *cis*- and *trans*-$[PtF(PCy_3)L_2][HF_2]$ (39) and (40)

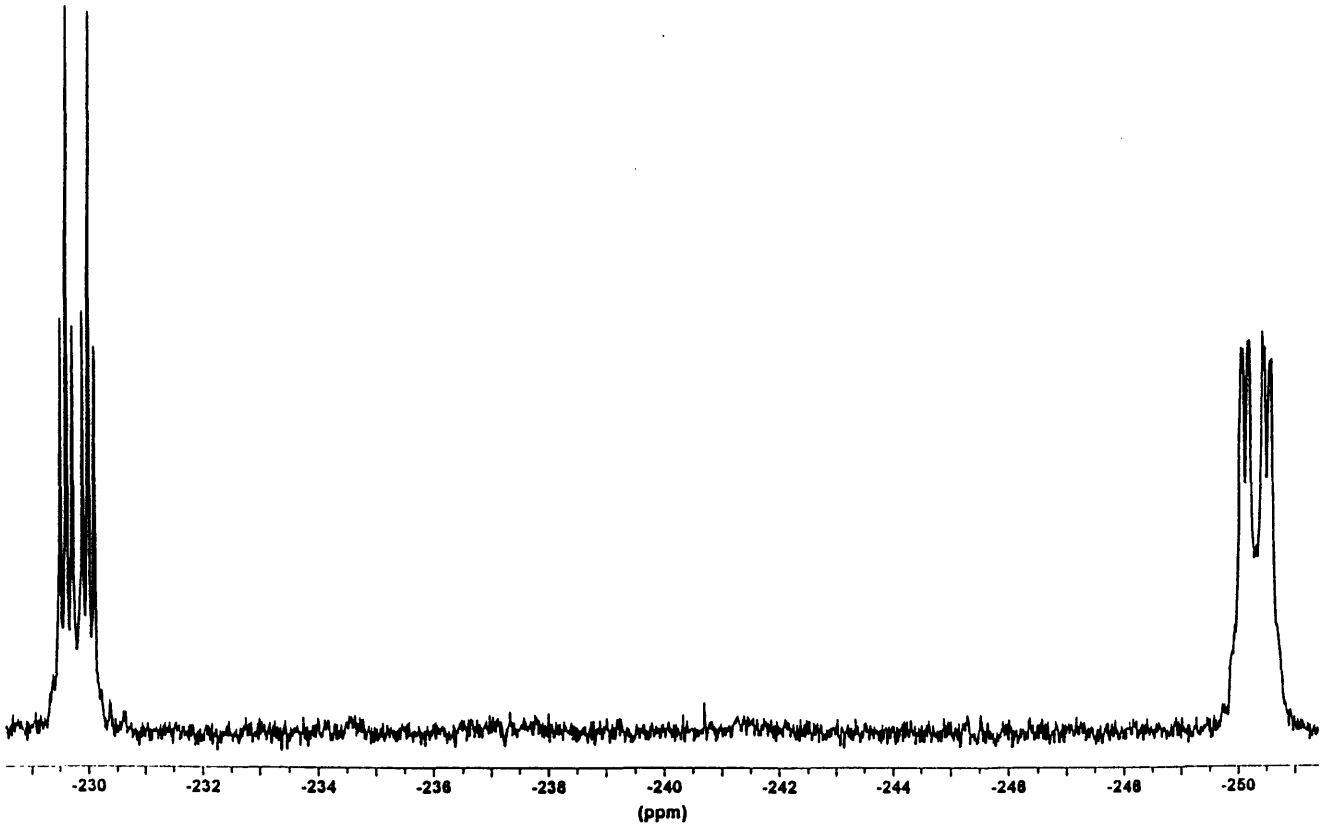

The tricyclohexylphosphine ligand is rather a strong Lewis base (pKa = 9.70),[35] moreover, it usually exhibits a large cone angle upon coordination to metal centres (170°).[35] According to electronic arguments, therefore, the PCy_3 ligand should be *trans* to the fluoride atom. However, according to steric arguments, the PCy_3 ligand should take the position *cis* to the fluoride instead of occupying the position between the two triarylphosphine ligands. The fact that both isomers are detected in solution and in a consistent ratio confirms the importance of both effects, electronic and steric in determining the final composition of the resulting product.

When comparing the NMR data of complexes (**38**) and (**39**) (Table 6.8), a large similarity in values is noticed. The difference is that in complex (**38**), the ligand *trans* to the fluoride atom is the *tris*-(*para*-methoxyphenyl)phosphine, while in complex (**39**), it is the tricyclohexylphosphine. The similarity in both sets of data suggests a similarity in the coordination chemistry of these two ligands in $[PtF(phosphine)_3]^+$ type of cations, taking into consideration both steric and electronic factors. The $P(4\text{-}CH_3OC_6H_4)_3$ ligand has a relatively small cone angle and a weak Lewis basicity, however the PCy_3 ligand has a relatively large cone angle and a strong Lewis basicity. It seems that the difference between both phosphine cone angles is balanced by the difference in Lewis basicities. Thus, both phosphine ligands have a similar impact on the bond strengths and electronic environments around the metal centres.

When comparing complex (**39**) (Table 6.8) with complex (**36**) (Table 6.6), in the former, the ligand *trans* to the fluoride atom is PCy_3 whereas in the latter, the ligand *trans* to the fluoride atom is PEt_3. The Lewis basicity of PCy_3 is larger than that of PEt_3, the pKa values are 9.70 and 8.69 respectively.[35] In contrast to the expected enhancement of the Pt-F bond strength and the chemical shifting of the fluoride signal to a lower frequency caused by the stronger Lewis base in complex (**39**), an opposite trend is observed. Thus, the steric effect in the former complex is dominating the electronic one. On the other hand, comparing the complexes (**37**) and (**40**), the difference is that in the former, the triphenylphosphine ligand is *cis* to the fluoride atom, however, in the latter the tricyclohexylphosphine is *cis* to the fluoride atom. In

the former complex, the P_{transP} coupling is 405 Hz. In the latter salt, the same type of coupling is 363 Hz. Moreover, in the complex (**40**), the $(4\text{-}CH_3OC_6H_4)_3P$-*cis*F coupling value is larger (44 Hz) and the Cy_3P-F coupling is smaller (17 Hz) than the average $^2J_{P\text{-}cisP}$ value (ca. 35 Hz) (Tables 6.6 and 6.8). Once again, the steric effect dominates over the electronic effect in determining the coupling intensities of the PCy_3 ligand to the other ligating groups. However, the strong Lewis basicity of the tricyclohexylphosphine is evidenced by the shifting of the fluoride signal to a lower frequency in complex (**40**) compared to that in complex (**37**).

6.5 Preparation and Characterisation of [*OC-6-13*][$MF_2(CO)_2(PR_3)_2$] (M = Os, Ru and PR_3 is a monodentate triarylphosphine ligand):

The ruthenium fluoride tetramer [{$RuF(\mu\text{-}F)(CO)_3$}$_4$] has been prepared by the reaction of ruthenium pentafluoride with carbon monoxide and was one of the earlier carbonyl fluoride complexes to be characterised by X-ray diffraction.[47,48] More recently, this compound and its osmium congener have been prepared by oxidation of the metal carbonyl with XeF_2.[49] The fluorination of the osmium carbonyl trimer [$Os_3(CO)_{12}$] with XeF_2 in anhydrous HF led initially to the formation of a mixture of four products. The main product was the *cis*-[$Os(CO)_4F_2$], in addition to $[Os(CO)_5F]^+$, [$Os_2(CO)_7F_4$] and $[Os_2(CO)_8F_3]^+$ as minor products. The formation of the fluoro osmium pentacarbonyl cation, which has a carbonyl:osmium ratio higher than that of the starting material, implies that carbonyl scrambling is taking place during the metal-metal bond cleavage. The removal of the aHF solvent results in the loss of carbonyl molecules yielding the tetrameric carbonyl fluoride osmium complex, [{$OsF(\mu\text{-}F)(CO)_3$}$_4$].[50] However, several disadvantages arise from the use of XeF_2 as a source of fluoride ligand specially in large scale reactions. This type of reactions needs constant venting in order to eliminate the large amount of xenon gas evolved, in addition to the high cost of XeF_2 starting material. Therefore, fluorine gas was investigated as a potential alternative fluorinating agent. In this work, the preparation of the osmium and ruthenium carbonyl fluoride tetramers was carried out in aHF, using fluorine gas as the fluorinating reagent.[51] The tetramers are obtained following removal of the solvent in vacuum.

The triruthenium dodecacarbonyl and its osmium analogue are soluble in aHF,[52] and since fluorine gas has a limited solubility in aHF, the fluorination of the metal trimers can be efficiently controlled. The reaction between the fluorine gas and the metal starting material takes place at the solution-gas interface which is detected by a change in colour at this interface. This makes the F_2/aHF system effectively a "mild" fluorinating system. The resulting products have been identified as the fluoride-bridged tetramers by comparison of NMR spectroscopic data with those in the literature.

The extremely moisture- and oxygen-sensitive solids $[\{MF_2(CO)_3\}_4]$ (M = Os or Ru) are hardly soluble in common organic solvents. However, it has been shown that the addition of a Lewis base such as a phosphine, at room temperature and under nitrogen, leads to a reaction between the tetramer and the phosphine ligand, accelerating the dissolution of the starting material in the organic solvent and yielding rather moisture- and oxygen-stable monomers, $[MF_2(CO)_2(\text{phosphine})_2]$.[53]

Figure 6.11
Five Possible Isomers of $[MX_2(CO)_2L_2]$

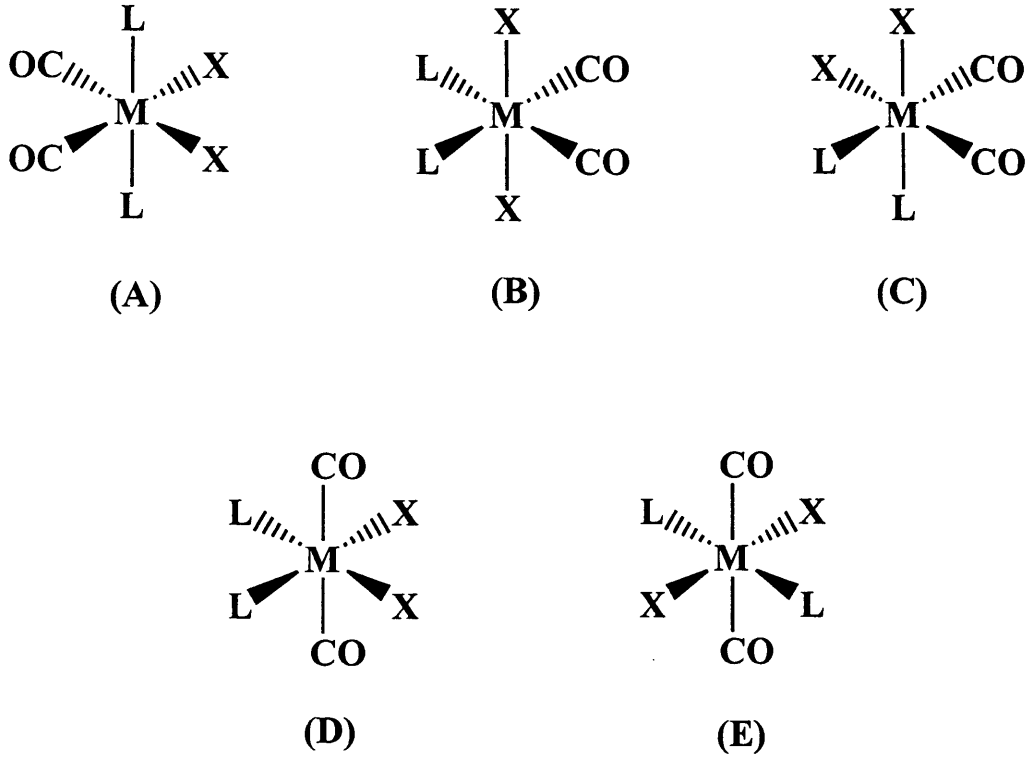

Five possible isomers could result from the reaction (Figure 6.11). For M = Ru and X = Cl, Br or I, all the five isomers have been identified.[54,55] Whilst for M = Os and X = Cl, Br or I, all the isomers except (**D**) were characterised. In contrast, the reaction of the $[\{MF_2(CO)_3\}_4]$ with the phosphine ligands affords only one isomer with structure (**A**), which is considered to be the thermodynamically favoured structure[54,56] and may be rationalised according to electronic and steric interpretations. The two phosphine ligands are *trans* to each other, reducing any possible steric interaction. The two fluoride atoms that are considered to be good π-electron donating ligands compared to the heavier halide atoms, are *trans* to the two carbonyl groups which are considered to be good π-electron acceptor ligands. In this present work, new ruthenium and osmium fluoride complexes with the *para*-derivatised triarylphosphines have been prepared according to the equation in Scheme 6.5.

Scheme 6.5

$$[\{MF_2(CO)_3\}_4] + 8\,PR_3 \rightarrow 4\,[OC\text{-}6\text{-}13][MF_2(CO)_2(PR_3)_2] + 4CO_{(g)}$$

M = Os or Ru.
PR_3 = $P(4\text{-}CH_3OC_6H_4)_3$ or $P(4\text{-}HOC_6H_4)_3$.

These reactions were carried out in a Schlenk flask, under nitrogen and in dried dichloromethane which was submitted to three freeze-thaw-degas cycles. The reaction solution was left stirring for three hours at room temperature and was periodically degassed to eliminate the liberated carbon monoxide.

6.5.1 Characterisation of *[OC-6-13]*[$RuF_2(CO)_2(PR_3)_2$]:

The ^1H NMR experiment carried out on the $[RuF_2(CO)_2\{P(4\text{-}CH_3OC_6H_4)_3\}_2]$ (**41**) complex, exhibits a multiplet at 7.69 ppm assigned to the aromatic protons in the *ortho*-positions. A second multiplet, at 6.98 ppm is assigned to the protons in the *meta*-positions. The methoxy groups give rise to a singlet at 3.86 ppm. The ^1H NMR spectrum of $[RuF_2(CO)_2\{P(4\text{-}HOC_6H_4)_3\}_2]$ (**42**) exhibits singlets at high frequencies (10.31 and 9.92 ppm) assigned for the hydroxy protons in addition to multiplets in the range 7.23 - 7.00 ppm assigned to the aryl protons of the ligands. The $^{31}P\{^1H\}$ NMR spectrum of complex (**41**) exhibits a triplet at 15.8 ppm with a P-F coupling of 22 Hz and that of complex (**42**) is at 14.0 ppm with a $^2J_{P\text{-}F}$ = 21 Hz. These NMR data are included in Table 6.9, together with relevant data for similar triarylphosphine ruthenium complexes.

Table 6.9
NMR Data for [*OC-6-13*][$RuF_2(CO)_2(PR_3)_2$]

PR_3	δ_P/ppm[d]	δ_F/ppm[d]	$^2J_{P-F}$/Hz	Δ_P/ppm[e]
PPh_3[a]	21.6	-324.3	20	27.6
$P(4\text{-}CH_3OC_6H_4)_3$ (**41**)[b]	15.8	-339.7	22	25.7
$P(4\text{-}HOC_6H_4)_3$ (**42**)[c]	14.0	-321.1	21	23.8
$P(4\text{-}FC_6H_4)_3$[a]	14.9	-333.1	22	23.7

[a] Ref. 51. Recorded in d^6-acetone. [b] Recorded in CD_2Cl_2. [c] Recorded in DMSO. [d] The signals' multiplicity is triplet. [e] $\Delta_P = \delta_{P(complex)} - \delta_{P(free\ ligand)}$.

From the data in Table 6.9 it can be seen that, as expected,[55,57] the introduction of the *para*-substituents decreases Δ_P, the coordination shift, and has a negligible effect on $^2J_{P-F}$ value. Of greater interest is the unusual δ_F value for the *tris*-(*para*-hydroxyphenyl)phosphine complex (**42**) which occurs to significantly higher frequency than that for complex (**41**). Although there is no direct NMR evidence for any interaction, the most plausible explanation for this unusual result is a hydrogen bonding interaction between the hydroxy group and the fluoride ligand {perhaps similar to the intermolecular OH-Cl interaction observed in the solid phase structure of *cis*-$[PtCl_2\{P(4\text{-}HOC_6H_4)_3\}_2]$ (**6**) (Chapter Two)} which is deshielding the fluorine nucleus. Support for a possible interaction comes from leaving the ruthenium(II) complex (**42**) in solution for 24 hours, when the $^{31}P\{^1H\}$ NMR spectrum exhibits a doublet at 19.1 ppm ($^2J_{P-F}$ = 18 Hz), while the intensity of the triplet at 14.0 ppm decreases. The hydrogen bonding between the hydroxy groups and the fluoride ligands facilitates the liberation of HF, which is detected by a singlet at -165.3 ppm in the ^{19}F NMR spectrum, and places the oxygen atoms in close proximity to the metal centres for bond formation. The doublet at 19.1 ppm ($^2J_{P-F}$ = 18 Hz) in the $^{31}P\{^1H\}$ NMR spectrum is assigned to two phosphine ligands, *trans* to each other, bound to the metal centre and coupling to one *cis*-fluoride ligand. This complex could be an intermediate

in which only one fluoride atom has been replaced by an oxygen atom. In this case, the *tris*-(*para*-hydroxyphenyl)phosphine would be acting as a bridging ligand between metal centres, using both types of ligating atoms, the phosphorus and the oxygen. However, none of the decomposition products from complex (**42**) could be isolated.

The positive ion FAB mass spectrum of complex (**41**) exhibits signals at 872, 853, 834 and 805 m/z assigned to $[M\text{-}CO]^+$, $[M\text{-}CO\text{-}F]^+$, $[M\text{-}CO\text{-}2F]^+$ and $[M\text{-}2CO\text{-}2F]^+$ fragments respectively. The spectrum of complex (**42**) was less informative. However, a signal at 667 m/z could be assigned to $[M\text{-}CO\text{-}F]^+$ fragment.

The infrared spectra of the Nujol mulls of complexes (**41**) and (**42**) show two bands in the ν_{CO} region, characteristic of two mutually *cis* carbonyl groups (Table 6.10).

Table 6.10
CO Stretching Frequencies for [*OC-6-13*][$RuF_2(CO)_2(PR_3)_2$] Complexes

PR_3	ν_{CO} / cm^{-1}	
	ν_s	ν_{as}
$P(4\text{-}CH_3OC_6H_4)_3$ (**41**)	2035,	1962
$P(4\text{-}HOC_6H_4)_3$ (**42**)	2055,	1982
PPh_3	2045,	1973
$P(4\text{-}FC_6H_4)_3$	2047,	1974

According to Table 6.10, adding either electron withdrawing substituents or electron donating substituents in the *para*-positions of the aryl rings did not affect the values of the carbonyl stretching frequencies when compared to their triphenylphosphine analogue. However, when comparing complexes (**41**) and (**42**), an obvious increase is observed when replacing the methoxy by the hydroxy groups. This may support the idea that there is an interaction between the hydroxy groups and the fluoride atoms.

This hydrogen bonding would strengthen the σ-bond between the metal centre and the fluoride and weaken the π-back bonding out of the filled p-orbitals of the fluoride atom. These two effects would result in an increase in both the symmetric and asymmetric carbonyl stretching frequencies.

A single crystal for the complex (**41**) has been isolated from a dichloromethane solution and characterised by X-ray diffraction. The structure is depicted in Figure 6.12.

Figure 6.12
Crystal structure of $[RuF_2(CO)_2\{P(4\text{-}CH_3OC_6H_4)_3\}_2]$ (41)

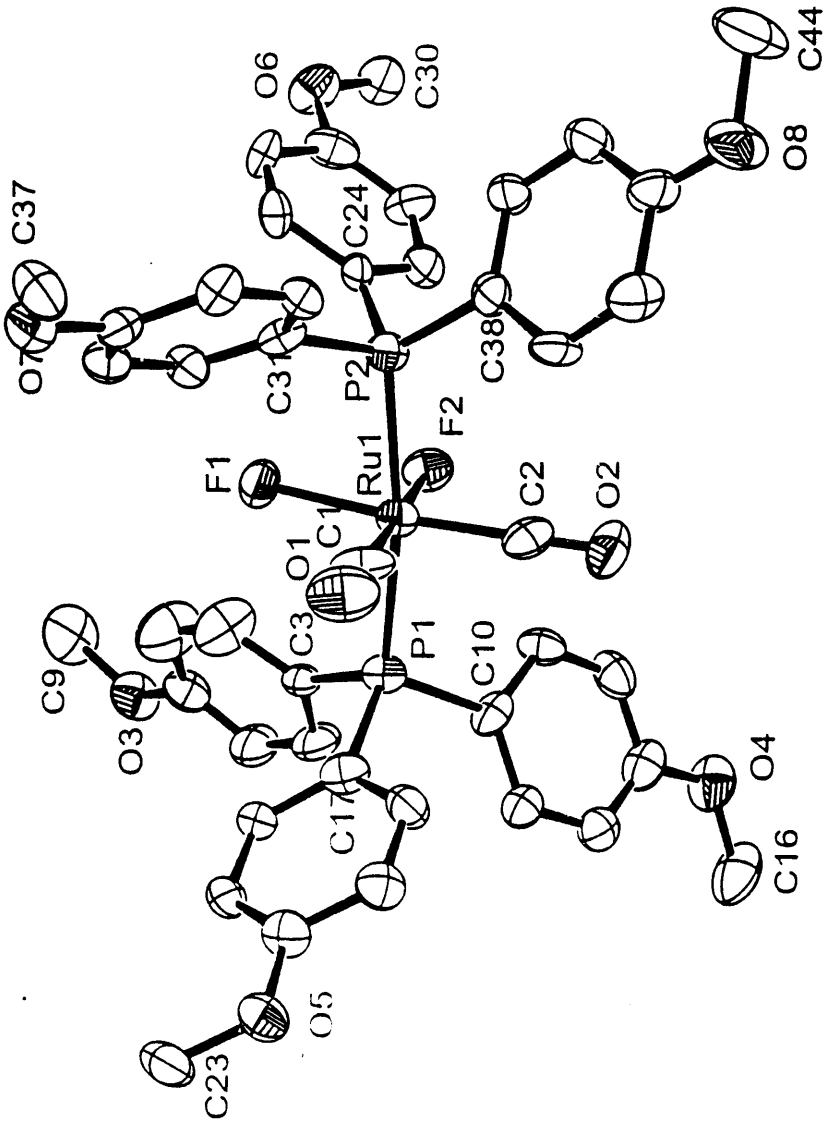

6.5.2 Characterisation of [*OC-6-13*][$OsF_2(CO)_2(PR_3)_2$]

The ^1H NMR spectrum of the $[OsF_2(CO)_2\{P(4\text{-}CH_3OC_6H_4)_3\}_2]$ (**43**), exhibits a multiplet at 7.63 ppm assigned to the aromatic protons in the *ortho* positions. A second multiplet, at 6.93 ppm, is assigned to the protons in the *meta* positions. The methoxy groups give rise to a singlet at 3.80 ppm. The ^1H NMR spectrum of $[OsF_2(CO)_2\{P(4\text{-}HOC_6H_4)_3\}_2]$ (**44**) exhibits a broad singlet at high frequency (10.05 ppm) assigned to the hydroxy protons in addition to multiplets in the range 7.42-6.83 ppm assigned to the aryl protons of the ligands. The $^{31}P\{^1H\}$ NMR experiment of complex (**43**) exhibits a triplet at -3.1 ppm with a P-F coupling of 30 Hz. The $^{31}P\{^1H\}$ NMR data for complex (**44**) exhibits one main signal in addition to several minor signals. The main signal is a triplet at -3.5 ppm with a $^2J_{P\text{-}F}$ = 30 Hz. NMR data are included in Table 6.11, together with relevant data for similar triarylphosphine osmium complexes.

Table 6.11
$^{31}P\{^1H\}$ NMR Data of [*OC-6-13*][$OsF_2(CO)_2(PR_3)_2$]

PR_3	δ_P/ppm[a]	δ_F/ppm[a]	$^2J_{P\text{-}F}$/Hz	Δ_P/ppm[b]
PPh_3[c]	1.0	-303.3	30	7.0
$P(4\text{-}CH_3OC_6H_4)_3$ (**43**)[d]	-3.1	-305.8	30	6.8
$P(4\text{-}HOC_6H_4)_3$ (**44**)[e]	-3.5	-301.2	30	6.3
$P(4\text{-}FC_6H_4)_3$[c]	-4.0	-308.8	32	4.8

[a] The signals' multiplicity is triplet. [b] $\Delta_P = \delta_{P(complex)} - \delta_{P(free\ ligand)}$. [c] Ref. 51. Recorded in d^6-acetone. [d] Recorded in $CDCl_3$. [e] Recorded in DMSO.

As seen for the ruthenium complexes (Table 6.9), the NMR data are generally unaffected by changing the *para*-substituent except for δ_F for (**44**). Here, the small

shift to higher frequency is reasonably explained by a hydrogen bonding interaction between the *para*-hydroxy groups and the metal-bound fluoride ligands.

The positive ion FAB mass spectrum of complex (**43**) exhibits signals at 989, 970 and 943 m/z assigned to $[M]^+$, $[M\text{-}F]^+$ and $[M\text{-}CO\text{-}F]^+$ fragments respectively. The spectrum of complex (**44**) was less informative. However, a signal at 887 m/z could be assigned to $[M\text{-}F]^+$ fragment.

The infrared spectra of the Nujol mulls of complexes (**43**) and (**44**) show two bands in the ν_{CO} region, characteristic of two mutually *cis* carbonyl groups (Table 6.11).

Table 6.11
CO Stretching Frequencies for [*OC-6-13*][$OsF_2(CO)_2(PR_3)_2$] Complexes

PR_3	ν_{CO} / cm^{-1}	
	ν_s	ν_{as}
$P(4\text{-}CH_3OC_6H_4)_3$ (**43**)	2014,	1930
$P(4\text{-}HOC_6H_4)_3$ (**44**)	2026,	1959
PPh_3	2017,	1937
$P(4\text{-}FC_6H_4)_3$	2035,	1962

In contrast to the ruthenium(II) complexes, the substituents on the aryl rings of the phosphine ligands incorporated in the osmium(II) complexes exhibited an influence on the carbon-oxygen bonding in the carbonyl group, as evidenced by the variations in the stretching frequencies, especially the asymmetric ones. It seems that significant differences between the magnitude of the symmetric stretching vibrations occur only between complex (**43**) and the complex incorporating arylphosphine ligand bearing fluorine in the *para*-positions. This confirms the increased electron donating

properties of the methoxy-substituted ligand compared to the fluorine-substituted ligand, inducing an increase in the electron density on the metal centre and an increase in the π-back-donation towards the carbonyl groups. However, when comparing complexes (**43**) and (**44**), an obvious increase is observed when replacing the methoxy by the hydroxy groups. Therefore, it can be concluded that there is an interaction between the hydroxy groups and the fluoride atoms, similar to that seen in the ruthenium analogue (**42**).

In contrast to the decomposition observed for complex (**42**), the *tris*-(*para*-hydroxyphenyl)phosphine osmium species (**44**) is stable in solution. This probably reflects the relative strengths of the osmium-fluoride and ruthenium-fluoride bonds which has been identified in the products from the reaction of ruthenium and osmium fluoride complexes with trimethylsilyl reagents.[55]

6.6 Summary:

The different characterisation data assigned to the low-valent late transition-metal fluoride complexes confirm the coexistence of two factors in stabilisation of the metal-fluoride bond. These two factors are: (i) an inductive withdrawing effect through the metal-fluoride σ-bond and (ii) a mesomeric donating effect out of the filled p-orbitals at the fluoride.

In general, the substituents in the aryl rings of the coordinated triarylphosphine ligands affect to different extents the coordination chemistry taking place in the inner sphere of the metal-fluoride complexes described in this chapter. Electron donating substituents strengthen the metal-phosphine and metal fluoride bonding as compared to a non-substituted triarylphosphine ligand {*cis*-$[PtF(PPh_3)\{P(4\text{-}CH_3OC_6H_4)_3\}_2]^+$ (**37**) *vs* $[PtF\{P(4\text{-}CH_3OC_6H_4)_3\}_3]^+$ (**38**)}. Moreover, trialkylphosphine ligands favour the *trans*-position to the fluoride as compared to the triarylphosphine ligands {*trans*-$[PtF(PEt_3)\{P(4\text{-}CH_3OC_6H_4)_3\}_2]^+$ (**36**) *vs* (**37**)}. On the other hand, the steric effect can exhibit a large influence on determining the configuration of the metal-fluoride complexes. In the complexes (**36**)-(**40**) series, bulky phosphine ligands favour the *cis*-position to the fluoride. It should be noted that in the metal-fluoride phosphine complexes incorporating $P(4\text{-}HOC_6H_4)_3$, a hydrogen bonding interaction has been detected between the hydroxy groups and the fluoride and probably favours elimination of HF and formation of metal-oxygen bond in the case of ruthenium complexes.

Chapter Six References

[1] G. W. Parshall, *Homogeneous Catalysis*, 2nd Ed, Wiley, New York, 1992.

[2] A. Spencer, *J. Organomet. Chem.*, 1980, **194**, 113.

[3] S. N. Blackburn, R. N. Hazeldine, R. V. Parish and J. H. Setchfield, *J. Organomet. Chem.*, 1980, **192**, 329.

[4] R. G. Pearson, *J. Chem. Ed.*, 1968, **45**, 581-587, 643.

[5] Kirk-Othmer, *Encyclopedia of Chemical Technology*, 2nd Edt, *Chemistry and Chemical Technology of the Fluorine*, John Wiley & Sons, 1966.

[6] C. L. Chernick, H. H. Claassen and B. Weinstock, *J. Am. Chem. Soc.*, 1961, **83**, 3165.

[7] P. L. Robinson and G. J. Westland, *J. Chem. Soc.*, 1956, 4481.

[8] B. Weinstock, J. G. Malm and E. E. Weaver, *J. Am. Chem. Soc.*, 1961, **83**, 4310.

[9] M. K. Whittlesey, R. N. Perutz, B. Greener and M. H. Moore, *Chem Commun.*, 1997, 187.

[10] E. F. Murphy, R. Murugavel and H. W. Roesky, *Chem. Rev.*, 1997, **97**, 3425 and references therein.

[11] R. W. Cockman, E. A. V. Ebsworth, J. H. Holloway, H. Murdock, N. Robertson and P. G. Watson, In: *Reaction of Non-metal Fluorides with some Platinum Metal Complexes*, J. Thrasher and S. Strauss (eds), ACS Symposium Series, ACS Books, 1994, 327.

[12] a) S. A. Brewer, J. H. Holloway, E. G. Hope and P. G. Watson, *J. Chem. Soc., Chem. Commun.*, 1992, 1577.

b) S. A. Brewer, A. K. Brisdon, J. H. Holloway, E. G. Hope, L. A. Peck and P. G. Watson, *J. Chem. Soc., Dalton Trans.*, 1995, 2945.

[13] a) C. A. Reed and W. R. Roper, *J. Chem. Soc., Dalton Trans.*, 1973, 1370.

b) G. R. Clark, C. A. Reed, W. R. Roper, B. W. Skelton, T. N. Waters, *J. Chem. Soc., Chem. Commun.*, 1971, 758.

c) R. J. Fitzgerald, N. Y. Sakkab, R. S. Strange and V. P. Narutis, *Inorg. Chem.*, 1973, **12**, 1081.

[14] N. M. Doherty and N. W. Hoffman, *Chem. Rev.*, 1991, 91, 553.

[15] J. H. Holloway and H. C. S. Clark , In: *Low Valent Transition Metal Fluorides*, T. Nakajima, B. Zemva and A. Tressaud (Eds.), Advanced Inorganic Fluorides: Synthesis, Characterisation and Applications, Elsevier Science S.A. Books, 2000, 51.

[16] H. E. Bryndza and W. Tam, *Chem. Rev.*, 1988, **88**, 1163.

[17] D. Foster, *Inorg. Chem.*, 1972, **11**, 1686.

[18] F. Araghizadeh, D. M. Branan, N. W. Hoffman, J. H. Jones, E. A. McElroy, N. C. Miller, D. L. Ramage, A. B. Salazar and S. H. Young, *Inorg. Chem.*, 1988, **27**, 3752.

[19] D. M. Branan, N. W. Hoffman, E. A. McElroy, N. C. Miller, D. L. Ramage, A. F. Schott and S. H. Young, *Inorg. Chem.*, 1987, **26**, 2915.

[20] L. Vaska and J. Peone, *J. Chem. Soc. Chem. Commun.*, 1971, 418.

[21] a) R. Brady, B. R. Flynn, G. L. Geoffry, H. B. Gray, J. Jr. Peone, and L. Vaska, *Inorg. Chem.*, 1976, **15**, 1485.

b) G. L. Geoffry, H. Isci, J. Litrenti and W. R. Mason, *Inorg. Chem.*, 1977, **16**, 1950.

c) G. L. Geoffry, M. S. Wrighton, G. S. Hammond and H. B. Gray, *J. Am. Chem. Soc.*, 1974, **96**, 3105.

[22] a) I. J. Colquhoun and W. J. McFarlane, *Mag. Res.*, 1982, **46**, 525.

b) C. Rüger, A. Mehlhoen and K. Schwetlick, *Z. Chem.*, 1974, **14**, 196.

c) R. R. Burch, R. L. Harlow and S. D. Ittel, *Organometallics*, 1987, **6**, 982.

[23] R. S. Drago, *Physical Methods for Chemists*, 2nd Edition, Saunders College Publishing, 1992.

[24] J. J. Dechter, *Prog. Inorg. Chem.*, 1982, **29**, 285, 1985, **33**, 393.

[25] G. Schiavon, S. Zecch, G. Pilloni and M. J. Martelli, *Inorg. Nucl. Chem.*, 1977, **39**, 115.

[26] J. T. Poulton, M. P. Sigalas, K. Folting, W. Streib, O. Eisensten and K. G. Caulton, *Inorg. Chem.*, 1994, **33**, 1476.

[27] J. McAvoy, K. C. Moss and D. W. Sharp, *J. Chem. Soc.*, 1965, 1376.

[28] R. D. W. Kemmitt, R. D. Peacock and J. Stocks, *J. Chem. Soc. (A)*, 1971, 846.

[29] M. A. Cairns, K. R. Dixon, J. J. McFarland, *J. Chem. Soc., Dalton Trans.*, 1975, 1159.

[30] N. M. Boag and M. S. Ravetz, *J. Chem. Soc., Dalton Trans.*, 1995, **21**, 3473.

[31] K. R. Dixon and D. J. Hawke, *Can. J. Chem.*, 1971, **49**, 3252.

[32] J. Chatt and J. M. Davidson, *J. Chem. Soc.*, 1959, 4020.

[33] H. C. S. Clark, J. Fawcett, J. H. Holloway, E. G. Hope, L. A. Peck and D. R. Russell, *J. Chem. Soc., Dalton Trans.*, 1998, 1249.

[34] a) L. A. Peck, *Ph.D. Thesis*, University of Leicester, 1995.

b) H. C. S. Clark, Leicester University, 1997-1999. Unpublished work.

[35] M. M. Rahman, H.-Y. Liu, K. Eriks, A. Prock and W. P. Giering, *Organometallics*, 1989, **8**, 1 and references cited therein.

[36] E. A. V. Ebsworth, N. Robertson and L. Y. Yellowlees, *J. Chem. Soc., Dalton Trans.*, 1993, 1031.

[37] a) R. G. Pearson, *J. Am. Chem. Soc.*, 1963, **85**, 3533.

b) R. G. Pearson, *J. Chem. Ed.*, 1968, **45**, 581.

[38] L. Vaska and J. Peone, *J. Chem. Soc. Chem. Commun.*, 1971, 418.

[39] D. R. Russell, M. A. Mazid and P. A. Tucker, *J. Chem. Soc., Dalton Trans.*, 1980, 1737.

[40] B. De Klerk-Engles, J. H. Groen, K. Vrieze, A. Mockel, E. Lindner and K. Coubitz, *Inorg. Chim. Acta*, 1992, **195**, 237.

[41] K. R. Dixon and J. J. McFarland, *J. Chem. Soc., Chem. Commun.*, 1972, 1274.

[42] a) H. C. Clark and J. D. Ruddick, *Inorg. Chem.*, 1970, **9**, 1226.

b) T. G. Appleton, M. H. Chisholm, H. C. Clark and L. E. Manzer, *Inorg. Chem.*, 1972, **11**, 1786.

[43] T. W. Dingle and K. R. Dixon, *Inorg. Chem.*, 1974, **13**, 846.

[44] G. Doyle, *J. Organomet. Chem.*, 1982, **224**, 355.

[45] E. R. Hammer, R. D. W. Kemmitt and M. A. R. Smith, *J. Chem. Soc., Dalton Trans.*, 1977, 261.

[46] G. G. Mather, A. Pidcock and G. J. N. Rapsey, *J. Chem. Soc., Dalton Trans.*, 1973, 2095.

[47] J. H. Holloway, R. D. Peacock and R. W. H. Small, *J. Chem. Soc.*, 1964, 644.

[48] C. J. Marshall, R. D. Peacock, R. D. Russell and I. L. Wilson, *J. Chem. Soc., Chem. Commun.*, 1970, 1643.

[49] A. J. Hewitt, J. H. Holloway, R. D. Peacock, J. B. Raynor and I. L. Wilson, *J. Chem. Soc., Dalton Trans.*, 1976, 579.

[50] S. A. Brewer, J. H. Holloway and E. G. Hope, *J. Chem. Soc., Dalton Trans.*, 1994, 1067.

[51] a) K. S. Coleman, *Ph.D. Thesis*, University of Leicester, 1996.
b) K. S. Coleman, J. Fawcett, J. H. Holloway, E. G. Hope and D. R. Russell, J. *Chem. Soc., Dalton Trans.*, 1997, 3557.

[52] S. A. Brewer, J. H. Holloway and E. G. Hope, *J. Fluorine Chem.*, 1995, **70**, 167.

[53] S. A. Brewer, K. S. Coleman, J. Fawcett. J. H. Holloway, E. G. Hope, D. R. Russell and P. G. Watson, *J. Chem. Soc., Dalton Trans.*, 1995, 1073.

[54] N. C. Thomas, *Coord. Chem. Rev.*, 1986, **70**, 121.

[55] B. R. James and L. D. Markham, *Inorg. Nucl. Chem. Lett.*, 1971, **7**, 373.

[56] N. C. Thomas, *Coord. Chem. Rev.*, 1989, **93**, 225.

[57] S. A. Brewer, K. S. Coleman, J. Fawcett, J. H. Holloway, E. G. Hope, D. R. Russell and P. G. Watson, *J. Chem. Soc., Dalton Trans.*, 1995, 1073.

CHAPTER SEVEN

REACTIONS OF LOW-VALENT PLATINUM GROUP METAL FLUORIDE COMPLEXES WITH HYBRID MULTIDENTATE PHOSPHINE LIGANDS

CHAPTER SEVEN

REACTIONS OF LOW-VALENT PLATINUM GROUP METAL FLUORIDE COMPLEXES WITH HYBRID MULTIDENTATE PHOSPHINE LIGANDS

7.1 Introduction:

The present chapter brings into a focus a further study of the low-valent late transition-metal-fluoride bond and in particular the reactivity of this bond upon coordination of the metal centre to hybrid multidentate chelating agents bearing, in addition to the phosphorus, either hydroxyl or vinyl groups.

Although the reactions of late transition-metal chloride, bromide and iodide complexes with bidentate and multidentate phosphine ligands have been extensively investigated, little coordination chemistry has been reported involving both multidentate ligands and fluoride. The main investigated areas describe single examples of fluorination of metal chelates rather than chelation at metal fluorides. For example, Cockman *et al.* revealed a non-concerted reaction between the $[Ir(dppe)_2]^+$ cation [dppe = *Bis*-(diphenylphosphinoethane)] and XeF_2.[1] When the reaction took place in deuterated dichloromethane at 240K, a fluorinated iridium(III) chelate (Figure 7.1a) was formed by the *trans* addition of the fluoride ligands to the metal centre. The $^{19}F\{^1H\}$ NMR spectrum revealed a quintet at δ -522.2 and the $^{31}P\{^1H\}$ NMR revealed a triplet at δ 8.8, $^2J_{P\text{-}F}$ = 18 Hz. However, when the same reaction was carried out in acetonitrile, the main product was a different fluorinated iridium(III) chelate (Figure 7.1b). The metal centre is bound to one fluoride and the *trans* position to the fluoride atom is occupied by an acetonitrile molecule. This time, the $^{31}P\{^1H\}$ NMR spectrum revealed a doublet at δ 11.0, $^2J_{P\text{-}F}$ = 20 Hz. Alternatively, on treating the $[Ir(dppe)_2S_2]^+$ cation with XeF_2 in deuterated dichloromethane, a *cis*-addition of fluoride ligands took place at the metal centre (Figure 7.1c). The ^{19}F and $^{31}P\{^1H\}$ NMR spectra revealed second order signals arising from an $AA'X_2X_2'$ spin system. The ^{19}F chemical signal is at δ -345.6 consistent with a fluoride *trans* to a phosphine ligand.[2]

Figure 7.1

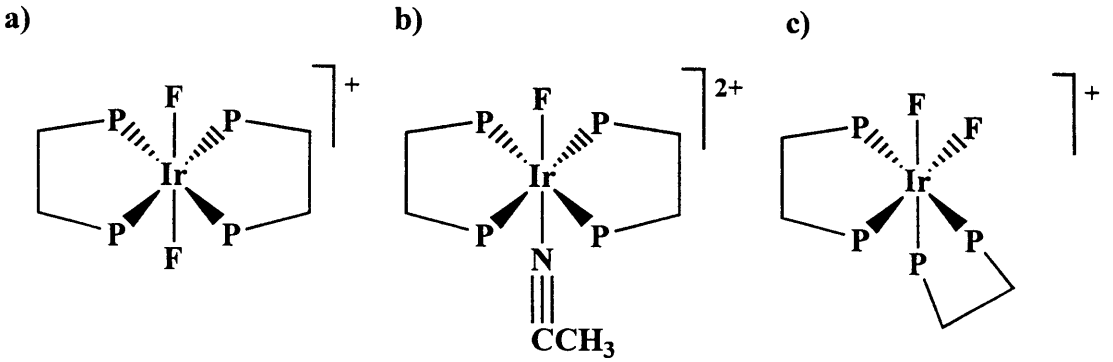

The second example is the reaction of *trans*-$[RuCl_2(dppe)_2]$ with $AgBF_4$ under one atmosphere of CO. The result is a mixture of two complexes, *trans*-$[Ru(CO)_2(dppe)_2][BF_4]_2$ and *trans*-$[RuF(CO)(dppe)_2][BF_4]$, as confirmed by the NMR data. It is thought that the fluoride ion is derived from the counterion, $[BF_4]^-$.[3]

In an additional example, Perutz *et al.*[4] investigated the C-F bond activation of hexafluorobenzene with *cis*-$[Ru(dmpe)_2H_2]$ (dmpe = $Me_2PCH_2CH_2PMe_2$) at -78°C and noticed the formation, in addition to *trans*-$[Ru(dmpe)_2(C_6F_5)H]$, of a second hydride bifluoride ruthenium complex, *trans*-$[Ru(dmpe)_2(H)(HF_2)]$ (Figure 7.2) in which the HF liberated in the C-F bond activation reaction has been trapped. It should be noted that the latter ruthenium complex was obtained in a higher yield by the reaction of the same starting material with $Et_3N.3HF$, triethylamine trihydrofluoride, at room temperature.[5]

Figure 7.2
***trans*-[Ru(dmpe)$_2$(H)(HF$_2$)]**

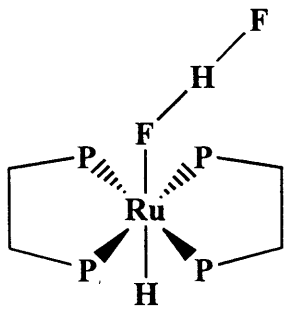

(dmpe = $Me_2PCH_2CH_2PMe_2$)

The reactions of low-valent late transition-metal fluoride complexes with multidentate donor ligands is still a very new area of chemistry. The main reason behind this delay in investigating this area is the difficulty in isolating stable low-valent late transition-metal fluoride complexes to be used as starting material for further reactions with desired ligands. However, as has been shown in Chapter Six, several platinum(II)- osmium(II) and ruthenium(II)- fluoride complexes have now been isolated as fairly stable complexes to be used as starting material for further reactions. The metal-fluoride bond reactivity can be expected to provide the driving force for the formation of new complexes the preparation of which should give a new insight into the low-valent late transition-metal fluoride chemistry. This chapter is an investigation of this type of chemistry.

7.2 Reaction of the Platinum(II) Fluoride Complex (35) with the P/O$^-$ Chelating System (23):

While studying the stability of different platinum(II) fluoride monomers,[14] it has been found that the $^1J_{Pt-F}$ in $[PtF(PPh_3)_3]^+$ cation is significantly smaller than that of $[PtF(PEt_3)_3]^+$ cation. This has been used to suggest that the Pt-F bond in the former complex is weaker than that in the latter. Indeed, the triethylphosphine complex showed stability in solution over extended periods and has been characterised crystallographically,[7a] whereas the triphenylphosphine analogue readily decomposed in solution. However, recently, it has been shown that this decomposition occurs by hydrolysis to form the $[Pt(OH)(PPh_3)_3]^+$ cation (Figure 7.3b),[7b] while in scrupulously dried solvents no decomposition occurs over many months, indicating that the variation in $^1J_{Pt-F}$ merely illustrates a change in the σ-bond strength and not a general bond weakening in going from the PPh_3 to the PEt_3 complex. However, more interestingly, the $[Pt(OH)(PPh_3)_3]^+$ cation was found to be unstable and decomposed over a period of two weeks when the OH group was displaced through an *ortho*-metalation (Figure 7.3c).

Figure 7.3

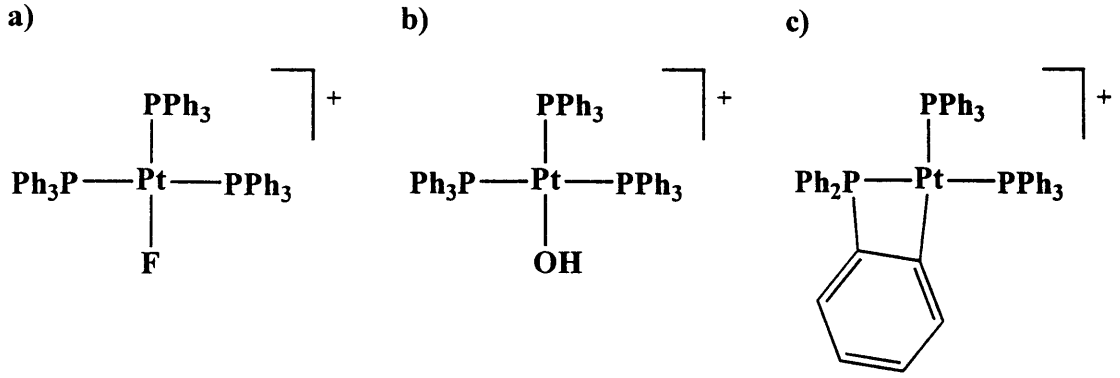

The coordination chemistry of the $P(2\text{-}HOC_6H_4)_3$ ligand on the one hand, and the platinum(II)-fluoride bond reactivity on the other, especially in the presence of moisture, gave the impetus to study the reaction between the doubly-fluoride bridged platinum(II) dimer (**35**) and the $P(2\text{-}HOC_6H_4)_3$ (**23**) ligand. It was anticipated that the Pt-F bond would be less stable than the Pt-O bond, strengthened by the "ring contribution" upon formation of the five-membered ring.

$[Pt_2(\mu\text{-}F)_2\{P(4\text{-}CH_3OC_6H_4)_3\}_4]^{2+}$ was allowed to react with $P(2\text{-}HOC_6H_4)_3$ in dichloromethane, according to Scheme 7.1.

Scheme 7.1

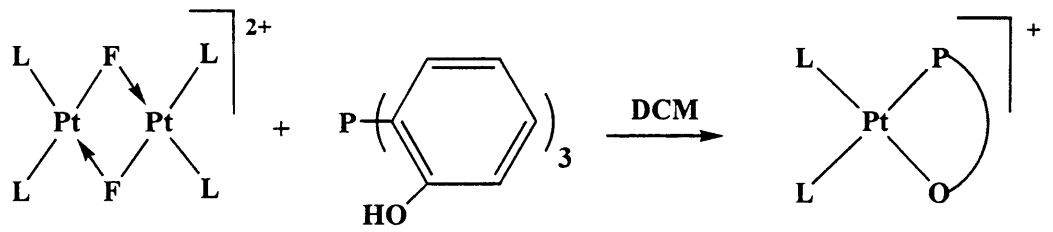

(45)

L = $P(4\text{-}CH_3OC_6H_4)_3$, P∩O = κ^2-$P(2\text{-}OC_6H_4)(2\text{-}HOC_6H_4)_2$ and

The *tris*-(*o*-hydroxyphenyl)phosphine was added to the platinum(II)-fluoride dimer (**35**) in dichloromethane solution in an FEP reaction vessel. The starting solution colour was yellow at room temperature and under nitrogen. The vessel containing the mixture was shaken for two minutes during which time the solution

colour changed to clearer yellow. According to the decomposition of the complex $[PtF(PPh_3)_3]^+$ already described,[7b] the oxygen atom was expected to replaced the fluoride on the platinum(II) centre, the driving force for this reaction being the elimination of HF and the formation of the five-membered ring. The product (**45**) has been characterised by ^1H and $^{31}P\{^1H\}$ NMR spectroscopies. Simulation[8] of the $^{31}P\{^1H\}$ NMR data has been carried out (Figure 7.4 and Table 7.1). $[Pt\{\kappa^2\text{-}P(2\text{-}OC_6H_4)(2\text{-}HOC_6H_4)_2\}\{P(4\text{-}CH_3OC_6H_4)_3\}_2]^+$ (**45**) incorporates a hydroxy-substituted arylphosphine ligand acting as a bidentate chelating agent. The other two coordination sites are still occupied by *tris*-(*p*-methoxyphenyl)phosphine ligands.

The $^{31}P\{^1H\}$ NMR spectrum of (**45**) exhibits two doublet of doublets at δ 35.0 and δ 24.2, assigned to the chelating agent and to the methoxy-substituted arylphosphine ligand in position *trans* to the phosphorus of this chelating agent, respectively. Additionally, a second order doublet of doublets, appearing like a triplet, at a lower frequency (δ 1.8) is assigned to the methoxy-substituted arylphosphine ligand in position *trans* to the phenoxy ligand (Figure 7.4).

The ^1H NMR spectrum exhibits a broad signal at δ 10.06 assigned to the hydroxy groups of the ligand. It also exhibits multiplets in the range δ 7.62-6.41 assigned to the aryl protons and two singlets at δ 3.61 and δ 3.56 assigned to the methoxy groups of the two phosphine ligands in different environments.

Figure 7.4 Experimental and Simulated $^{31}P\{^{1}H\}$ NMR Spectra of $[Pt\{\kappa^2\text{-}P(2\text{-}OC_6H_4)(2\text{-}HOC_6H_4)_2\}\{P(4\text{-}CH_3OC_6H_4)_3\}_2]^+$ (45)

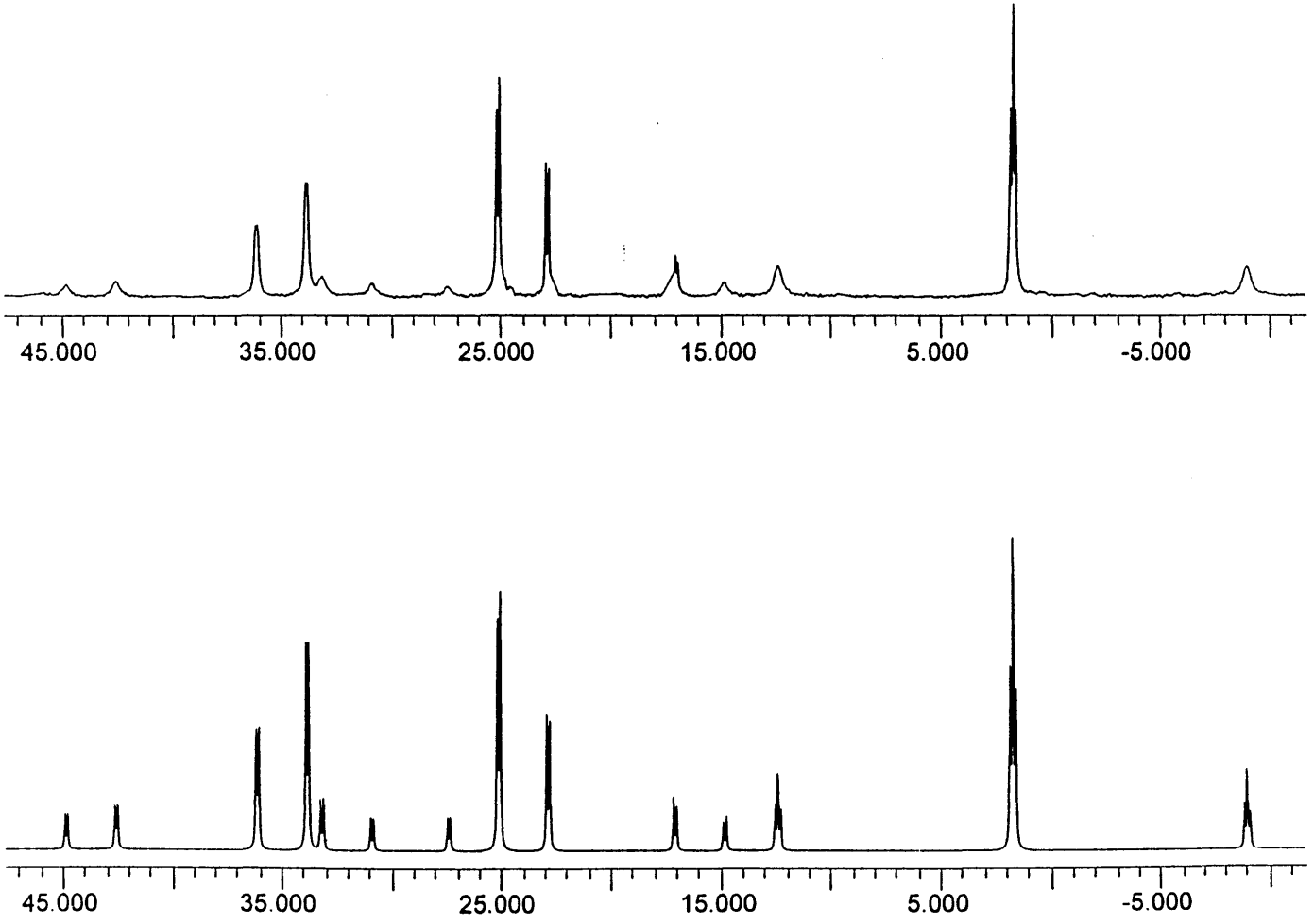

Figure 7.5
Structure of the Complex
$[Pt\{\kappa^2\text{-}P(2\text{-}OC_6H_4)(2\text{-}HOC_6H_4)_2\}\{P(4\text{-}CH_3OC_6H_4)_3\}_2]^+$ (45)

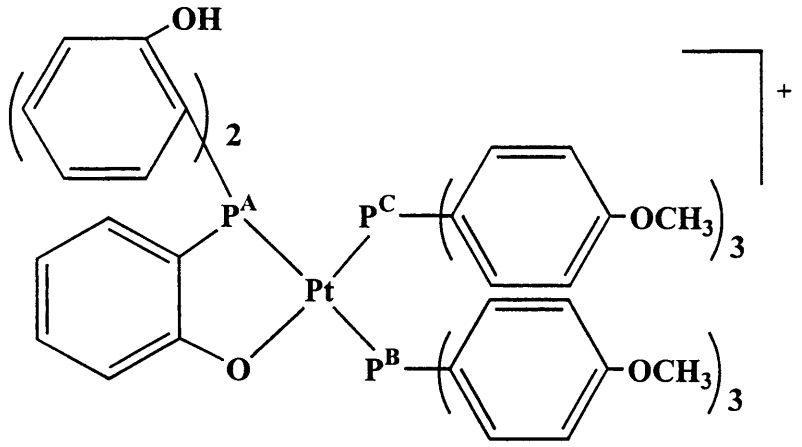

Table 7.1
$^{31}P\{^1H\}$ Simulated NMR Data[8] for Complex (45) in Figure 7.5.

X	δP/ppm	Δ/ppm[a]	$^2J_{PA\text{-}X}$/Hz	$^2J_{PB\text{-}X}$/Hz	$^1J_{Pt\text{-}X}$/Hz
P_A	35.0	84			2824
P_B	24.2	34.0	368		2605
P_C	1.8	11.6	19	22	3469

[a] **Coordination chemical shift ($\delta_{P(complex)} - \delta_{P(free\ phosphine)}$).**

The phosphino-alcohol chelating agents generally undergo deprotonation to yield phosphino-phenoxy-metal chelates,[9,10] favoured by the liberation of HF. The relatively high coordination chemical shift of the P_A signal implies that the ligand is chelating the platinum(II) centre and is incorporated in a five-membered ring.[11] This five-membered ring allows a good delocalisation of the negative charge by conjugation through the aromatic ring, between the phosphorus and the oxygen ligating atoms of the chelating agent. The signal assigned to P_A exhibits a broadness that could be due to a fluxionality caused by competition involving three oxygen

atoms over one coordination site at the platinum centre. The high frequency phosphorus chemical shifts of P_A and P_B (δ 35.0 and δ 24.2 respectively) are in accordance with their position *cis* to the electronegative element, oxygen. The phosphorus chemical shift of P_C (δ 1.8) is in accord with its position *trans* to the oxygen (see other $[PtX(phosphine)_3]^+$ cations in Chapter Six). The 368 Hz value corresponds to a $P_{trans}P$ coupling.[12] The 19 and 22 Hz values are common for a $P_{cis}P$ coupling.[13] The 2824 and 2605 Hz Pt-P coupling constants fall in the range of $^1J_{Pt-P}$ values where the phosphine ligands are mutually *trans*.[14] The value $^1J_{Pt-P}$ = 2824 Hz is very similar to that of $[Pt\{\kappa^2\text{-}P(2\text{-}OC_6H_4)(2\text{-}HOC_6H_4)_2\}_2]$ (**24**), $^1J_{Pt-P}$ = 2887 Hz (Chapter Four). The 3469 Hz Pt-P coupling constant falls in the range of $^1J_{Pt-P}$ values where the phosphorus atom is *trans* to an electronegative element.[6,15]

7.3 Reaction of the Platinum(II) Fluoride Complex (35) with the P/Vinyl Chelating System (31):

A second reaction was carried out using the doubly-fluoride bridged platinum(II) dimer (**35**) and a chelating agent. This time the chelating agent was the *ortho*-styryldiphenylphosphine ligand (**31**).

In the previous chapters, the coordination chemistry of the *tris*-(*ortho*-hydroxyphenyl)phosphine ligand (**23**) was compared with that of the SP ligand (**31**). This was mainly concerned with the electronic state of the metal centre and the steric requirements around this centre and how these factors affect the chelating capabilities of the chelating agents. In this chapter, a new factor is considered which is the existence of the fluoride as a ligand on the platinum(II) metal centre. Thus, in addition to the comparison of the chelating capabilities of the two chelating agents, it may be possible to detect variations in the platinum(II)-fluoride bond reactivity.

The formation of HF by the deprotonation of the hydroxy group and cleavage of the platinum(II)-fluoride bond, is considered one of the driving forces for the completion of the formation of the metal chelate (**45**). This is not expected to occur in the reaction of the same metal fluoride starting material with the ligand (SP) and

could, therefore, give an insight into the importance of the formation and elimination of HF.

Two milligrams of the ligand (SP) (**31**) were added to a dichloromethane solution of the platinum(II)-fluoride dimer (**35**) and ^{1}H, $^{31}P\{^{1}H\}$ and $^{19}F\{^{1}H\}$ NMR experiments were carried out on the resulting solution. The product was *trans*-$[PtF\{PPh_2(CH_2CHC_6H_4)\}\{P(4\text{-}CH_3OC_6H_4\}_2]^+$ (**46**) in which the (SP) ligand is acting in a monodentate mode.

The ^{1}H NMR spectrum reveals a broad singlet at 11.36 ppm assigned to the HF_2^-, which is the counterion. It also reveals a set of multiplets in the range 7.89-6.44 ppm assigned to the aryl protons of the phosphine ligands. Additionally, two signals appear at 5.54 and 5.04 ppm. The former is a doublet of doublets ($J_{H3\text{-}H2}$ = 1 Hz and $J_{H3\text{-}H1}$ = 17 Hz) assigned to the proton H_3 of the coordinated ligand (SP) to the metal centre (Figure 7.6). The latter signal is a doublet ($J_{H2\text{-}H1}$ = 11 Hz) and is assigned to the proton H_2 of the coordinated ligand (SP) to the metal centre (Figure 7.6). The signal assigned to H_1 could be beneath the aryl protons' signals (For references see Chapter Five). A singlet at ca. 3.70 ppm is assigned to the methoxy groups in the *para*-positions of the aryl rings of the phosphine ligands. The chemical shifts of the signals assigned to the vinyl protons in complex (**46**), as well as the coupling constant values between these protons, are very similar to those of the free ligand (SP) and to those of $[(\eta^5\text{-}C_5Me_5)RhCl_2(SP)]$ (**33**) (Chapter five). This similarity confirms that the ligand has its vinyl group un-coordinated to the metal centre.

Figure 7.6
***trans*-[PtF{$PPh_2(CH_2CHC_6H_4)$}{$P(4\text{-}CH_3OC_6H_4)_2$}]$^+$ (46)**

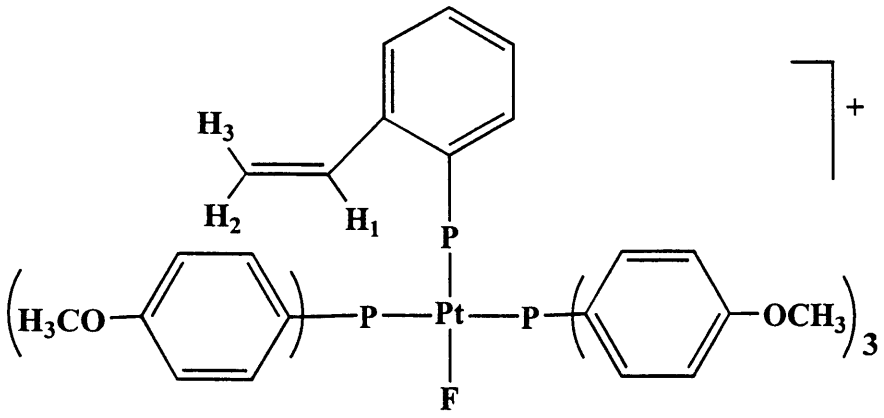

The $^{31}P\{^1H\}$ NMR spectrum of (**46**) exhibits a doublet of doublets at 24.5 ppm and a doublet of triplets at -0.2 ppm, but unfortunately, the platinum satellites could not be resolved. The $^{19}F\{^1H\}$ NMR spectrum of (**46**) exhibits a doublet of triplets at -228.8 ppm flanked with satellites. The data with assignments are summarised in Table 7.2 along with those of closely related platinum-fluoride cations.

Table 7.2
NMR Data of Complexes (36), (38) and (46).[a, e]

	trans-$[PtF(PEt_3)L_2]^+$ (36)	$[PtFL_3]^+$ (38)	*trans*-$[PtF(SP)L_2]^+$ (46)
δ_{Pa} [b]	25.0	23.4	24.5
δ_{Pb} [c]	0.7	-1.2	-0.2
$^2J_{Pa-Pb}$ [d]	20	18	18
$^2J_{Pa-F}$ [d]	32	37	37
$^2J_{Pb-F}$ [d]	141	144	144
δ_F [f]	-254.2	-229.8	-228.8
$^1J_{Pt-F}$ [d]	246	ca. 180	ca. 175

[a] NMR experiments of (36) and (38) are recorded in d^6 acetone and that of (46) is recorded in D_2O. [b] $\delta_{P\ cisF}$ /ppm (dd). [c] $\delta_{P\ trans\text{-}F}$ /ppm (dt). [d] In Hz. [e] L = P(4-$CH_3OC_6H_4)_3$. [f] In ppm (dt).

As expected, the phosphorus chemical shift assigned to the ligand *trans* to the fluoride atom is at lower frequency than those of the phosphine ligands *cis* to the fluoride atom. This is attributed to the π-back-bonding of the fluoride atom affecting mainly the ligand *trans* to itself. The high nucleophilicity of the alkylphosphine ligand PEt_3 in complex (**36**) causes an increase in the platinum-fluoride coupling and a shift to a lower frequency in δ_F when compared to those for complexes (**38**) and (**46**). An increase in the electron density on the metal centre induces an increase in the electron withdrawing effect through the σ-bonding between the platinum(II) centre and the fluoride ligand.

Figure 7.7 $^{31}F\{^{1}H\}$ NMR Spectra of *trans*-$[PtF\{PPh_2(CH_2CHC_6H_4)\}\{P(4\text{-}CH_3OC_6H_4\}_2]^+$ (46)

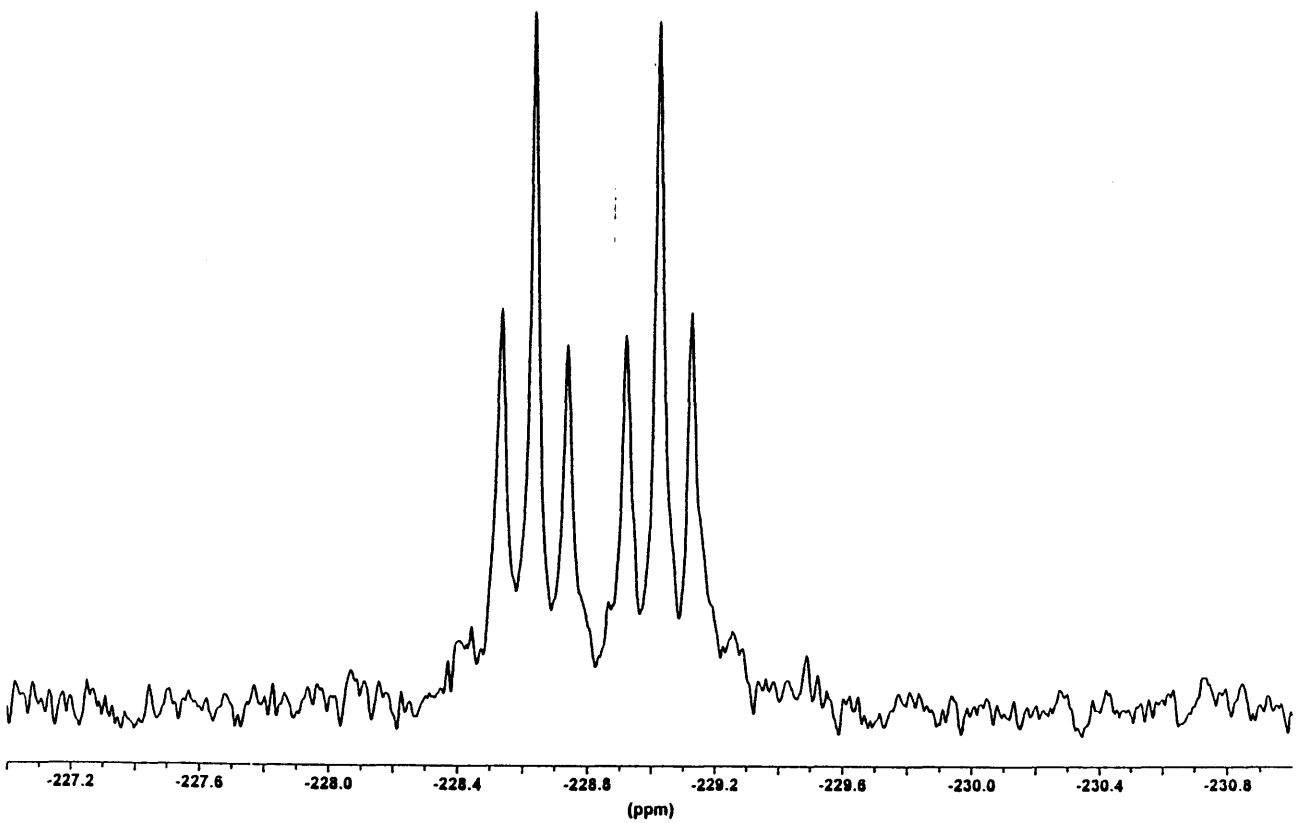

7.4 Reaction of Osmium(II) and Ruthenium(II) Carbonyl Fluoride Complexes with Hybrid Multidentate Phosphine Ligands:

The coordination chemistry of the highly moisture- and oxygen-sensitive ruthenium and osmium fluoride tetramers $[\{MF(\mu\text{-}F)(CO)_3\}_4]$ (M = Os, Ru) with monodentate triarylphosphine ligands has already been described in Chapter Six. In the present chapter, the coordination chemistry of the same tetramers with multidentate hybrid phosphine ligands is highlighted. The phosphine ligands are the *tris*-(*ortho*-hydroxyphenyl)phosphine (**23**) and the *ortho*-styryldiphenylphosphine (**31**). In general, the same experimental procedures are followed.[18] The tetramer and the phosphine ligand are mixed together in a Schlenk flask under nitrogen, in a 1:8 ratio. Dried and degassed dichloromethane is added to the mixture and the resulting solution is degassed periodically to ensure the elimination of any liberated carbon monoxide.

7.4.1 Reaction of $[\{MF(\mu\text{-}F)(CO)_3\}_4]$, (M = Ru, Os) with the P/O$^-$ Chelating System (23):

The reactions of the tetramers $[\{MF(\mu\text{-}F)(CO)_3\}_4]$ (M = Ru, Os) with the *tris*-(*ortho*-hydroxyphenyl)phosphine ligand (**23**), in dichloromethane, afforded purple solutions. In both cases, the NMR spectra revealed the formation of one main product, in addition to minor by-products that could be eliminated by slow recrystallisation from acetone or dichloromethane:hexane in the case of the osmium complex and by an acetone:hexane recrystallisation in the case of the ruthenium complex. A single crystal, suitable for X-ray diffraction, has been isolated for the osmium complex. The NMR experiments carried out on these crystals proved that they correspond to the main product from the reaction of the osmium tetramer with the P/O$^-$ chelating system. The formulae of the resulting products are: $[OC\text{-}6\text{-}13][Os(CO)_3\{\kappa^3\text{-}(2\text{-}OC_6H_4)_2P(2\text{-}HOC_6H_4)\}]$ (**47**) and $[TB\text{-}5][Ru(CO)_2\{\kappa^3\text{-}(2\text{-}OC_6H_4)_2P(2\text{-}HOC_6H_4)\}]$ (**48**) (Figure 7.8). In both complexes the phosphine ligand is coordinated to the metal centre in a η^3-P,O,O trihapto fashion.

Figure 7.8
Structures of the Complexes [*OC-6-13*][$Os(CO)_3\{\kappa^3$-$(2\text{-}OC_6H_4)_2P(2\text{-}HOC_6H_4)\}$] (47) and [*TB-5*][$Ru(CO)_2\{\kappa^3$-$(2\text{-}OC_6H_4)_2P(2\text{-}HOC_6H_4)\}$] (48)

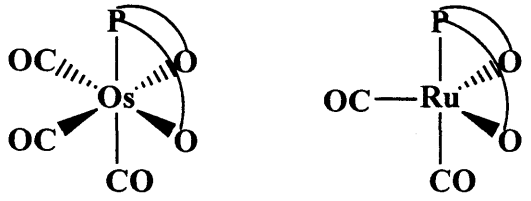

(47) (48)

The importance of the coordination chemistry of P,O-mixed donor ligands to late transition metals has been established in the literature[16] and has already been highlighted in this work (Chapter Four). However, the formation of the trihapto-mode by a phosphino-two phenoxide coordination was unknown until recently,[17] when $[\{(\eta^6\text{-}1,2,3,4\text{-}Me_4C_6H_2)RuCl_2\}_2]$ dimer was allowed to react with *tris*-(2,4,6-trimethoxyphenyl)phosphine ligand in order to achieve η^3-P,O,O bonding after loss of two methyl groups upon formation of two five-membered chelate rings. It was obvious that the steric bulkiness of the phosphine ligand (large cone angle, 184°)[18] was the main driving force for the formation of the chelation, forcing a close contact between the metal centre and the oxygen atoms. The product is $[(\eta^6\text{-}1,2,3,4\text{-}Me_4C_6H_2)Ru[P(2\text{-}OC_6H_3\text{-}6\text{-}OMe)_2\{C_6H_3(OMe)_2\text{-}2,6\}]$ and a crystal structure determination revealed a piano stool geometry at the metal centre (Figure7.9).

Figure 7.9
Structure of $[(\eta^6\text{-}1,2,3,4\text{-}Me_4C_6H_2)Ru[P(2\text{-}OC_6H_3\text{-}6\text{-}OMe)_2\{C_6H_3(OMe)_2\text{-}2,6\}]$[17]

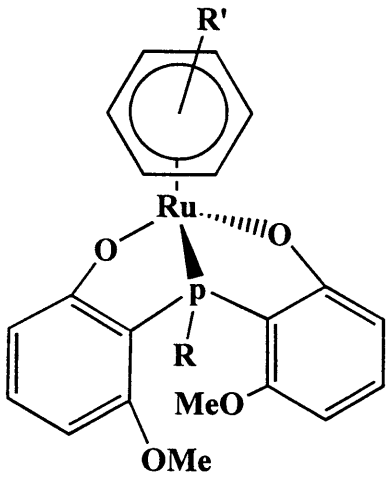

R = $C_6H_3(OMe)_2$-2,6

A possible pathway to this ruthenium complex starts with the formation of the ruthenium-phosphorus bond by cleavage of chloride bridges, and, indeed, the relevant complex incorporating the monohapto phosphine ligand has been isolated. The next step is the successive elimination of 2 molecules of MeCl *via* four-centered intermediates or transition states, yielding the metal chelate complex.

In the formation of complexes (**47**) and (**48**), the two fluoride atoms are replaced by oxygen atoms following the elimination of HF, which was detected in the $^{19}F\{^1H\}$ NMR spectra by a singlet at ca. -165.2 ppm [complex (**47**)] and at ca. -176.1 ppm [complex (**48**)]. The ^1H NMR spectra reveal broad singlets at ca. 11.14 ppm (**47**) and at ca. 4.80 ppm (**48**) assigned to the hydroxy protons. Additionally, they each reveal a set of multiplets in the range 7.58 - 6.16 ppm (**47**) and 7.58-6.50 ppm (**48**). The $^{31}P\{^1H\}$ NMR spectra exhibit a singlet in each case at 34.5 ppm (**47**) and at 30.2 ppm (**48**). The corresponding coordination chemical shifts of the phosphorus signals ($\Delta_P = \delta_{P(complex)} - \delta_{P(free\ ligand)}$) are 83.5 ppm and 79.2 ppm respectively. These are almost identical to the coordination shift (Δ_P = 84 ppm) observed for $[Pt\{\kappa^2\text{-}P(2\text{-}OC_6H_4)(2\text{-}HOC_6H_4)_2\}\{P(4\text{-}CH_3OC_6H_4)_3\}_2]^+$ (**45**). Hence, these values indicate that the phosphorus is incorporated into five-membered rings following chelation at the metal centre.

The positive ion FAB mass spectrum of complex (**47**) exhibits signals at 585, 557, 528 and 499 m/z assigned to $[M]^+$, $[M\text{-}CO]^+$, $[M\text{-}2CO]^+$ and $[M\text{-}3CO]^+$ fragments respectively. The similar mass spectrum of complex (**48**) exhibits signals at 441 and 409 m/z assigned for $[M\text{-}CO]^+$ and $[M\text{-}2CO]^+$ fragments respectively.

The infrared spectra of the Nujol mulls of complexes (**47**) and (**48**) show three and two bands, respectively, in the ν_{CO} region (Table 7.3).

Table 7.3
CO Stretching Frequencies for $[Os(CO)_3\{\kappa^3\text{-}(2\text{-}OC_6H_4)_2P(2\text{-}HOC_6H_4)\}]$ (47) and $[Ru(CO)_2\{\kappa^3\text{-}(2\text{-}OC_6H_4)_2P(2\text{-}HOC_6H_4)\}]$ (48)

Complexes	ν_{CO} / cm^{-1}
(**47**)	2113, 2043, 2002
(**48**)	2059, 2001

The infrared spectrum of complex (**47**) exhibits two bands at relatively high frequencies, 2113 and 2043 cm^{-1}. These bands are assigned to the carbonyl groups *trans* to the phenoxy ligands in the main plane of the molecule. The band at 2002 is assigned to the carbonyl group in position *trans* to the phosphorus.

Table 7.4
CO Stretching Frequencies for Osmium(II) Phosphine Complexes

Complexes	ν_{CO} / cm^{-1}	
	ν_s	ν_{as}
$[OsF_2(CO)_2\{P(4\text{-}CH_3OC_6H_4)_3\}_2]$ (**43**)	2014,	1930
$[OsF_2(CO)_2\{P(4\text{-}HOC_6H_4)_3\}_2]$ (**44**)	2026,	1959
$[Os(CO)_3\{\kappa^3\text{-}(2\text{-}OC_6H_4)_2P(2\text{-}HOC_6H_4)\}]$ (**47**)	2113,	2043

Comparing the data in Table 7.4, the stretching frequencies of complex (**47**), where the carbonyl groups are *trans* to the oxygen atoms, are higher than those of complexes (**43**) and (**44**), where the carbonyl groups are *trans* to the fluoride atoms. This difference is attributable to the larger π-back-donation of the fluoride ligand compared to that of the phenoxy ligand. In addition, the relatively high stretching frequencies assigned to the carbonyl groups in the ruthenium complex (**48**) are due to the 16e configuration around the metal.

Figure 7.10
Crystal Structure of $[Os(CO)_3\{\kappa^3\text{-}(2\text{-}OC_6H_4)_2P(2\text{-}HCC_6H_4)\}].C_3H_6O$ (47)

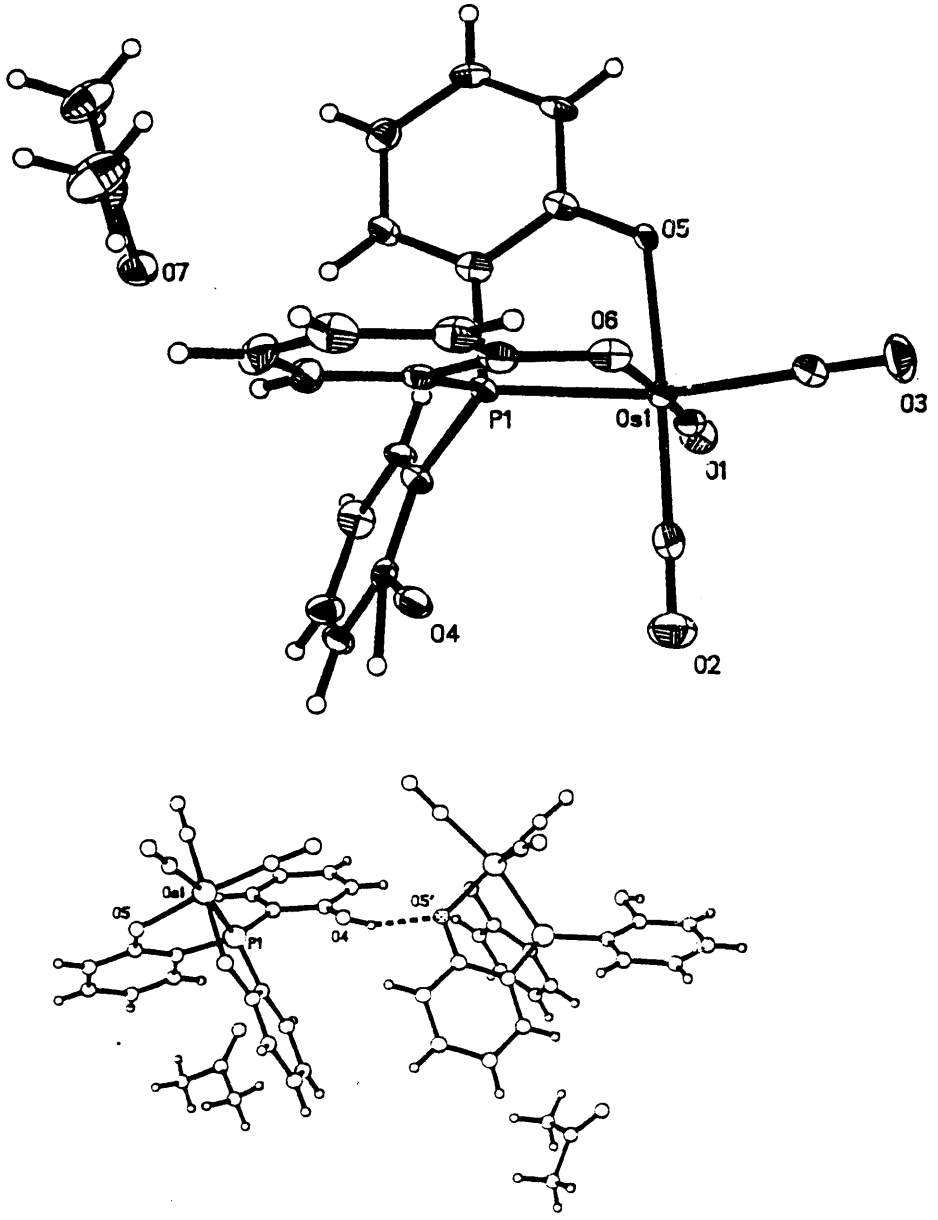

A single crystal, suitable for X-ray diffraction, has been isolated for the osmium complex $[Os(CO)_3\{\kappa^3\text{-}(2\text{-}OC_6H_4)_2P(2\text{-}HOC_6H_4)\}]$ (**47**) (Figure 7.10) which crystallised with one molecule of acetone. The tridentate phosphine ligand is *trans* to three carbonyl groups. Therefore, there was no loss of carbon monoxide molecules and a possible pathway could be fluoride-bridge cleavage by the formation of a metal-phosphorus bond followed by the elimination of HF and the replacement of the fluoride atoms by oxygen atoms.

Table 7.5
Selected Bond Distances (Å) and Angles (°) with e.s.d. in Parentheses about Os(II) for $[Os(CO)_3\{\kappa^3\text{-}(2\text{-}OC_6H_4)_2P(2\text{-}HOC_6H_4)\}].C_3H_6O$ (47)

Os(1)-C(1)	1.890(9)	O(1)-C(1)	1.140(10)
Os(1)-C(2)	1.891(10)	O(2)-C(2)	1.143(11)
Os(1)-C(3)	1.984(10)	O(3)-C(3)	1.130(11)
O(6)-C(36)	1.360(7)	Os(1)-O(6)	2.083(6)
O(5)-C(21)	1.367(6)	Os(1)-O(5)	2.106(5)
O(4)-C(16)	1.344(10)		
O(4) ...H... O(5')	2.620(8)	Os(1)-P(1)	2.345(2)
C(1)-Os(1)-C(2)	92.7(4)	C(1)-Os(1)-C(3)	95.6(4)
C(1)-Os(1)-O(6)	173.5(3)	C(1)-Os(1)-O(5)	90.5(3)
C(1)-Os(1)-P(1)	92.5(3)		
C(2)-Os(1)-C(3)	91.4(4)	C(2)-Os(1)-O(6)	90.0(3)
C(2)-Os(1)-O(5)	176.2(3)		
C(3)-Os(1)-O(6)	90.3(3)	C(3)-Os(1)-O(5)	90.4(3)
O(6)-Os(1)-O(5)	86.7(2)	O(6)-Os(1)-P(1)	81.26(18)
O(5)-Os(1)-P(1)	80.69(15)		

Selected angles and bond distances for complex (**47**) are included in Table 7.5. According to the tabulated data, the structure is a distorted octahedron around the osmium(II) centre. This distortion can be detected by the differences in the bond distances and angles around the metal centre. The two osmium-oxygen (phenyl) bond lengths are different. The same observation applies to the osmium-carbon (CO) bond distances. There is not a large difference between the carbon-oxygen bond lengths when comparing the two types of carbonyl groups. However, the osmium-carbon (*trans* to phosphorus) bond length is larger than that of osmium-carbon (*trans* to oxygen). This difference is attributed to the difference in the *trans*-influence of the phosphine ligand compared to that of the phenoxy group. The three osmium-carbon bond lengths are longer than those in the $[OsF_2(CO)_2(PPh_3)_2]$ complex [1.832(9) Å][20] and the carbon-oxygen (CO) bond lengths are shorter than those of the reference complex [1.178(9) Å]. On the other hand, when comparing the three oxygen-carbon (phenyl) bond lengths, those incorporated in a five-membered chelation ring are larger than that corresponding to the free hydroxy group. This is due to the fact that when the oxygen is un-coordinated to the metal centre, its π-electron density is interacting more with that of the phenyl group compared to the case where the oxygen is bound to the metal. This electron delocalisation towards the aryl group induces a multiple O-C bond character, shortening the O-C (phenyl) bond. However, the osmium-phosphorus bond length in (**47**) is relatively short compared to that of $[OsF_2(CO)_2(PPh_3)_2]$ complex [2.419(2) Å].[20] The bite angles at the metal centre caused by the formation of the five-membered rings are 81.26 (18) and 80.69(15)° and are comparable to values from the literature such as in the case of the [*OC-6-13*][$RuCl_2\{\eta^2$-(2,6-$(MeO)_2C_6H_3)PPh_2\}$] complex where the average bite angle is 79.8°].[17]

A relatively strong intermolecular hydrogen bond is observed between a hydroxy group and an oxygen atom bound to the metal centre.[21] This could be due to the fact that the oxygen atoms bound to the osmium(II) centre are electron-rich.

7.4.2 Reaction of $[\{MF(\mu\text{-}F)(CO)_3\}_4]$, (M = Ru, Os) with the P/Vinyl Chelating System (31):

The reaction of the tetramers $[\{MF(\mu\text{-}F)(CO)_3\}_4]$ (M = Ru, Os) with eight equivalents of the *ortho*-styryldiphenylphosphine ligand (**31**), in dichloromethane for three hours, afforded a white solution in the case of M = Os and a yellow solution in the case of M = Ru. In both cases, the NMR spectra revealed the formation of one main product, in addition to minor by-products that were hard to eliminate. Extending the time of the reaction led to the formation of additional products. These results will be discussed later.

Figure 7.11
$[OC\text{-}6\text{-}13][MF_2(CO)_2(SP)_2]$ (M = Os (49), Ru (50))

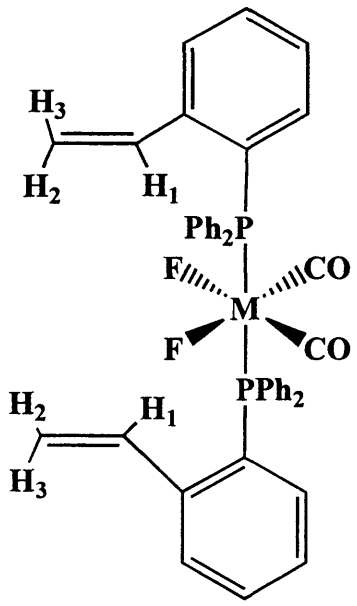

The main product from these reactions is $[OC\text{-}6\text{-}13][MF_2(CO)_2(SP)_2]$ (M = Os (**49**), Ru (**50**)) (Figure 7.11), where the phosphine ligand is acting in a phosphorus-bound monodentate mode. The absence of chelation could be due either to a steric hindrance impeding any close contact between the vinyl group and the metal centre, or to the fact that the metal centre, being bound to two fluoride atoms, is electron deficient and would not favour the allocation of the vinyl group to one coordination

site. Similar behaviour has been observed in the rhodium(III) complex in Chapter Five.

The structure of complexes (**49**) and (**50**) has been confirmed by different characterisation techniques. The ^{1}H NMR spectrum of the [*OC-6-13*][$OsF_2(CO)_2(SP)_2$] (**49**) complex, revealed a set of multiplets in the range 7.87-6.71 ppm assigned to the aromatic protons. A doublet of doublets at 5.57 ppm (J_{H3-H1} = 17 Hz and J_{H3-P} = 1 Hz) is assigned to the H_1 proton of an SP ligand coordinated to the metal centre in a monodentate mode. Another doublet of doublets at 5.54 ppm (J_{H3-H1} = 17 Hz and J_{H3-H2} = 1 Hz) is assigned to the H_1 proton of an un-coordinated SP ligand. A doublet of doublets at 5.13 ppm (J_{H2-H1} = 11 Hz and J_{H3-H2} = 1 Hz) is assigned to the H_2 proton of a coordinated SP ligand. In addition to these signals, the ^{1}H NMR spectrum revealed a doublet of doublets at 5.08 ppm (J_{H2-H1} = 8 Hz and J_{H3-H2} = 1 Hz). Such a signal is usually assignable to the H_2 proton of a vinyl group bound to the metal centre (see Chapter Five), mainly due to the relatively low H_2-H_3 coupling value.[22] The signal which exhibited broadness in the range 3.20-1.60 ppm might be attributed to one of the by-products of the reaction. The $^{19}F\{^{1}H\}$ NMR spectrum of complex (**49**) exhibited a broad singlet at -308.4 ppm assigned to a fluoride *trans* to a carbonyl group on an osmium metal (see Chapter Six) and two singlets at -154.2 and -169.6 ppm assigned to BF_4^- and SiF_6^{2-} respectively, which result from the reaction of HF with the glass of the reaction vessel.

The ^{1}H NMR spectrum of the [*OC-6-13*][$RuF_2(CO)_2(SP)_2$] (**50**) complex, revealed a set of multiplets in the range 7.79-6.95 ppm assigned to the aromatic protons. A doublet of doublets at 6.77 ppm (J_{H1-H2} = 11 Hz and J_{H1-H3} = 17 Hz), a doublet at 5.56 ppm (J_{H3-H1} = 17 Hz) and a doublet at 5.05 ppm (J_{H1-H2} = 11 Hz) are assigned to the H_1, H_3 and H_2 protons, respectively, of an SP ligand coordinated to the metal centre in a monodentate mode through the phosphorus atom. The related $^{19}F\{^{1}H\}$ NMR was inconclusive.

Table 7.6
NMR Data of [*OC-6-13*][$MF_2(CO)_2(PR_3)_2$] (M = Os, Ru)

PR_3	δ_P/ppm[f]		δ_F/ppm[f]		$^2J_{P-F}$/Hz		Δ_P/ppm[d]	
	Os	Ru	Os	Ru	Os	Ru	Os	Ru
$P(4\text{-}CH_3OC_6H_4)_3$[a]	-3.1	15.8	-305.8	-339.7	30	22	6.8	25.7
$P(4\text{-}HOC_6H_4)_3$[b]	-3.5	14.0	-301.2	-321.1	30	21	6.3	23.8
PPh_3[c]	1.0	21.6	-303.3	-324.3	30	20	7.0	27.6
$P(4\text{-}FC_6H_4)_3$[c]	-4.0	14.9	-308.8	-333.1	32	22	4.8	23.7
SP[e]	0.9	21.7	-308.4[g]	-	31	20	14.7	35.5

[a] Recorded in CD_2Cl_2. [b] Recorded in DMSO. [c] Ref. 20. Recorded in d^6-acetone. [d] $\Delta_P = \delta_{P(complex)} - \delta_{P(free\ ligand)}$. [e] The osmium complexes are recorded in $CDCl_3$ and those of ruthenium in CD_2Cl_2. [f] The signals' multiplicity is triplet. [g] Broad singlet.

The $^{31}P\{^1H\}$ NMR signal multiplicity, assigned for complexes (**49**) and (**50**), is a triplet at 0.9 ppm ($^2J_{P-F}$ = 31 Hz) and 21.7 ppm ($^2J_{P-F}$ = 20 Hz) respectively. These data, together with those related to other osmium and ruthenium fluoride phosphine complexes, are included in Table 7.6. When comparing the phosphorus-fluoride coupling constant values included therein, a high similarity is observed, which implies similarity in the bonding in these complexes. Therefore, the introduction of the vinyl group as a substituent on the *ortho*-position of the aryl ring does not affect the bonding of the phosphine ligand. It has been observed in Chapter Six that while the various *para*-substituents affect the ^{31}P and ^{19}F chemical shifts, the phosphorus-fluoride coupling is relatively unaffected by these variations. It has been concluded that the electronic variations caused by these substituents have a negligible influence on the coupling constant values. However, when comparing the coordination chemical shift values of both ruthenium and osmium complexes included in Table 7.6, a significant increase is observed when adding one vinyl group on the *ortho*-position of an aryl ring. If the discussion is based on the steric effect, one would argue that the

increased bulkiness of the phosphine ligand caused by the *ortho*-substituent would favour a lengthening in the distance separating the phosphorus atom from the electropositive metal centre, inducing a chemical shifting of the phosphorus signal to lower frequencies when compared to less bulky phosphine ligands. Since this is not the case, the electronic factor should be the dominant factor since, having the phosphorus atom and the vinyl group on the same aryl double bond, this allows an electron delocalisation between both groups inducing a shift of the phosphorus signal to a higher frequency.

The positive ion FAB mass spectrum of complex (**49**) exhibits signals at 843, 823, 793 and 768 m/z assigned to $[M\text{-}F]^+$, $[M\text{-}2F]^+$, $[M\text{-}2F\text{-}CO]^+$ and $[M\text{-}2F\text{-}2CO]^+$ fragments respectively. The similar mass spectrum of complex (**50**) exhibits signals at 753, 725, 705 and 675 m/z assigned to $[M\text{-}F]^+$, $[M\text{-}F\text{-}CO]^+$, $[M\text{-}2F\text{-}CO]^+$ and $[M\text{-}2F\text{-}2CO]^+$ fragments respectively.

Table 7.7
CO Stretching Frequencies for [*OC-6-13*][$MF_2(CO)_2(PR_3)_2$] Complexes

	M = Os		**M = Ru**	
PR_3	**ν_{CO} / cm^{-1}**		**ν_{CO} / cm^{-1}**	
	ν_s	**ν_{as}**	**ν_s**	**ν_{as}**
$P(4\text{-}CH_3OC_6H_4)_3$	2014,	1930	2035,	1962
$P(4\text{-}HOC_6H_4)_3$	2026,	1959	2055,	1982
PPh_3	2017,	1937	2045,	1973
$P(4\text{-}FC_6H_4)_3$	2035,	1962	2047,	1974
SP	2021,	1940	2040,	1967

The infrared spectra of the Nujol mulls of complexes (**49**) and (**50**) show two bands in the ν_{CO} region, assigned to the two mutually *cis* carbonyl groups (Table 7.7). In Chapter Six, it has been noticed that adding either electron withdrawing substituents or electron donating substituents in the *para*-positions of the aryl rings in the phosphine ligands did not affect the carbonyl bond stretchings in the ruthenium complexes, when compared to their triphenylphosphine analogue. This observation is also valid for the *ortho*-styryldiphenylphosphine complex as no significant changes are observed when comparing the symmetric and asymmetric values of both complexes [*OC-6-13*][$MF_2(CO)_2(SP)_2$] and their triphenylphosphine analogue.

The complex [*OC-6-13*][$RuF_2(CO)_2(SP)_2$] (**50**) tends to be unstable in dichloromethane solution. When complex (**50**) is left in solution for twenty-four hours at room temperature, in addition to the signals observed in the proton NMR spectrum, broad signals are detected at 4.22, 3.64 ppm and a doublet at 3.16 ppm (J_{H-H} =13 Hz). These could be a sign of a vinyl bound to the metal centre. The $^{31}P\{^1H\}$ NMR spectrum of the same solution revealed two signals coupling to each other. These are two doublets at 58.8 ppm ($^2J_{P-F}$ = 18 Hz and $^2J_{P\text{-}trans\text{-}P}$ = 272 Hz) and 43.0 ppm ($^2J_{P-F}$ = 18 Hz and $^2J_{P\text{-}trans\text{-}P}$ = 272 Hz). While the intensity of these signals was increasing, that of the triplet at 21.7 ppm, assigned for the complex (**50**), was decreasing. According to the $^{31}P\{^1H\}$ NMR data, the ruthenium centre is bound to two inequivalent phosphorus atoms which are mutually *trans*. The inequivalence between the two SP ligands would arise from the fact that one of these ligands is chelating the metal centre while the other is not. The chelation state was, therefore, confirmed by the low frequency vinyl proton signals in the ^1H NMR spectrum. The infrared spectrum revealed, in addition to the out-of-plane deformation bands at 998 and 917 cm^{-1}, characteristic of an un-coordinated vinyl group, a weak signal at 1587 cm^{-1} that could correspond to the stretching of a weakly bound vinyl group to the ruthenium centre. The proposed structure of the resulting product from the decomposition of complex (**50**) is [*OC-6-13*][$RuF(CO)_2\{\kappa^2\text{-}(\eta^2\text{-}2\text{-}CH_2CHC_6H_4)PPh_2\}\{PPh_2(2\text{-}CH_2CHC_6H_4)\}$] (**51**) depicted in Figure 7.12.

Figure 7.12
The decomposition product of [*OC-6-13*][$RuF_2(CO)_2(SP)_2$]

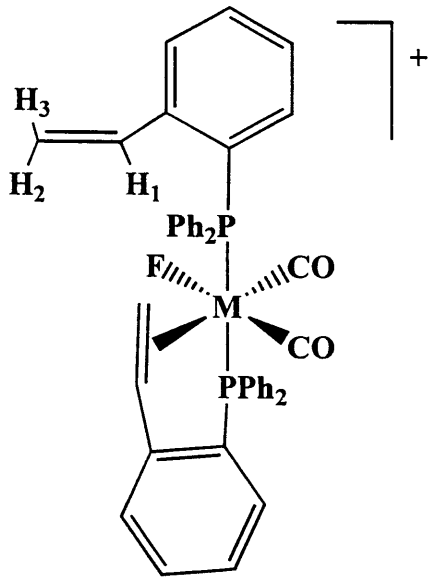

(51)

Additionally, the $^{19}F\{^1H\}$ NMR spectrum exhibited two singlets at -139.5 and -153.6 ppm. The latter is assigned to BF_4^- resulting from the reaction of HF with the glass of the reaction vessel. However, the former signal could be assigned to a product of solvent fluoridation or an additon reaction on the vinyl group of the SP ligand. Nevertheless, there were no additional data from other characterisation techniques to confirm any assignment for additional by-products.

The complex [*OC-6-13*][$OsF_2(CO)_2(SP)_2$] (**49**) also tends to decompose in dichloromethane solution, however, the nature of its decomposition is not clear.

7.5 Summary:

The *tris*-(*ortho*-hydroxyphenyl)phosphine ligand (**23**) has shown a wide variety of hapticities. It is mainly influenced by the steric and electronic requirements of the metal centre. Three coordination modes were detected in this work for the same ligand. It has acted as a monohapto-ligand, e.g. $[PtS_2\{P(2\text{-}HOC_6H_4)_3\}_2]$ (**26**), as a dihapto-ligand forming one five-membered ring on the metal centre, e.g. $[Pt\{\kappa^2\text{-}P(2\text{-}OC_6H_4)(2\text{-}HOC_6H_4)_2\}\{P(4\text{-}CH_3OC_6H_4)_3\}_2]^+$ (**45**), and as a trihapto-ligand forming two five-membered rings on the same metal centre, e.g. $[Os(CO)_3\{\kappa^3\text{-}(2\text{-}OC_6H_4)_2P(2\text{-}HOC_6H_4)\}]$ (**47**). The *ortho*-styryldiphenylphosphine ligand (**31**) has acted in two modes; in a monodentate fashion by bonding through the phosphorus atom, e.g. *trans*-$[PtF\{PPh_2(CH_2CHC_6H_4)\}\{P(4\text{-}CH_3OC_6H_4\}_2]^+$ (**46**) and in a bidentate fashion by using both ligating groups, the phosphorus atom and the vinyl group, such as in the complex *[OC-6-13]*$[RuF(CO)_2\{\kappa^2\text{-}(\eta^2\text{-}2\text{-}CH_2CHC_6H_4)PPh_2\}\{PPh_2(2\text{-}CH_2CHC_6H_4)]$ (**51**).

It was found that the *tris*-(*ortho*-hydroxyphenyl)phosphine ligand (**23**) readily yielded a transition-metal chelate when allowed to react with a transition-metal fluoride complex. This could be due to the ease of fluoride replacement with an oxygen and the liberation of HF. However, the chelation of the transition-metal fluoride complexes with the *ortho*-styryldiphenylphosphine ligand (**31**) was not as straightforward as that of (**23**). This has been attributed to the repulsion of the vinyl group by the metal centre due to electronic and steric factors. The fact of having the metal bound to fluoride, reduces the electron density at the metal. As a result of this electronic state, the metal does not favour coordination of the vinyl group which is considered to be, predominantly, an electron acceptor ligand. On the other hand, the vinyl group in the *ortho*-position of the aryl ring of the phosphine ligand induces a steric hindrance. As a result of this hindrance, the distance between the metal centre and the vinyl group is expected to be large. Therefore, the interaction between the two entities is disfavoured.

Chapter Seven References

[1] R. W. Cockman, A. V. Ebsworth, J. H. Holloway, H. Murdoch, N. Robertson and P. G. Watson, *Inorganic Fluorine Chemistry: Toward the 21st Century,* Chapter 20, *Reaction of Nonmetal Fluorides with Some Platinum Metal Complexes*, 326.

[2] L. A. Peck, *Ph.D. Thesis*, University of Leicester, 1995.

[3] G. Smith, D. J. Cole-Hamilton, A. C. Gregory and N. G. Gooden, *Polyhedron*, 1982, **1**, 97.

[4] M. K. Whittlesey, R. N. Perutz, B. Greener and M. H. Moore, *J. Chem. Soc., Chem. Commun.*, 1997, 187.

[5] a) R. Franz, *J. Fluorine Chem.*, 1980, **15**, 423.
b) M. A. McClinton, *Aldrichchim. Acta*, 1995, **28**, 31.

[6] M. A. Cairns, K. R. Dixon and J. J. McFarland, *J. Chem. Soc. Dalton Trans.*, 1975, 1159.

[7] a) D. R. Russell, M. A. Mazid and P. A. Tucker, *J. Chem. Soc., Dalton Trans.*, 1980, 1737.
b) H. C. S. Clark, J. Fawcett, J. H. Holloway, E. G. Hope, L. A. Peck, and D. R. Russell, *J. Chem. Soc., Dalton Trans.*, 1998, 1249.

[8] gNMR, version 3.6, Cherwell Scientific Publishing Ltd., Oxford, 1995.

[9] H. D. Empsall, B. L. Shaw and B. L. Turtle, *J. Chem. Soc. Dalton Trans.*, 1976, 1500.

[10] R. T. Boeré, C. D. Montgomery, N. C. Payne and C. J. Willis, *Inorg. Chem.*, 1985, **24**, 3680.

[11] L. S. Merriwether and J. R. Leto, *J. Am. Chem. Soc.*, 1961, **83**, 3182.

[12] J. M. Jenkins and B. L. Shaw, *Proc. Chem. Soc.*, 1963, 279.

[13] N. W. Alcock, A. W. G. Platt and P. Pringle, *J. Chem. Soc. Dalton Trans.*, 1987, 2273.

[14] J. A. Pople and D. P. Santry, *Mol. Phys.*, 1964, **8**, 1.

[15] E. R. Hammer, R. D. W. Kemmitt and M. A. R. Smith, *J. Chem. Soc. Dalton Trans.*, 1977, 261.

[16] a) J. C. Jeffrey and T. B. Rauchfuss, *Inorg. Chem.*, 1979, **18**, 2658.

b) M. Canestrari, B. Chaudret, F. Dahan, Y.-S. Huang, R. Poilblanc, T.-C. Kim and M. Sanchez, *J. Chem. Soc., Dalton Trans.*, 1990, 1179.

c) I. Le Gall, P. Laurent, E. Soulier, J.-Y. Salaün and H. des Abbayes, *J. Organomet. Chem.*, 1998, **567**, 13.

d) M. B. Smith and A. M. Z. Slawin, *Inorg. Chim. Acta*, 2000, **299**, 172.

e) D. D. Ellis, G. Harrison, A. G. Orpen, H. Phetmung, P. G. Pringle, J. G. deVries and H. Oevering, *J. Chem. Soc., Dalton Trans.*, 2000, 671.

[17] Y. Yamamoto, R. Sato, F. Matsuo, C. Sudoh and T. Igoshi, *Inorg. Chem.*, 1996, **35**, 2329.

[18] M. Wada and A. Tsuboi, *J. Chem. Soc., Perkin Trans.*, 1987, 151.

[19] P. E. Garrou, *Chem.Rev.*, 1981, **81**, 229.

[20] a) K. S. Coleman, *Ph.D. Thesis*, University of Leicester, 1996.

b) K. S. Coleman, J. Fawcett, J. H. Holloway, E. G. Hope and D. R. Russell, J. *Chem. Soc., Dalton Trans.*, 1997, 3557.

[21] J.-C. Shi, C.-H. Yueng, D.-X. Wu, Q.-T. Liu and B.-S. Kang, *Organometallics*, 1999, **18**, 3796.

[22] C. N. Banwell and N. Sheppard, *Mol. Phys.*, 1960, **3**, 351.

CHAPTER EIGHT

EXPERIMENTAL

CHAPTER EIGHT
EXPERIMENTAL

Throughout this work, the air- and moisture-sensitive compounds were handled on either a glass vacuum line, under dinitrogen, using standard Schlenk line techniques, or on a metal vacuum line with facilities to connect glass or fluoroplastic vessels *via* Teflon^{TM} couplings. Reactions requiring the use of aHF were carried out inside FEP reaction vessels.

8.1 Metal Vacuum Line:

The metal vacuum line consisted of 316-stainless steel or Monel Autoclave Engineers valves (AE-30 series) [Autoclave Engineers Inc., Erie, Pennsylvania, U. S. A.] connected *via* Autoclave Engineers high-pressure connectors. Argon arc welded "U" traps were incorporated in the metal manifold in order to allow separation and condensation of gases. Inlets for fluorine [Distillers MG] and argon [BOC Special Gases] were positioned as shown in Figure 8.1. Rough pump vacuum outlets were connected *via* a stainless steel soda-lime chemical scrubber unit (volume 1 dm^3) to a rotary pump [Model PSR/2, NGN Ltd.] which provided a vacuum of 10^{-2} mmHg. The soda-lime chemical scrubber neutralised the fluorine gas and HF. The high vacuum was achieved *via* outlets to a mercury diffusion pump coupled to a second rotary pump [Edwards High Vacuum International, Model RV5]. This provided, typically, a vacuum in the region of 10^{-5} mmHg. The high vacuum system was protected from volatile products that remained after using the rough vacuum system, by a glass trap immersed in liquid nitrogen (-196°C). A second glass trap cooled by solid carbon dioxide (-78°C) was employed between the mercury diffusion pump and the rotary pump in order to protect this last unit from mercury vapour. Pressures of 0 - 1500 mmHg were measured by Bourdon tube gauges [Type IF/66Z, Budenberg Gauge Co., Broadheath, Greater Manchester]. The high vacuum was measured by a Penning gauge situated between the metal outlets and the liquid nitrogen trap.

Figure 8.1
Metal Vacuum Line

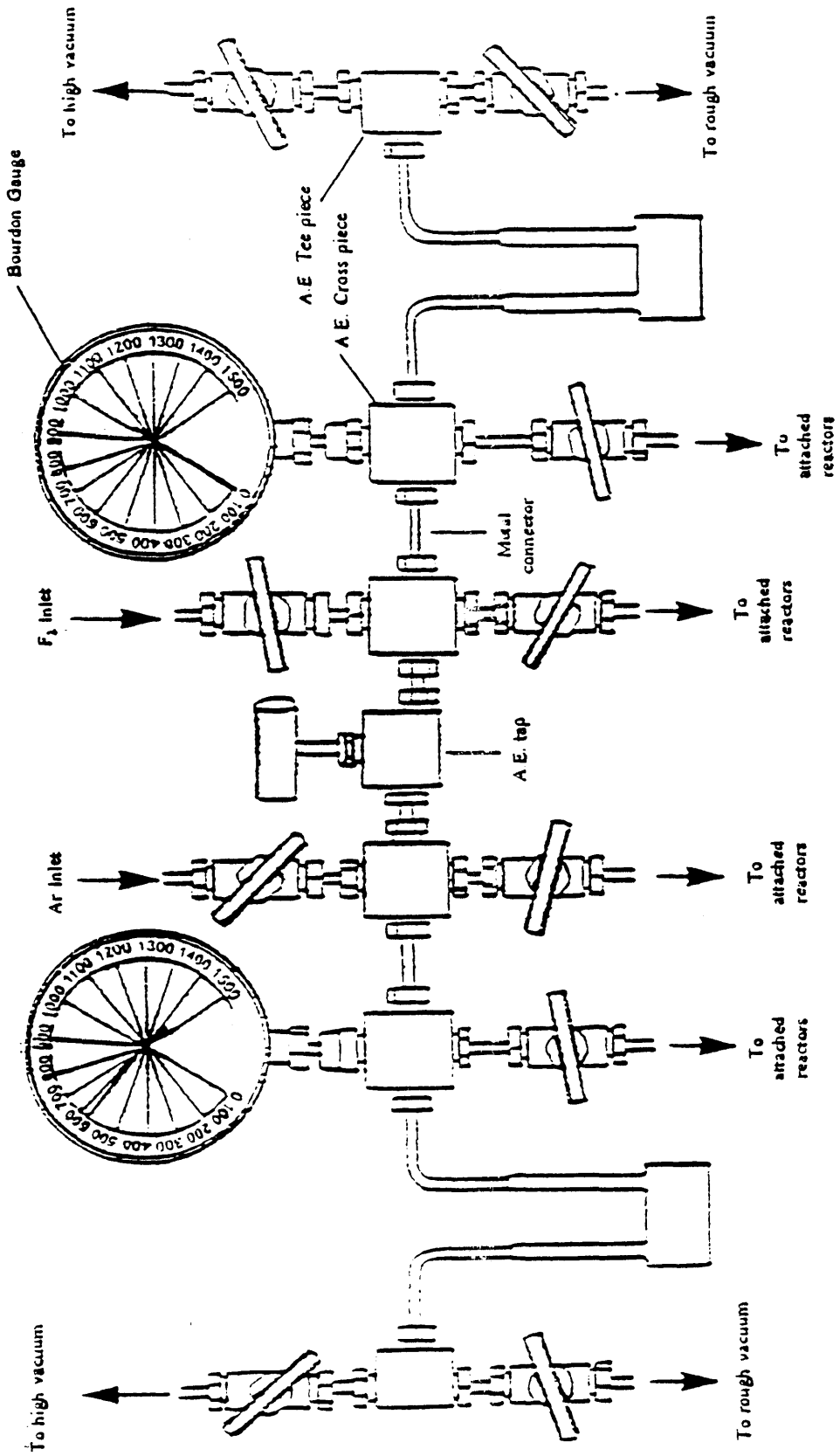

8.2 Glass Vacuum Line (Schlenk Line):

This apparatus was used in order to handle materials less reactive to oxygen and moisture compared to those handled on the metal vacuum line. The glass line consisted of a vacuum and dinitrogen manifold fitted with greased vacuum taps. The reaction vessels are connected to the outlets of the manifold by Neoprene tubing. The vacuum (0.1 mmHg) was achieved using a rotary pump protected by a glass trap immersed in liquid nitrogen.

8.3 Reaction Vessels Used on the Metal Vacuum Line:

The extremely air- and moisture-sensitive compounds were handled on the metal vacuum line. The vessels used were made of either glass or FEP. The glass vessels were fitted with Young's greaseless taps. These vessels are usually used for dried and degassed organic solvent storage.

The FEP reactors, in which all the reactions took place, consisted of straightened 4mm O.D. x ca. 25 cm long FEP tube (0.05 cm wall thickness) [Production Techniques Ltd.]. The tubes were sealed at one end by heat moulding into a 5 mm O.D. NMR glass tube. These tubes were then connected to Chemcon™ coarse-control needle valves [Type STD/VC-4, Production Techniques] by a PTFE compression union 'O' ring.

Before the introduction of the reagents, the FEP reactors were passivated. The passivation consisted of an evacuation to 10^{-4} mmHg to ensure that a vacuum tight system had been obtained, followed by the admission of ca. 500 mmHg of fluorine gas for ca. 0.5 hrs.. The fluorine gas was than removed using the rough pump. A high vacuum was then achieved.

Non-volatile reagents were loaded into the FEP vessels in the dry box, while the solvents and the volatile reagents were transferred into the FEP vessels under static vacuum (see Figure 8.2).

Figure 8.2
Apparatus Used for the Transfer of Volatile Reagents and Solvents under Static Vacuum

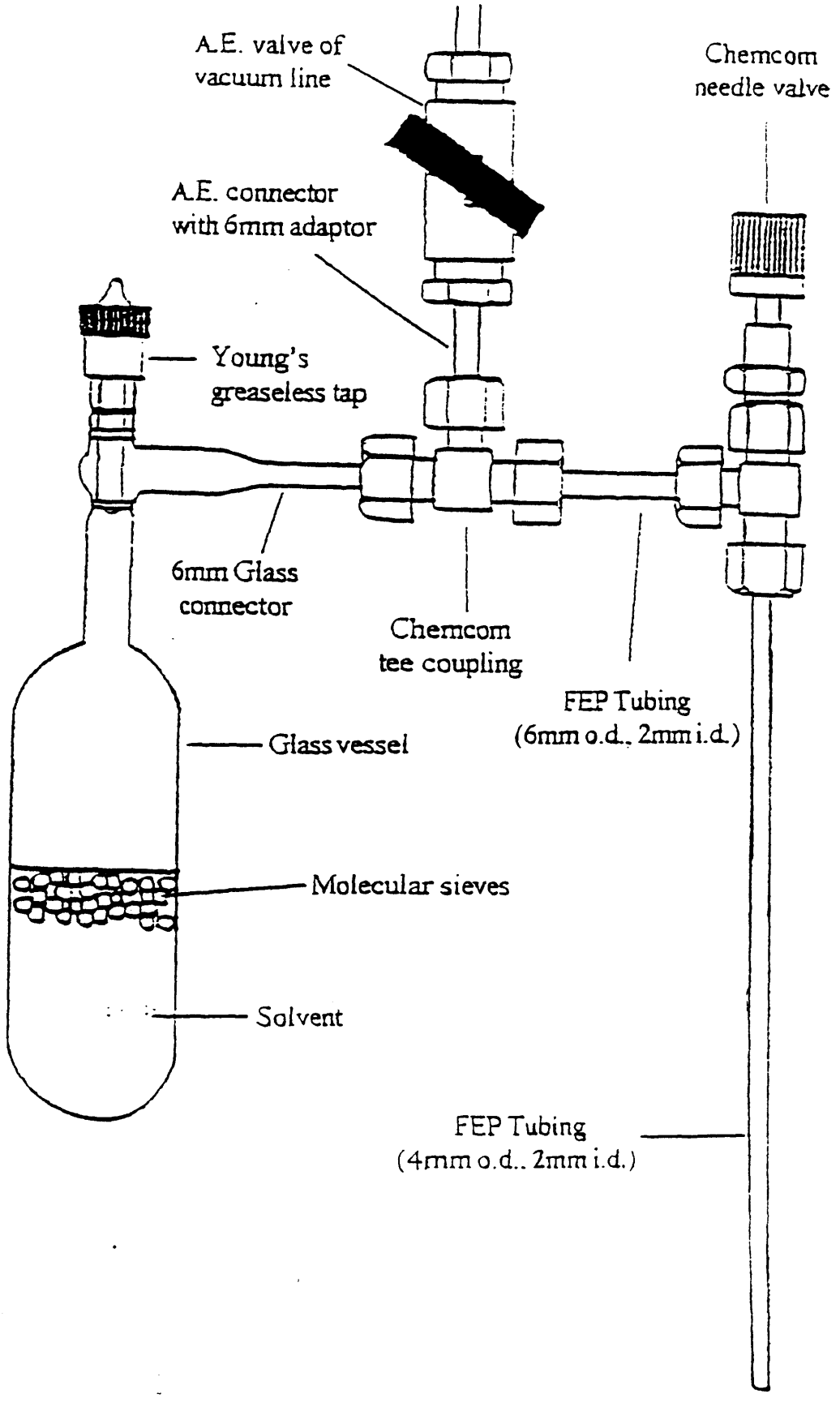

After reaction, the solvent was either removed to manipulate the product, or sealed at the top, under vacuum, using a small ring oven, whilst the solution remained frozen at -196°C. The resulting sealed tubes could then be examined by NMR spectroscopy.

8.4 Inert Atmosphere Dry Box:

The manipulation of involatile materials was carried out in an auto-recirculating positive pressure dry box [Vacuum Atmosphere Co., VAC NE 42-2 Dri Lab.]. It provided an atmosphere of dinitrogen and an oxygen and water content of less than 5 ppm. The inertness and dryness of the box atmosphere was maintained by circulation through a column of manganese oxide and a column of molecular sieves for the removal of oxygen and moisture respectively. The dry box was equipped with a Sartorius balance [Model 1601 MP8].

8.5 Analytical Techniques:

8.5.1 Nuclear Magnetic Resonance Spectroscopy:

NMR spectra were recorded on Bruker ARX 250, Bruker DPX 300, or Bruker DRX 400 spectrometers. ^{1}H NMR spectra were recorded at 250.13, 301.50, 400.13 MHz, referenced internally using the residual protio solvent resonance relative to tetramethylsilane (δ = 0 ppm). ^{31}P NMR spectra were recorded at 101.26, 122.05, 161.98 MHz, referenced externally to 85% H_3PO_4 (δ = 0 ppm). ^{19}F NMR specra were recorded at 376.50 MHz, referenced externally to $CFCl_3$ (δ = 0 ppm). ^{13}C NMR spectra were recorded at 75.78 MHz (on a Bruker DPX 300 machine) referenced externally to tetramethylsilane (δ = 0 ppm). ^{195}Pt NMR spectra were recorded at 86.02 MHz, referenced externally to Na_2PtCl_6 / D_2O (δ = 0 ppm). All chemical shifts were quoted in δ (ppm) and coupling constants in Hz using the high-frequency positive convention.

Figure 8.3
NMR Sample in 4 mm FEP Tube

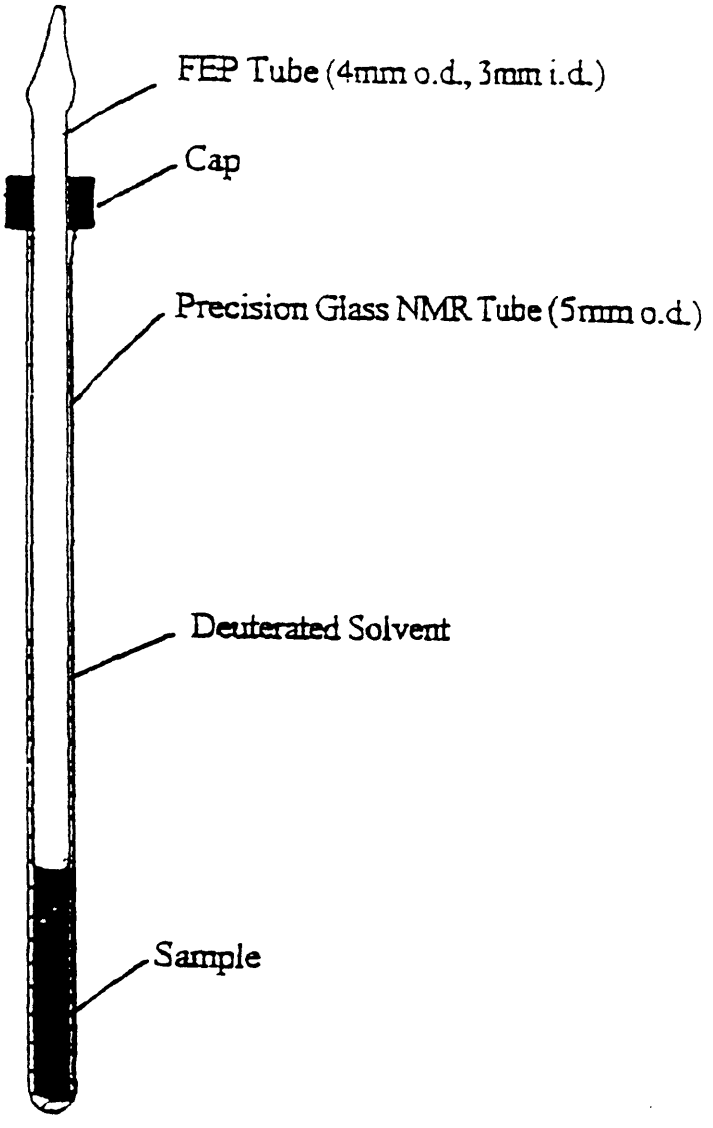

Abbreviations used in multiplicities are: s = singlet, d = doublet, t = triplet, q = quartet, m = multiplet, b = broad. For the fluorine containing platinum complexes, spectra were recorded in FEP tubes (outside diameter of 4mm) held coaxially in 5mm precision glass NMR tubes containing a small amount of deuterated solvent as lock substance (Figure 8.3).

8.5.2 Infrared Spectroscopy:

Infrared spectra were recorded as Nujol mulls, sandwiched between KBr plates on a *Bio-Rad* FTS40 Fourier Transform Infrared Spectrometer. In the case of low frequency detection, the Nujol-compound dispersion was laid on polythene plates. Abbreviations used in multiplicities are: s = strong, m = medium, w = weak, b = broad.

8.5.3 Microanalysis:

Elemental Analyses were carried out by *Butterworth Laboratories Ltd.*, Waldegrave Road, Teddington, Middlesex, TW11 8LG UK.

8.5.4 Mass Spectrometry:

Mass spectra (Electron Impact EI and Fast Atom Bombardment FAB using 3-Nitrobenzyl Alcohol as matrix) were recorded on a Kratos Concept Mass Spectrometer and those of electrospray (ES) were recorded on a **Z** SPRAY™ Micromass' quantum LC spectrometer.

8.5.5 X-Ray Diffraction:

The single crystals were glued to the end of thin glass-fibres using epoxy resins. Intensity data were measured on a Siemens P4 diffractometer, using Mo-Kα radiation (λ = 0.71073 Å). The structures were solved using SHELXTL-pc[1] and

refined using the program package SHELXL-93.[2] The above equipment and programs were used to solve the structures of all the crystals mentioned in this work except that of $[RuF_2(CO)_2\{P(4\text{-}CH_3OC_6H_4)_3\}_2]$ (**41**) which was solved using an Enraf Nonius Kappa CCD diffractometer, using Mo-Kα radiation (λ = 0.71069 Å). The structure was solved using Patterson DIRDIF methods[11] and refined using SHELXL-97.[12]
The crystal data and structure refinement for each crystal structure determined in this work can be found in the Appendix.

8.6 Solvents:

The diethyl ether used in this work, was stored over sodium wire for a minimum period of three days, then distilled under dinitrogen from sodium and benzophenone. The dichloromethane was distilled under dinitrogen, from calcium hydride. The THF and hexane were distilled under dinitrogen from potassium and then stored over molecular sieves, in ampoules stopped by Youngs' PTFE valves. The aHF was purified by vacuum transfer, dried by repetitive fluorination at room temperature and stored in Kel-F tubes over dry BiF_5. The methanol, DMSO and acetone were used as supplied.
The dichloromethane used on the metal vacuum line required a more rigorous drying method and additional purification. It was shaked with portions of concentrated H_2SO_4 until the acid layer remained colourless, followed by washing with water, aq. 5% Na_2CO_3 and then water again. The solvent was then predried over $CaCl_2$, distilled under dinitrogen from P_2O_5 and finally from CaH_2.
All the solvents were from BDH Ltd., Spectroscopic Grade, except aHF which was from Johnson Matthey.

8.7 Chemical Reagents:

Chemical	Source	Purification / Special storage
4-Bromoanisole	1	A
Trichlorophosphine, PCl_3	1	B
Ammonium chloride, NH_4Cl	5	A
Magnesium sulfate, $MgSO_4$	5	A
Hydrobromic acid, HBr	1	A
Sodium hydroxide, NaOH	5	A
Bis-acetonitrileplatinum-dichloride, $[PtCl_2(CH_3CN)_2]$	Prepared according to the literature route.[9]	C
Bis-acetonitrilepalladium-dichloride, $[PdCl_2(CH_3CN)_2]$	Prepared according to the literature route.[9]	C
Triethylphosphinechloro-platinumchloride bridged dimer, $[\{PtCl(\mu\text{-}Cl)(PEt_3)\}_2]$	Prepared according to the literature route.[10]	C
Methyllithium, MeLi	1	D
dicarbonylrhodiumchloride bridged dimer, $[\{Rh(CO)_2(\mu\text{-}Cl)\}_2]$	1	E
Pentamethylcyclopentadi-enylchlororhodium-chloride bridged dimer, $[\{Rh(\eta^5\text{-}C_5Me_5)(CO)(\mu\text{-}Cl)\}_2]$	1	A
2-Bromoanisol	1	A
Chlorodiphenylphosphine, PPh_2Cl	1	B
Anhydrous hydrofluoric acid, aHF	4	See Section 8.6
Fluorine gas, F_2	3	A
Potassium metal	6	A
Sodium metal	1	A

Chemical	Source	Purification / Special storage
Calciumhydride, CaH_2	1	A
Pentafluoridebismuth, BiF_5	4	F
Silvertetrafluoroborate, $AgBF_4$	1	A
Phosphoruspentoxide, P_2O_5	1	A
Triethylphosphine, PEt_3	1	B
Triphenylphosphine, PPh_3	2	F
Tricyclohexylphosphine, PCy_3	1	F
Tricarbonylfluoroosmium-fluoride bridged dimer, $[\{Os(CO)_3F(\mu\text{-}F)\}_2]$	Prepared according to the literature route.[8]	C
Tricarbonylfluoro-rutheniumfluoride bridged dimer, $[\{Ru(CO)_3F(\mu\text{-}F)\}_2]$	Prepared according to the literature route.[8]	C

(1) Aldrich Chemical Company Ltd.

(2) Lancaster Chemical Company Ltd.

(3) Fluorochem.

(4) Johnson Matthey.

(5) BDH, Laboratory Supplies.

(6) Fisons Laboratory reagent.

(A) used as supplied.

(B) stored in a glass ampoule fitted with a Youngs' tap and degassed prior to use.

(C) dried prior to use.

(D) used as supplied, stored in a firmly closed container at low temperature (ca. 5°C).

(E) used as supplied, stored in a closed container at low temperature (ca. 5°C).

(F) used as supplied, stored under dinitrogen.

8.8 Preparation of $P(4\text{-}CH_3OC_6H_4)_3$ (3):

The phosphine ligand (**3**) was prepared according to the literature[3] route with few modifications.

All procedures were performed under nitrogen. The first step in the synthesis of (**3**) was the preparation of the Grignard reagent (*p*-methoxyphenylmagnesiumbromide). 4-bromoanisole (25 g, 133.7 mmol) in dried THF (20 ml) was added dropwise into a three necked (250 ml) r.b.f. fitted with a reflux condenser containing Mg turnings (4 g, 164.5 mmol) stirring in dried THF (30 ml) with a couple of drops of 1,2-dibromoethane. The start of the reaction was detected by elevation of the temperature as a result of the exothermic reaction. To prevent a vigorous temperature elevation, the r.b.f. was kept in an ice bath during the 4-bromoanisole addition. The colour of the resulting solution was dark green. After the complete addition of the 4-bromoanisole, the solution was heated to reflux for an hour.

The Grignard reagent was then transfered *via* a cannular to a three necked r.b.f. (500 ml) containing dried THF (150 ml), ensuring that the excess of unreacted Mg turnings remained in the first flask. PCl_3 (3.89 ml, d 1.574) in THF (50 ml) was added dropwise to the solution while the r.b.f. was kept in an ice bath. The addition of the PCl_3, which took three hours, turned the solution to a clear green colour. The solution was stirred at room temperature overnight, during which its colour turned to dark red. A concentrated, degassed, aqueous solution of NH_4Cl was added to the mixture while the r.b.f. was kept in an ice bath. The colour of the solution went from dark red to green to yellow. The two phases were separated and the organic phase was dried over $MgSO_4$ for two hours. The solvent was then removed *in vacuo.* The ligand (**3**) was purified by washing with methanol at room temperature, and then dried *in vacuo.* The ligand (**3**) is air-sensitive in solution and is soluble in chloroform, dichloromethane, THF, toluene, methanol (at high temperature), and slightly soluble in ether. Yield 12.7 g, 81 %. δ ^1H NMR ($CDCl_3$) 7.22 (6H, dd, $^3J_{H\text{-}H}$ = 8 Hz, $^3J_{H\text{-}P}$ = 8 Hz, *ortho*-Ar.H), 6.80 (6H, d, $^3J_{H\text{-}H}$ = 8 Hz, *meta*-Ar.H), 3.79 (9H, s, CH_3O-) and δ $^{31}P\{^1H\}$ NMR ($CDCl_3$) -9.9 (s). Electron Impact mass Spectrum, m/z 352 ($[M]^+$), 337 ($[M - Me]^+$) and 322 ($[M - 2Me]^+$) (calculated $[M]^+$ = 352.12283, found $[M]^+$ = 352.12289).

Elemental Analysis, calculated: C 71.6 %, H 6.0 %, N 0.0 % and P 8.8 %, found: C 71.0 %, H 6.0 %, N < 0.3 % and P 9.1 %.

8.9 Preparation of $P(4\text{-}HOC_6H_4)_3$ (5):

The *tris*-(*p*-hydroxyphenyl)phosphine was prepared according to the literature route[3] with few modifications. The ligand (**3**) (2.43 g, 6.9 mmol) was dissolved in hydrobromic acid, HBr, (16 ml, d 1.49, 0.29 mol) under nitrogen and the resulting solution was heated to reflux overnight. The starting solution colour was clear yellow. The resulting solution showed the precipitation of a white solid which is the *tris*-(*p*-hydroxyphenyl)phosphine hydrobromide (**4**).Yield 1.9 g, 70 %. The hydrobromide salt was then washed with hexane and recrystallized from methanol-HBr (4.8 ml methanol + 0.3 ml HBr). δ ^{1}H NMR (MeOD) 7.20 (ddd, $^3J_{H\text{-}H}$ = 7 Hz, $^3J_{H\text{-}P}$ = 8 Hz, $^4J_{H\text{-}H}$ = 1 Hz, *ortho*-Ar.H), 6.80 (m, *meta*-Ar.H), 3.70 (bs, Ar.OH), δ ^{31}P{^{1}H} NMR (MeOD) 1.2 (s). The hydrobromide salt (1.67 g, 4.3 mmol) was solubilised in degassed 3% NaOH solution (50 ml), and the *tris*-(*p*-hydroxyphenyl)phosphine (**5**) was precipitated out of the solution by a dropwise addition of couple of milliliters of glacial acetic acid. The ligand (**5**) precipitated as a gummy white solid which was washed with water, then hexane and left under vacuum overnight. Recrystallisation from ether-hexane purified the ligand (**5**) which was dried *in vacuo* to yield 1.12 g, 84 %. δ ^{1}H NMR (d^6 acetone) 8.50 (bs, OH-), 7.00 (6H, dd, $^3J_{H\text{-}H}$ = 9 Hz, $^3J_{H\text{-}P}$ = 7 Hz, *ortho*-Ar.H), 6.70 (6H, dd, $^3J_{H\text{-}H}$ = 9 Hz, $^4J_{H\text{-}H(OH)}$ = 1 Hz *meta*-Ar.H), 3.20 (q, $^3J_{H\text{-}H}$ = 7 Hz, -CH_2-ether) and 0.94 (t, $^3J_{H\text{-}H}$ = 7 Hz, CH_3-ether). δ ^{31}P{^{1}H} NMR (d^6 acetone) -9.8 (s). δ ^{13}C{^{1}H} NMR (d^6 acetone) 159.33 (s, *para*-Ar.C), 136.17 (d, $J_{P\text{-}C}$ = 21 Hz, *ortho*-Ar.C), 129.33 (d, $J_{P\text{-}C}$ = 8 Hz, Ar.C-P) and 116.87 (d, $J_{P\text{-}C}$ = 8 Hz, *meta*-Ar.C). Electron Impact mass Spectrum, m/z calculated $[M]^+$ = 310.07588 , found $[M]^+$ = 310.07591.

8.10 Preparation of *cis*- (6) and *trans*-[$PtCl_2\{P(4\text{-}HOC_6H_4)_3\}_2$] (7):

Bis-(acetonitrile)dichloroplatinum(II) (0.196 g, 0.56 mmol) was dissolved with an excess of the ligand (**5**) (0.38 g, 1.22 mmol) in acetone (50 ml) in an r.b.f. (100 ml) fitted with a condenser. The solution was heated to reflux for two hours under nitrogen. The starting solution colour was green which went to clear after refluxing. The resulting solution was concentrated on the rotary evaporator to 10 ml, and the addition of hexane favoured the precipitation of a yellow-green solid. By fractional recrystallisation from acetone-hexane, two isomers were separated from the resulting product, and dried *in vacuo*: *cis*- and *trans*-[$PtCl_2\{P(4\text{-}HOC_6H_4)_3\}_2$].

cis-isomer (**6**): yield 0.060 g. δ ^{1}H NMR (d^6 acetone) 7.20 (12H, dd, $^3J_{H\text{-}H}$ = 8 Hz, $^3J_{H\text{-}P}$ = 9 Hz, *ortho*-Ar.H), 6.50 (12H, d, $^3J_{H\text{-}H}$ = 8 Hz, *meta*-Ar.H), 4.81 (s, Ar.OH) and 2.05 (b, acetone). δ $^{31}P\{^1H\}$ NMR (d^6 acetone) 11.4 (s, $^1J_{Pt\text{-}P}$ = 3762 Hz). FAB mass spectrum, m/z 886 ([M]$^+$), 851 ([M - Cl]$^+$) and 814 ([M - 2Cl]$^+$). Elemental Analysis of *cis*-[$PtCl_2\{P(4\text{-}HOC_6H_4)_3\}_2$].4$C_3H_6O$, calculated: C 51.53 % and H 4.86 %, found: C 51.55 % and H 5.45 %.

trans-isomer (**7**): yield 0.020 g. δ ^{1}H NMR (d^6 acetone) 8.75 (bs, Ar.OH), 7.40 (12H, dd, $^3J_{H\text{-}H}$ = 8 Hz, *ortho*-Ar.H), 6.75 (12H, d, $^3J_{H\text{-}H}$ = 8 Hz, *meta*-Ar.H) and 1.88 (m, acetone). δ $^{31}P\{^1H\}$ NMR (d^6 acetone) 16.9 (s, $^1J_{Pt\text{-}P}$ = 2598 Hz). FAB mass spectrum, m/z 886 ([M]$^+$), 850 ([M - Cl]$^+$) and 814 ([M - 2Cl]$^+$). Elemental Analysis, calculated: C 48.77 %, H 3.41 %, Cl 8.00 %, N 0.00 % and P 6.99 %, found: C 46.81 %, H 3.84 %, Cl 7.04 %, N < 0.3 % and P 6.13 %. Infrared (Nujol mull): 3408bs, 2830m, 1599s, 1580s, 1499w, 1467s, 1377s, 1271s, 1147s, 1096s, 825s, 530s, 475s, 462s, 453s and 345s cm^{-1}.

8.11 Preparation of [$PtCl\{P(4\text{-}HOC_6H_4)_3\}_3$]Cl (8):

The synthesis of complex (**8**) was achieved by starting from either complexes (**6**) and (**7**), or bis-(acetonitrile)dichloroplatinum(II). In the former case, the reaction was carried out by the reaction of complexes (**6**) and (**7**) with the ligand (**5**) in a 1:1

ratio. In the latter case, the reaction was carried out by the reaction of bis-(acetonitrile)dichloroplatinum(II) with the ligand (**5**) in a 1:3 ratio, respectively. The reactions in both cases were carried out in acetone heated to reflux, under nitrogen, for two hours. The resulting solution was concentrated on the rotary evaporator, to 10 ml. The addition of hexane brought about the precipitation of a creamy oil which solidified after drying under vacuum. The complex $[PtCl\{P(4\text{-}HOC_6H_4)_3\}_3]Cl$ (**8**) was a clear green solid, and was purified by recrystallisation from acetone-hexane. yield 60 %. δ ^1H NMR (MeOD) 7.14 (12H, dd, $^3J_{H\text{-}H}$ = 9 Hz, *ortho*-Ar.H *cis* to Cl), 7.00 (6H, dd, $^3J_{H\text{-}H}$ = 7 Hz, $^3J_{H\text{-}P}$ = 11 Hz, *ortho*-Ar.H *trans* to Cl), 6.56 (12H, d, $^3J_{H\text{-}H}$ = 9 Hz, *meta*-Ar.H *cis* to Cl), 6.35 (6H, d, $^3J_{H\text{-}H}$ = 7 Hz, *meta*-Ar.H *trans* to Cl), 4.77 (s, Ar.OH) and 3.19 (bs, methanol). δ $^{31}P\{^1H\}$ NMR (MeOD) 20.3 (2P, d, $^2J_{P\text{-}P}$ = 18 Hz, $^1J_{Pt\text{-}P}$ = 2483 Hz, P *cis* to Cl),) and 9.0 (1P, t, $^1J_{Pt\text{-}P}$ = 3701 Hz, P *trans* to Cl). FAB mass spectrum, m/z 1161 ($[M - Cl]^+$), 851 ($[M - L_2 - Cl]^+$) and 503 ($[M - 2L_2 - 2Cl]^+$). Infrared (Nujol mull) 3245bs, 1687w, 1600s, 1580s, 1500s, 1464s, 1378s, 1271s, 1231s, 1177s, 1097s, 827s, 650w, 641w, 532s, 523s, 498w, 474s, 463s, 449s, 424w and 317w cm^{-1}.

To make sure that the counter ion in (**8**) is Cl^-, analysis for chlorine was carried out: 6.68×10^{-5} mole of the complex (**6**) was dissolved in methanol, and analysed with 0.1M $AgNO_3$ aqueous solution. A white precipitate came down, which is $AgCl_{(s)}$. After adding a couple of drops of concentrated nitric acid to the solution, and more $AgNO_3$ solution, another quantity of $AgCl_{(s)}$ came down. Adding concentrated HNO_3 ensured that all the chlorine atoms are free in solution, in Cl^- form. The total mole number of precipitated $AgCl_{(s)}$ is 1.4×10^{-4} mole, which corresponds to two equivalents of chlorine in each one mole of (**6**).

8.12 Preparation of $[PtCl\{P(4\text{-}CH_3OC_6H_4)_3\}_3]Cl$ (9):

The synthesis of complex (**9**) was carried out by the reaction of bis-(acetonitrile)dichloroplatinum(II) with the ligand (**3**) in a 1:3 ratio, in dichloromethane. The solution was left stirring overnight, at room temperature. The result was a white mixture of two complexes: *cis*-$[PtCl_2\{P(4\text{-}CH_3OC_6H_4)_3\}_2]$ and

$[PtCl\{P(4\text{-}CH_3OC_6H_4)_3\}_3]Cl$ (**9**). At a certain stage, the conversion of the former to the latter complex stopped and the concentrations of both complexes reached an equilibrium in solution.

Complex $[PtCl\{P(4\text{-}CH_3OC_6H_4)_3\}_3]Cl$ (**9**): yield ca. 60 %. δ ^1H NMR ($CDCl_3$) 7.54-6.47 (m, Ar.H), 3.77 (9H, s, CH_3O- of the ligand (**3**) *trans* to Cl)) and 3.74 (18H, s, CH_3O- of the ligand (**3**) *cis* to Cl). δ $^{31}P\{^1H\}$ NMR ($CDCl_3$) 21.4 (2P, d, $^1J_{Pt\text{-}P}$ = 2469 Hz, $^2J_{P\text{-}P}$ = 18 Hz, P *cis* to Cl) and 10.1 (1P, t, $^1J_{Pt\text{-}P}$ = 3676 Hz, P *trans* to Cl). FAB mass spectrum, m/z 1287 ($[M - Cl]^+$), 1252 ($[M - 2Cl]^+$), 935 ($[M - Cl - L]^+$) and 899 ($[M - 2Cl - L]^+$), where L is the phosphine ligand.

Complex *cis*-$[PtCl_2\{P(4\text{-}CH_3OC_6H_4)_3\}_2]$: δ ^1H NMR ($CDCl_3$) 7.23 (6H, m, *ortho*-Ar.H), 6.50 (6H, d, $^3J_{H\text{-}H}$ = 8 Hz, *meta*-Ar.H) and 3.61 (9H, s, CH_3O-). δ $^{31}P\{^1H\}$ NMR ($CDCl_3$) 11.0 (s, $^1J_{Pt\text{-}P}$ = 3703 Hz).[4]

8.13 Preparation of *cis*-$[PtCl_2(PEt_3)\{P(4\text{-}CH_3OC_6H_4)_3\}]$ (10):

The dimer *sym.trans*-$[\{PtCl(\mu\text{-}Cl)(PEt_3)\}_2]$ (0.104 g, 0.136 mmol) was allowed to react with the phosphine ligand (**3**) (0.1 g, 0.27 mmol) in acetone (30 ml) heated to reflux for three hours, under nitrogen. The starting solution colour was green which turned to clear after refluxing. The resulting solution was concentrated on the rotary evaporator and the addition of petroleum ether brought about the precipitation of a white solid out of the solution. It was dried *in vacuo*. The white solid is a mixture of two products according to the NMR data. The main one is complex (**10**) and the by-product is the complex *cis*-$[PtCl_2\{P(4\text{-}CH_3OC_6H_4)_3\}_2]$ already described in Section 8.12. Yield ca. 30 %. δ ^1H NMR ($CDCl_3$) 8.00-6.70 (m, Ar.H), 3.80 (s, CH_3O-), 1.70 (m, CH_2-) and 1.10 (m, CH_3-). δ $^{31}P\{^1H\}$ NMR ($CDCl_3$) 9.0 (1P, d, $^1J_{Pt\text{-}P}$ = 3798 Hz, $^2J_{P\text{-}P}$ = 16 Hz, P of the ligand (**3**)) and 5.9 (1P, d, $^1J_{Pt\text{-}P}$ = 3430 Hz, P of PEt_3).

8.14 Preparation of *cis*-$[PtMe_2\{P(4\text{-}CH_3OC_6H_4)_3\}_2]$ (11):

Scrupulously anhydrous conditions need to be maintained throughout this reaction because of the high air-sensitivity of the methyl lithium (starting material). All the apparatus were heated to remove as much moisture as possible.

The complex *cis*-[$PtCl_2\{P(4\text{-}CH_3OC_6H_4)_3\}_2$] (0.15 g, 0.15 mmol) was allowed to react with a large excess of methyl lithium (0.033 g, 1.5 mmol) in dried THF (50 ml), under nitrogen, in a dry ice bath (-78°C). The yellow solution was then left stirring overnight, at room temperature. A concentrated aqueous NH_4Cl solution was added dropwise to the solution at 0°C. After adding the NH_4Cl solution, the solution colour turned clear. That indicated that the excess of methyl lithium had reacted with NH_4Cl. The organic phase was separated, and dried over $MgSO_4$ for two hours. The THF was removed *in vacuo*, and the resulting crystalline white product was recrystallised from dried DCM:dried hexane, filtered, then dried *in vacuo* to yield a clear translucent crystals. Yield 0.2 g, 76 %, δ ^1H NMR (CD_2Cl_2) 7.10 (12H, dd, $^3J_{H\text{-}H}$ = 9 Hz, $^3J_{H\text{-}P}$ = 9 Hz, *ortho*-Ar.H), 6.50 (12H, d, $^3J_{H\text{-}H}$ = 9 Hz, *meta*-Ar.H), 3.60 (18H, s, CH_3O-), 0.14 (6H, dd, $^3J_{P1\text{-}H}$ = 6.5 Hz, $^3J_{P2\text{-}H}$ = 6.7 Hz, $^2J_{Pt\text{-}H}$ = 75 Hz, CH_3 bound to platinum). δ $^{31}P\{^1H\}$ NMR (CD_2Cl_2) 24.4 (s, $^1J_{Pt\text{-}P}$ = 1932 Hz). FAB mass spectrum: m/z 914 ($[M - CH_3]^+$) and 898 ($[M - 2CH_3]^+$). Elemental Analysis, calculated: C 56.83 %, H 5.20 %, N 0.00 % and P 6.66 %, found: C 56.43 %, H 5.18 %, N < 0.3 % and P 7.26 %. Infrared (Nujol mull): 2875m, 1593s, 1567s, 1499s, 1404s, 1378s, 1290s, 1253s, 1175s, 1094s, 1031s, 652w, 641w, 635w, 625w, 533s, 508s and 425s cm^{-1}.

8.15 Reaction of cis-$[PdCl_2(CH_3CN)_2]$ with $P(4\text{-}HOC_6H_4)_3$ (5):

Bis-(acetonitrile)dichloropalladium(II) (0.081 g, 0.31 mmol) was dissolved with the ligand (**5**) (0.192 g, 0.62 mmol) in acetone (50 ml) in an r.b.f. (100 ml) fitted with a condenser, and refluxed for three hours under nitrogen. The starting solution colour was yellow, which remained unchanged throughout the refluxing. The resulting solution was concentrated on the rotary evaporator to 10 ml, and a yellow-orange oil deposited after the addition of hexane. This oil solidified after drying under vacuum. The main product was the dimer $[(L_2)_4Pd_2(\mu\text{-}Cl)_2]^{2+}$ (**12**). Yield 0.170 g, 68 %. δ ^1H NMR (d^6 acetone) 9.06 (bs, Ar.OH), 7.53 (m, *ortho*-Ar.H), 6.89 (d, $^3J_{H\text{-}H}$ = 9 Hz, *meta*-Ar.H), 3.00 (s, Ar.OH) and 2.07 (quintet, acetone). δ $^{31}P\{^1H\}$ NMR 20.1 (s) and smaller signals at 30.8 (bs) and 29.1 (bs).

Adding an excess of phosphine ligand (**5**) to the dimer (**12**) in acetone and in a 2:1 ratio and stirring the resulting solution for two hours, produced the monomer $[PdCl(L_2)_3]^+$ (**13**) as the main product, which was purified by recrystallisation from acetone:hexane. δ ^{1}H NMR (d^6 acetone) 7.14 (12H, dd, $^3J_{H-H}$ = 9 Hz, *ortho*-Ar.H *cis* to Cl), 6.97 (6H, dd, $^3J_{H-H}$ = 7 Hz, *ortho*-Ar.H *trans* to Cl), 6.56 (12H, d, $^3J_{H-H}$ = 9 Hz, *meta*-Ar.H *cis* to Cl), 6.35 (6H, d, $^3J_{H-H}$ = 7 Hz, *meta*-Ar.H *trans* to Cl) and 4.77 (s, Ar.OH). δ $^{31}P\{^1H\}$ NMR (d^6 acetone) 30.5 (1P, t, $^2J_{P-P}$ = 14 Hz, P *trans* to Cl) and 26.6 (2P, d, P *cis* to Cl). Infrared (Nujol mull): 3425bs, 1596s, 1574s, 1560w, 1540w, 1499s, 1272s, 1211s, 1119w, 1008w, 826s, 648w, 641w, 527s, 492w, 473w, 457w and 446w cm^{-1}.

8.16 Preparation of *trans*-$[Rh(CO)Cl\{P(4\text{-}HOC_6H_4)_3\}_2]$ (14):

The dimer $[\{Rh(CO)_2(\mu\text{-}Cl)\}_2]$ (0.101 g, 0.26mmol) was allowed to react with the ligand $P(4\text{-}HOC_6H_4)_3$ (**5**) (0.322 g, 1 mmol) in a 1:4 ratio, respectively, in acetone (50 ml) heated to reflux for two hours under nitrogen. The starting solution colour was yellow, which remained unchanged throughout the reaction. The acetone was removed *in vacuo* to yield the product as an air-sensitive yellow powder. Yield 0.3 g, 75 %, δ ^{1}H NMR (d^6 acetone) 8.93 (bs, OH), 7.60 (m, *ortho*-Ar.H), 6.93 (m, *meta*-Ar.H) and 2.13 (s, acetone). δ $^{31}P\{^1H\}$ NMR (d^6 acetone) 24.9 (d, $^1J_{Rh-P}$ = 123 Hz). Electron Impact mass spectrum, m/z 758 ($[M - CO]^+$) and 723 ($[M - CO - Cl]^+$). Infrared (Nujol mull): 3144b, 1980s, 1697s, 1602s, 1588s, 1499s, 1282m, 1267m, 1225m, 1178m, 833s, 660s, 565s and 536s cm^{-1}.

8.17 Preparation of $[Rh(\eta^5\text{-}C_5Me_5)Cl_2\{P(4\text{-}CH_3OC_6H_4)_3\}]$ (15):

The dimer $[\{Rh(\eta^5\text{-}C_5Me_5)Cl(\mu\text{-}Cl)\}_2]$ (0.094 g, 0.151 mmol) was allowed to react with the phosphine ligand (**3**) (0.12 g, 0.34 mmol) in a 1:2 ratio in dichloromethane (50 ml) heated to reflux for three hours under nitrogen. The starting solution colour was dark red which remained unchanged throughout the reaction. The solvent was removed on the rotary evaporator. The resulting product was an orange crystalline solid which was purified by recrystallization from dichloromethane:hexane,

and dried *in vacuo*. Yield 0.18 g, 90 %, δ ^{1}H NMR (CD_2Cl_2) 7.60 (6H, dd, *ortho*-Ar.H), 6.70 (6H, m, *meta*-Ar.H) 5.20 (s, dichloromethane), 3.70 (9H, s, CH_3O-) and 1.30 (15H, d, J_{P-H} = 3 Hz, H (C_5Me_5)). δ $^{31}P\{^1H\}$ NMR (CD_2Cl_2) 27.3 (d, $^1J_{Rh-P}$ = 143 Hz). FAB mass spectrum, m/z 625 ($[M - Cl]^+$) and 590 ($[M - 2Cl]^+$), calculated $[M]^+$ = 625.11457 , found $[M]^+$ = 625.11476. Elemental Analysis, calculated: C 51.50 %, H 5.13 % and N 0.00 %, found: C 51.91 %, H 5.13 % and N < 0.3 %. Infrared (Nujol mull), 1594s, 1499s, 1254s, 1182s, 1178s, 1023s, 840s, 831s, 799s, 651w, 626w and 528w cm^{-1}.

8.18 Preparation of $[Rh(\eta^5\text{-}C_5Me_5)Cl_2\{P(4\text{-}HOC_6H_4)_3\}]$ (16):

The dimer $[\{Rh(\eta^5\text{-}C_5Me_5)Cl(\mu\text{-}Cl)\}_2]$ (0.199 g, 0.323 mmol) was allowed to react with the phosphine ligand (**5**) (0.2 g, 0.65 mmol) in a 1:2 ratio in acetone (50 ml) heated to reflux for two hours under nitrogen. The starting solution colour was dark red, which turned slightly brighter on heating. The acetone was removed on the rotary evaporator, and the solid was dried *in vacuo*. The final product was an orange solid, and was found to be soluble solely in dimethylsulfoxide (DMSO). Yield 0.36 g, 90 %, δ ^{1}H NMR (d^6 DMSO) 9.87 (bs, OH), 7.35 (6H, dd, $^3J_{H-H}$ = 9 Hz, *ortho*-Ar.H), 6.64 (6H, m, *meta*-Ar.H), 1.08 (15H, d, J_{P-H} = 3 Hz, H(C_5Me_5)). δ $^{31}P\{^1H\}$ NMR (d^6 DMSO) 29.0 (d, $^1J_{Rh-P}$ = 144 Hz). Electron Impact mass spectrum, m/z 583 ($[M - Cl]^+$), 548 ($[M - 2Cl]^+$) and 237 ($[M - L_2 - 2Cl - 2H]^+$). Elemental Analysis, calculated: C 54.30 %, H 4.88 %, Cl 11.45 %, N 0.00 % and P 5.00 %, found: C 53.68 %, H 4.89 %, Cl 10.92 %, N < 0.3 % and P 4.08 %. Infrared (Nujol mull), 3292bs, 1600s, 1586s, 1574s, 1500s, 1418w, 1273s, 1231s, 1220s, 1204s, 1175s, 1015s, 947w, 855s, 833s, 805s, 668w, 660w, 640w, 621w, 586w, 537s, 516s, 480s, 459s, 440s, 435s, 421s, 402s, 289s and 286s cm^{-1}.

8.19 Preparation of $P(2\text{-}CH_3OC_6H_4)_3$ (17) and $PPh_2(2\text{-}CH_3OC_6H_4)$ (18):

The synthesis of the ligands (**17**) and (**18**) followed the same steps as in the synthesis of the ligand (**3**) (Section 8.8).[3] However, the 2-bromoanisole was used in both cases instead of the 4-bromoanisole used in the case of preparation of ligand (**3**).

Subsequently, PCl_3 was used in the preparation of the ligand (**17**), whilst PPh_2Cl was used in the preparation of the ligand (**18**). The phosphine ligands (**17**) and (**18**) were purified by washing with methanol at -78°C and at room temperature respectively. Both ligands were then dried *in vacuo*.

Characterisation of the ligand (**17**): Yield 20.0 g, 85 %. δ ^{1}H NMR ($CDCl_3$) 7.20 (6H, m, Ar.H), 6.70 (6H, m, Ar.H) and 3.70 (9H, s, CH_3O-). δ $^{31}P\{^1H\}$ NMR ($CDCl_3$) -39.3 (s). Electron Impact mass spectrum, m/z 352 ($[M]^+$), 321 ($[M - CH_3O]^+$) and 290 ($[M - 2CH_3O]^+$) (calculated $[M]^+ = 352.12283$, found $[M]^+ = 352.12280$).

Characterisation of the ligand (**18**): yield 14.7 g, 76 %. δ ^{1}H NMR ($CDCl_3$) 7.30 (11H, m, 1H on the *ortho* position of the substituted aryl ring and 10H of the non-substituted aryl rings), 6.88 (2H, m, *meta*-Ar.H of the substituted aryl ring), 6.66 (1H, m, *para*-Ar.H of the substituted aryl ring) and 3.75 (3H, s, CH_3O-). δ $^{31}P\{^1H\}$ NMR ($CDCl_3$) -16.9 (s). FAB mass spectrum, m/z 292 ($[M]^+$), 261 ($[M - CH_3O]^+$). Elemental Analysis, calculated: C 78.07 %, H 5.86 %, N 0.00 % and P 10.59 %, found: C 76.83 %, H 5.60 %, N < 0.3 % and P 9.48 %.

8.20 Reaction of $[PtCl_2(CH_3CN)_2]$ with $P(2\text{-}CH_3OC_6H_4)_3$:

The reaction of the platinum(II) complex $[PtCl_2(CH_3CN)_2]$ (0.255 g, 0.73 mmol) with two equivalents of the phosphine ligand (**17**) (0.514 g, 1.46 mmol), in dichloromethane and at room temperature, afforded one main platinum(II) phosphine complex:

Unsym.*cis*-$[Pt_2(\mu\text{-}Cl)_2Cl_2\{P(2\text{-}CH_3OC_6H_4)_3\}_2]$ (**19**). Yield ca. 55 %. δ ^{1}H NMR (CD_2Cl_2) 8.00 - 6.50 (m, Ar.H), 5.26 (s, dichloromethane) and 3.40 (bs, CH_3O-). δ $^{31}P\{^1H\}$ NMR ($CDCl_3$) 11.0 (s, $^1J_{Pt\text{-}P} = 2814$ Hz). Electron Impact mass spectrum, m/z 1199 ($[M - Cl]^+$) and 1164 ($[M - 2Cl]^+$). Infrared (Nujol mull), 1579s, 1250w, 1203w, 1150w, 1021s, 891w, 797s, 662s, 561s, 516s, 501s, 491s, 467s, 427s.

A conversion was observed in dichloromethane solution from the unsymmetrical *cis* configuration to the symmetrical *trans* one, complex (**20**). This affected the $^{31}P\{^1H\}$ NMR data. The correspondent new signal was at -10.4 ppm (s, $^1J_{Pt\text{-}P} = 4240$ Hz). The experiment was run in CD_2Cl_2.

8.21 Preparation of *trans*-$[PtCl_2\{P(2\text{-}CH_3OC_6H_4)Ph_2\}_2]$ (21):

Bis-(acetonitrile)dichloroplatinum(II) (0.123 g, 0.35 mmol) was dissolved with the ligand (**18**) (0.21 g, 0.7 mmol) in dichloromethane (50 ml) in a Schlenk flask (100 ml). The solution was stirred overnight under nitrogen. The starting solution colour was clear yellow which remained unchanged during the reaction. The resulting solution was concentrated on the rotary evaporator to 10 ml, and the addition of hexane resulted in the precipitation of yellow crystals. Yield 1.965g, 67 %. δ ^{1}H NMR (CD_2Cl_2) 7.80-6.80 (14H, m, Ar.H), 5.25 (s, dichloromethane) and 3.70 (3H, s, CH_3O-). δ $^{31}P\{^1H\}$ NMR (CD_2Cl_2) 15.1 (s, $^1J_{Pt\text{-}P}$ = 2716 Hz). FAB mass spectrum, m/z 850 ($[M]^+$), 815 ($[M - Cl]^+$) and 779 ($[M - 2Cl]^+$). Elemental Analysis, calculated: C 53.6 %, H 4.03 %, Cl 8.34 %, N 0.00 % and P 7.28 %, found: C 53.27 %, H 3.68 %, Cl 8.77 %, N < 0.3 % and P 7.10 %. Infrared (Nujol mull), 1584w, 1462s, 1315w, 1307w, 1281w, 1273w, 1243w, 1183w, 1157w, 1074w, 1044w, 1020s, 999w, 850w, 793s, 771s, 764s, 755s, 744s, 696s, 686s, 576s, 550s, 523s, 511s, 494s, 476s, 435w, 413w and 338w cm^{-1}.

8.22 Preparation of $[Rh(\eta^5\text{-}C_5Me_5)Cl_2\{P(2\text{-}CH_3OC_6H_4)Ph_2\}]$ (22):

The dimer $[\{Rh(\eta^5\text{-}C_5Me_5)Cl(\mu\text{-}Cl)\}_2]$ (0.154 g, 0.25 mmol) was dissolved with the ligand (**18**) (0.143 g, 0.49 mmol) in dichloromethane (50 ml) in a Schlenk flask (100 ml). The solution was stirred overnight under nitrogen. The resulting product was a dark red-brown powder. Yield 0.237 g, 79 %. δ ^{1}H NMR ($CDCl_3$) 8.15 (1H, m, *meta*-Ar.H of the substituted ring), 7.85 (4H, dd, *ortho*-Ar.H of the non-substituted ring), 7.51 (1H, m, *ortho*-Ar.H of the substituted ring), 7.30 (6H, m, *meta* and *para*-Ar.H of the non-substituted ring), 7.10 (1H, m, *para*-Ar.H of the substituted ring), 6.83 (1H, dd, *meta*-Ar.H of the substituted ring (at the same time *para* to the methoxy group)), 3.30 (3H, s, CH_3O-) and 1.34 (15H, d, $J_{H\text{-}H(Cp^*)}$ = 3 Hz, Cp* protons). δ $^{31}P\{^1H\}$ NMR 28.4 (d, $^1J_{Rh\text{-}P}$ = 142 Hz). FAB mass spectrum, m/z 565 ($[M - Cl]^+$) and 530 ($[M - 2Cl]^+$). Elemental Analysis, calculated: C 57.92 %, H 5.36 %, and N 0.00 %, found: C 57.03 %, H 5.09 % and N < 0.3 %. Infrared (Nujol mull), 1586s, 1460s, 1277s, 1255s, 1188w, 1181s, 1160s, 1157s, 1086s, 1069w, 1047w,

1022s, 998w, 866w, 860w, 804s, 759s, 756s, 749s, 732w, 698s, 673w, 583s, 546w, 528s, 508s, 487s, 477s, 444s and 413w cm^{-1}.

8.23 Preparation of $P(2\text{-}HOC_6H_4)_3$ (23):

The *tris*-(*o*-methoxyphenyl)phosphine (1.1 g, 3.12 mmol) was dissolved in degassed hydrobromic acid HBr (15 ml, d 1.49, 0.27 mol) under nitrogen, the solution was heated to reflux overnight. The starting solution colour was yellow-orange. The resulting solution exhibited, at low temperature, the precipitation of a white solid which was the *tris*-(*o*-hydroxyphenyl)phosphine hydrobromide. Yield 1.1 g, 90 %.
The hydrobromide salt was then washed with dried and degassed hexane. The hydrobromide salt (1.67 g, 4.3 mmol) was solubilised in degassed 3% NaOH solution (50 ml), and the free *tris*-(o-hydroxyphenyl)phosphine was precipitated out of the solution by a dropwise adding of a degassed acetic acid glacial.
The *o*-hydroxy-substituted arylphosphine ligand was purified by recrystallisation from degassed and dried ether:hexane solvents, followed by drying *in vacuo* to yield 0.95 g, 71 %. δ ^1H NMR (in diethylether, the lock-solvent is $CDCl_3$) 8.40 (b.s., HO-), 7.80 (1H, m, *meta*-Ar.H (at the same time *ortho* to the hydroxy group)), 7.60 (1H, m, *ortho*-Ar.H) and 7.4 (2H, m, *meta*- and *para*-Ar.H). δ $^{31}P\{^1H\}$ NMR (in diethylether, the lock-solvent is $CDCl_3$) -49.0 (s.). Electron Impact mass spectrum, m/z 310 ($[M]^+$) and 293 ($[M - OH]^+$), (calculated $[M]^+ = 310.07588$, found $[M]^+ = 310.07581$).

8.24 Preparation of $[Pt\{\kappa^2\text{-}P(2\text{-}OC_6H_4)(2\text{-}HOC_6H_4)_2\}_2]$ (24):

The *bis*-(acetonitrile)platinumdichloride $[PtCl_2(CH_3CN)_2]$ (0.064 g, 0.185 mmol) was treated, at room temperature, with *tris*-(*o*-hydroxyphenyl)phosphine(0.115 g, 0.371 mmol), in dichloromethane (50 ml) and under nitrogen. The mixture was left stirring overnight. The resulting solution was clear translucent. The solvent was separated *in vacuo*, and the white solid product was hardly soluble in any solvent, except in dimethylsulfoxide (DMSO). Yield 0.110 g, 70 %. δ ^1H NMR (d^6 DMSO) 7.80 - 6.30 (m., Ar.H), 3.85 (b.s., HO-), 2.52 (s, DMSO). δ $^{31}P\{^1H\}$ (d^6 DMSO) 23.6 (bs, $^1J_{Pt\text{-}P} = 2887$ Hz). FAB mass spectrum, m/z 855 ($[M + CH_3CN]^+$) and 814 ($[M]^+$),

assuming that three coordination sites on the platinum(II) centre are occupied by two phosphine ligands, one is chelating, the other is not. The fourth coordination site is occupied by an acetonitrile molecule. Infrared (Nujol mull), 3408bs, 1587s, 1297s, 1262s, 1221s, 1159w, 1017s, 946w, 905w, 854w, 833w, 799s, 750s, 701w, 689w, 560s, 542s, 520s, 509s, 487s and 401s cm^{-1}.

8.25 Preparation of $[Pt(S)\{\kappa^2\text{-}P(2\text{-}OC_6H_4)(2\text{-}HOC_6H_4)_2\}\{P(2\text{-}HOC_6H_4)_3\}]$ (25) and $[Pt(S)_2\{P(2\text{-}HOC_6H_4)_3\}_2]$ (26):

A single crystal was isolated from the NMR experiment solution of complex (**24**), and structurally characterised by X-Ray diffraction studies as $[Pt\{\kappa^2\text{-}P(2\text{-}OC_6H_4)(2\text{-}HOC_6H_4)_2\}_2]$. The isolated crystals' colour was clear yellow. However, when dissolved in deuterated chloroform, the solution colour turned to dark orange. The proposed products were: $[Pt(DMSO)\{\kappa^2\text{-}P(2\text{-}OC_6H_4)(2\text{-}HOC_6H_4)_2\}\{P(2\text{-}HOC_6H_4)_3\}]$ (**25**) and $[Pt(DMSO)_2\{P(2\text{-}HOC_6H_4)_3\}_2]$ (**26**). Both products were characterised by the following data: δ ^1H NMR (d^6 DMSO) 9.75, 9.29, and 8.91 (b.s., HO-groups in three different chemical environments), 7.54-6.57 (m, Ar.H) and 3.46 (bs, coordinated DMSO). δ $^{31}P\{^1H\}$ NMR (d^6 DMSO) 21.3 (d, $^2J_{Pt\text{-}P}$ = 387 Hz, P of the chelating phosphine ligand in complex (**25**)), 10.7 (d, $^2J_{Pt\text{-}P}$ = 387 Hz, P of the un-chelating phosphine ligand in complex (**25**)) and 15.6 (s, $^1J_{Pt\text{-}P}$ = 2742 Hz, P in complex (**26**)).

8.26 Preparation of $[Rh(\eta^5\text{-}C_5Me_5)Cl_2\{\kappa^2\text{-}P(2\text{-}OC_6H_4)(2\text{-}HOC_6H_4)_2\}]$ (29):

The mixture of the dinuclear rhodium(III) complex $[\{Rh(\eta^5\text{-}C_5Me_5)Cl(\mu\text{-}Cl)\}_2]$ (0.043 g, 0.08 mmol) and two equivalents of $P(2\text{-}HOC_6H_4)_3$ (0.05 g, 0.16 mmol) were stirred in dichloromethane (20 ml), at room temperature and under nitrogen. The colour of the solution went from dark red to dark orange after one hour and a half, then to orange after leaving it stirring overnight. Yield 0.090 g, 96 %. NMR experiments were run on a sample taken from the resulting dichloromethane solution. δ ^1H NMR ($CDCl_3$) 8.29 (bs, HO-), 7.54-6.67 (m, Ar.H) and 1.28 ($J_{P\text{-}H}$ = 3.5

Hz). δ $^{31}P\{^{1}H\}$ NMR ($CDCl_3$) 19.5 ($^{1}J_{Rh-P}$ = 137 Hz). FAB mass spectrum, m/z 547 ($[M - Cl]^+$). Infrared (Nujol mull), 3396bs, 1589s, 1294s, 1255w, 1221w, 1025w, 836s, 754s, 565s, 522s, 502s, 482s and 459w cm^{-1}.

8.27 Reaction of $[\{Rh(\mu\text{-}Cl)(CO)_2\}_2]$ with $P(2\text{-}HOC_6H_4)_3$:

The dinuclear rhodium(I) complex $[\{Rh(\mu\text{-}Cl)(CO)_2\}_2]$ (0.063 g, 0.16 mmol) was treated with two equivalents of $P(2\text{-}HOC_6H_4)_3$ (0.1 g, 0.32 mmol) in dichloromethane (50 ml), at room temperature and under nitrogen. The solution was left stirring overnight. A white solid precipitated out. It was thought to be the $[Rh(CO)\{\kappa^2\text{-}P(o\text{-}OC_6H_4)(o\text{-}HOC_6H_4)_2\}\{ P(2\text{-}HOC_6H_4)_3\}]$ (**30**). Yield 0.216 g, 90 %. δ ^{1}H NMR (d^6-acetone) 11.72 and 10.68 (s., HO-), 9.77 and 9.21 (bs, HO-), 7.64-6.29 (m, Ar.H), 5.49 (s, dichloromethane) and 2.77 (bs, HO-). δ $^{31}P\{^{1}H\}$ NMR (d^6-acetone) 41.6 (dd, $|^{1}J_{Rh-P}|$ = 93 Hz, $^{2}J_{P-P}$ = 472 Hz) and 34.7 (dd, $|^{1}J_{Rh-P}|$ = 93 Hz, $^{2}J_{P-P}$ = 472 Hz). FAB mass spectrum, m/z 721 ($[M - CO]^+$). Infrared (Nujol mull), 3456bs, 2082s, 1582s, 1556w, 1265w, 1225w, 1126w, 1026w, 848s, 798s, 747s, 565s, 536s, 516s, 500s, 483s and 465s cm^{-1}.

8.28 Preparation of $PPh_2(2\text{-}C_2H_3C_6H_4)$ (31):

The preparation of the *ortho*-styryldiphenylphosphine ligand followed a similar route to that of the (*ortho*-methoxyphenyl)diphenylphosphine ligand (**18**). However, instead of the 2-bromoanisole, the 2-bromostyrene was used as the starting material. The purification of the final product was achieved by a quick wash with methanol at -78°C. The characterisation data obtained in this work concur with data already published in the literature.[6,7]

8.29 Preparation of $[Pt\{\kappa^2\text{-}(C_2H_3C_6H_4)PPh_2\}Cl_2]$ (32):

The *bis*-(acetonitrile)platinumdichloride $[PtCl_2(CH_3CN)_2]$ (0.188 g, 0.54 mmol) was treated, at room temperature, with *ortho*-styryldiphenylphosphine (0.156

g, 0.54 mmol), in dichloromethane (50 ml) and under nitrogen. The starting solution colour was clear green. The mixture was left stirring for two days. The colour of the solution remained unchanged throughout the experiment. The solvent was separated *in vacuo*, and the white solid product was analysed. Yield 0.170 g, 57 %. δ ^{1}H NMR ($CDCl_3$) 7.92-7.25 (m., Ar.H), 5.98 (dd, J_{H1-H2} = 8 Hz, J_{H1-H3} = 13 Hz and J_{H1-Pt} = 62 Hz, H_1), 5.30 (s, dichloromethane), 5.22 (dd, J_{H1-H2} = 8 Hz, J_{H3-H2} < 0.5 Hz and J_{H2-Pt} = 70 Hz, H_2) and 3.58 (ddd, J_{H3-P} = 3 Hz, J_{H3-H1} = 13 Hz, J_{H3-H2} < 0.5 Hz and J_{H3-Pt} = 55 Hz, H_3). δ ^{31}P{^{1}H} ($CDCl_3$) 23.6 (s, $^{1}J_{Pt-P}$ = 3234 Hz). FAB mass spectrum, m/z 554 ($[M]^+$), 519 ($[M - Cl]^+$) and 482 ($[M - 2Cl]^+$). Elemental Analysis, calculated: C 43.33 %, H 3.09 %, Cl 12.79 %, N 0.00 % and P 5.59 %, found: C 41.89 %, H 3.02 %, Cl 13.35 %, N < 0.3 % and P 5.28 %. Infrared (Nujol mull), 1582s, 1481w, 1437s, 1434w, 1335w, 1330w, 1280w, 1256s, 1220s, 1191s, 1186s, 1166s, 1161s, 1137s, 1106s, 1076s, 1024s, 1007s, 997s, 984w, 966s, 950w, 874s, 830s, 789s, 757s, 751s, 748s, 739w, 708s, 691s, 684w, 598s, 562s, 541s, 534s, 507s, 502s, 462w, 448w, 429w, 342w, 334w and 302w cm^{-1}.

8.30 Preparation of $[Rh(\eta^5\text{-}C_5Me_5)Cl_2\{(PPh_2C_2H_3C_6H_4)\}]$ (33):

The mixture of the dinuclear rhodium(III) complex $[\{Rh(\eta^5\text{-}C_5Me_5)Cl(\mu\text{-}Cl)\}_2]$ (0.171 g, 0.277 mmol) and two equivalents of the *ortho*-styryldiphenylphosphine (0.160 g, 0.55 mmol) were stirred in dichloromethane (50 ml), at room temperature and under nitrogen. The colour of the solution (dark red) remained the same throughout the reaction, when it was stirred overnight. Yield 0.276 g, 84 %. δ ^{1}H NMR (CD_2Cl_2) 7.69-7.27 (m, Ar.H) 6.89 (dd, J_{H1-H2} = 11 Hz and J_{H1-H3} = 17 Hz, H_1), 5.46 (dd, J_{H3-H2} < 1 Hz and J_{H3-H1} = 17 Hz, H_3), 4.83 (dd, J_{H2-H1} = 11 Hz and J_{H2-H3} < 1 Hz, H_2) and 1.27 (d, $J_{P-H(Cp^*)}$ = 1.3 Hz). δ ^{31}P{^{1}H} NMR (CD_2Cl_2) 32.6 (d, $^{1}J_{Rh-P}$ = 143 Hz). ES mass spectrum, m/z 561 ($[M - Cl]^+$) and 525 ($[M - 2Cl]^+$). Elemental Analysis, calculated: C 60.32 %, H 5.40 %, Cl 11.87 %, N 0.00 % and P 5.18 %, found: C 60.24 %, H 5.42 %, Cl 11.05 %, N < 0.3 % and P 4.03 %. Infrared (Nujol mull), 1623w, 1588s, 1535s, 1209w, 1194w, 1082s, 1131w, 1092s, 1082w, 1027s, 1005w, 916s, 715s - 692s cm^{-1}.

8.31 Preparation of $[Rh(\eta^5\text{-}C_5Me_5)Cl\{\kappa^2\text{-}(C_2H_3C_6H_4)PPh_2\}][BF_4]$ (34):

The complex $[Rh(\eta^5\text{-}C_5Me_5)Cl_2\{(PPh_2C_2H_3C_6H_4)\}]$ (**33**) (0.037 g, 0.0617 mmol) was allowed to react with $AgBF_4$ (0.012 g, 0.0617 mmol) in dichloromethane (10 ml) and at room temperature. The start of the reaction was detected by the precipitation of a white solid thought to be AgCl. The solution was stirred for three hours followed by a filtration. The solvent was taken off on the rotary evaporator. The complex (**34**) had an orange colour and it was characterised. Yield 0.035 g, 87 %. δ ^{1}H NMR (CD_2Cl_2) 7.78-7.21 (m, Ar.H) 6.38 (dd, $J_{H1\text{-}H2}$ = 9 Hz and $J_{H1\text{-}H3}$ = 14 Hz, H_1), 4.76 and 4.52 (bs, H_2 and H_3) and 1.54 (d, $J_{P\text{-}H(Cp^*)}$ = 3 Hz). δ $^{31}P\{^1H\}$ NMR (CD_2Cl_2) 50.3 (bd, $^1J_{Rh\text{-}P}$ = 122 Hz). δ ^{19}F NMR (CD_2Cl_2) -152.7 (s, BF_4^-). FAB mass spectrum, m/z 561 ($[M - BF_4]^+$) and 526 ($[M - BF_4 - Cl]^+$). Infrared (Nujol mull), 1850s - 1492s, 1250s, 1062s, 1021s, 797s, 750w, 691w, 656w, 568s - 433s cm^{-1}.

8.32 Preparation of $[Pt_2(\mu\text{-}F)_2\{P(4\text{-}CH_3OC_6H_4)_3\}_4][HF_2]_2$ (35):

The *cis*-[*tris*-(*p*-methoxyphenyl)phosphine]dimethyl-platinum(II) complex (**11**) (0.050 g, 0.052mmol) was loaded, under nitrogen (in a dried box), into a passivated FEP tube, which was then transfered to the metal line along with a Kel-F tube containing anhydrous HF. All the connections were then passivated. The aHF was transfered to the tube containing the complex (**11**) by condensation; whilst the temperature of the FEP tube was taken down to -196°C, the aHF was condensed under vacuum. After adding ca. 0.5 ml of aHF (d 0.97), the solution was warmed to room temperature, at which point the complex (**11**) was completely dissolved in the solution. The start of the reaction was evidenced by methane gas evolution. The methane gas was eliminated by evacuating the tube after freezing down the solution. The addition of the aHF was stopped when the methane evolution ceased upon the addition of an excess of aHF. The resulting solution colour was dark orange. The aHF was subsequently removed by pumping slowly through the rough pump by judicious cooling of the FEP tube in liquid nitrogen. The resulting product was a bright yellow solid. It was dissolved in dried DCM (enough volume for the NMR experiments),

frozen in liquid nitrogen whilst under vacuum, and the FEP tube was sealed by heat moulding using a small ring oven. The tube is kept at -196°C to avoid the risk of the decomposition of the product at higher temperatures. NMR experiments were run on the sample, δ ^{1}H NMR (d^6 acetone, used as the lock substance) 10.97 (bs, HF_2^-), 6.20 (m, *ortho*-Ar.H), 5.70 (d, $^{3}J_{H\text{-}H}$ = 8Hz, *meta*-Ar.H), 4.27 (s, CH_2Cl_2), 2.70 (s, CH_3O-). δ ^{31}P{^{1}H} NMR (d^6 acetone) 2.9 (s, $^{1}J_{P\text{-}Pt}$ = 3763 Hz). δ ^{195}Pt NMR (d^6 acetone) -4061 (t, $^{1}J_{P\text{-}Pt}$ = 3778 Hz). δ ^{19}F{^{1}H} NMR (d^6 acetone, at -20°C) -257 (s, $^{1}J_{Pt\text{-}P}$ = ca. 262 Hz).

In the next sections (8.34-8.37), the same experimental procedures were followed. Either two drops of a liquid phosphine or two milligrams of a solid phosphine, were added to a DCM NMR solution of the dimer (**35**) in an FEP tube, inside a dry box. The reaction routes are depicted in Chapter Six. The resulting solution was frozen, the reaction vessel evacuated, and then sealed and kept at -196°C to avoid the risk of decomposition at higher temperatures. NMR experiments were run on the sample.

8.33 Preparation of *trans*-[PtF(PEt$_3$){P(4-CH$_3$OC$_6$H$_4$)$_3$}$_2$][HF$_2$] (36):

The starting solution colour was yellow. It turned to bright yellow after adding PEt_3. δ ^{1}H NMR (d^6 acetone, used as the lock substance) 10.93 (bs, HF_2^-), 6.25 (dd, *ortho*-Ar.H), 5.90 (d, *meta*-Ar.H), 4.35 (s, CH_2Cl_2), 1.0 (m, CH_2- of coordinated PEt_3), 0.4 (m, CH_2- of free PEt_3), 0.2 (m, CH_3- of coordinated PEt_3), 0.0 (m, CH_3- of free PEt_3). δ ^{31}P{^{1}H} NMR (d^6 acetone) 25.0 (2P, dd, $^{2}J_{P\text{-}P}$ = 19.2 Hz, $^{2}J_{P\text{-}F}$ = 32.0 Hz, $^{1}J_{P\text{-}Pt}$ = 2361 Hz, P of P(4-$CH_3OC_6H_4$)$_3$), 0.7 (1P, dt, $^{2}J_{P\text{-}P}$ = 18.7 Hz, $^{2}J_{P\text{-}F}$ = 140.7 Hz, $^{1}J_{P\text{-}Pt}$ = 3391 Hz, P of PEt_3), -10.0 (s, free ligand P(4-$CH_3OC_6H_4$)$_3$). δ ^{19}F{^{1}H} NMR (d^6 acetone) -169.8 (s, HF_2^-), -254.2 (dt, $^{2}J_{F\text{-}transP}$ = 141 Hz, $^{2}J_{F\text{-}cisP}$ = 32 Hz, $^{1}J_{F\text{-}Pt}$ = 246 Hz).

8.34 Preparation of *cis*-[PtF(PPh$_3$){P(4-CH$_3$OC$_6$H$_4$)$_3$}$_2$][HF$_2$] (37):

δ ^{1}H NMR (d^6 acetone) 6.25 (dd, *ortho*-Ar.H), 5.60 (d, *meta*-Ar.H), 4.25 (s, CH_2Cl_2). δ ^{31}P{^{1}H} NMR (d^6 acetone) 23.6 (2P, ddd, $^2J_{P\text{-}cisP}$ = 16 Hz, $^2J_{P\text{-}transP}$ = 405 Hz, $^2J_{P\text{-}F}$ = 32 Hz, $^1J_{P\text{-}Pt}$ = 2608 Hz, P of P(4-CH$_3$OC$_6$H$_4$)$_3$ and PPh$_3$), -0.85 (1P, dt, $^2J_{P\text{-}P}$ = 20 Hz, $^2J_{P\text{-}F}$ = 146 Hz, $^1J_{P\text{-}Pt}$ = 3693 Hz, P of P(4-CH$_3$OC$_6$H$_4$)$_3$ *trans* to F). δ ^{19}F{^{1}H} NMR (d^6 acetone) -169.8 (s, HF_2^-), -229.5 (dt, $^2J_{F\text{-}cisP}$ = 38 Hz, $^2J_{F\text{-}transP}$ = 143 Hz, $^1J_{F\text{-}Pt}$ = 544 Hz).

8.35 Preparation of [PtF{P(4-CH$_3$OC$_6$H$_4$)$_3$}$_3$][HF$_2$] (38):

δ ^{1}H NMR (d^6 acetone) 7.20 (m, *ortho*-Ar.H of the *cis*- and *trans*-P(4-CH$_3$OC$_6$H$_4$)$_3$ to F), 6.75 (d, $^3J_{H\text{-}H}$ = 9 Hz, *meta*-Ar.H *cis*- to F), 6.70 (d, $^3J_{H\text{-}H}$ = 8 Hz, *meta*-Ar.H *trans*- to F), 5.30 (s, CH_2Cl_2), 3.80 (18H, s, CH$_3$O- of P(4-CH$_3$OC$_6$H$_4$)$_3$ *cis*-F), 3.7 (9H, s, CH$_3$O- of P(4-CH$_3$OC$_6$H$_4$)$_3$ *trans*-F). δ ^{31}P{^{1}H} NMR (d^6 acetone) 23.4 (2P, dd, $^2J_{P\text{-}P}$ = 18 Hz, $^2J_{P\text{-}F}$ = 37 Hz, $^1J_{P\text{-}Pt}$ = 2590 Hz, P *cis*-F), -1.2 (1P, dt, $^2J_{P\text{-}P}$ = 18 Hz, $^2J_{P\text{-}F}$ = 144 Hz, $^1J_{P\text{-}Pt}$ = 3729 Hz, P *trans*-F). δ ^{19}F{^{1}H} NMR (d^6 acetone) -169.8 (s. HF_2^-), -229.78 (dt, $^2J_{F\text{-}cisP}$ = 37 Hz, $^2J_{F\text{-}transP}$ = 141 Hz, $^1J_{F\text{-}Pt}$ = 181 Hz).

8.36 Preparation of *trans*- and *cis*-[PtF{PCy$_3$}{P(4-CH$_3$OC$_6$H$_4$)$_3$}$_2$][HF$_2$] (39) and (40):

δ ^{1}H NMR (d^6 acetone) 6.80 (m, Ar.H), 5.30 (s, CH_2Cl_2), 3.80 (4s, CH$_3$O- of P(4-CH$_3$OC$_6$H$_4$)$_3$ in four different environments), 1.70 (m, hydrogen atoms of Cy *cis*-F), 1.2 (m, hydrogen atoms of Cy *trans*-F).

δ ^{31}P{^{1}H} NMR (d^6 acetone) [L = P(4-CH$_3$OC$_6$H$_4$)$_3$] assigned to the *cis*-isomer: 31.0 (dt, $^2J_{P(Cy3)\text{-}cisP}$ = $^2J_{P(Cy3)\text{-}F}$ = 17 Hz, $^2J_{P(PCy3)\text{-}transP}$ = 362 Hz, P of PCy$_3$), 20.5 (dd, $^2J_{P(cisF)\text{-}F}$ = 44 Hz, $^2J_{P(L\text{-}cisF)\text{-}P(trans\text{-}F)}$ = 19 Hz, $^2J_{P(L\text{-}cisF)\text{-}PCy3}$ = 363 Hz), -2.1 (dt, $^2J_{P(transF)\text{-}F}$ = 140 Hz, $^2J_{P\text{-}cisP}$ = 18 Hz).

δ ^{31}P{^{1}H} NMR (d^6 acetone) assigned to the *trans*-isomer: 23.4 (dd, $^2J_{P(L)\text{-}F}$ = 38 Hz, $^2J_{PCy3\text{-}P(L)}$ = 18 Hz, $^1J_{Pt\text{-}P(L)}$ = 2590 Hz P of P(4-CH$_3$OC$_6$H$_4$)$_3$), -1.2 (dt, $^2J_{PCy3\text{-}F}$ = 141 Hz, $^2J_{P(L)\text{-}cisP}$ = 18 Hz).

δ $^{19}F\{^1H\}$ NMR (d^6 acetone) -172.6 (s, HF_2^-), the signals assigned to the *cis* isomer: -250.3 (ddd, $^2J_{F\text{-}cisP(L)}$ = 44 Hz, $^2J_{F\text{-}transP}$ = 146 Hz, $^2J_{F\text{-}cisP(PCy3)}$ = 15 Hz, $^1J_{F\text{-}Pt} \cong$ 175 Hz). the signals assigned to the *trans* isomer: -229.8 (dt, $^2J_{F\text{-}cisP}$ = 38 Hz, $^2J_{F\text{-}transP}$ = 145 Hz, $^1J_{F\text{-}Pt} \cong$ 175 Hz).

8.37 Preparation of $[MF_2(CO)_2(L)_2]$, (M = Os, Ru):

A weighed amount of $[\{MF_2(CO)_3\}_4]$ (ca. 0.10 g) was loaded into a Schlenk flask in the dry box along with 8 molar equivalents of the corresponding phosphine ligand (**L**). In the case of the $P(4\text{-}HOC_6H_4)_3$ ligand (**5**), an FEP vessel was used instead of the Schlenk flask due to the reactivity of the metal fluoride tetramer with glass when these were left in contact for a long period. The low solubility of the phosphine ligand (**5**) in the dichloromethane solvent prolonged the reaction time, therefore the FEP vessel was more convenient than the glass flask in order to obtain a high yield for the final product. The Schenk flask (or the FEP tube) was then attached to the glass vacuum line and the tubing degassed (three successive cycles of pumping and introducing dry dinitrogen). The next step was the introduction of freshly dried and distilled dichloromethane (ca. 20 ml) that was submitted as well to three freeze - thaw - degas cycles. The start of the reaction was evidenced by the evolution of a gas expected to be carbon monoxide. The solutions were continuously degassed in order to ensure the elimination of the liberated carbon monoxide. The solvent was then removed *in vacuo* and the resulting product recrystallised from dichloromethane:hexane mixture. The yields from these reactions were in the range 20-30 %.

The characterisation data of the resulting complexes were the following:

$[RuF_2(CO)_2\{P(4\text{-}CH_3OC_6H_4)_3\}_2]$ (41):

δ ^1H NMR (CD_2Cl_2) 7.69 (12H, m, *o*-Ar.H), 6.98 (12H, d, *m*-Ar.H), 5.36 (s, CH_2Cl_2), 3.86 (18H. s, CH_3O-). δ $^{31}P\{^1H\}$ NMR (CD_2Cl_2) 15.8 (t, $^2J_{P\text{-}F}$ = 22 Hz). δ $^{19}F\{^1H\}$ NMR (CD_2Cl_2) -339.7 (t, $^2J_{P\text{-}F}$ = 22 Hz). FAB mass spectrum, m/z 872 ($[M - CO]^+$), 853 ($[M - CO - F]^+$), 834 ($[M - CO - 2F]^+$) and 805 ($[M - 2CO - 2F]^+$).

Elemental Analysis of $[RuF_2(CO)_2\{P(4\text{-}CH_3OC_6H_4)_3\}_2].3CH_2Cl_2$, calculated: C 48.89 %, H 4.19 % and N 0.00 %, found: C 48.24 %, H 3.98 % and N < 0.0 %. Infrared (Nujol mull), 2035s, 1962s, 1592s, 1568s, 1501s, 1406w, 1290s, 1255s, 1183s, 1026s, 882w, 828s, 799s, 657s, 634w, 626w, 601s, 536s, 506w, 477w, 452w, 430s cm^{-1}.

$[RuF_2(CO)_2\{P(4\text{-}HOC_6H_4)_3\}_2]$ (42):

δ ^1H NMR (d^6 DMSO) 10.31 (bs, OH-), 9.92 (bs, OH-), 7.23 (dd, $J_{H\text{-}H}$ = 8 Hz, *o*-Ar.H), 7.00 (m, *m*-Ar.H), 3.39 (s, HO-). δ $^{31}P\{^1H\}$ NMR (d^6 DMSO) 14.0 (d, $^2J_{P\text{-}F}$ = 21 Hz). δ $^{19}F\{^1H\}$ NMR (d^6 DMSO) -165.3 (s), -321.1 (t). FAB mass spectrum, m/z 667 ($[M - CO - F]^+$). Infrared (Nujol mull), 2055s, 1982s, 1600s, 1578s, 1504s, 1294s, 1253s, 1176s, 1120s, 1010s, 892w, 833s, 677w, 526s, 494s, 456s, 431s cm^{-1}.

$[OsF_2(CO)_2\{P(4\text{-}CH_3OC_6H_4)_3\}_2]$ (43):

δ ^1H NMR ($CDCl_3$) 7.63 (m, *o*-Ar.H), 7.28 ($CHCl_3$), 6.93 (d, $^3J_{H\text{-}H}$ = 9 Hz, *m*-Ar.H), 5.29 (s, CH_2Cl_2), 3.80 (s, CH_3O-). δ $^{31}P\{^1H\}$ NMR ($CDCl_3$) -3.1 (t, $^2J_{P\text{-}F}$ = 30 Hz). δ $^{19}F\{^1H\}$ NMR ($CDCl_3$) -153.8 (s), -305.8 (t, $^2J_{P\text{-}F}$ = 22 Hz). FAB mass spectrum, m/z 989 ($[M]^+$), 970 ($[M - F]^+$) and 943 ($[M - CO - F]^+$). Elemental Analysis of $[OsF_2(CO)_2\{P(4\text{-}CH_3OC_6H_4)_3\}_2].2CH_2Cl_2$, calculated: C 47.68 %, H 4.00 % and N 0.00 %, found: C 48.41 %, H 3.97 % and N < 0.3 %. Infrared (Nujol mull), 2014s, 1930s, 1593s, 1565s, 1501s, 1406w, 1300s, 1286s, 1255s, 1184s, 1024s, 829w, 801w, 653w, 535s, 500s, 472w, 453w, 435w, 423w cm^{-1}.

$[OsF_2(CO)_2\{P(4\text{-}HOC_6H_4)_3\}_2]$ (44):

δ ^1H NMR (d^6 DMSO) 10.40-9.70 (bs, OH-), 7.42 - 6.83 (m, Ar.H), 5.83 (s, dichloromethane), 3.46-2.58 (s, HO-). δ $^{31}P\{^1H\}$ NMR (d^6 DMSO) 4.2 (d, J = 27 Hz), -2.4 (d, J = 23 Hz), -3.5 (d, $^2J_{P\text{-}F}$ = 30 Hz). δ $^{19}F\{^1H\}$ NMR (d^6 DMSO) -166.5 (s), -301.2 (t). FAB mass spectrum, m/z 887 ($[M - F]^+$). Infrared (Nujol mull), 2026s, 1959s, 1602s, 1581s, 1503s, 1286s, 1260s, 1176s, 1120s, 1031w, 947w, 893w, 832s, 676w, 642w, 633w, 525s, 491s, 459s, 432s, 402s cm^{-1}.

8.38 Preparation of $[Pt\{\kappa^2\text{-}P(2\text{-}OC_6H_4)(2\text{-}HOC_6H_4)_2\}\{P(4\text{-}CH_3OC_6H_4)_3\}_2]^+$ (45) and *trans*-$[PtF\{PPh_2(CH_2CHC_6H_4)\}\{P(4\text{-}CH_3OC_6H_4\}_2]^+$ (46):

The reactions of the dimer $[Pt_2(\mu\text{-}F)_2\{P(4\text{-}CH_3OC_6H_4)_3\}_4][HF_2]_2$ (**35**) with the phosphine ligands $P(2\text{-}HOC_6H_4)_3$ (**23**) and $P(2\text{-}C_2H_3C_6H_4)_3$ (**31**) were carried out following the same procedures as in Sections 8.34 - 8.37. The NMR experiments were carried out using D_2O as the lock substance.

Complex (**45**): δ ^1H NMR (D_2O) 10.06 (bs, OH-), 7.62-6.41 (m, Ar.H), 5.21 (s, dichloromethane), 3.61, 3.56 (2s, CH_3O-). δ $^{31}P\{^1H\}$ NMR (D_2O) 35.0 (dd, $^2J_{P\text{-}transP}$ = 368 Hz, $|^2J_{P\text{-}cisP}|$ = 19 Hz and $^1J_{Pt\text{-}P}$ = 2824 Hz, P∩O), 24.2 (dd, $^2J_{P\text{-}transP}$ = 368 Hz, $|^2J_{P\text{-}cisP}|$ = 22 Hz and $^1J_{Pt\text{-}P}$ = 2605 Hz, P_{cisO}) and 1.8 (dd, $|^2J_{P\text{-}cisP}|$ = 22 Hz, $|^2J_{P\text{-}cisP'}|$ = 19 Hz and $^1J_{Pt\text{-}P}$ = 3469 Hz, P_{transO}). δ $^{19}F\{^1H\}$ NMR (D_2O) -152.0 (s, BF_4^-).

Complex (**46**): δ ^1H NMR (D_2O) 11.36 (bs, HF_2^-), 7.89-6.44 (m, Ar.H), 5.54 (dd, $J_{H3\text{-}H2}$ = 1 Hz and $J_{H3\text{-}H1}$ = 17 Hz, H_3), 5.04 (d, $J_{H2\text{-}H1}$ = 11 Hz, H_2) and 3.70 (s, CH_3O-). δ $^{31}P\{^1H\}$ NMR (D_2O) 24.5 (dd, $^2J_{P\text{-}cisP}$ = 18 Hz, $^2J_{P\text{-}cisF}$ = 37 Hz, $P(4CH_3OC_6H_4)_3$) and -0.2 (dt, $^2J_{P\text{-}cisP}$ = 18 Hz, $^2J_{P\text{-}transF}$ = 144 Hz, SP). δ $^{19}F\{^1H\}$ NMR (D_2O) -168.0 (s, HF_2^-) -228.8 (dt, $^2J_{P\text{-}cisF}$ = 38 Hz, $^2J_{P\text{-}transF}$ = 145 Hz, $^1J_{Pt\text{-}F}$ = 176 Hz).

8.39 Preparation of Osmium and Ruthenium Carbonyl fluoride Complexes (47), (48), (49) and (50):

The preparation of these complexes was carried out following the same procedures as in Sections 8.38. However, the complexes (**47**) and (**48**) were purified by a recrystallisation from acetone:hexane, while the complexes (**49**) and (**50**) were purified by a recrystallisation from dichloromethane:hexane.

[*OC-6-33*][$Os(CO)_3\{\kappa^3$-$(2\text{-}OC_6H_4)_2P(2\text{-}HOC_6H_4)\}$] (47):

δ ^1H NMR (d^6 DMSO) 11.14 (bs, OH-), 7.58-6.50 (m, Ar.H). δ $^{31}P\{^1H\}$ NMR (d^6 DMSO) 34.5 (s). δ $^{19}F\{^1H\}$ NMR (d^6 DMSO) -165.2 (s). FAB mass spectrum, m/z 585 ($[M]^+$), 557 ($[M - CO)]^+$, 528 ($[M - 2CO)]^+$ and 449 ($[M - 3CO)]^+$. Elemental Analysis of $[Os(CO)_3\{\kappa^3$-$(2\text{-}OC_6H_4)_2P(2\text{-}HOC_6H_4)\}].0.5CH_2Cl_2$, calculated: C 44.05 %, H 2.63 % and N 0.00 %, found: C 44.09 %, H 2.80 % and N < 0.3 %. Infrared (Nujol mull), 2113s, 2043s, 2002s, 1584s, 1301s, 1262w, 1224w, 1159w, 1130w, 1075w, 1015w, 908w, 850s, 837s, 800w, 751s, 697w, 596s, 575w, 560w, 544w, 526w, 516w, 491w, 481w, 461w, 420w cm^{-1}.

[*TB-5*][$Ru(CO)_2\{\kappa^3$-$(2\text{-}OC_6H_4)_2P(2\text{-}HOC_6H_4)\}$] (48):

δ ^1H NMR (MeOD) 7.58-6.50 (m, Ar.H), 4.80 (s, HO-). δ $^{31}P\{^1H\}$ NMR (MeOD) 30.2 (s). δ $^{19}F\{^1H\}$ NMR (MeOD) -176.1 (s). FAB mass spectrum, m/z 441 ($[M - CO]^+$) and 409 ($[M - 2CO)]^+$. Infrared (Nujol mull), 2059s, 2001s, 1585s, 1558s, 1407w, 1302s, 1264s, 1245w, 1232w, 1158w, 1152w, 1130s, 1077w, 1064w, 1030w, 1023w, 854s, 797w, 755s, 697w, 685w, 667w, 648w, 630w, 597w, 570s, 536w, 521w, 506w, 500w, 491s, 467s, 435s, 421s, 327w cm^{-1}.

[*OC-6-13*][$OsF_2(CO)_2(SP)_2$] (49):

δ ^1H NMR ($CDCl_3$) 7.87-6.71 (m, Ar.H), δ 5.57 (dd, $J_{H3\text{-}H1}$ = 17 Hz and $J_{H3\text{-}P}$ = 1 Hz, H_1 of coordinated SP), 5.13 ($J_{H2\text{-}H1}$ = 11 Hz and $J_{H3\text{-}H2}$ = 1 Hz, H_2 of coordinated SP) and 3.20 - 1.60 (broadness). δ $^{31}P\{^1H\}$ NMR ($CDCl_3$) 0.9 (t, $^2J_{P\text{-}F}$ = 31 Hz). δ $^{19}F\{^1H\}$ NMR ($CDCl_3$) -308.4 (bs), -154.2 (s, BF_4^-) and -169.6 (s, SiF_6^{2-}). FAB mass spectrum, m/z 843 $[M\text{-}F]^+$, 823 $[M\text{-}2F]^+$, 793 $[M\text{-}2F\text{-}CO]^+$ and 768 $[M\text{-}2F\text{-}2CO]^+$. Infrared (Nujol mull), 2021s, 1940s, 1588w, 1261s, 1185s, 1158w, 1023s, 998w, 915s, 875s, 797s, 743w, 708w, 695w, 582w, 514s, 394w cm^{-1}.

[*OC-6-13*][$RuF_2(CO)_2(SP)_2$] (50):

δ ^1H NMR ($CDCl_3$) 7.79-6.95 (m, Ar.H), δ 6.77 (dd, J_{H1-H3} = 17 Hz and J_{H1-H2} = 11 Hz, H_1 of coordinated SP), 5.56 (J_{H1-H3} = 17 Hz, H_3 of coordinated SP) and 5.05 (J_{H1-H2} = 11 Hz, H_2 of coordinated SP). δ $^{31}P\{^1H\}$ NMR ($CDCl_3$) 21.7 (t, $^2J_{P-F}$ = 20 Hz). FAB mass spectrum, m/z 753 $[M-F]^+$, 725 $[M-F-CO]^+$, 705 $[M-2F-CO]^+$ and 675 $[M-2F-2CO]^+$. Infrared (Nujol mull), 2040s, 1967s, 1587w, 1436s, 1261s, 1187w, 1159w, 1116w, 1071w, 1026w, 998w, 917w, 795s, 744s, 694s, 603w, 581w, 521s, 508s, 478w, 452w, 396w cm^{-1}.

Chapter Eight References

[1] G. M. Sheldrick, SHELXTL-pc Release 4.2, Seimens Analytical X-Ray Instruments, Madison, WI, 1991.

[2] G. M. Sheldrick, SHELXL-93, Program for Crystal Structure Refinement, University of Göttingen, 1993.

[3] A. E. Sinear, W. Valient and J. Wirth, *J. Org. Chem.*, 1960, **25**, 2001.

[4] S. O. Grim, R. L. Keiter and W. McFarlane, *Inorg. Chem.*, 1967, **6**, 1133.

[5] T. B. Rauchfuss, F. T. Patino and M. D. Roundhill, *Inorg. Chem.*, 1975, **14**, 653.

[6] M. A. Bennett, R. S. Nyholm and D. Saxby, *J. Organometal. Chem.*, 1967, **10**, 301.

[7] M. A. Bennett, R. N. Johnson and I. B. Tomkins, *Inorg. Chem.*, 1974, **13**, 346.

[8] K. S. Coleman, *Ph.D. Thesis*, University of Leicester, 1996.

[9] F. R. Hartley, S. G. Murray and C. A. McAuliffe, *Inorg. Chem.*, 1979, **18**, 1394.

[10] R. J. Goodfellow and L. M. Venanzi, *J. Chem. Soc.*, 1965, 7533.

[11] a) P. T. Beurskens, G. Admiraal, G. Beurskens, W. P. Bosman, S. Garcia-Granda, R. O. Gould, J. M. M. Smits and C. Smykalla, 1992. The DIRDIF program system, Technical Report of the Crystallography Laboratory, University of Nijmegen, The Netherlands.

b) P. T. Beurskens, G. Admiraal, G. Beurskens, W. P. Bosman, R. de Gelder, R. Israel and J. M. M. Smits, 1994, The DIRDIF-94 program system, Technical Report of the Crystallography Laboratory, University of Nijmegen, The Netherlands.

[12] G. M. Sheldrick, SHELXL-97, Program for Crystal Structure Refinement, University of Göttingen, 1997.

APPENDIX

X-Ray Crystal Data Collection, Solution and Refinement Details for the Compounds (3), (6), (7), (15), (19), (21), (24), (32) and (47)

Compound	(3)	(6)	(7)
Formula	$C_{21}H_{21}O_3P$	$C_{42}H_{42}Cl_2O_8P_2Pt$	$C_{27}H_{33}ClO_6PPt_{0.50}$
Formula Weight	352.35	1002.69	617.50
Temperature (K)	290(2)	190(2)	200(2)
Crystal System	Monoclinic	Monoclinic	Triclinic
Space Group	$P2_1/c$	$P2_1/c$	$P\bar{1}$
Unit Cell Dimensions (Å and °)	a = 9.866(2) b = 9.6238(12) c = 19.792(3) α = 90, β = 92.02(2) γ = 90	a = 10.5810(19) b = 25.591(7) c = 15.661(5) α = 90, β = 102.10(2) γ = 90	a = 9.853(3) b = 12.950(3) c = 13.124(4) α = 64.22(2), β = 83.95(3) γ = 68.52(2)
Volume / $Å^3$	1878.1(5)	4146.4(19)	1400.2(7)
Z	4	4	2
Density (calc.) / Mg/m^3	1.246	1.606	1.465
Absorption Coefficient (mm^{-1})	0.162	3.641	2.716
F(000)	744	2000	628
Crystal Size (mm)	0.64 × 0.55 × 0.17	0.35 × 0.35 × 0.16	0.54 × 0.41 × 0.38
Limiting Indices	-1 ≤ h ≤ 11 -1 ≤ k ≤ 11 -23 ≤ l ≤ 23	-13 ≤ h ≤ 0 -33 ≤ k ≤ 1 -19 ≤ l ≤ 20	-1 ≤ h ≤ 13 -15 ≤ k ≤ 16 -18 ≤ l ≤ 18
Reflections Collected	4430	10379	7781
Independent Reflections	3306 (R_{int} = 0.0167)	9462 (R_{int} = 0.1146)	7527 (R_{int} = 0.0490)
Refinement Method	Full-matrix least-squares on F^2	Full-matrix least-squares on F^2	Full-matrix least-squares on F^2
Data / Restraints / Parameters	3305 / 0 / 226	9462 / 0 / 419	7527 / 0 / 322
Goodness-of-fit on F^2	1.010	1.046	1.023
Final R Indices	R1 = 0.0456, wR2 = 0.0900	R1 = 0.0827, wR2 = 0.1714	R1 = 0.0376, wR2 = 0.0865
R Indices (all data)	R1 = 0.0907, wR2 = 0.1091	R1 = 0.1833, wR2 = 0.2297	R1 = 0.0398, wR2 = 0.0881
Largest Diff. Peak and Hole ($eÅ^{-3}$)	0.192 and -0.151	3.454 and -2.332	1.868 and -1.713

Compound	(15)	(19)	(21)
Formula	$C_{32}H_{38}Cl_4O_3PRh$	$C_{42}H_{42}Cl_4O_6P_2Pt_2.2CH_2Cl_2$	$C_{38}H_{34}Cl_2O_2P_2Pt$
Formula Weight	746.30	1406.53	850.58
Temperature (K)	180(2)	293(2)	190(2)
Crystal System	Monoclinic	Monoclinic	Monoclinic
Space Group	$P2_1$	P2/n	P2(1)/c
Unit Cell Dimensions (Å and °)	a = 8.734(3) b =17.027(4) c = 10.863(3) α = 90, β = 96.41(3) γ = 90	a = 14.399(2) b = 11.187(5) c = 15.365(2) α = 90, β = 107.750(10) γ = 90	a = 13.518(9) b = 10.150(5) c = 37.34(3) α = 90(2), β = 95.13(6) γ = 90
Volume / $Å^3$	1605.4(8)	2357.2(11)	5103(6)
Z	2	2	6
Density (calc.) / Mg/m^3	1.544	1.982	1.661
Absorption Coefficient (mm^{-1})	0.947	6.497	4.409
F(000)	764	1356	2520
Crystal Size (mm)	0.45 × 0.44 × 0.17	0.32 × 0.28 × 0.12	0.32 × 0.26 × 0.08
Limiting Indices	-1 ≤ h ≤ 10 -1 ≤ k ≤ 21 -13 ≤ l ≤ 13	0 ≤ h ≤ 18 -1 ≤ k ≤ 14 -18 ≤ l ≤ 18	-1 ≤ h ≤ 16 -1 ≤ k ≤ 12 -46 ≤ l ≤ 46
Reflections Collected	3604	5590	13298
Independent Reflections	3364 (R_{int} = 0.0948)	4888 (R_{int} = 0.0403)	10538 (R_{int} = 0.1601)
Refinement Method	Full-matrix least-squares on F^2	Full-matrix least-squares on F^2	Full-matrix least-squares on F^2
Data / Restraints / Parameters	3364 / 1 / 370	4888 / 0 / 278	10538 / 0 / 172
Goodness-of-fit on F^2	1.035	1.094	1.046
Final R Indices	R1 = 0.0369, wR2 = 0.0971	R1 = 0.0604, wR2 = 0.1329	R1 = 0.0877, wR2 = 0.2256
R Indices (all data)	R1 = 0.0402, wR2 = 0.0997	R1 = 0.1022, wR2 = 0.1629	R1 = 0.2868, wR2 = 0.2999
Largest Diff. Peak and Hole ($eÅ^{-3}$)	1.023 and -1.041	2.554 and -3.873	4.129 and -2.851

Compound	(24)	(32)	(47)
Formula	$C_{22}H_{24}O_5PPt_{0.50}S_2$	$C_{20}H_{17}Cl_2PPt$	$C_{24}H_{19}O_7OsP$
Formula Weight	561.05	555.29	640.56
Temperature (K)	200(2)	180(2)	190(2)
Crystal System	Monoclinic	Monoclinic	Monoclinic
Space Group	$P2_1/n$	$P2_1/n$	P2(1)/c
Unit Cell Dimensions (Å and °)	a = 10.6871(12) b =16.9593(16) c = 12.8075(15) α = 90, β = 90.685(12) γ = 90	a = 9.1895(13) b = 18.032(3) c = 11.331(2) α = 90, β = 106.580(12) γ = 90	a = 15.981(3) b = 9.503(2) c = 15.802(4) α = 90, β = 102.131(18) γ = 90
Volume / $Å^3$	2321.1(4)	1799.5(5)	2346.3(8)
Z	4	4	4
Density (calc.) / Mg/m^3	1.605	2.046	1.813
Absorption Coefficient (mm^{-1})	3.327	8.182	5.545
F(000)	1128	1056	1240
Crystal Size (mm)	0.26 × 0.19 × 0.17	0.42 × 0.40 × 0.22	0.24 × 0.20 × 0.09
Limiting Indices	$0 \le h \le 14$ $-1 \le k \le 22$ $-16 \le l \le 16$	$-12 \le h \le 1$ $-1 \le k \le 23$ $-14 \le l \le 14$	$-19 \le h \le 20$ $-12 \le k \le 1$ $-20 \le l \le 1$
Reflections Collected	6244	4979	5757
Independent Reflections	5574 (R_{int} = 0.0495)	4344 (R_{int} = 0.0505)	5111 (R_{int} = 0.0555)
Refinement Method	Full-matrix least-squares on F^2	Full-matrix least-squares on F^2	Full-matrix least-squares on F^2
Data / Restraints / Parameters	5574 / 0 / 277	4344 / 0 / 217	5111 / 0 / 263
Goodness-of-fit on F^2	1.009	0.993	0.982
Final R Indices	R1 = 0.0574, wR2 = 0.1144	R1 = 0.0529, wR2 = 0.1243	R1 = 0.0453, wR2 = 0.0875
R Indices (all data)	R1 = 0.1151, wR2 = 0.1354	R1 = 0.0784, wR2 = 0.1243	R1 = 0.1015, wR2 = 0.1057
Largest Diff. Peak and Hole ($eÅ^{-3}$)	1.139 and -1.158	6.320 and -2.504	1.132 and -1.885